ERRATA

Page 11, line last:	For m^{o}_{p/M_u}, read M^{o}_{p/M_u}
Page 12, line 1:	For m^{s}_{p/M_u}, read M^{s}_{p/M_u}
Pages 15,32,33:	For $\underline{F}$, read $\bar{\underline{F}}$
Page 16, line 20:	After solution, insert , applied to the elastic structure
Page 20, para 1:	For 47,600, 154,800, 12,300, 181,400, read -47,600, +154,800, -12,300, +181,400
Page 40, para 3, line 2:	For lock, read lack
Page 45, equation 3.5:	After $\underline{m}^{t}$, insert ds
Page 50, para 4, line 3:	For 1.4, read 0.2
Page 59, para 2, line 16:	For has, read have
Page 78, equation 4.16:	For A_1, read Z_1
Page 81, equation 4.31:	After $F_2\ \xi_{c2}$, insert)
Page 134, para 3, line 7:	For thich, read which
Page 152, para 1, line 2:	After moment, insert distribution
Page 183, para 1, lines 1 to 4:	Delete 'The identification .... Plage 7.3'.
Page 245, para 2, line 6:	For: LaGrance, read LaGrange
Equations 6.15, 6.17, 6.18, 6.24 to 6.27:	In last term before $\underline{m}^{T}$, insert Σ
Equation 4.4:	For d, read e
Equations 4.39, 4.40:	For l, read 1
Page 138, para 3, line 3:	Delete in positional cordinates $_{c}^{s}$
Equation 4.7:	For $\dfrac{4 + c_c - 4{,}000}{2{,}000}$, read $(4 + \dfrac{c_c - 4000}{2{,}000})$

THE ULTIMATE STRENGTH OF STATICALLY INDETERMINATE PRESTRESSED CONCRETE STRUCTURES

by

Brajendra Kumar Gupta

A thesis submitted for the Degree of
Doctor of Philosophy
in the Faculty of Engineering of the
University of London

Imperial College of Science and Technology
London

November, 1967

ABSTRACT

The up to date research in prestressed concrete has been briefly reviewed and conflicting opinions in respect of ultimate flexural strength and flexural stress-resultant deformation characteristic of a prestressed concrete section have been examined in the light of author's test results of two-span beams and fixed portal frames.

Based on the usual strain-compatibility approach but on the assumption that the maximum moment of resistance of a section need not occur at any fixed value of concrete strain, a method has been presented to calculate the complete moment-curvature relationship, including the falling branch, for a prestressed concrete section. This requires that the stress-strain curve of concrete in flexural compression is completely defined. The effect of various parameters studied suggest that the divergence in the experimental moment-curvature characteristics for similar sections could result from the variation in the concrete strain corresponding to the peak stress of the stress-strain curve of concrete.

Results of some previous tests on different types of statically indeterminate prestressed concrete skeletal structures have been reviewed and examined in the light of a theory presented which shows that full-redistribution, in general, would not take place in such structures.

A design method has been proposed which creates conditions so that a statically indeterminate prestressed concrete structure carries the ultimate load by simultaneously developing the maximum moment of resistance at each of the critical sections which form the collapse mechanism, and at the same time maximum output from each such critical section is ensured. It is also shown how other criteria can be used.

The effect of linear transformation has been studied by considering both the 'equilibrium' and the 'compatibility' criteria.

To substantiate the proposed design method and to study its merits and demerits with respect to the existing methods of design, four tests on two-span beams and five tests on fixed portal frames were carried out, which are described in some detail. The force-moment transducer devised to measure vertical and horizontal forces and moment simultaneously in frames is also described in some detail.

ACKNOWLEDGEMENTS

The work reported herein was carried out in the Concrete Structures and Technology Section of the Civil Engineering Department under the supervision of Professor A.L.L. Baker whose benevolent interest is acknowledged. Thanks are due to Dr. A.D. Edwards for his day to day guidance and interest.

The author wishes to thank Dr. C.W. Yu and Mr. R. Loveday for their interest in all the experimental work and providing facilities in the laboratory. Thanks are due to Dr. J.C. Chapman and Mr. J. Neal for allowing the use of many of the equipment belonging to the Engineering Structures Section. The author is specially thankful to the Engineering Structures Section and Mr. J.S. Teraszkiewicz for sparing their rig for the author's tests on beams.

The author wishes to acknowledge the valuable suggestions and assistance of Messrs. R. Loveday and N.D. Scott in developing the Force-Moment transducer reported in Chapter 8.

A large number of laboratory and workshop staff were associated in the experimental work. The author is indebted to Messrs. C. Mortlock, H.G. Wilson, J.R. Turner, P. Jelus, F. Turner, S. Finch, J. Mepham, J. Jeffers, J. Baulch, R. Glen and J. Audsley of the Concrete Structures and Technology Section; Messrs. L. Tidey and G. Jaskulski of the Workshop section; and B. Philpot and G. Scopes of the Engineering Structures Section. The author is especially grateful to Mr. G. Jaskulski, who produced two units of the finally developed Force-Moment transducer, and Messrs. J.R. Turner and J. Audsley who were very generous with their time.

A large number of colleagues helped the author by way of recording data during testing and discussions and he wishes to thank Messrs. D.D.O. Paranagama, R. Matheson, T. Tankut, E.A.W. Maunder,

A.K. Chatterji, K.M. Price, K.C. Michael. Messrs. Michael and Price were particularly generous with their time and the author especially acknowledges their assistance. Thanks are due to Mr. A.Q. Samartin Quiroga for his assistance in developing the equation of stress-strain curve given in Chapter 4.

All computations were carried out on the Atlas computer at the University of London, Institute of Computer Science. The co-operation of the staff at the Institute is gratefully acknowledged.

The author wishes to thank the Punching Section of the Centre for Computing and Automation of the College for punching all his test data, Miss Joyce Gurr for preparing the photoplates, Miss Pat Kerridge for typing the thesis, and Miss Sandra Rumble for preparing some of the drawings.

The author also wishes to thank his wife Usha for her untiring assistance in fixing gauges on many of the concrete specimens and arranging experimental data for punching.

Last, but not least, the author is thankful to the Association of Commonwealth Universities, London, and Ministry of Education, Government of India for awarding a Commonwealth Scholarship, and State Government of Rajasthan for granting the leave of absence. The interest shown by Mr. B.D. Mathur, Chief Engineer and Mr. H.D. Gupta, Additional Chief Engineer is gratefully acknowledged.

CONTENTS

SIGN CONVENTION AND NOTATION

All symbols have been defined where they first appear in the text. However, the following is the list of symbols more frequently used. When a symbol is used to denote the corresponding functional matrix in positional co-ordinates s , bar is placed at the bottom of the symbol.

SIGN CONVENTION

Only stresses, stress-sesultants and corresponding deformations and applied actions, cable eccentricity (e_s) and depths measured from the extreme compressive fibres, i.e. d, e_1, e_2, and h have algebraic values. All other quantities have numerical values only unless otherwise stated.

Basis:-

Extreme fibres are denoted arbitrarily 1 and 2.

Direct stresses: compression + ve
tension - ve

Stress-Resultants

(a) Moment: a + ve moment is one which produces + ve stress in fibre 2.

(b) Shear: as in structural analysis

(c) Thrust: compression + ve
tension - ve

Cable eccentricity and depths

e_s: a + ve eccentricity is one which is measured in the direction of fibre 2.

d, e_1, e_2 and h: depth measured from fibre 2 towards fibre 1 is + ve and that measured from fibre 1 towards fibre 2 is - ve.

NOTATION

Stress-resultants

P = Concrete prestressing force stress-resultant, or prestress conceived as an external force applied to concrete section, in general (+ ve)

P_e = initial effective prestress

P_{cr1}, P_{cr2} = prestressing forces at cracking in fibres 1 and 2 respectively

P_u = prestress at ultimate load

C = total compressive force resisted by the concrete compression zone

T = total tensile force resisted by the prestressing steel

M = moment (absolute)

S = shear

N = thrust

M, M_a = absolute and apparent moments respectively, in general

M_A, M_{aA} = actual absolute and apparent moments respectively at section A

M_u, M_{au} = absolute and apparent ultimate moments respectively, in general

M_u^+, M_u^- = positive and negative absolute ultimate moments respectively, in general

M_r = moment at a section due to inelasticity taking place in the structure

$(M_u)_A$, $(M_{au})_A$ = absolute and apparent ultimate moments respectively of Section A

$(M_{au})_1$, $(M_{au})_n$ = apparent ultimate moments of the first and the last hinge respectively

M_{cr}, M_{acr} = absolute and apparent cracking moments respectively, in general

M_{cr1}, M_{acr1} = absolute and apparent moments respectively when cracking in fibre 1 commences

M_{cr2}, M_{acr2} = absolute and apparent moments respectively when cracking in fibre 2 commences

$\overline{M}_{cr1}$, $\overline{M}_{cr2}$ = moments measured from the state of prestress, i.e. including the secondary prestress moments when cracking takes place in fibres 1 and 2 respectively

$M_{(d+1)}$, $M_{\nu(d+1)}$ = absolute moments due to loads $(d+1)$ and $\nu(d+1)$ respectively, applied to the elastic structure

$(M_{\nu(d+1)})_1$, $(M_{\nu(d+1)})_n$ = absolute moments at the first and the last hinge respectively due to load $\nu(d+1)$ applied to the elastic structure

M_p = total absolute moment due to prestress

M_p^o = pure prestress moment $(= Pe_s)$, or moment due to prestress applied to the reduced structure

M_p^s = secondary prestress moment

$(M_p^s)_1$, $(M_p^s)_n$ = secondary prestress moments at the first and the last hinge respectively

M_a^e = apparent moment calculated according to the elastic theory, in general

$\left[M_{aA}^e\right]_{th}$ = theoretical apparent moment at the section A according to the elastic theory

$(M_{a\,\nu(d+1)}^e)_1$, $(M_{a\nu(d+1)}^e)_n$ = apparent ultimate moments at the first and the last hinge respectively due to load $\nu(d+1)$, applied to the elastic prestressed structure $(=M_{\nu(d+1)}+M_p^s)$

m = bending moment due to unit bi-action applied at a release of the reduced structure, in general

$m_1\ m_2\ ..\ m_\alpha$ = bending moments due to unit bi-action applied at 1, 2 .. α releases respectively of the reduced structure

$m_p^o = M_p^o / M_u$

m_p^s = m_p^s / M_u

N_p^o = thrust due to prestress applied to the reduced structure

n = thrust due to unit bi-action applied at a release of the reduced structure, in general

$n_1, n_2 \ldots n_\alpha$ = thrusts due to unit bi-action applied at 1, 2 $\ldots \alpha$ releases respectively of the reduced structure

$\underline{H}$ = functional matrix in positional co-ordinates s and corresponds to $3 \times \alpha$ stress-resultant distributions due to unit bi-action applied in turn at each release of the reduced structure

$\underline{x}^t$ = functional matrix in positional co-ordinates s and corresponds to the total solution for the given loading configuration and intensity

$\underline{x}_p^o$ = functional matrix in positional co-ordinates s and corresponds to the particular solution due to prestress

Applied actions (actions relative to concrete)

W = applied point load in general

W_u = ultimate load

w = self weight per unit length

$(d+1)$ = working load

$\nu(d+1)$ = factored working load to denote design ultimate load

P, etc. = as defined above.

Geometrical Properties

A_c = gross concrete cross sectional area

A_s = total area of prestressing steel

A_{si} = area of prestressing steel in the ith layer

a = distance of the point of actual crushing from the theoretical critical section

b = breadth of rectangular section

D = total depth of section

d = effective depth, i.e. depth of the centroid of the prestressing steel, measured from the extreme compression fibre, i.e. either fibre 1 or 2

d_i = depth of the centroid of the prestressing steel in the ith layer, measured from the extreme compression fibre, i.e. either fibre 1 or 2

e_1, e_2 = distances of the centroid of the section from fibres 1 and 2 respectively

e_s = cable eccentricity, i.e. the distance of the centroid of the prestressing force P from the centroid of the section

h = depth from extreme compression fibre to fibre of zero strain, (extreme comp. fibre can be either fibre 1 or 2)

I = second moment of area

L = length of span

l_B, l_D etc. = lengths of the members pertaining to the critical sections B, D, etc. respectively over which inelasticity spreads

S = area under the stress-strain curve of concrete

z = distance from the theoretical critical section to the point of contraflexure

Z_1 = I/e_1

Z_2 = I/e_2

Material Properties

c_c = 6 x 12 in. cylinder strength of concrete

c_u = 6 in. cube strength of concrete

c_r = modulus of rupture of concrete

f_{co} = stress corresponding to the peak of the stress-strain curve of concrete

f_c = stress in the extreme compression fibre of concrete

f_s = tensile steel stress in general $\left(= \psi(\varepsilon_s) \right)$; also used to denote tensile stress in prestressing steel assumed concentrated at its centroid

f_{si} = tensile stress in prestressing steel in the ith layer

ε_{co} = strain corresponding to the peak of the stress-strain curve of concrete

E_c = modulus of elasticity for concrete

E_s = modulus of elasticity for steel

Stresses

f = stress in general

f_1^p, f_2^p = stresses in fibres 1 and 2 respectively due to prestress

f_1^{cr}, f_2^{cr} = changes in stresses in fibres 1 and 2 respectively, when cracking commences in that fibre

Strains

ε = strain in general

ε_{cu} = maximum strain in concrete in compression at failure

ε_c = concrete compressive strain in the extreme compression fibre, in general (+ ve)

$\bar{\varepsilon}_{c1}$ = distance of the centroid of the area under the stress-strain curve of concrete from the zero strain

$\bar{\varepsilon}_{c2}$ = $\varepsilon_c - \bar{\varepsilon}_{c1}$

ε_c^p = compressive strain in concrete due to prestress at the centroidal level of the prestressing steel

ε_{ci}^p = compressive strain in concrete due to prestress at the centroidal level of the ith layer of the prestressing steel

ε_s = tensile strain in prestressing steel, in general; the steel assumed concentrated at its centroid (+ ve)

ε_{si} = tensile strain in prestressing steel at the ith layer; the steel assumed concentrated at its centroid

ε_s^o = effective prestrain (tensile) in prestressing steel

$\varepsilon_s^{cr1}, \varepsilon_s^{cr2}$ = tensile strains in prestressing steel at cracking in fibres 1 and 2 respectively

ε_s' = tensile strain in concrete at the centroidal level of the prestressing steel

ε_{si}' = tensile strain in concrete at the centroidal level of the ith layer of the prestressing steel

Deformations

ϕ, ϕ_a = absolute and apparent curvatures respectively, in general; ϕ when so specified also used to denote inelastic curvature which is the difference between the elastic and actual curvatures

ϕ_p = curvature due to prestress, including the effect of secondary prestress moment

ϕ_{cr1}, ϕ_{cr2} = absolute curvatures when cracking takes place in fibres 1 and 2 respectively

$\underline{\theta} = (\theta_1, \theta_2 .. \theta_\alpha)$ = functional matrix corresponding to idealized plastic rotations at α critical sections of the structure

Stress-resultant-deformation characteristics

$\underline{\bar{F}}$ = functional matrix in positional co-ordinates s and corresponds to stress-resultant-deformation section properties pertaining to bending moment, shear and thrust

$\underline{F}$ = elastic flexibility matrix of the members in positional co-ordinates s.

$\underline{K}$ = the functional matrix in positional co-ordinates s and corresponds to the flexural stress-resultant deformation section peoperty i.e. moment-curvature relationship

$\underline{k}$, $\underline{g}$ = elastic bending and thrust flexibility matrices respectively

Coefficients and ratios

α = number of indeterminancies in a structure

β = total number of critical sections in a structure

γ = depth of the centroid of the concrete stress block from the extreme compression fibre, divided by the depth of compression zone

λ = Somes' coefficient to represent enhanced concrete strength at a critical section

F_1 F_2 = bond strain compatibility factors for concrete in compression and tension respectively

p = complementary solution coefficient in general

p_p^s = complementary solution coefficient corresponding to prestress applied to the elastic structure

$p_{\nu(d+1)}$ = complementary solution coefficient corresponding to load $\nu(d+1)$ applied to the elastic structure

p_r = complementary solution coefficient corresponding to the final inelastic curvatures which represent the difference between the elastic solution and final inelastic solution

Sc = factor to denote scope for redistribution

Suffices and use of brackets = suffices in general after the round brackets refer to the sections and those after the square brackets to the structures

CHAPTER 1

INTRODUCTION

1.1 INTRODUCTION

The inelastic characteristics of structural concrete were recognised by the early authors of the nineteenth century such as Thullie, Ritter, etc., who proposed theories that incorporated the inelasticity of concrete. However, such studies were discontinued towards the end of the nineteenth century, at which time the linear elastic theory and the concept of stress factor of safety became accepted in design throughout the world. The concept of stress factor of safety met with some opposition at first, but the design formulae resulting from the linear elastic theory proved too attractive. A renewed interest in the ultimate strength of structural concrete began about 1930. Since then much research has been carried out with respect to the stress distribution in the compression zone and the ultimate strength of reinforced or prestressed concrete sections subject to flexure with or without shear and/or axial load. Excellent reviews[1,2,3] of this development have been published in many languages.

Except for the work of Hognestad et al[2,4], Moenart[5], and Rüsch[6], who studied the stress distribution in the compression zone of concrete through prism tests, most of the other studies[7,8,9,10] were made through the interpretation of results of simply supported beams tested to destruction. Although the various investigators have made different assumptions with respect to the stress distribution in the concrete compression zone, they have produced formulae which predict the ultimate strength to a high degree of accuracy. These investigations, however, did not study the deformations corresponding to the stress-resultants and thus their results cannot be extended to the field of statically indeterminate structures. The conclusions

reached by Hognestad and Rusch were based on idealized conditions and take no account of shear and other restraints present in practice, which are discussed in Chapter 3. Cooke[11], and Somes[12] have recently reported that the gradient of the bending moment diagram influences the ultimate strength of a prestressed concrete section. Mattock[13], however, has shown that this gradient has little influence on the ultimate strength compared to its influence on the ultimate deformation. The author, in Chapter 3, examines his results in the light of the above work.

Recently there have been several attempts[14,15,16] to obtain the complete stress-strain curve of concrete for both concentrically and eccentrically loaded prisms. There is fair agreement up to the point of maximum stress but beyond this the results differ considerably. The divergence of results is probably due to the method of testing and the characteristic of the testing machine rather than the characteristic of concrete.

Before 1949 little work was done on the problem of the behaviour of reinforced and prestressed concrete continuous structures in inelastic range. The early research mainly consisted of a few tests by Kazinczy[17], and Glanville and Thomas[18] on reinforced concrete continuous beams. These tests demonstrated that there was a redistribution of stress-resultants as ultimate load was reached and it was necessary to consider the 'inelastic' phenomenon for the complete understanding of the behaviour of a statically indeterminate concrete structure. Baker[19] suggested, in 1949, a method for the design of continuous beams, which incorporated the limited ductility of concrete and inelastic behaviour of steel and concrete. Since then several ultimate load theories[20,21,22] have been proposed for structural concrete. All these theories include a compatibility requirement for deformations and are dependent in some form or the other on moment-curvature or moment-rotation relationship. One of the aspects of

research in prestressed concrete has been to study such deformation characteristics of individual sections, mainly through tests on simply supported beams, to arrive at safe limiting values so that such information may tentatively be used for the ultimate load design of statically indeterminate structures. At present, opinions with regard to the moment-curvature relationship for a prestressed concrete section differ. While one school of throught regards it as the basic relationship to describe the behaviour of an indeterminate structure, there are other investigators[23] whose tests have led them to believe that there is no unique moment-curvature relationship for a prestressed concrete section. The author's test-results and conclusions are set out in Chapter 4. However, it is certain that the moment-curvature relationship has a rising characteristic with gradually decreasing rate of increase of bending moment with increase of curvature until the maximum moment is reached, when the rate of increase of bending moment reduces to zero. After this the shape of the moment-curvature diagram depends upon many factors such as rate of loading, reinforcement ratio, transverse binding, etc. and there is little experimental evidence about the exact shape of this portion.

The other aspect of research has been to study the behaviour of continuous structures as ultimate load is approached and to establish ultimate load theories for statically indeterminate structures.

A large number of different types of continuous prestressed concrete structures ranging from two-span beams to fixed portal frames have been tested in the past under varying degrees of scope for redistribution and considerable redistribution in the stress-resultants has been observed, but the information made available through such tests is so varying that it does not lead to conditions which justify the application of the 'Simple Plastic Theory' for

prestressed concrete continuous structures. Based on the test-results various investigators[11,14,24,25,26] have suggested empirical methods for design of certain categories of statically indeterminate prestressed concrete structures. Extensive series of tests have been carried out at University of Leeds by Bennett and his co-workers, at Cambridge University by Davies and LaGrange, and at Indian Institute of Technology, Kharagpur by Mallick and his co-workers. Two different findings have emerged from these tests. Tests at Leeds and Kharagpur show that full redistribution in prestressed concrete continuous structures does not take place due to the limited ductility of concrete and confirm, to some extent, the theories put forward by Baker[20], Guyon[21], and Macchi[22] and the Report of Institution of Civil Engineers Research Committee[27]. Tests at Cambridge again show that full redistribution does not occur. This is not taken as evidence of lack of ductility but emphasis is placed on the negative sloping portion of the moment-curvature relationship. Thus, just before collapse of the structure some critical sections may be sustaining less and less moment even though the total load on the structure is increasing. There is little experimental evidence to confirm this theory but the phenomenon of falling moment at increasing curvatures has been accepted theoretically and computer programmes[28] have been written incorporating such behaviour.

The plastic theory of structural steel is based on the fact that the stress-strain curve of mild steel has a long region of constant stress, whereas neither the steel nor the concrete used in the prestressed concrete work has such a flat plateau of stress. But this does not disqualify the theory immediately. The necessary and sufficient condition for applying the theory is that if a structure is loaded, a stage must be reached when there are certain number of sections where deformation can increase without any changes in the stresses taking place anywhere in the structure.

At this stage a 'mechanism' is formed and the hinges rotate but the curvatures in the members between the hinges do not change as deflexions increase. From this point of view plastic theory can be applied to prestressed concrete if the moment-curvature relationship has a long flat region after maximum moment is reached, which, as stated above, may or may not be available. Thus on the face value it appears that plastic theory, in general, cannot be applied to prestressed concrete structures. Now consider a structure whose critical sections forming the collapse mechanism have maximum moments of resistance in the same ratio as the bending moments caused by the maximum applied load. Such a structure would resist the maximum load by simultaneously developing the maximum moment at each of the critical section and at that instant plastic theory would be applicable. Many prestressed concrete structures with concordant cable profile, tested in the past, failed in a manner very close to this. The behaviour of the structure immediately before and after this condition is unimportant, but to design a structure for such conditions in usual manner would be uneconomical. In Chapter 6 a theory has been proposed which ensures maximum output from each of the critical section and creates above conditions.

In English literature the present practice of design of prestressed concrete continuous structures consists in determining the cross sectional areas of steel and concrete and cable profile on the basis of elastic distribution of stress-resultants at working load. The cable profile can either be concordant or linearly transformed or arbitrary nonconcordant. To ensure that individual section has adequate ultimate strength for certain specified factor times the elastic stress-resultants at working load, untensioned steel is added. In the past, most of the tests have been carried out on structures designed in the above manner. Since the cable profile was based on elastic stress-resultant distribution, such tests had the disadvantage that they did not create most severe conditions for redistribution.

The Russian practice for the design of statically indeterminate prestressed concrete structures consists in choosing an ultimate load stress-resultant distribution in equilibrium with the applied load semiempirically and designing the sections accordingly for the ultimate strength. To ensure a satisfactory performance at cracking load, the requisite stress-resultant distribution is obtained by creating certain discontinuities by partially stressing the structure in the statically determinate state with eccentric hinges. The Russian practice along with its merits and demerits will be discussed in Chapter 2 but the obvious disadvantage in the Russian practice is that it only ensures the satisfactory performance at the specified cracking load; whether such a structure would always withstand the specified ultimate load cannot be said.

1.2 OBJECT AND SCOPE

The overall objective of this thesis is to examine and establish why, in general, full redistribution does not occur in statically indeterminate prestressed concrete structures and to present a theory which creates conditions such that the structure carries the ultimate load by simultaneously developing the maximum moment of resistance at each of the critical sections which form the collapse mechanism and at the same time ensures maximum output from each such critical section. As an extension of the above theory it has been shown how the criterion of cracking, or the criterion used by the Russians can be adopted for design.

The effect of linear transformation, which has so far been theoretically studied[11,36,37] by considering only the 'equilibrium' criterion , has been investigated by taking into account both the 'equilibrium' and 'compatibility' criteria.

To substantiate the proposed theory and to study its merits and demerits with respect to the existing methods of design, four tests on two-span beams and five tests on fixed portal frames. have been included in the thesis and are described in Chapter 7. In order to measure the reactions of the frame, a special force-moment transducer which can measure precisely both the vertical and horizontal forces and also the moment simultaneously has been developed and is reported in Chapter 8.

One explanation for full redistribution not occuring in statically indeterminate prestressed concrete structure is the 'limited rotational capacity of concrete hinge'. The author by presenting a simple theory to describe the behaviour of a statically indeterminate structure with a drooping moment-curvature characteristic, near collapse examines in Chapter 5 the previous test results of two and three-span prestressed concrete beams and shows that full redistribution, in general, would not occur in prestressed concrete structures, which is the result of the drooping branch of the moment-curvature diagram for a prestressed concrete section.

The stress-resultant-deformation characteristics of all sections must be known or assumed before any prediction of the ultimate strength of an indeterminate structure can be made. These characteristics must again be based on the material characteristics and in Chapter 3 the author has examined his test results in the light of the C.E.B. recommendations[29] and the recent suggestions made by Somes, and Mattock. In Chapter 4 a method similar to that suggested by Davies[55] and LaGrange[14] has been presented for the calculation of the ultimate moment and the moment-curvature relationship. The results of this approach and of those due to the C.E.B. recommendations are compared with each other and with the author's test results.

The studies in this thesis have been restricted to simple planar skeletal structures, that is continuous beams and frames loaded monotonically in their own plane. It has been assumed that only flexural deformations are significant. The work described here, with suitable modifications would also be applicable to other loading systems and other complex planar and space structures.

The criterion of ultimate load considered in this thesis is that of collapse, that is the ultimate load has been defined as the actual maximum load which the structure would carry under the given set of internal and external conditions.

CHAPTER 2

EFFECT OF PRESTRESS IN A STATICALLY INDETERMINATE CONCRETE STRUCTURE

2.1 INTRODUCTION

In prestressed concrete, unlike the other structural materials, before the external loads are applied prestress itself sets up certain stress-resultants and deformations. The various terms of structural mechanics, if used in this context, would demand special care. For example, in the commonly used sense, probably on the analogy of reinforced concrete, the ultimate moment of a prestressed concrete section is defined as the force in the reinforcement times the distance between the lines of action of this force and the compressive force, at collapse. For a reinforced concrete section the ultimate moment so defined is the actual moment at the section and is also equal to the moment due to the applied ultimate load. But for a prestressed concrete section due to the presence of the prestress moment the ultimate moment so defined, although equal to the moment due to the applied load for a statically determinate structure, is not the actual moment at the section. If all we wish to calculate is the ultimate load for a statically determinate prestressed concrete structure, then the above definition suffices provided the moment due to the external loads is measured from the state of pure prestress.

In a statically indeterminate structure, where the prestress, in addition to the pure prestress moment, also sets up secondary prestress stress-resultants and where for analysis stress-resultant-deformation characteristics are to be considered, the situation becomes all the more complex. It is obvious that the stress-resultant deformation characteristics or load-moment relationship for any section of a statically indeterminate prestressed concrete structure must include the

moments and curvatures set up before the application of the load. In some previous investigations, as discussed in Chapter 3, secondary prestress moments have been omitted. To facilitate the consideration of the moments and deformations caused by the prestress, following definitions are introduced.

2.2 APPARENT AND ABSOLUTE MOMENT

A combination of steel and concrete at a section, in general, is capable of resisting certain bending moment of particular sense, measured from the zero curvature, in one direction and some other value of bending moment of opposite sense in the other direction. The moment measured from the zero curvature is the absolute moment at the section, and in structural mechanics terminology is known as moment. To be more specific, the moment measured from the zero curvature will be called absolute moment and denoted by M. In the elastic range of a reinforced concrete structure the moment due to the applied load $M_{(d+l)}$ is the absolute moment at the section, and the common practice of describing $M_{(d+l)}$ as the moment at the section is justified. But in prestressed concrete, even for a section of a simply supported beam, because of the pure prestress moment M_p^o, the moment due to the applied load $M_{(d+l)}$ is not the absolute moment at the section, and to describe $M_{(d+l)}$ as the moment on the section, which is loosely done at present, is little justified. The absolute moment on the section in this case is equal to $M_{(d+l)} + M_p^o$. However, if instead of measuring the moment from the zero curvature we measure it from the state of pure prestress, then $M_{(d+l)}$ can be described as the moment at the section. But in the true sense of structural mechanics it cannot be called moment. To distinguish it from the absolute moment M, it will be called apparent moment and denoted by M_a.

Thus, for a section of a statically determinate prestressed concrete structure in elastic state

$$M = M_p^o + M_{(d+1)}$$

or

$$M - M_p^o = M_a = M_{(d+1)} \quad \ldots\ldots (2.1)$$

or considering the structure as a whole, we have in matrix notation

$$\underline{M} - \underline{M}_p^o = \underline{M}_a = \underline{M}_{(d+1)} \quad \ldots\ldots (2.2)$$

where bar at the bottom denotes the corresponding functional matrix in positional co-ordinates s.

In a statically indeterminate structure, in addition to the pure prestress moment, prestress also sets up secondary prestress stress-resultants if the cable profile is nonconcordant. If M_p^s denotes the secondary prestress moment (also known as parasitic moment) at a section, then M_p^s can have the same sense as that of M_p^o or otherwise.

Thus, for a section of a statically indeterminate structure in elastic state

$$M = M_p^o + M_p^s + M_{(d+1)}$$

or

$$M - M_p^o = M_a = M_p^s + M_{(d+1)} \quad \ldots\ldots (2.3)$$

or considering the structure as a whole, we have in matrix notation

$$\underline{M} - \underline{M}_p^o = \underline{M}_a = \underline{M}_p^s + \underline{M}_{(d+1)} \quad \ldots\ldots (2.4)$$

From equation 2.3 it is clear that if the moment at a section is measured from the state of pure prestress, that is

apparent moment is measured, then the moment corresponding to no external load is not zero but equal to M_p^s, which can only be zero for a statically determinate structure or for a statically indeterminate structure with concordant cable profile.

Introduction of above definitions requires the definition of ultimate moment to be re-examined. With reference to Figure 2.1 the absolute positive ultimate moment M_u^+ is defined as the maximum positive absolute moment which the section can resist and similarly the absolute negative ultimate moment M_u^- is defined as the maximum negative absolute moment which the section can resist.

Here it will be necessary to define what is positive absolute moment. The moment measured from the zero curvature and producing positive stress in fibre 2 is defined as positive absolute moment and that producing negative stress in fibre 2 as negative.

Thus, for a section of a statically determinate structure at ultimate load

$$M_u = M_p^o + M_\nu(d+1)$$

or

$$M_u - M_p^o = M_\nu(d+1) \qquad \ldots\ (2.5)$$

or considering the structure as a whole, we have

$$\underline{M}_u - \underline{M}_p^o = \underline{M}_\nu(d+1) \qquad \ldots\ (2.6)$$

$M_u - M_p^o$ is the ultimate moment defined in the commonly used sense and is what the various theoretical formulae calculate for the ultimate moment. According to the definitions introduced this is the apparent ultimate moment denoted by M_{au}, i.e.

$$M_{au} = M_u - M_p^o \qquad \ldots\ (2.7)$$

In a statically indeterminate structure at ultimate load, consideration is also to be made of the inelasticity occuring at the various sections. If M_r denotes the moment at a section due to inelasticity taking place in the structure, then for a section of a statically indeterminate structure at ultimate load

$$M_u = M_p^o + M_p^s + M_{\nu(d+1)} + M_r$$

or

$$M_u - M_p^o = M_{au} = M_p^s + M_{\nu(d+1)} + M_r \quad \ldots\ (2.8)$$

or considering the structure as a whole, we have

$$\underline{M}_u - \underline{M}_p^o = \underline{M}_{au} = \underline{M}_p^s + \underline{M}_{\nu(d+1)} + \underline{M}_r \quad \ldots\ (2.9)$$

2.3 MEASURE OF REDISTRIBUTION

In studying the results of tests on statically indeterminate structures, one is faced with the problem of devising a suitable parameter to define the degree of redistribution at the ultimate load. Various parameters have been proposed; Macchi[22], at the second F.I.P. Congress, defined the degree of redistribution as the ratio of the actual ultimate load to the fully plastic load; Bennett[23] defined it as the increase of the actual ultimate load above that for elastic distribution, expressed as the ratio of the difference of the loads between the elastic distribution and full redistribution. Consider two structures designed to have the same plastic load and also the same elastic load. If the two structures carry the same ultimate load, then according to the above definitions they would have the same redistribution irrespective of their deformations. In prestressed concrete, as will be seen in Chapter 6, it is often

possible to have structures carrying the same ultimate load but with different deformations. Obviously, a deformation criterion would be more suitable to measure redistribution. Such a criterion, although cumbersome for theoretical work, would be quite convenient for studying the results of tests. For tests on structures designed for the same plastic load, one such criterion may be to compare their load-deflection curves (W/W_u versus δ). Redistribution in the author's tests will be studied in this manner.

For theoretical work, a criterion based on 'equilibrium' alone would be more convenient. By rearranging terms and dividing both sides by M_{au}, we have from equation 2.8

$$1 - \frac{M_r}{M_{au}} = \frac{M_{\nu(d+1)} + M_p^s}{M_{au}} \qquad \ldots\ (2.10)$$

Equation 2.10 suggests that the ratio $(M_{\nu(d+1)} + M_p^s)/M_{au}$ would be some measure of redistribution at a section. This ratio at the first hinge divided by the same ratio at the last hinge would then give an idea of redistribution for the whole structure and can be taken as the measure of redistribution for the whole structure. Thus, if Sc denotes the measure of redistribution for the whole structure, then

$$Sc = \frac{\left[(M_{\nu(d+1)})_1 + (M_p^s)_1\right] \Big/ (M_{au})_1}{\left[(M_{\nu(d+1)})_n + (M_p^s)_n\right] \Big/ (M_{au})_n}$$

$$= \frac{\left[(M_{\nu(d+1)})_1 + (M_p^s)_1\right]}{\left[(M_{\nu(d+1)})_n + (M_p^s)_n\right]} \cdot \frac{(M_{au})_n}{(M_{au})_1} \qquad \ldots\ (2.11)$$

where the subscripts 1 and n after the round brackets refer to the first and the last hinge respectively.

If we measure all our moments from the state of pure prestress, then

$$M_{\nu(d+1)} + M^{s}_{p} = M^{e}_{a\,\nu\,(d+1)} \qquad \ldots\ (2.12)$$

where $M^{e}_{a\,\nu\,(d+1)}$ is the apparent moment at a section if the ultimate load is applied to the elastic structure.

Hence

$$Sc = \frac{(M^{e}_{a\,\nu\,(d+1)})_{1}}{(M^{e}_{a\,\nu\,(d+1)})_{n}} \frac{(M_{au})_{n}}{(M_{au})_{1}} \qquad \ldots\ (2.13)$$

Equation 2.13 is the same as defined by LaGrange[14], but obtained in a slightly different manner. Sc was called by LaGrange as 'scope for redistribution' and will be referred by the same term in this thesis. It will be noted that it is the same as Macchi's 'disproportion factor', see reference 22.

It will be seen from equation 2.11 that scope for redistribution in a structure can be varied by varying the secondary prestress stress-resultant distribution.

2.4 MOMENT-CURVATURE RELATIONSHIP

The common practice to plot the moment-curvature relationship for a prestressed concrete section is to plot the apparent moment, expressed as the ratio of the apparent ultimate moment, versus apparent curvature. When a dimensionless relationship is preferred, the curvature is also expressed as the ratio of the ultimate apparent curvature. In structural steel or reinforced concrete, because of the absence of the initial moment like the prestress moment, there is nothing like apparent moment and apparent curvature and the usual moment-curvature curve relates

to the absolute moment and absolute curvature. Ideally, for prestressed concrete also the moment-curvature relationship should pertain to the absolute moment and absolute curvature, that is the moment and curvature should be measured from the state of zero curvature and for this reason the moment-curvature curves in this thesis will be plotted between the absolute moment and absolute curvature. However, to study as how the two plots would differ, for some test results they have been plotted in both ways, see Figures 7.25 and 7.26. The basic shapes of the two plots are similar and one is obtainable from the other by transfer of origin and modifying the constants.

In the present investigation the ultimate curvature corresponding to the same ultimate moment has been found to vary widely from section to section. To give an idea of this variation, the moment-curvature relationships have been plotted between M/M_u and ϕ.

2.5 STRUCTURES WITH CONCORDANT AND LINEARLY TRANSFORMED CABLE PROFILES

The design of a prestressed concrete element for working loads is essentially based on satisfying the basic inequalities, which represent the design conditions. The solution of these inequalities and the evaluation of the prestressing force and its eccentricity (design procedure) has, in general, been set out by many authors[31,32,33,34]. Having fixed the sectional properties and prestress, it is possible to establish the cable domain. To obtain a concordant cable profile for an indeterminate structure, the problem then reduces to finding a cable profile lying within this domain such that

$$\int_s \underline{H}^T \underline{F} \underline{x}_p^o ds = 0 \qquad \ldots\ldots (2.14)$$

where $\underline{H}$ is a functional matrix in positional co-ordinates s and for a planar structure corresponds to $3x\alpha$ stress-resultant distributions (m s n) due to unit bi-action applied in turn at each release of the reduced structure;

$\underline{F}$ is the elastic flexibility matrix of the members in positional co-ordinates s; and

$\underline{x}_p^o$ is the particular solution due to prestress.

It is usual to neglect shear deformations and equation 2.14 reduces to

$$\int_s \underline{m}^T \underline{k}\, \underline{M}_p^o\, ds + \int_s \underline{n}^T \underline{g}\, \underline{N}_p^o\, ds = 0 \qquad \ldots\ (2.15)$$

where $\underline{m}(= \underline{m}_1\, \underline{m}_2 \ldots \underline{m}_\alpha)$ and $\underline{n}(= \underline{n}_1\, \underline{n}_2 \ldots \underline{n}_\alpha)$ are the functional matrices in positional co-ordinates s and correspond to bending moment and thrust distributions respectively due to unit bi-action applied in turn at each release of the reduced structure; $\underline{k}$ and $\underline{g}$ are the elastic bending and thrust flexibility matrices respectively of the members in positional co-ordinates s; and $\underline{M}_p^o$ and $\underline{N}_p^o$ are the functional matrices in positional co-ordinates s corresponding to bending moment and thrust distributions respectively due to prestress applied to the reduced structure.

Equation 2.15 represents α (where α is the indeterminancy number) linearly independent equations and, except for very simple indeterminate structures, a concordant cable profile can only be established through a trial and error procedure. A method dealing with this procedure has been outlined by Morice[35]. The author, however, found the following procedure more expedient for the particular case of monotonically increasing applied load.

A structure has β number of critical sections which, in general, are in excess of its indeterminacy number α. If the eccentricities at $(\beta - \alpha)$ critical sections are fixed, then,

assuming the shape of the cable profile same as that of bending moment diagram, the eccentricities at the remaining α critical sections can be evaluated by solving equations 2.15. The $(\beta - \alpha)$ critical sections where the eccentricities are fixed should be those where the cable zone width is small and there is not much scope for manoeuvring. The cable profile so determined should then be checked for lying within the cable zone; if not, another trial would be necessary until it is satisfied.

Many of the structures tested in the past[11,14,36,37] had concordant or linearly transformed cable profiles based on the working load stress-resultant distribution, which had the disadvantage that full output was not obtained from all the critical sections. Many such structures with concordant cable profile had also the disadvantage that the changes in bending moments at the critical sections during loading to failure were approximately equal to the elastic moments due to the ultimate load applied to a completely elastic structure and the scope for redistribution was small.

Remembering that $M_p^s = 0$ for a concordant cable profile, we have from equation 2.11

$$\left[Sc\right]_C = \frac{\left(M_{\nu(d+1)}\right)_1}{\left(M_{\nu(d+1)}\right)_n} \frac{\left(M_{au}\right)_n}{\left(M_{au}\right)_1} \qquad \ldots\ (2.16)$$

where suffix C after the square brackets refers to the structure with a concordant cable profile.

If P_u is the prestress force at a section at the ultimate load and d is the depth of the centroid of the prestress from the extreme compression fibre, then

$$M_{au} = k_u P_u d \qquad \ldots\ (2.17)$$

where k_u is a constant.

Therefore

$$\left[Sc\right]_C = \frac{(M_{\nu(d+1)})_1}{(M_{\nu(d+1)})_n} \frac{(k_u P_u d)_n}{(k_u P_u d)_1} \quad \ldots\ldots (2.18)$$

Equation 2.18 is true algebraically and since the sign convention of 'M' and 'd' has been defined to match with each other (see SIGN CONVENTION AND NOTATION), it would hold good numerically as well.

If all sections are assumed under-reinforced and have the same prestress, then in equation 2.18, $(k_u)_1 \simeq (k_u)_n$ and $(P_u)_1 \simeq (P_u)_n$. Now if d is approximately proportional to $M_{\nu(d+1)}$ at a section, then from equation 2.18 $\left[Sc\right]_C$ would be nearly equal to unity. That is, a structure with such a concordant cable profile would exhibit little redistribution. This was observed by Cooke[11] for three-span beams and Raina[37] for two-span beams. The author observed this for the fixed portal frames. The frame F-1, which had a concordant cable profile designed in the above manner, had a horizontal deflection of 1.10 inches and a vertical deflection of 0.62 inches at ultimate load; the corresponding deflections for frames F-2,3,4 and 5 were 1.30 and 0.82, 2.70 and 1.37, 1.32 and 1.00, and 1.38 and 0.975 inches respectively; see Figures 7.21 to 7.24. Frame F-2 had a linearly transformed cable profile obtained from F-1, and frames F-3 to 5 were designed differently as described in Chapter 7 with maximum eccentricities at all the critical sections of the apparent collapse mechanism.

The linear transformation, which consists in adding a certain linear combination of complementary solution diagrams to a cable profile, alters the eccentricities at the critical sections and also sets up certain secondary prestress stress-resultant distribution. Depending upon the linear transformation employed, redistribution is either reduced or increased and mode

of collapse would also change. The problem becomes quite complex to study in general terms by considering both equilibrium and compatibility criteria. Morice and Lewis[36] considering only the equilibrium criterion and assuming the apparent ultimate moment of a section proportional to its effective depth have shown that no variation in ultimate load of a structure should occur due to linear transformation. Raina[37], on the other hand, has shown that a variation in ultimate load would occur due to linear transformation. Raina, like Morice and Lewis, also considers only the equilibrium criterion, but assumes that failure takes place by ultimate concrete strain. He expresses the steel strain in terms of the effective depth and concrete strain, and by representing the load-strain curve of the H.T. steel tendon by a term of a sine series obtains the apparent ultimate moment of a critical section after solving a transcendental equation, which enables him to show a variation in ultimate load due to linear transformation.

Raina, for his test specimens which are described in Chapter 7, calculated that, as compared to beam CB-1 which had the parent concordant cable profile, the ultimate loads for beams CB-2 and 3 which had upward linear transformations should change by +2.0% and +5.5% respectively, and those for beams CB-4 and 5 which had downward linear transformations by +7.9% and +21.8% respectively. The corresponding figures as obtained from the tests are +1.35%, +4.71%, +2.42% and -12.62% respectively. The variation, except for beam CB-5, is practically of the same order as the accuracy of experimental measurements, and it supports Morice and Lewis's assumption. There is other experimental evidence[11,14] which also supports the simplifying assumption for continuous beams and hinged portal frames.

The experimental evidence[14] available for fixed portal frames does not support the above assumption. To the author's

knowledge, so far only four fixed portal frames employing linearly transformed cable profiles have been tested. These tests were carried out by LaGrange[14] at Cambridge University, who concluded that "in portal frames with fixed feet, linear transformations would almost invariably change the load carrying capacity of the frame". This is not confirmed by the author's tests on frame F-2 which had a linearly transformed cable profile and carried practically the same ultimate load as the parent frame F-1 with concordant cable profile. To the author, the above statement appears misleading. Linear transformation which consists in adding a certain linear combination of complementary solution diagrams to a cable profile does not affect 'equilibrium' and therefore as long as the collapse mechanism is not changed due to linear transformation, the ultimate load based on 'equilibrium criterion' should remain practically unaltered. To LaGrange, linear transformation meant adding linear functions to the eccentricities of the concordant cables and he changed the strengths of the critical sections in some parts of the frame by linear transformation, without changing the eccentricity of the cable in some other part. Linear transformation in its true sense cannot do this. The above conclusion is therefore based on a different meaning of linear transformation, and should be interpreted accordingly. Before the effect of linear transformation (in its true sense) in fixed portal frames is established, more experimental evidence is necessary.

There are, however, certain odd cases, for example Raina's beam CB-5 which carried 12.62% less ultimate load as compared to the parent concordant beam, which shows that it may not always be realistic to consider only equilibrium criterion. The author, in Chapter 6, considering both equilibrium and compatibility criteria has tried to study the effect of linear transformation in general terms, but without success, and it appears that each case will have to be studied individually.

The effect of linear transformation, as pointed out by LaGrange[14], is not significant on factor Sc. Consider two structures, namely one with a concordant cable profile and the other with a linearly transformed cable profile obtained from the first. Let the two structures be assumed to carry the same ultimate load, i.e. $M_{v(d+1)}$ is the same in both the cases.

If d is the effective depth at any section in the concordant case, then the effective depth in the linearly transformed case would be $(d + M_p^s/P_e)$, where P_e is the initial prestress. Thus from equation 2.11 we have

$$\left[Sc\right]_{LT} = \frac{(M_{v(d+1)})_1 + (M_p^s)_1}{(M_{v(d+1)})_n + (M_p^s)_n} \quad \frac{\left((d + \frac{M_p^s}{P_e})k_u P_u\right)_n}{\left((d + \frac{M_p^s}{P_e})k_u P_u\right)_1}$$

$$= \frac{(M_{v(d+1)})_1 + (M_p^s)_1}{(M_{v(d=1)})_n + (M_p^s)_n} \quad \frac{(k_u d P_u)_n + (M_p^s k_u \frac{P_u}{P_e})_n}{(k_u d P_u)_1 + (M_p^s k_u \frac{P_u}{P_e})_1}$$

.... (2.19)

where subscript LT after the square brackets refers to the linearly transformed case.

Equation 2.19 holds good algebraically in general, and since the sign convention for 'M' and 'd' have each been defined to match with each other (see SIGN CONVENTION AND NOTATION), equation 2.19 would also be true numerically if the sign of $(M_p^s)_1$ is

related with $(M_{\nu(d+1)})_1$ and $(d)_1$, and that of $(M^s_p)_n$ with $(M_{\nu(d+1)})_n$ and $(d)_n$. The linear transformation which numerically reduces the effective depth at a critical section sets up M^s_p which acts opposite to $M_{\nu(d+1)}$ and vice versa, with the result that there is not much effect on Sc.

2.6 RUSSIAN CODE RECOMMENDATIONS

The Russians design statically indeterminate prestressed concrete structures for both working load and ultimate load criteria. An ultimate load stress-resultant distribution in equilibrium with the applied loads is assumed semi-empirically. The required section sizes, the area and position of steel are estimated throughout the structure. The critical section strengths are checked to ensure adequate ultimate load carrying capacity; an equilibrium method is used, compatibility of strain across a section is ignored. The assumed stress-resultant distribution is reduced in the ratio of allowable cracking load to ultimate load. The cracking moments of the critical sections are calculated on the basis of a concordant cable. If the cracking moments at the critical sections are not satisfactory, the working load stress-resultant distribution is modified by the addition of a linear stress-resultant distribution, that is linear combination of the complementary solution diagrams. The final assumed elastic moment distribution due to the applied working loads now conforms to the cracking moments at the critical sections. The stress-resultant distribution due to the working loads applied to the true structure is now determined. The difference between the assumed and true distributions at working loads is a linear distribution.

The cracking moments were based on a concordant cable profile, but this profile was arbitrarily assumed. It remains

therefore to ensure that the secondary prestress moments are made equal to the difference between the assumed and true elastic distributions. The required secondary moments with a given profile is obtained by building in a specified lack of fit. The structure is made statically determinate by providing hinges, usually eccentric to the centre line of the section, and the structure is then partially stressed. The hinges are concreted solid, and the remaining prestress applied. The final secondary stress-resultant distribution together with the elastic stress-resultant distribution due to the applied loads is thus made equal to the assumed cracking moment distribution. The effect of creep is allowed by applying a factor of 2 to the difference between the assumed and true stress-resultant distributions at working load.

Creep is a phenomenon which is still not fully understood. The introduction of creep factor in the above method has resulted in certain empiricism. Saeed-un-din and Hall[38] have shown that linear creep has no effect, other than that causing loss of prestress, on the stress-resultant distribution set up by prestressing a structure in a statically indeterminate state; the results of author's tests are set out in Chapter 6. The creep factor should therefore be applied only to the stress-resultant distribution set up during the statically determinate state.

The assumed stress-resultant distribution at cracking load has been ensured by building in a lock of fit, and, in theory, such a structure would carry the specified cracking load satisfactorily. But, whether such a structure would always carry the specified ultimate load without the rupture of any section or the structure as a whole or part becoming kinematically unstable, cannot be said.

The results of frame F-5 which was designed according to the above method but with creep factor applied to the stress-resultant distribution set up in the statically determinate state will be discussed in Chapter 6.

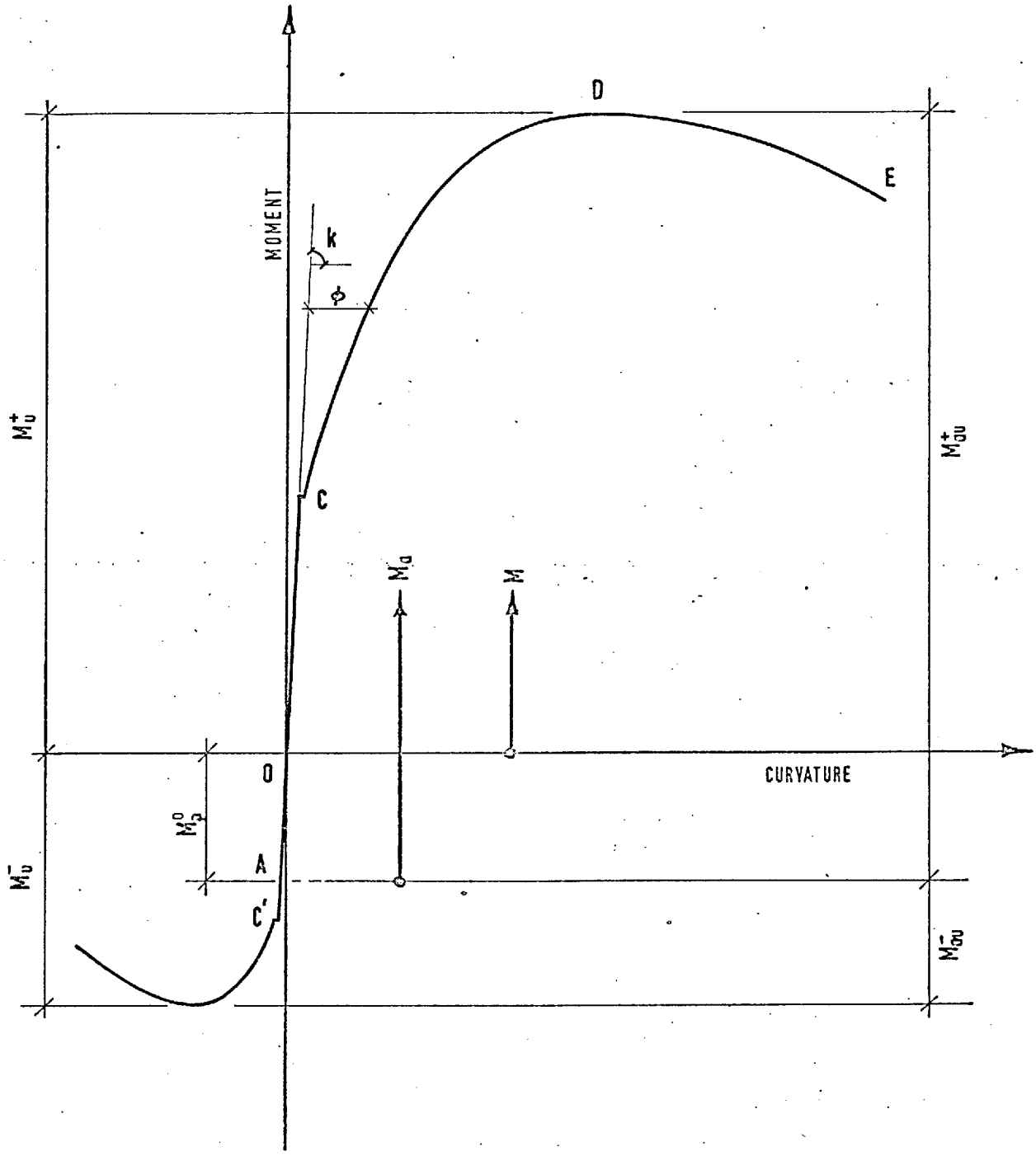

Fig. 2·1 : MOMENT CURVATURE RELATIONSHIP FOR ECCENTRICALLY PRESTRESSED SECTION

CHAPTER 3

ULTIMATE LOAD ANALYSIS OF STATICALLY INDETERMINATE CONCRETE STRUCTURES

3.1 PRINCIPLES AND ASSUMPTIONS OF STANDARD ANALYSIS

There are three conditions that any problem of structural mechanics or of stress analysis must satisfy:-

(1) Equilibrium
(2) Compatibility
(3) Material Properties

For a statically determinate structural system the problem is relatively straightforward, since conditions (1) are sufficient to give all the stress-resultants. Conditions (2) and (3) may then be applied afterwards if the displacements of the structure are required. But for the analysis of a statically indeterminate structure it is necessary to consider all the three conditions. This thesis is concerned with skeletal structures like continuous beams and frames, and for such structures the three requirements are satisfied as follows.

A skeletal structure, where the member lengths are much greater than either of the overall dimensions of their cross section, is idealized into member lines with each point on the member line endowed with section properties in a plane at right angles to the member line. The section properties are obtained by integrating the idealized material properties over the two cross sectional dimensions. In a composite material like prestressed concrete, in addition to material properties, consideration is also required for their relative percentages and position, condition of grout, etc. The distribution of stress-resultants due to any condition of loading applied to this idealized structure is then found by

satisfying both equilibrium and geometric compatibility requirements. This can either be done by the 'Displacement (or Stiffness) Method' or the 'Force (or Flexibility) Method'. In the displacement method the compatibility conditions used first give rise to equations of equilibrium, whereas in the force method the equilibrium conditions first satisfied lead to the equations of compatibility. The early treatises on these methods are by Jenkins[39], who dealt with the force method, and Argyris and Kelsey[40] who dealt with both the force and displacement methods. In this thesis force method will be used.

3.2 BASIC EQUATIONS

Consider an α times statically indeterminate structure and let it be planar subject to planar loading. The compatibility requirement states that:-

$$\int_s \underline{H}^T \overline{\underline{F}}\, \underline{x}^t \, ds = 0 \qquad \ldots\ldots (3.1)$$

where $\underline{H}$ is the functional matrix in positional co-ordinates s and corresponds to $3x\alpha$ stress-resultant distributions due to unit bi-action applied in turn at each release of the reduced structure;

$\overline{\underline{F}}$ is the functional matrix in positional co-ordinates s and corresponds to stress-resultant deformation section properties pertaining to bending moment, shear and thrust; and

$\underline{x}^t$ is the functional matrix in positional co-ordinates s and corresponds to the required total solution for the given loading configuration and intensity, that is three total stress-resultant distributions (bending moment m, shear s and thrust n) at all positions of the structure.

Equation 3.1 represents α compatibility equations (α being the indeterminancy number) for a given equilibrium system. These equations are linearly independent, and provided $\underline{\bar{F}}$ is known, they can be solved for any load conditions, including the ultimate load.

This thesis is concerned with skeletal planar structures with planar loading, where major deformations due to the applied load are caused by bending, and deformations due to shear and thrust are neglected such that

$$\underline{H} = \left[\underline{m}_1 \; \underline{m}_2 \cdots \underline{m}_\alpha \right] = \underline{m} \qquad \ldots\ (3.2)$$

$$\underline{\bar{F}} = \underline{K} \qquad \ldots\ (3.3)$$

$$\underline{x}^t = \underline{m}^t \qquad \ldots\ (3.4)$$

where $\underline{m}$ is the functional matrix in positional co-ordinates s and corresponds to $1 \times \alpha$ bending moment distribution due to unit bi-action applied in turn at each release of the reduced structure;

$\underline{K}$ is the functional matrix in positional co-ordinates s and corresponds to the flexural stress-resultant deformation section property, that is moment-curvature relationship at a section; and

$\underline{m}^t$ is the functional matrix in positional co-ordinates s and corresponds to total bending solution for the given load configuration and intensity.

Thus, for the structure where only flexural deformations are significant equation 3.1 reduces to

$$\int_s \underline{m}^T \underline{K} \underline{m}^t = 0 \qquad \ldots\ (3.5)$$

Thus, provided the moment-curvature relationships for all sections are known, a solution can be found for any load condition, including the ultimate load. The solution is somewhat cumbersome if the moment-curvature-relationship is not linear, but in theory

it would be quite easy on a computer. Depending upon the moment-curvature relationship, failure may be said to occur either when one or more cross sections rupture, or when the structure as a whole or part of it becomes kinematically unstable.

3.3 ULTIMATE FLEXURAL STRENGTH

The apparent and absolute ultimate moments as applicable to prestressed concrete have been defined in Chapter 2. It is the apparent ultimate moment which the various theoretical formulae estimate for prestressed concrete and which will be considered in this Section.

The main difficulty in the study of the ultimate flexural strength of a reinforced or prestressed concrete section is the lack of knowledge of the actual stresses in the flexural compression zone of concrete at collapse. The behaviour of compression zone of concrete at collapse has been related by many of the investigators to the compressive strain ε_{cu} in the extreme comparison fibre and at that strain by coefficients relating to:-

1) the average stress over the area divided by the strength of the concrete in direct compression, and

2) the depth of the centre of compression divided by the depth of compression zone.

The early work in this field was done by Whitney[7], Jensen[8], Gaston[9], Billet and Appleton[10], etc. Their work was based on the interpretation of beam test results, and, because of one less equation available than the number of unknowns involved, each of them made one or the other assumption; with the result their findings differed from one another. Surprisingly each of them produced formula which predicts the ultimate flexural strength to a high degree of accuracy. The work on prisms by Hognestad et al[4],

Moenart[5], and Rüsch[6] has produced better understanding of the behaviour of the flexural compression zone of concrete and their results are in reasonable agreement. The conclusions reached by Hognestad, and Rusch are based on studies made under simulated conditions of pure flexure, and, strictly speaking, should be applicable to such idealized conditions. However, their results when applied to reinforced and prestressed concrete beams met in practice have shown fairly accurate correlation.

Naughton[41], during his investigations on two-span, and Cooke[11], on three-span prestressed concrete beams, found that the ultimate flexural strength of similar sections situated at the support or at the load point varied appreciably. The apparent ultimate moment of each critical section was obtained experimentally, and where only one section failed at collapse, it was obtained by continuing the test beyond the maximum load. It was discovered that the experimental values represented two separate relationships depending upon whether the section considered was at the support or at the load point. Considering only the equilibrium of forces acting on the concrete section, the dimensionless relationship for the apparent ultimate moment of a section was written by Cooke in the form:-

$$\frac{M_{au}}{bd^2 c_u} = \beta \left(\frac{A_s f_{su}}{bd\, c_u}\right)\left[\eta - \frac{\gamma}{\alpha}\left(\beta \frac{A_s f_{su}}{bd\, c_u}\right)\right] \qquad \ldots\ (3.6)$$

where f_{su} is the ultimate tensile stress of tensioned steel;

β is the ratio of maximum stress in tensioned steel to ultimate tensile strength (f_{su});

and α is the ratio of mean compressive stress (rectangular distribution) to 6 in. cube crushing strength c_u.

(The remaining symbols have the same meaning as explained

under 'SIGN CONVENTION AND NOTATION', but have numerical values only).

Cooke, for his three-span beam series, found Υ/α = 0.67 and β for support section as 0.95, and for the intermediate span section which was the load point as 1.20. Naughton, for his two-span beams, which had practically the same effective depth in all cases at each critical section, found the ultimate moment of resistance of support section about 7-18% higher than that of the span section.

A number of possible reasons were advanced by Cooke for the above variation in his tests such as (1) reduction of the peak moment by dispersion of the concentrated load, (2) formation of a bulb of stress under the reaction plate which increases the flexural strength of the concrete depending upon the value of the reaction as found by Frocht[42] for an elastic medium, (3) increase in the longitudinal stress of concrete due to the presence of transverse stress, (4) the statistical probability that the strength of the section at which failure occurs will be greater at a concentrated load than the weakest section in a length of beam; this means that with an increase in the outer span length, probability of increase in the strength of the failure section becomes less. Cooke, for his beams, obtained a variety of values of ultimate moment of resistance for similar sections situated at the supports, depending upon the outer span length. He observed an enhancement in its value with the increase in the gradient of the bending moment diagram. But, somehow, instead of pursuing this reason, he got involved in the above reasoning; although the first three of them could not explain to Cooke himself the order of the experimental variation.

An examination of the load-moment curves plotted by Cooke for his test beams shows that moment corresponding to zero load is zero for all beams, whether employing a concordant or a linearly transformed cable profile. This would be consistent from test to test if it is assumed that moments were measured from the state of prestress, that is including both the pure prestress moment M_p^o and the secondary prestress moment M_p^s ; but such a moment will neither be an apparent moment nor an absolute moment. In the light of this, Cooke's results and equation 3.6 may be susceptible to some discrepancy, but Naughton's results which were obtained from concordant beams cannot be disputed. However, the order of variation in them is somewhat less as compared to the Cooke's results. The above phenomenon, although first observed by Naughton, and Cooke, is a real one, and there must be some explanation for this.

Somes[12] examined in detail the difference between the idealized conditions of Hognestad, and Rüsch's tests and the actual conditions pertaining to the concrete zone which eventually fails at a critical section. Hognestad and Rüsch's results have been derived from studies in a region of pure flexure in which no transverse confinement other than that due to stirrups exists, see Figure 3.1(a). Unlike this, the compression zone of a critical section usually met in practice is associated with confinement due to the presence of loading plate or the beam column interconnection as shown in Figure 3.1. Somes examined the published work on the effect of transverse reinforcement in bound concrete, and postulated that for conditions typical of the concrete zone which eventually fails at a critical section the actual flexural compressive strength would be greater than that defined for pure flexure. According to him the enhancement results from the following two effects acting together:-

1) Transverse loading on the beam sets up a local system of biaxial or even triaxial compression close to the section, which enhances the maximum moment of resistance. But the capacity of the member may depend upon the resistance of some section away from the moment peak where the transverse loading has diminished.

2) The critical section away from the load is restrained on one side by a region of effectively stronger concrete while on the other side flexural stress falls away rapidly with the bending moment diagram.

The two effects jointly serve to confine the critical zone, and according to Somes this confinement depends upon the gradient of the bending moment diagram close to and on the appropriate side of the section. Somes has postulated that the enhanced compressive strength of concrete would be equal to a factor λ times the one defined for pure flexure, where

$$\lambda = 1 + \frac{D}{z} + 5\left(\frac{D}{z}\right)^2 \qquad \ldots\ (3.7)$$

where D is the total depth of the section; and
z is the distance from the critical section to the appropriate point of contraflexure.

It has been suggested that the value of λ should be restricted to 1.4 which corresponds to $D/z = 0.2$; when D/z is greater than 1.4, λ will be influenced by a shear-bending interaction, a phenomenon not yet well understood.

Somes substantiated his postulate by comparing Mallick's[25] and his experimental results with the theoretical ones. It should be noted that Somes's measured values of ultimate moment refer to the maximum moment in the beam when crushing moment of some point is reached, that is in the continuous beams tested by Cooke, Naughton, the author, etc. Somes's calculated values of ultimate

moment would refer to the theoretical critical section. Somes has, however, warned that the value of λ, derived by him, would not be applicable to the analysis which attempts to take account of the displacement of the crushing zone from the peak of the bending moment distribution.

Mattock[13], in November 1964, published the results of thirty-seven simply supported reinforced concrete beams involving many variables, including the distance from the point of maximum moment to the point of zero moment. There is some scatter in the measured values of ultimate moments, but nevertheless they show a trend similar to that observed by Cooke, and Somes, that is the ultimate flexural strength tends to increase slightly with increase in the gradient of the bending moment diagram. Mattock did not comment on this feature; probably being small it did not draw his attention. However he observed another phenomenon, that is the increase in the maximum concrete compression strain with the decrease in the distance of the point of maximum moment from the point of zero moment, which resulted in increased ultimate curvatures. Mattock has tentatively suggested the following empirical expression for ultimate flexural strain of concrete.

$$\varepsilon_{cu} = 0.003 + \frac{0.5}{z} \qquad \ldots\ (3.8)$$

where z is the distance from the point of maximum moment to the point of zero moment and is measured in inches, and 0.003 is the strain value used for ultimate strength calculations in the ACI Building Code[43], ACI 318-63 and corresponds to the region of constant moment.

It would be noted that equation 3.8 is not dimensionally consistent.

The confining effect on concrete by transverse loading was also observed by Warwaruk[44] in his tests on ungrouted beams loaded at the centre of their span and by Yamashiro and Siess[45] in tests on beam-column connections.

3.4 DISCUSSIONS IN THE LIGHT OF AUTHOR'S TEST RESULTS

It is a fact that transverse loading on a beam sets up a local system of biaxial or even triaxial compression, and close to the loading point the ultimate flexural strength is appreciably increased; but the load carrying capacity of the member is not always governed by this. In general, it would depend upon the resistance of some section away from the moment peak (theoretical critical section) where the effect of transverse loading is not present. The author observed in his tests, which are described in Chapter 7, that in two-span beams failure always took place by crushing of concrete away from the theoretical critical section; the actual distance varied slightly from test to test depending upon the critical section considered, and is given in Table 3.1. However, in the frames crushing took place very close to the theoretical critical sections. This was probably due to the method of construction and the fact that there was a discontinuity in the duct-tubing at each of the critical sections. For the frames, therefore, only the theoretical critical sections have been considered here.

The maximum apparent moments measured at the various theoretical critical sections and at the corresponding points where crushing of concrete actually took place are given in Table 3.1 for the test beams. The values of the apparent ultimate moments M_{au} calculated according to the C.E.B. recommendations[46] are also given in this Table. These values have been calculated by

taking $f_{co} = 1.05\, c_c$ and $F_2 = 0.8$ (see SIGN CONVENTION AND NOTATION), as assumed throughout the thesis. It will be seen that the measured moments at the theoretical critical sections of the test beams are about 15% higher than those evaluated from the C.E.B. recommendations, and that there is a general trend of increase in their values with increase in D/z ratio, which is in accordance with Somes's postulate. However, such an increase was not noticed for the test frames; D/z ratio varied largely for the various critical sections, but the measured ultimate moments did not show any marked variation. This shows that Somes's postulate would not always be true, and the real explanation for the increase in the maximum moments measured at the theoretical critical sections of the test beams lies somewhere else.

Although there is a variation in the maximum moments measured at the various theoretical critical sections of the test beams, they do not show any uniform trend as noticed by Naughton or Cooke. For example, Naughton for his two-span beams always observed that the maximum moments measured at the support section were higher than those measured at the span sections. In the author's tests this was only noticed for beams B-1 to 3, and for beam B-4 higher moment was observed at the span section. Similarly, according to Cooke higher moments should have always been measured at the load section, but for beams B-1 to 3 they were measured at the support section. It appears to the author that Naughton or Cooke's findings are not applicable in general.

A comparison of the maximum moments measured at the points where crushing of concrete actually took place in the test beams and frames has been made with those evaluated according to the C.E.B. recommendations in Figure 3.2, which shows that they are in reasonable agreement. The apparent ultimate moments according to the C.E.B. recommendations have been calculated

with $f_{co} = 1.05\ c_c$, and $F_2 = 0.8$ for beams and 0.5 for frames, as assumed throughout the thesis.

The author is therefore of the opinion that failure of a beam takes place by crushing of concrete at a section somewhat displaced from the theoretical critical section and where the effect of loading plate has disappeared. The ultimate strength of this section would be equal to that evaluated according to the C.E.B. recommendations, but at this instant the moment measured at the theoretical critical section would be greater than that measured at the above section due to the gradient of the bending moment distribution. It would be appreciated that the value of the maximum moment measured at the theoretical critical section does not relate to its ultimate strength, since the failure does not usually occur there; it is only a hypothetical quantity. It would be seen from Table 3.1 that the distance between the actual crushing point and the theoretical critical section varied from 0.33 to 1.1 D, and on an average a value of 0.75 D can be assumed. For this distance being fixed, it can easily be seen that depending upon the gradient of the bending moment distribution a variety of values for the maximum moment at the theoretical critical section can be obtained. The value of the moment which Somes's postulate calculates is the above hypothetical quantity, but he evaluates it in an indirect manner by introducing the factor λ.

Figure 3.3 shows a portion of the structure between the points of zero and maximum moments. A is the point of zero moment, C the peak point of bending moment distribution and B is the point where crushing of the concrete occurs at collapse. If ADE denotes the bending moment distribution, then BD = M_{au}, i.e. the apparent ultimate moment evaluated according to the C.E.B. recommendations.

From similar triangles ABD and DEF we have

$$\frac{\delta M_{au}}{M_{au}} = \frac{a}{z - a} = \frac{a}{z}\left(1 - \frac{a}{z}\right)^{-1}$$

Expanding the R.H.S. and neglecting higher powers of $\frac{a}{z}$, we have

$$\frac{\delta M_{au}}{M_{au}} = \frac{a}{z}\left[1 + \left(\frac{a}{z}\right)\right]$$

or $$\delta M_{au} = M_{au}\left[\left(\frac{a}{z}\right) + \left(\frac{a}{z}\right)^2\right]$$

$$CE = M_{au} + \delta M_{au}$$

$$= M_{au}\left[1 + \left(\frac{a}{z}\right) + \left(\frac{a}{z}\right)^2\right] \quad \ldots\ldots (3.9)$$

The apparent moments at collapse at the various theoretical critical sections of the authors beams calculated according to the above and Somes's methods are given in Table 3.1 and have been compared with the measured values in Figure 3.4, which shows that the above postulate results in reasonable agreement.

In view of the above, the author is of the opinion that the explanation for the variation in the values of the ultimate moments of similar sections, as observed by Naughton, Cooke, Somes, and the author, lies in the fact that the moments were not measured at the points where crushing of concrete actually took place but at the theoretical critical sections.

Thus, the strength of a theoretical critical section at collapse can be calculated either by:-

1) the enhancement of the flexural strength of the actual critical section as suggested above; or

2) the artificial enhancement of the actual concrete strength to give an enhanced ultimate flexural strength to correspond to the strength of the theoretical critical section at collapse, as suggested by Somes.

There is, in addition to the phenomenon discussed above, the problem of enhanced concrete strength due to strain gradient across the cross section, which has been observed by Baker and Amarakone[47], and Sturman, Shah and Winter[16]. It would appear, however, that if the actual critical section is used as the basis for calculating the hypothetical strength of the theoretical critical section at collapse, then the effect of this parameter is small. However, before final conclusion is reached, more research would be necessary.

The concrete strain measurements could not be taken right up to the collapse load, for many of the strain gauges were damaged before the maximum load was reached. The values of concrete strain in the extreme compression fibre, and curvature were obtained from the measurement of concrete strains at three levels. For the test frames, except the centre of the transome, the gauges were fixed about $\frac{1}{4}$"-$\frac{3}{4}$" displaced from the theoretical critical sections. The values of concrete strain and curvature pertain to such points whereas the stress-resultants refer to the theoretical critical sections. This, although not accurate, was accepted since the distance was small and it would only have underestimated the curvatures and concrete strains slightly. The measured strain values used in Figure 3.5 therefore correspond to such conditions under the maximum load. But it would be seen that they vary from 0.0021 to 0.0083 as against 0.0035 recommended by the C.E.B. This shows that there is no fixed value for ultimate

concrete compressive strain. This was noticed by Mattock who suggested equation 3.8 to evaluate the ultimate concrete strain. In Figure 3.5 the measured concrete strains have been compared with those calculated according to equation 3.8. Although there is a considerable scatter, it shows a general trend of increase in the value of the ultimate concrete strain as suggested by Mattock, but the calculated values are considerably large as compared to the measured values. Mattock's equation 3.8 is based on the experimental results of reinforced concrete beams. The above disparity shows that results of reinforced concrete would not apply to prestressed concrete.

Qualitatively equation 3.8 suggests that the ultimate concrete strain should increase with the gradient of the bending moment distribution. The gradient of the bending moment distribution provides some sort of restraint and under the effect of such a restraint it would be reasonable to expect concrete to crush at an increased ultimate strain. But it appears doubtful, or at least has not been confirmed by the author's test results, that concrete in a structure at a particular critical section, irrespective of its sectional properties, would crush at the same value of the ultimate strain. The results of author's suggestion are set out in Chapter 4.

Figures 7.32 to 7.45 show that Somes's contention that when crushing occurred just away from the loading plate, the strains beneath the plate were frequently greater than the strains where crushing was taking place need not always be true.

3.5 MOMENT-CURVATURE RELATIONSHIP

The usual property which represents the characteristics of a structural material is its stress-strain relationship. Thus, provided the stress-strain relationships for concrete and prestressing steel and their relative percentages and position are known, it should

theoretically be possible to establish the moment-curvature relationship for any prestressed concrete section. This thesis is concerned with monotonically increasing loads where the effect of plasticity occuring during the previous loadings is neglected. That is, theoretically there should exist a unique moment-curvature relationship. There is relatively little experimental evidence for prestressed concrete of the moment-curvature relationship after the maximum moment of resistance is reached. But up to the maximum moment of resistance it has been obtained for both statically determinate and indeterminate structures by many investigators. The experimental moment-curvature relationship obtained for a section of a statically determinate structure rarely agrees with that obtained for a corresponding section of a statically indeterminate structure. And in the same indeterminate structure the moment-curvature relationships obtained for any two critical sections with identical sectional and material properties also seldom agree with each other. For example, Mallick and his co-workers[25,26,30], at the Indian Institute of Technology, Kharagpur, observed for two and three-span prestressed concrete beams and reinforced concrete pinned portal frames that the ultimate curvatures measured at the first hinge were considerably higher than those obtained at the second hinge. On the contrary, the author for his beam B-4 obtained an absolute ultimate curvature of 0.0026 in^{-1} for the first hinge and 0.003 in^{-1} at the second hinge, which suggests that there is no unique moment-curvature relationship for prestressed concrete and that arbitrary rules such as those suggested by Mallick do not hold good.

The sectional and material properties of many of the critical sections of the beams and frames tested by the author were the same, and theoretically each of them should have exhibited the same moment-curvature relationship; but, as will be seen from Figures 7.25 to 7.31, they differed considerably from one another.

In Figure 3.6 some of the author's extreme cases have been compared with those obtained according to the C.E.B. recommendations. It will be seen that the experimental M-ϕ relationships when compared with the C.E.B. recommendations vary widely. It is obvious that until and unless this variation can be predicted, any theoretical approach based on the moment-curvature concept for the analysis of a statically indeterminate prestressed concrete structure will bear little correlation with experimental results.

The experimental moment-curvature relationships could not be obtained by the author beyond the maximum moment of resistance, since by that time many of the strain gauges at the critical sections were damaged. In future experiments it would be desirable to incorporate some strain and curvature measuring devices which remain in tact even after the maximum moment of resistance is reached. As discussed in detail in Chapter 6, there is sufficient evidence (see Figures 7.10 to 7.18) which show that at the maximum load many of the critical sections had passed the maximum moment of resistance and were retaining moment somewhat smaller than their ultimate moment. If the moment-curvature relationship up to the maximum moment of resistance could exhibit variation as shown in Figure 3.6, then the variation expected beyond this, if not more, would at least be of the same order. Difficulties of using moment-curvature relationship with falling branch for the analysis of a statically indeterminate structure has been discussed by Rosenblueth and Cossio[48].

3.6 ANALYSIS BASED ON MOMENT-ROTATION RELATIONSHIP

Baker[20] has overcome the theoretical difficulties inherent in the use of the moment-curvature relationship by considering the deformations over a finite length. He estimates the total inelastic rotation that can be accommodated over a

'plastic hinge' length by means of a semi-empirical formula. The theoretical discontinuities at α hinge positions (α being the statical indeterminacy number) due to an arbitrary stress-resultant distribution in equilibrium with applied loads are calculated from equation 3.5. The sections between hinge positions are assumed to act elastically but the stress-resultant-section property characteristic is calculated from a non-linear stress-strain diagram for concrete and linear-stress-strain relationship for steel. Account can be taken of the inelastic rotations, other than plastic hinge rotations, which occur at critical sections. The theoretical rotations are compared with the estimated capacity of rotation, due account being taken of the sign. If the theoretical rotation is in excess of the expected capacity of any hinge, an adjustment is made to the assumed initial bending moment distribution. Macchi[22] has suggested a similar approach called the 'Method of Imposed Rotations'. Here inelastic rotations are imposed on an 'elastic structure' and the resulting bending moment distribution found. This distribution when added to the elastic distribution of bending moments constitutes the final solution.

The above methods, in effect, assume unique moment-rotation relationship, which has been found reasonably true in many of the cases. However, Mallick and Sastry[26], in December 1966, published the results of tests on twenty-seven three-span and twelve two-span prestressed concrete beams, which showed that the rotations measured at the first and the second hinge varied considerably, inspite of their similar geometric properties. Some of their results for three-span beams are summarized in Table 3.2. Although there is considerable scatter in the test results, the variation from one critical section to another in the same test is quite conspicuous and appears to result from the fact that there is no unique moment-curvature relationship.

3.7 CONCLUSIONS

(1) The flexural ultimate strengths measured at the actual points of crushing of the concrete were in reasonable agreement with those estimated according to the C.E.B. recommendations, but the corresponding curvatures, concrete compressive strains (extreme fibre), and the flexural stress-resultant deformation characteristics for sections with similar geometric properties showed a considerable divergence.

(2) It is suggested that the enhanced flexural strength at the theoretical critical sections of a prestressed concrete structure at collapse is the result of the displacement of the actual point of crushing of the concrete from the theoretical critical section, and the gradient of the apparent bending moment distribution.

Structure reference	cylinder strength, lb/in^2	overall cross sectional dimensions b x D, in.	section reference	effective depth, in.	Tension reinforcement	$\frac{d_n}{D}$	Dist. of pt. of crushing from theo. crit. section, in.	Maximum apparent moment, 10^3 lb in.					Ratio (xii)/(ix)	Ratio (xiii)/(ix)	Remarks
								Theoretical M_{au} according to			Measured at				
								C.E.B.	Somes	Author	Theo. crit. section	Pt.of crushing			
(i)	(ii)	(iii)	(iv)	(v)	(vi)	(vii)	(viii)	(ix)	(x)	(xi)	(xii)	(xiii)	(xiv)	(xv)	(xvi)
B-1	5706	4 x 6	B	4.1	3 No. 0.276 in. dia. H.T. wires	0.22	6(l)	117	130	139	140	110	1.20	0.94	
			D'	4.3		0.11	3(l)	125	132	136	119	112	0.95	0.90	Excluded for reaons given in text
			D	4.3		0.11	2(r)	125	132	136	138	133	1.10	1.05	
B-2	5980	4 x 6	B	4.3		0.21	3.5(l)	128	140	151	154	135	1.20	1.05	
			D'	4.3		0.11	2.5(l)	128	134	139	135	129	1.05	1.01	
			D	4.3		0.11	3(r)	128	134	139	143	135	1.12	1.05	
B-3	6103	4 x 6	B	4.3		0.21	4.5(r)	129	141	153	161	135	1.25	1.05	
			D'	4.3		0.11	3(l)	129	135	140	150	141	1.16	1.09	
			D	4.3		0.11	3.5(r)	129	135	140	145	136	1.12	1.05	
B-4	6023	4 x 6	B	4.3		0.06	4(l)	128	131	134	143	138	1.12	1.08	
			D	4.3		0.11	7(r)	128	134	139	150	130	1.15	1.02	
												Average	1.15	1.05	excluding D' of B-1

TEST BEAMS - MEASURED ULTIMATE MOMENTS AND THEIR COMPARISON WITH VARIOUS THEORETICAL METHODS

TABLE 3.1

ROTATIONS AT FAILURE IN MALLICK AND SASTRY'S THREE-SPAN BEAMS

Beam (cross section 4 x 6 in.)	End span, ft	Central span, ft	Cube strength, lb/in^2	Effective depth at load section, in.	Effective depth at support section, in.	Rotation, rad. x 10^3		Ratio $\frac{(vii)}{(viii)}$
						Load section, Hinge 1	Support section-Hinge 2	
(i)	(ii)	(iii)	(iv)	(v)	(vi)	(vii)	(viii)	(ix)
3A-1	9	6	6,500	4.30	4.30	56.40	38.60	1.46
3A-3	9	6	7,500	4.80	4.80	52.00	43.00	1.21
3B-2	8.5	7	5,500	3.00	3.00	42.00	25.80	1.63
3B-3	8.5	7	4,800	4.00	4.00	37.60	30.95	1.21
3C-4	8	8	5,000	4.00	4.00	46.00	28.20	1.63
3C-5	8	8	6,500	4.25	4.25	66.00	38.00	1.74
3C-6	8	8	6,500	4.00	4.00	61.00	29.40	2.08
3C-7	8	8	5,850	3.00	3.00	35.60	19.90	1.79
3D-2	7.25	9.5	7,250	4.00	4.00	73.60	32.10	2.29
3E-2	7	10	7,000	4.50	4.50	73.80	37.60	1.96
3E-3	7	10	4,900	4.00	4.00	59.80	28.40	2.11
3E-4	7	10	6,250	3.25	3.25	62.40	31.00	2.01
3E-5	7	10	6,500	4.50	4.50	72.00	34.60	2.08
3E-6	7	10	6,500	4.00	4.00	72.80	34.00	2.14
3F-3	6	12	7,000	4.50	4.50	84.40	35.00	2.41

TABLE 3.2

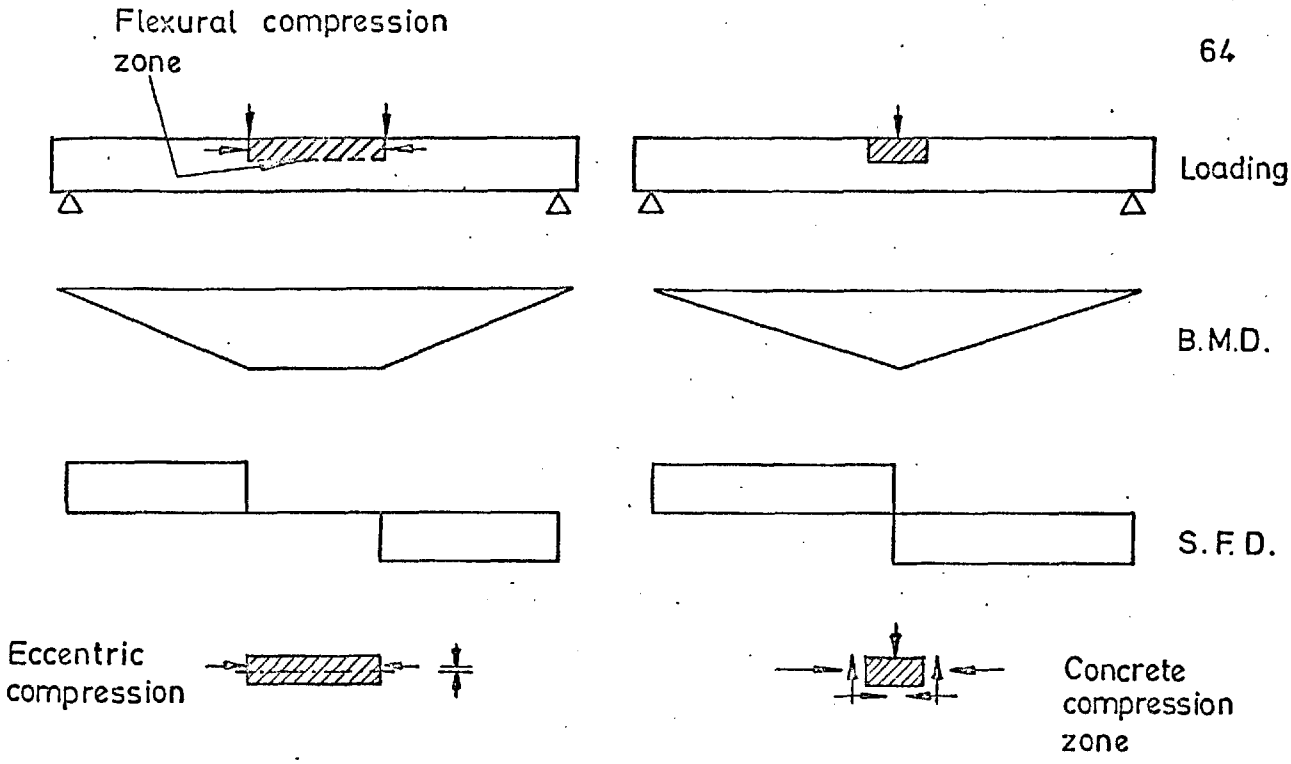

(a) PURE FLEXURE

(b) POINT LOAD IN SPAN

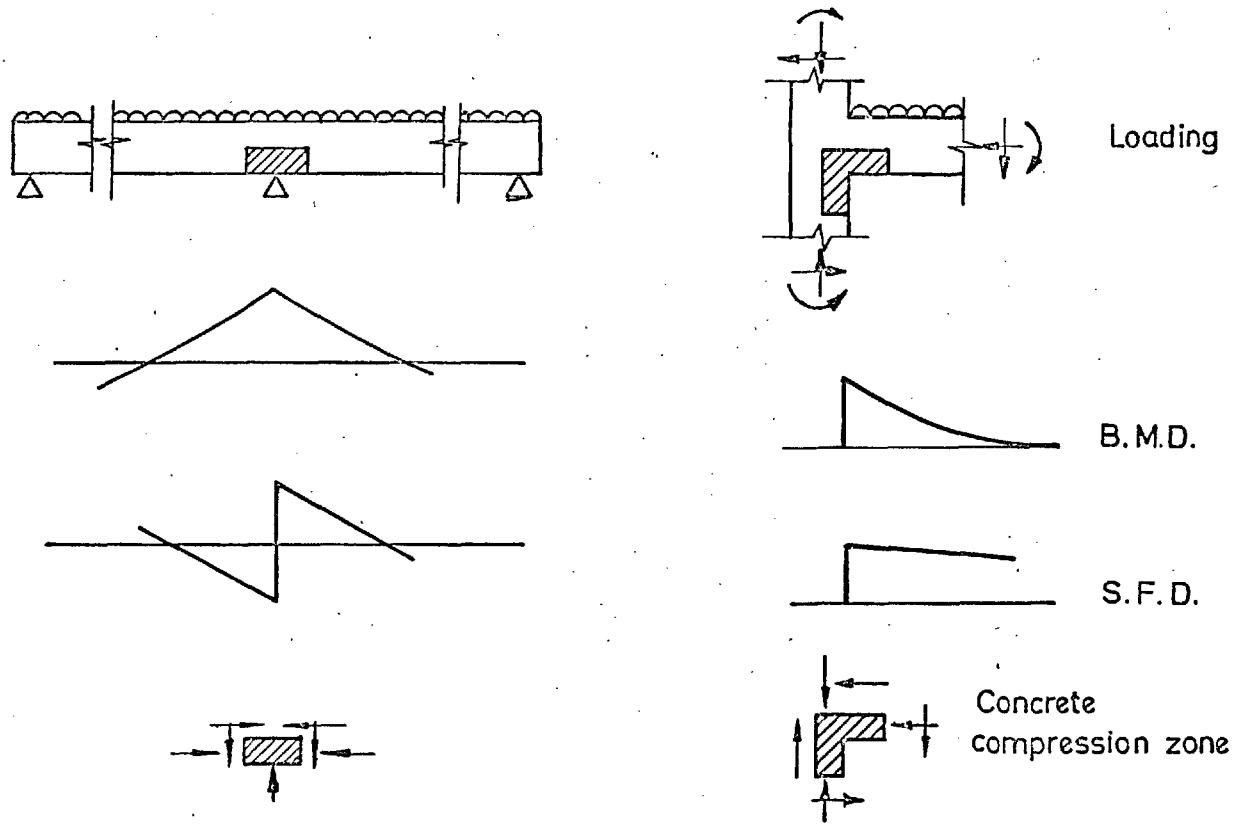

(c) SUPPORT OF CONTINUOUS BEAM

(d) BEAM-COLUMN INTERSECTION

Fig 3.1 TYPICAL STATES OF CONCRETE IN FLEXURAL COMPRESSION AS MET IN PRACTICE

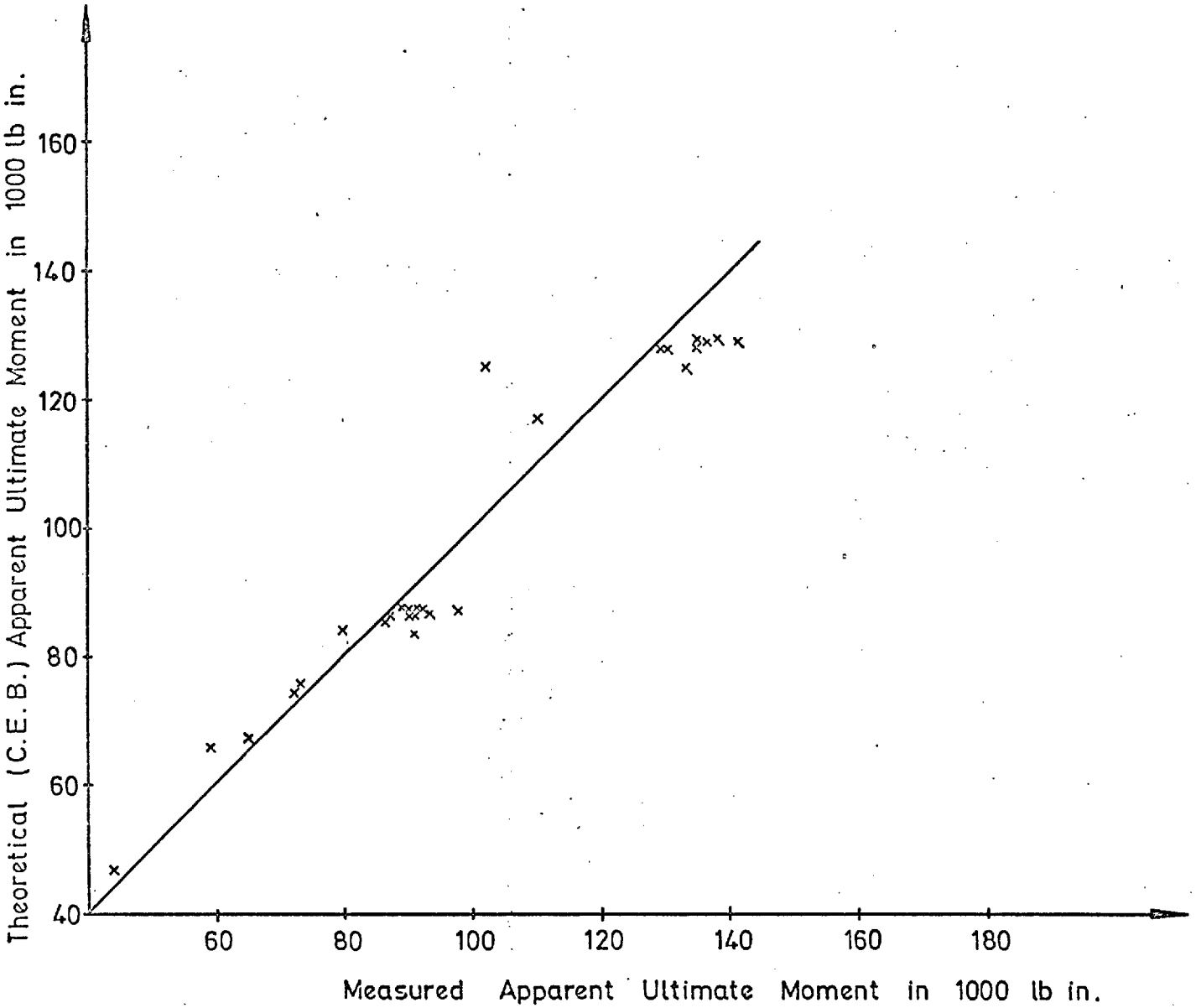

Fig 3.2 : COMPARISON OF MEASURED ULTIMATE MOMENTS WITH C.E.B. RECOMMENDATIONS

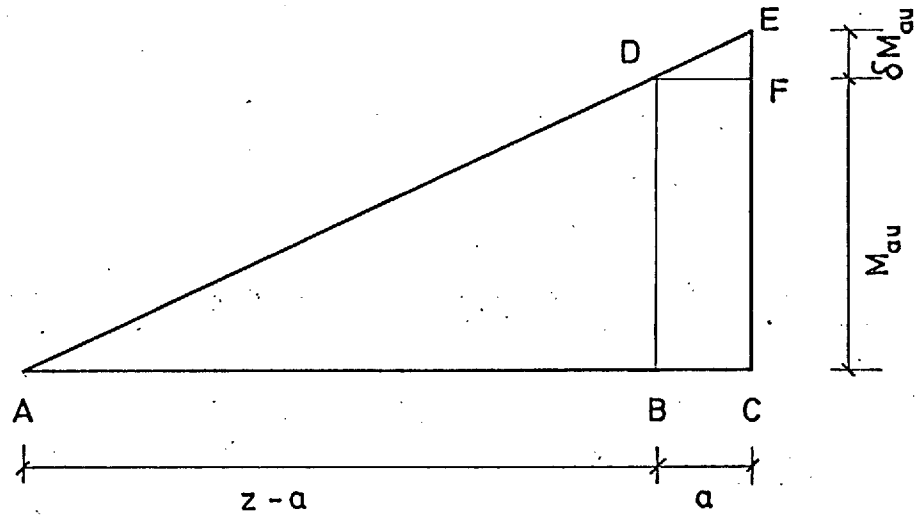

Fig. 3.3: BENDING MOMENT DISTRIBUTION BETWEEN POINTS OF ZERO AND MAXIMUM MOMENT

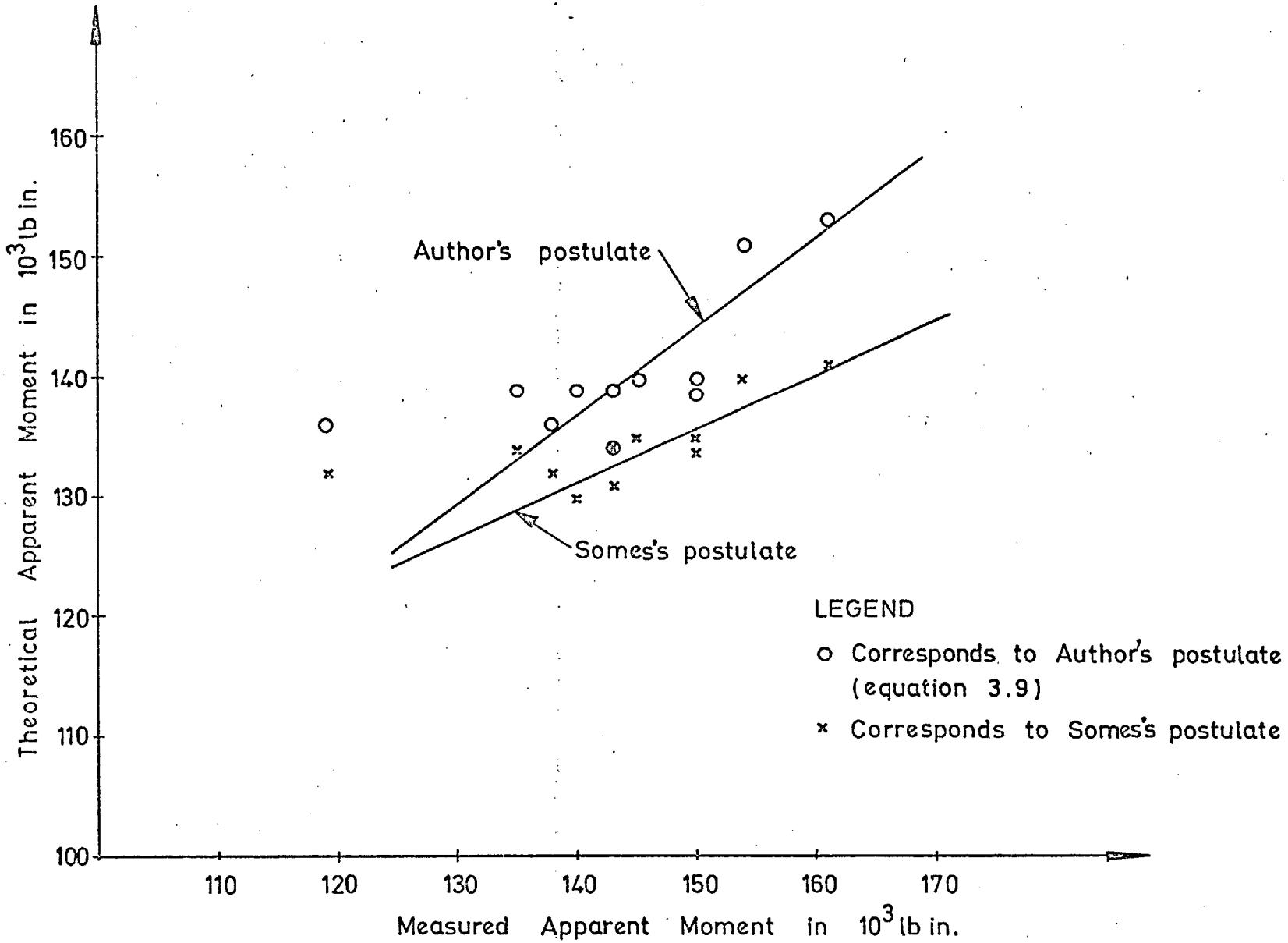

Fig. 3.4: COMPARISON OF MOMENTS AT COLLAPSE AT THEORETICAL CRITICAL SECTIONS OF AUTHOR'S BEAMS

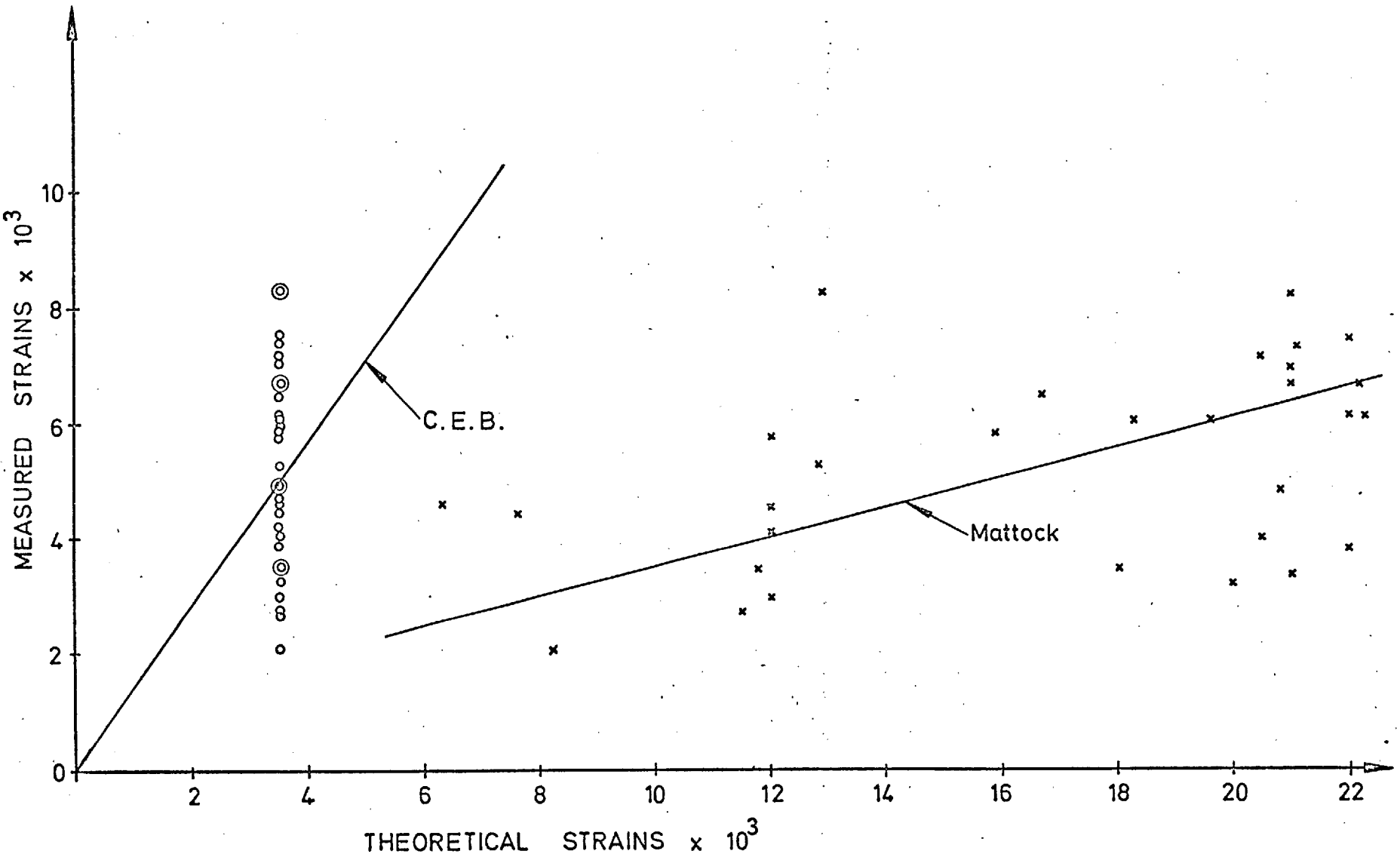

Fig. 3.5: COMPARISON OF ULTIMATE FLEXURAL COMPRESSIVE STRAINS OF CONCRETE FOR AUTHOR'S TEST SPECIMENS

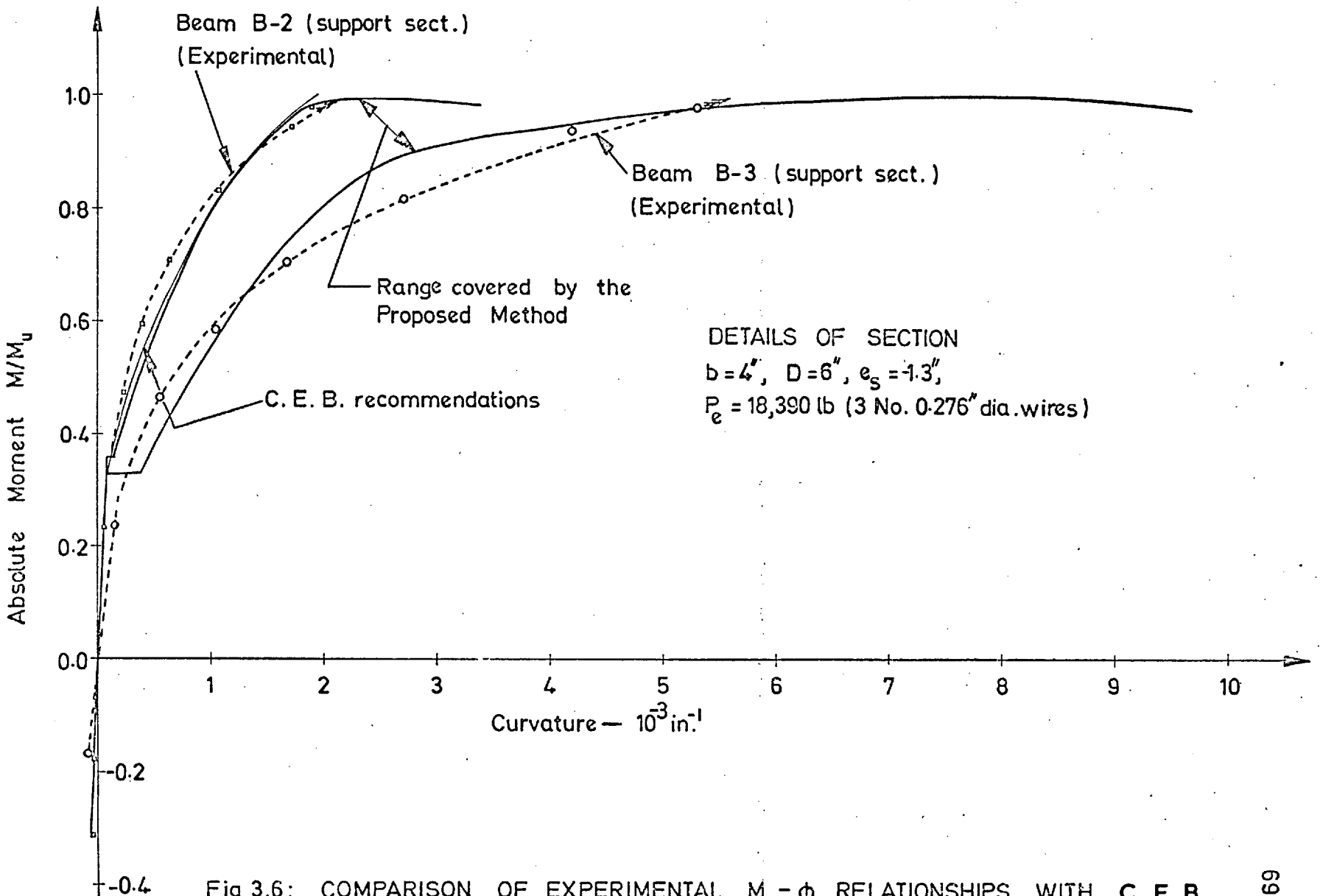

Fig 3.6: COMPARISON OF EXPERIMENTAL M – ϕ RELATIONSHIPS WITH C.E.B. RECOMMENDATIONS AND PROPOSED METHOD.

CHAPTER 4

PROPOSED METHOD FOR THE ANALYSIS OF FLEXURAL STRESS-RESULTANT-DEFORMATION CHARACTERISTIC OF PRESTRESSED CONCRETE

4.1 INTRODUCTION

The flexural stress-resultant-deformation characteristic of a section is defined by the relationship between the resisting moment and the corresponding curvature. It was seen in Chapter 3 that the measured maximum flexural strengths are in reasonable agreement with those calculated according to the C.E.B. recommendations but there is considerable divergence in the flexural stress-resultant-deformation characteristics. The flexural stress-resultant-deformation characteristic of a prestressed concrete section depends upon the characteristics of prestressing steel and concrete and the sectional properties. The sectional properties and characteristic of prestressing steel can be estimated quite accurately. The major factor which cannot be assessed accurately is the characteristic of concrete. The usual property that defines the characteristic of a structural material is its stress-strain relationship. The common stress-strain curve of concrete as recommended by the C.E.B.[29] consists of either a parabolic rectangle or a parabola which terminates at a strain of 0.0035. This limit on strain has probably been fixed under the belief that as in tension concrete in compression also behaves as a 'brittle' material incapable of shortening beyond a certain value of strain. However, in actual tests on simply supported and continuous reinforced concrete beams, maximum concrete compressive strains as large as 0.015-0.05 have been measured by various investigators[13,15,48,49]. It appears that unlike structural steel, which is a strain-hardening material, concrete is strain-softening in compression; or in other words, the

stress-stress curve of concrete in compression exhibits a distinct maximum stress after which the stress decreases with increasing strain. This property results in a considerable difficulty. When a concrete specimen is tested in a 'constant load' type of testing machine, the specimen is suddenly crushed as soon as the maximum stress is reached. This behaviour led in the past to the belief that concrete behaves as a 'brittle' material. Similarly, when simply supported concrete beams are tested by applying 'constant load', the beams are observed to fail suddenly as soon as the strain in the extreme compression fibre reaches a value somewhat greater than the strain at the maximum stress in a compression specimen.

4.2 THE CONCRETE STRESS-STRAIN CURVE IN COMPRESSION

It is now widely realized that while the internal failure mechanism of concrete may be brittle on the microscopic scale, it is not brittle on the macroscopic or structural scale. Recently, by devising stiff constant strain-rate testing machines, several investigators[14,15,50 to 53] have obtained the complete stress-strain curve of concrete for both concentrically and eccentrically loaded prisms. There is a fair agreement up to the point of maximum stress but beyond this the results differ considerably. The divergence of results is probably due to the method of testing and the characteristic of the testing machine rather than the characteristic of concrete. The author postulates that like any other structural material the shape of the concrete stress-strain curve would always be the same.

The stress-strain curve of concrete up to the point of maximum stress may be defined accurately by either of the following equations:-

$$f_c = f_{co}\left[2\left(\frac{\varepsilon_c}{\varepsilon_{co}}\right) - \left(\frac{\varepsilon_c}{\varepsilon_{co}}\right)^2\right] \quad \ldots\ldots (4.1)$$

$$f_c = \frac{2f_{co}\left(\frac{\varepsilon_c}{\varepsilon_o}\right)}{1 + \left(\frac{\varepsilon_c}{\varepsilon_{co}}\right)^2} \quad \ldots\ldots (4.2)$$

where f_c is the concrete stress corresponding to concrete strain of ε_c;

f_{co} is the maximum concrete stress; and

ε_{co} is the concrete strain corresponding to the maximum concrete stress.

The C.E.B. and many of the investigators define the concrete stress-strain curve up to the point of maximum stress by equation 4.1, and the same will be done in this thesis. For the descending portion the author considered equation 4.2, which was originally suggested by Desayi and Krishnan[54], and the following equation:

$$f_c = f_{co}\, e^{-k\left[\left(\frac{\varepsilon_c}{\varepsilon_{co}}\right) - 1\right]^{\eta}} \quad \ldots\ldots (4.3)$$

where k and η are the arbitrary constants.

In the absence of any reliable data for the descending portion of the concrete stress-strain curve, the only alternative was to evaluate k and η indirectly. The object was to obtain the correct stress-strain curve of concrete in flexural compression and the available check was that the calculated value of apparent maximum moment and the corresponding concrete strain in the extreme compression fibre and curvature reasonably agree with the corresponding measured quantities. To this end, the above quantities were studied

according to the theory presented in Section 4.4 by varying λ and η over a wide range. Some of the results are summarized and compared with the C.E.B. recommendations in Table 4.1. It will be seen from the Table that the shape of the concrete stress-strain curve does not have appreciable effect on the above quantities and there should be additional factors influencing the above quantities, which will be discussed later.

However, equation 4.3 with $\lambda = 0.14$ and $\eta = 1.5$ results in somewhat better correlation with the text results. The curve defined by the equations 4.1 and 4.3 has been compared in Figure 4.1 with that obtained by Soliman[53] for an eccentrically loaded prism, which shows good agreement. The complete stress-strain curve of concrete is, therefore, tentatively defined as

$$f_c = f_{co}\left[2\left(\frac{\varepsilon_c}{\varepsilon_{co}}\right) - \left(\frac{\varepsilon_c}{\varepsilon_{co}}\right)^2\right], \text{ for } \varepsilon_c \leqslant \varepsilon_{co}$$

and $$f_c = f_{co}\, d^{-0.14\left[\left(\frac{\varepsilon_c}{\varepsilon_{co}}\right) - 1\right]^{1.5}}, \text{ for } \varepsilon_c \geqslant \varepsilon_{co} \qquad \ldots\ (4.4)$$

Amongst the several equations, Soliman has recently defined the stress-strain curve for bound concrete in flexure by a parabola up to the point of maximum stress f_{co} and strain ε_{co} followed by a straight line at a constant stress f_{co} up to a strain of ε_{cs}, and thereafter by a sloping straight line which corresponds to a strain of ε_{cf} for a stress of $0.8 f_{co}$, where

$$\begin{aligned} f_{co} &= 0.9\, c_c(1 + 0.05q'') \\ \varepsilon_{co} &= 0.55 f_{co} \times 10^{-6} \\ \varepsilon_{cs} &= 0.0025\ (1 + q'') \\ \varepsilon_{cf} &= 0.0045\ (1 + 0.85\, q'') \end{aligned} \qquad \ldots\ (4.5)$$

q" is a factor defined by Soliman to represent the effect of binders, and for unbound concrete q" = 0. If we consider concrete with a cylinder strength of about 6000 lb/in^2, we have ε_{co} = 0.00294 which is greater than ε_{cs}. Clearly, it is not valid fo use Soliman's equation for unbound concrete with cylinder strength greater than 5000 lb/in^2.

Equation 4.4 defines the shape but to obtain the actual stress-strain curve for any concrete the values of f_{co} and ε_{co} must be defined. There is little published data on this subject. Many of the investigators take f_{co} as 0.8-1.0 times the 6 x 12 in. cylinder strength. Sturman, Shah, and Winter[16] have recently found that for the strain gradients considered the peak of the flexural curve was located at a strain about 50% larger and at a stress about 20% larger than the peak of the curve for concentric compression. The strain gradient as mentioned in Chapter 3 provides some sort of restraint and it would be reasonable to expect concrete to carry higher strains and stresses. In practice there could be many restraints other than the strain gradient such as the cable profile, the loading plate, the beam-column intersection, etc. The author is of the opinion that in practice the peak of the flexural stress-strain curve would vary much more than that observed by Sturman, Shah and Winter. This can only be confirmed by exhaustive research. Alternatively, it could be verified indirectly by studying the flexural strengths and deformations of the critical sections of beams and frames tested to destruction. The latter course has been adopted here.

There is little evidence to show appreciable variation in the peak stress. In this thesis f_{co} taken equal to 1.05 times the 6 x 12 in. cylinder strength gave consistent results throughout.

The value of ε_{co} is usually taken 0.002. The author is, however, of the opinion that it could vary considerably from 0.0015 to 0.006 depending upon the restraint present. Based on the study of the author's test results, tentative suggestions which are subject to modification in the light of further research are given in Section 4.6.

4.3 ASSUMPTIONS OF ANALYSIS

It was seen in Chapter 3 that for the critical sections of the continuous beams and frames tested by the author the maximum concrete strain corresponding to the maximum flexural strength varied from 0.0021 to 0.0083. This suggests that it is not necessary that the maximum strength of a critical section would always be reached by attaining a particular value of the maximum concrete strain, as has been assumed by most of the investigators. The author like Davies[55], and LaGrange[14] is of the opinion that the maximum flexural strength of a section would occur at different values of the maximum concrete strain, which would depend upon the material characteristics and sectional properties. The best way to obtain the maximum flexural strength and the corresponding maximum concrete strain would be to express the apparent moment of resistance near crushing in terms of the variables defining the material characteristics and sectional properties and impose a mathematical argument.

Except for the above difference, the basis followed here is the strain-compatibility approach used by other investigators. The following assumptions are made:-

1) that only the flexural deformations are significant, the effect of thrust and shear force has been neglected;

2) the material characteristics are defined by their respective stress-strain relationship; the stress-strain relationship for steel is the same as obtained in a standard tension test and that for concrete would be as suggested in the previous Section;

3) before cracking plane sections remain plane and usual assumptions of the theory of elasticity hold good;

4) after cracking the change in the strain within the compression zone varies linearly with the distance from the zero compression boundary;

5) changes in strain in the reinforcement may be derived by continuing the strain-change profile of the compression zone to the steel levels; due account being taken of bond conditions; and

6) after cracking the contribution of the concrete tensile resistance is negligible.

Assumption 2 in respect of stress-strain of concrete has been discussed in the previous Section and is reasonable in the light of present research. Assumptions 1 and 5 are easily demonstrated with calculations and the remaining ones are justified by the actual measurements on the beams.

4.4 DERIVATION OF MOMENT-CURVATURE RELATIONSHIP FOR A BONDED RECTANGULAR SECTION

The basic moment-curvature relationship for a prestressed section is shown in Figure 2.1. Before the application of any external load there is a curvature A due to prestress. Cracking can take place either in fibre 1 (point C) or fibre 2 (point C'). Over the portion CC' the relationship is linear elastic. At C or C' the section cracks and theoretically there is a discontinuity in the moment-curvature diagram. After C or C'

the relationship becomes non-linear and elastic theory no longer holds good.

Elastic phase

During this phase a prestressed concrete section is assumed to behave according to the linear elastic theory. There are two particular stages, namely the prestress stage and the cracking stage which need to be considered.

The deformations and stresses in a section subjected to flexure are shown in Figures 4.2(a) to 4.2(c).

The effect of prestress at a section off a statically indeterminate structure is to set up a moment M_p which is equal to the sum of the pure prestress moment M_p^o and the secondary prestress moment M_p^s. The section at this stage is therefore subjected to a direct force P_e and a moment $(M_p^o + M_p^s)$.

The curvature ϕ_p produced by the prestress is

$$\phi_p = \frac{M_p^o + M_p^s}{E_c I} \qquad \ldots\ (4.6)$$

where E_c is the elastic modulus of elasticity, which according to the British Standard Code of Practice 115[63] is

$$E_c = \frac{4 + c_c - 4{,}000}{2{,}000} \times 10^6 \qquad \ldots\ (4.7)$$

Stresses in fibres 1 and 2 due to prestress are

$$f_1^p = \frac{P_e}{A_c} + \frac{M_p^o + M_p^s}{Z_1} \qquad \ldots\ (4.8)$$

$$f_2^p = \frac{P_e}{A_c} + \frac{M_p^o + M_p^s}{Z_2} \qquad \ldots\ (4.9)$$

Cracking can take place in fibre 1 or 2. Before cracking commences in fibre 1, the stress in fibre 1 must be changed by an approximation to f_1^{cr} such that

$$\overline{f}_1^{cr} = c_r - f_1^p \qquad \ldots\ (4.10)$$

At this instant effective prestrain in steel will have become

$$\varepsilon_s^{cr1} = \varepsilon_s^o - \frac{\overline{f}_1^{cr}\, e_s}{E_c\, e_1} \qquad \ldots\ (4.11)$$

and the prestress force will have become

$$P_{cr1} = P_e \frac{\varepsilon_s^{cr1}}{\varepsilon_s^o} \qquad \ldots\ (4.12)$$

Similarly, when cracking commences in fibre 2

$$\overline{f}_2^{cr} = c_r - f_2^p \qquad \ldots\ (4.13)$$

$$\varepsilon_s^{cr2} = \varepsilon_s^o - \frac{\overline{f}_2^{cr}\, e_s}{E_c\, e_2} \qquad \ldots\ (4.14)$$

$$P_{cr2} = P_e \frac{\varepsilon_s^{cr2}}{\varepsilon_s^o} \qquad \ldots\ (4.15)$$

$$f_1^{cr} = c_r - \frac{\varepsilon_s^{cr1}}{\varepsilon_s^o}\left(\frac{P_e}{A_c} + \frac{M_p^o}{A_1}\right) - \frac{\overline{M}_p^s}{Z_1} \qquad \ldots\ (4.16)$$

$$f_2^{cr} = c_r - \frac{\varepsilon_s^{cr2}}{\varepsilon_s^o}\left(\frac{P_e}{A_c} + \frac{M_p^o}{Z_2}\right) - \frac{\overline{M}_p^s}{Z_2} \qquad \ldots\ (4.17)$$

where $\overline{M}_p^s$ is the modified secondary prestress moment at the section.

Hence moment $\bar{M}_{cr1}$ (measured from the state of prestress) when cracking takes place in fibre 1 is given by

$$\bar{M}_{cr1} = Z_1 \left[c_r - \frac{\varepsilon_s^{cr1}}{\varepsilon_s^o} \left(\frac{P_e}{A_c} + \frac{M_p^o}{Z_1} \right) - \frac{\bar{M}_p^s}{Z_1} \right] \quad \ldots\ (4.18)$$

In a statically determinate or a statically indeterminate structure with a concordant cable profile $\bar{M}_p^s = 0$ and $\bar{M}_{cr1} = M_{acr1}$

Absolute moment when cracking takes place in fibre 1 is therefore given by

$$M_{cr1} = \bar{M}_{cr1} + M_p^o + \bar{M}_p^s$$

$$= Z_1 \left[c_r - \frac{\varepsilon_s^{cr1}}{\varepsilon_s^o} \left(\frac{P_e}{A_c} + \frac{M_p^o}{Z_1} \right) \right] + M_p^o \quad \ldots\ (4.19)$$

Similarly,

$$M_{cr2} = Z_2 \left[c_r - \frac{\varepsilon_s^{cr2}}{\varepsilon_s^o} \left(\frac{P_e}{A_c} + \frac{M_p^o}{Z_2} \right) \right] + M_p^o \quad \ldots\ (4.20)$$

The absolute curvatures when cracking takes place are

$$\phi_{cr1} = \frac{f_1^{cr}}{E_c e_1} + \phi_p \quad \ldots\ (4.21)$$

and

$$\phi_{cr2} = \frac{f_2^{cr}}{E_c e_2} + \phi_p \quad \ldots\ (4.21)$$

Post-elastic phase

After cracking the strain and stress distributions in the section are shown in Figures 4.2(d) to 4.3(g).

Consider an instant when the concrete strain in the extreme compression fibre is ε_c.

From the compatibility of strains we have (See Figures 4.2(d) and 4.2(e)).

$$\frac{\varepsilon_c}{\varepsilon'_s} = \frac{|h|}{|d| - |h|} \qquad \ldots\ (4.22)$$

But as shown in Figure 4.2(g) we have

$$\varepsilon'_s = \frac{1}{F_2}(\varepsilon_s - \varepsilon_s^o - F_1\ \varepsilon_c^p) \qquad \ldots\ (4.23)$$

Substituting for ε'_s from equation 4.23, we have from equation 4.22

$$|h| = \frac{F_2\ \varepsilon_c\ |d|}{F_2\ \varepsilon_c + \varepsilon_s - \varepsilon_s^o - F_1\ \varepsilon_c^p} \qquad \ldots\ (4.24)$$

In Figure 4.2(f) is shown the stress-strain curve of concrete with the area under the curve up to a strain of ε_c equal to S and centroid at G. According to assumption 2 the concrete stress block in Figure 4.2(e) is similar in shape to the stress-strain curve of concrete shown in Figure 4.2(f); the average stress in Figure 4.2(e) would be same as in Figure 4.1(f) and is equal to S/ε_c.

The compressive force resisted by concrete is therefore

$$C = b\ |h|\ \frac{S}{\varepsilon_c} \qquad \ldots\ (4.25)$$

If the stress-strain curve of steel is defined by $f_s = \psi(\varepsilon_s)$, then the force resisted by steel is

$$T = A_s\ \psi(\varepsilon_s) \qquad \ldots\ (4.26)$$

From the equilibrium of forces acting on the section we have

$$A_s\ \psi(\varepsilon_s) = b\ |h|\ \frac{S}{\varepsilon_c} \qquad \ldots\ (4.27)$$

Substituting $|h|$ from equation 4.24

$$A_s \psi(\varepsilon_s) = \frac{F_2 b |d| S}{F_2 \varepsilon_c + \varepsilon_s - \varepsilon_s^o - F_1 \varepsilon_c^p} \quad \ldots\ (4.28)$$

The distance of the centroid of the concrete stress block in Figure 4.2(e) is

$$\gamma h = \frac{\bar{\varepsilon}_{c2}}{\varepsilon_c + \varepsilon_s'} d \quad \ldots\ (4.29)$$

The apparent resisting moment is therefore given by

$$M_a = \frac{F_2 b |d| S d}{F_2 \varepsilon_c + \varepsilon_s - \varepsilon_s^o - F_1 \varepsilon_c^p} \left(1 - \frac{\bar{\varepsilon}_{c2}}{\varepsilon_c + \varepsilon_s'}\right) \quad \ldots\ (4.30)$$

Substituting ε_s' from equation 4.23 we have

$$M_a = b |d| d \frac{F_2 S(F_2 \varepsilon_c + \varepsilon_s - \varepsilon_s^o - F_1 \varepsilon_c^p - F_2 \bar{\varepsilon}_{c2}}{(F_2 \varepsilon_c + \varepsilon_s - \varepsilon_s^o - F_1 \varepsilon_c^p)^2} \quad \ldots\ (4.31)$$

It would, in principle, be possible to eliminate ε_s from equations 4.28 and 4.31 and express M_a in terms of ε_c only. But, because of the stress-strain relationships of concrete and steel being non-linear, the equations 4.28 and 4.31 can only be solved by trial and error, which although cumbersome can easily be programmed for a computer. However, equations 4.28 and 4.31 in effect gives M_a and ε_s for an assumed value of ε_c.

The absolute moment and curvature may now be calculated from the following expressions, and the depth of compression zone from equation 4.24.

$$M = M_a + M^o_p \qquad \ldots\ (4.32)$$

$$\phi = \frac{\varepsilon_c + \varepsilon'_s}{d}$$

$$= \frac{F_2\varepsilon_c + \varepsilon_s - \varepsilon^o_s - F_1\varepsilon^p_c}{F_2 d} \qquad \ldots\ (4.33)$$

Cracking

When cracking first takes place, the contribution of the concrete tensile strength to the resisting moment becomes negligible and there will be discontinuity in the M-ϕ diagram. With dead load or load-maintaining loading device it would be necessary for the steel force to increase and hence the curvature increases from ϕ_{cr} to ϕ'_{cr} for M_{cr} to be maintained. At this stage the behaviour of the section is defined by equations 4.28 and 4.31 and it would be possible to get a value of ε_c which gives M_a equal to M_{acr} and hence ϕ'_{cr}.

Maximum moment of resistance

Once M_a is expressed in terms of ε_c it would, in principle, be possible to maximize M_a by varying ε_c but for reasons mentioned above it is not possible to do it analytically. It is, however, quite easy on the computer.

Several layers of steel

It has so far been assumed that the resultant of the steel forces coincides with the centroid of the steel. The assumption is reasonable if the steel is situated in layers close to one another but if the steel layers are spread all over the section the assumption is not correct. Because of the linear strain distribution across the section, the deeper layers

are stressed more and the resultant of the steel forces does not coincide with the centroid of the steel. In such a case it would be necessary to consider each layer separately.

Figure 4.3(a) shows a section with n layers of steel. The strain and stress distributions in the post-elastic stage are shown in Figure 4.3(b) and 4.3(c).

Considering layers 1 and i we have from the compatibility of strains

$$\frac{\varepsilon_c}{-\varepsilon'_{s1}} = \frac{|h|}{|h| - |d_1|} \qquad \ldots\ (4.34)$$

$$\frac{\varepsilon_c}{\varepsilon'_{si}} = \frac{|h|}{|d_i| - |h|} \qquad \ldots\ (4.35)$$

Eliminating $|h|$ from equations 4.34 and 4.35 we have

$$\varepsilon'_{si} = \frac{|d_i| - |d_1|}{|d_1|}\,\varepsilon_c + \frac{|d_i|}{|d_1|}\,\varepsilon'_{s1} \qquad \ldots\ (4.36)$$

Equations similar to 4.23 for the 1st and ith layers are

$$\varepsilon'_{s1} = \frac{1}{F_2}\,(\varepsilon_{s1} - \varepsilon^o_{s1} - F_1\,\varepsilon^p_{c1}) \qquad \ldots\ (4.37)$$

$$\varepsilon'_{si} = \frac{1}{F_2}\,(\varepsilon_{si} - \varepsilon^o_{si} - F_1\,\varepsilon^p_{ci}) \qquad \ldots\ (4.38)$$

Substituting ε'_{s1} and ε'_{si} from equations 4.37 and 4.38 we have from equation 4.36 on simplification

$$\varepsilon_{si} = F_2\left[\frac{|d_i| - |d_1|}{|d_1|}\,\varepsilon_c + \frac{|d_i|}{|d_1|}\,\frac{1}{F_2}\,(\varepsilon_{s1} - \varepsilon^o_{s1} - F_1\varepsilon^p_{c1})\right] +$$

$$\varepsilon^o_{si} + F_1\,\varepsilon^p_{ci}$$

$$= \alpha_i + \beta_i\,\varepsilon_{s1} \qquad \ldots\ (4.39)$$

where

$$\alpha_i = F_2 \frac{|d_i| - |d_1|}{|d_1|} \varepsilon_c - \frac{|d_i|}{|d_1|} (\varepsilon^o_{s1} + F_1 \varepsilon^p_{c1}) + \varepsilon^o_{si} + F_1 \varepsilon^p_{ci} \quad \ldots\ (4.40)$$

$$\beta_i = \frac{|di|}{|d_1|} \quad \ldots\ (4.41)$$

The equations 4.28 and 4.31 will therefore reduce to

$$\sum_{i=1}^{n} A_{si} \psi_i (\alpha_i + \beta_i \varepsilon_{s1}) = \frac{F_2 b |d_1| S}{F_2 \varepsilon_c + \varepsilon_{s1} - \varepsilon^o_{s1} - F_1 \varepsilon^p_{c1}} \quad \ldots\ (4.42)$$

where ψ_i is the function relating the strain ε_{si} to the steel force f_{si}

$$M_a = \sum_{i=1}^{n} \left[A_{si} \psi_i (\alpha_i + \beta_i \varepsilon_{s1}) \left(d_i - \frac{F_2 \bar{\varepsilon}_{c2} d_1}{F_2 \varepsilon_c + \varepsilon_{s1} - \varepsilon^o_{s1} - F_1 \varepsilon^p_{c1}} \right) \right] \quad \ldots\ (4.43)$$

Now in a manner similar to that mentioned above it is possible to eliminate ε_{s1} from equations 4.42 and 4.43 and express M_a in terms of ε_c.

4.5 VARIABLES AFFECTING THE MOMENT-CURVATURE RELATIONSHIP

The basic equations that govern the M-Ø relationship in the post-elastic phase are 4.28 and 4.31, and 4.42 and 4.43. They are dependent on the section properties, the bond strain compatibility factors F_1 and F_2 and the stress-strain relationships for steel and

concrete. As mentioned earlier, the section properties and stress-strain relationship of steel can be assessed quite accurately. F_1 is usually taken equal to unity, which is supported by research and is reasonable. Thus, the only factors that could lead to the variation observed in the author's test results are F_2 and the stress-strain relationship for concrete. The latter in the light of Section 4.2 would only vary by change in the co-ordinates of its apex.

Before these parameters are studied, it would be desirable to examine whether a perchance variation in the prestress or the concrete strength at the different critical sections with similar geometric properties could have resulted in the observed variation. The effects of variation in the prestress and the concrete strength by $\pm$15% have been studied in Figures 4.4 and 4.5 respectively. For reasons that will be obvious later the other parameters were fixed as $\varepsilon_{co} = 0.002$, $f_{co} = 1.05\ c_c$, and $F_2 = 0.8$ for beams and 0.5 for frames. It will be seen that the variation in concrete strength has some effect on the curvature corresponding to the ultimate moment. The variation in concrete strength also results in the variation of the maximum flexural strength. Since the measured maximum flexural strengths of the different critical sections with similar geometric properties were practically the same, the above factor cannot be taken to account for the observed variation in the moment-curvature relationships.

We are now left with F_2, and ε_{co} and f_{co} only. For the reason given above, f_{co} should have practically the same value at all the critical sections with similar geometric properties, which means that f_{co} would be related to the cylinder strength c_c by the same factor; f_{co} taken equal to $1.05\ c_c$ gave consistent results throughout. The factors that need to be considered are therefore F_2 and ε_{co}. The measured quantities available for checking are the maximum apparent moment of resistance and the corresponding curvature and concrete strain in the extreme compression

fibre. Now if the variation of F_2 and ε_{co} confirms the observed data, then the author's postulate and the theory presented in Section 4.4 would seem reasonable.

The variations of F_2 and ε_{co} have been studied in Figures 4.6 and 4.7 where the theoretical ultimate apparent moments and the corresponding curvatures and concrete strains in the extreme compression fibre have been plotted against F_2; results for $F_2 < 0.2$ were found to oscillate and have not been included. It will be seen from Figures 4.6 and 4.7 that F_2 has little effect. In the tests the value of F_2 should have lain between 0.2 to 1.0. Extensive research would be necessary to determine factor F_2 for different bond conditions. In the present investigation the diameter of the duct-tubing used in the frame members was small and bond with the grout was not expected as good as that in the beams which had a comparatively larger diameter duct-tubing. A value of F_2 equal to 0.8 for the beams and 0.5 for the frames gave consistent results throughout.

In Figures 4.6 and 4.7 the results have been calculated for $\varepsilon_{co} = 0.002$ and 0.004 only. They show a large variation in the curvatures and concrete strains and little variation in the ultimate flexural strengths. It appears to the author that the value of ε_{co} varied considerably at the different critical sections in the author's tests, which resulted in the different M-Ø relationships for identical sections. The authors extreme experimental M-Ø relationships for similar sections have been compared with the corresponding theoretical M-Ø relationships obtained by taking different values of ε_{co} in Figures 4.8 and 4.9, which show a reasonable agreement throughout and confirm that the M-Ø relationships for sections with similar geometric properties could vary by virtue of change in ε_{co}.

4.6 AUTHOR'S TEST RESULTS AND TENTATIVE SUGGESTIONS

The experimental moment-curvature relationships for the various critical sections of the authors continuous beams and frames are given in Figures 7.25 to 7.31. Working backwards the author has determined the values of ε_{co} which result in theoretical M-ϕ relationships that have a fairly reasonable agreement with the measured relationships. The results of such an analysis for the critical sections with similar geometric properties are given in Table 4.2, which along with the values of ε_{co} gives the resulting theoretical maximum moments of resistance and the corresponding curvatures and concrete strains in the extreme compression fibre. The corresponding experimental results are also given in this Table. Comparison between the flexural strengths is extremely good except for the cases where grouting was not satisfactory. The comparison between the curvatures and concrete strains is not so good, but if we take into account the fact that the curvatures and strains correspond to moments lying between 0.89-0.98 of the maximum moments, and that for many of the critical sections, as pointed out in Chapter 3, they pertain to the points displaced $\frac{1}{4}$-$\frac{3}{4}$ in. from the critical sections, and represent under-measured values, then the curvatures would also show a fairly reasonable agreement, but the concrete strains do not show such a good agreement. The explanation for this, to the author, lies in the fact that near collapse there is some redistribution in the concrete stress block, with the result the neutral axis rises and for the same curvature the concrete strain in the extreme compression fibre gets somewhat reduced. This, in other words, amounts to the fact that near collapse the strain distribution in the concrete compression zone does not remain linear, as assumed. The experimental strain distribution near failure in the compression zone was non-linear, although it could reasonably be approximated to a linear variation.

Table 4.2 has been prepared with a view to examine whether the test results could lead to any pattern which may be useful for analysing statically indeterminate structures. It was postulated that the value of ε_{co} is varied by the presence of a restraint - the more severe the restraint the higher the value of ε_{co}. The restraint in a prestressed concrete structure results from the following:-

1) The beam-column interconnection,
2) The gradient of the absolute bending moment distribution at failure,
3) The transverse gradient of the strain distribution on the section,
4) The structural configuration,
5) Truss action.

The critical sections of the test beams included in Table 4.2 had identical geometric properties. It will be seen from Table 4.2 that, except those of beam B-3, for all the critical sections of beams ε_{co} varies from 0.002 to 0.004. The value of ε_{co} for the critical sections of beam B-3 is 0.006, which is rather high as compared to those for the other similar critical sections. It is difficult to exactly find out the reason for this. However, an examination of the experimental M-ϕ diagrams for the critical sections of beam B-3 shows that the range of the initial linear portion is somewhat less compared to that for the other similar critical sections. This suggests that the prestress available at the critical sections of beam B-3 was less than that available at the other critical sections. A reduction in prestress has an effect of shifting the M-ϕ diagram towards right (see Figure 4.4). It appears to the author that the results of beam B-3 are misleading and should not be considered. From the other results it would be reasonable to assume that for the critical sections of the test beams ε_{co}, on an average, was

0.003. The restraint conditions of the various critical sections were practically similar and to have the same value for ε_{co} is reasonable.

The critical sections of the test frames included in Table 4.2 had identical geometric properties. It will be seen from the Table that for the critical sections other than C, the value of ε_{co} is 0.006 in most of the cases. The restraint conditions at these critical sections, i.e. A, D_1, D_2 and E were practically similar from test to test and it is reasonable to obtain the same value for ε_{co}. The restraint conditions at the critical section C varied from test to test, which resulted in the variation of ε_{co} for this critical section. The factors contributing towards the restraint at the critical section C were practically same except for the 'gradient of the absolute bending moment distribution at failure', which was sharp in the case of frames F-4 and 5 and shallow for F-3 by virtue of positioning of the prestressing cable (see Figure 7.5). Thus the restraint available at C in F-4 and 5 was more severe than that in F-3, and to obtain ε_{co} equal to 0.004-0.005 for F-4 and 5 and 0.0015 for F-3 seems reasonable. Similarly, the restraint conditions available at the critical sections A, D_1, D_2 and E of the test frames were more severe than those for the critical sections of the test beams, and to obtain ε_{co} equal to 0.006 for the frames and 0.003 for the beams also seems reasonable.

The author's experimental data is too meagre to make any recommendations. However, based on the author's limited experimental evidence the following tentative suggestions are made, which are subject to modification in the light of further research. Depending upon the actual restraint conditions, the following values for ε_{co} may be assumed:-

	Characteristics of restraint	Suggested ε_{co}
1.	SEVERE RESTRAINT such as those met at the beam-column intersections of frames	0.006
2.	MODERATELY SEVERE RESTRAINT such as those met at the loading plates of the continuous structures but with additional restraint due to prestressing cables	0.0045
3.	MODERATE RESTRAINT such as those met at the loading plates of the continuous structures	0.003
4.	LITTLE RESTRAINT such as those met at the loading plates of simply supported beams	0.002
5.	VERY LITTLE RESTRAINT such as those met in the region of constant moment	0.0015

4.7 CONCLUSIONS

(1) The theory presented for the analysis of flexural stress-resultant-deformation characteristic of a prestressed concrete section shows that the maximum moment of resistance of a section would not occur at any fixed value of concrete strain in the extreme compression fibre, and requires the stress-strain curve of concrete in flexural compression to be completely defined.

(2) The stress-strain curve of concrete which is tentatively suggested to be defined by equations 4.4 shows reasonable agreement with Soliman's experimental curve for an eccentrically loaded prism.

(3) The divergence in the experimental moment-curvature relationships for sections with similar geometric properties could result from the variation in the concrete strain corresponding to the maximum stress of the stress-strain curve of concrete, which depends upon the degree of restraint available at a particular critical section.

TABLE 4.1

EFFECT OF CONCRETE STRESS BLOCK ON ULTIMATE FLEXURAL STRENGTH AND CORRESPONDING DEFORMATIONS

($\varepsilon_{co} = 0.002$, $f_{co} = 1.05\ c_c$, $F_2 = 0.8$ for beams and 0.5 for frames)

Concrete stress block	Apparent ultimate moment, lb in.	corresponding curvature, in^{-1}	corresponding max. concrete strain
C.E.B. (parabolic rectangle)	127,700 (87,100)	0.0020 (0.0027)	0.0035 (0.0035)
$f_c = \dfrac{2f_{co}(\frac{\varepsilon_c}{\varepsilon_{co}})}{1 + (\frac{\varepsilon_c}{\varepsilon_{co}})^2}$	127,000 (86,200)	0.0023 (0.0031)	0.0040 (0.0041)
$f_c = f_{co}\left[2(\frac{\varepsilon_c}{\varepsilon_{co}}) - (\frac{\varepsilon_c}{\varepsilon_{co}})^2\right]$, for $\varepsilon_c \leq \varepsilon_{co}$ $f_c = f_{co}e^{-0.08\left[\frac{\varepsilon_c}{\varepsilon_{co}} - 1\right]^4}$, for $\varepsilon_c \geq \varepsilon_{co}$	129,200 (87,500)	0.0026 (0.0035)	0.0045 (0.0045)

(Continued)

Table 4.1 (Cont.)

Concrete Stress block	Apparent ultimate moment, lb in.	corresponding curvature, in^{-1}	corresponding max. concrete strain
$f_c = f_{co}\left[2\left(\frac{\varepsilon_c}{\varepsilon_{co}}\right) - \left(\frac{\varepsilon_c}{\varepsilon_{co}}\right)^2\right]$, for $\varepsilon_c \leq \varepsilon_{co}$ $f_c = f_{co}e^{-0.12\left[\frac{\varepsilon_c}{\varepsilon_{co}} - 1\right]^3}$, for $\varepsilon_c \geq \varepsilon_{co}$	128,600 (87,100)	0.0023 (0.0035)	0.0041 (0.0045)
$f_c = f_{co}\left[2\left(\frac{\varepsilon_c}{\varepsilon_{co}}\right) - \left(\frac{\varepsilon_c}{\varepsilon_{co}}\right)^2\right]$, for $\varepsilon_c \leq \varepsilon_{co}$ $f_c = f_{co}e^{-0.16\left[\frac{\varepsilon_c}{\varepsilon_{co}} - 1\right]^2}$, for $\varepsilon_c \geq \varepsilon_{co}$	127,800 (86,700)	0.0023 (0.0034)	0.0041 (0.0045)
$f_c = f_{co}\left[2\left(\frac{\varepsilon_c}{\varepsilon_{co}}\right) - \left(\frac{\varepsilon_c}{\varepsilon_{co}}\right)^2\right]$, for $\varepsilon_c \leq \varepsilon_{co}$ $f_c = f_{co}e^{-0.14\left[\frac{\varepsilon_c}{\varepsilon_{co}} - 1\right]^{1.5}}$ for $\varepsilon_c \geq \varepsilon_{co}$	127,900 (86,900)	0.0026 (0.0039)	0.0046 (0.0052)

Figures without brackets refer to the beam section, i.e. 4 x 6 in. concrete section with 3 No. 0.276 in. dia. prestressing wires at 4.3 in. effective depth; and those with brackets refer to the frame section, i.e. $3\frac{1}{2}$ x 6 in. concrete section with 2 No. 0.276 in. dia. prestressing wires at 4.1 in. effective depth.

TABLE 4.2

COMPARISON OF EXPERIMENTAL AND THEORETICAL (PROPOSED METHOD) ULTIMATE FLEXURAL STRENGTHS AND CORRESPONDING CURVATURES AND CONCRETE STRAINS IN EXTREME COMPRESSION FIBRE

		Theoretical			Experimental				
Struct	Critical section	ε_{co}	M_{au} lb in.	ϕ at M_{au} in^{-1}	ε_c at M_{au}	M_{au} lb in.	Max. ϕ in^{-1}	Max. ε_c	Characteristics of restraint	Remarks
B-1	D'	0.002	128,000	.0026	.0046	112,000	.0017	.003	moderate	grouting not satisfactory
B-2	D'	0.0015)avg.	126,000	.0022	.004	129,000	.0046	.0046	"	
	D	0.004) .0027	134,000	.0054	0.01	135,000	-	-	"	
	B	0.002	128,000	.0026	.0046	135,000	.0019	.0033	"	
B-3	D	0.006	139,000	.0078	.016	136,000	.0044	.0058	"	
	B	0.006	139,000	.0078	.016	135,000	.0053	.007	"	
B-4	D	0.004	134,000	.0054	0.01	130,000	.003	.0042	"	
	B	0.003	131,000	.0039	.007	138,000	.0026	.0045	"	
F-2	A	0.006	95,000	.0118	.018	87,000	.0071	.0083	Severe	
	D_1 & D_2 avg.	0.006	95,000	.0118	.018	86,000	.0069	.0074	"	
	E	0.006	95,000	.0118	.018	90,500	.005	.0075	"	
F-3	A	0.006	95,000	.0118	.018	90,500	.007	.0059	"	
	C	0.0015	86,000	.0028	.0036	85,000	.0013	.0021	Very little	
	D_2	0.006	95,000	.0118	.018	79,500	.0067	.0062	Severe	grouting not satisfactory
	E	0.006	95,000	.0118	.018	92,000	.007	.0074	"	
F-4	A	0.006	95,000	.0118	.018	90,000	.008	.0061	"	
	C	0.004	91,000	.0079	.011	89,500	.0049	.0047	moderately severe	
	D_1	0.006	95,000	.0118	.018	92,500	.0084	.0072	Severe	
	D_2	0.005	93,000	.010	.015	92,000	.006	.0041	"	
	E	0.006	95,000	.0118	.018	91,000	.0062	.0060	"	
F-5	A	0.004	91,000	.0079	.011	90,500	.003	.0035	"	
	C	0.005	93,000	.010	.015	93,000	.004	.0039	moderately severe	
	D_2	0.006	95,000	.0118	.018	85,000	.0049	.0049	Severe	grouting not satisfactory
	E	0.006	95,000	.0118	.018	97,500	.0056	.0067	"	

Note The experimental curvatures and concrete strains in the extreme compression fibre are under-measured values since they correspond to moments lying between 0.88-0.98 of the maximum moments and were measured in many of the cases at points displaced $\frac{1}{4}$-$\frac{3}{4}$ in. from the critical sections.

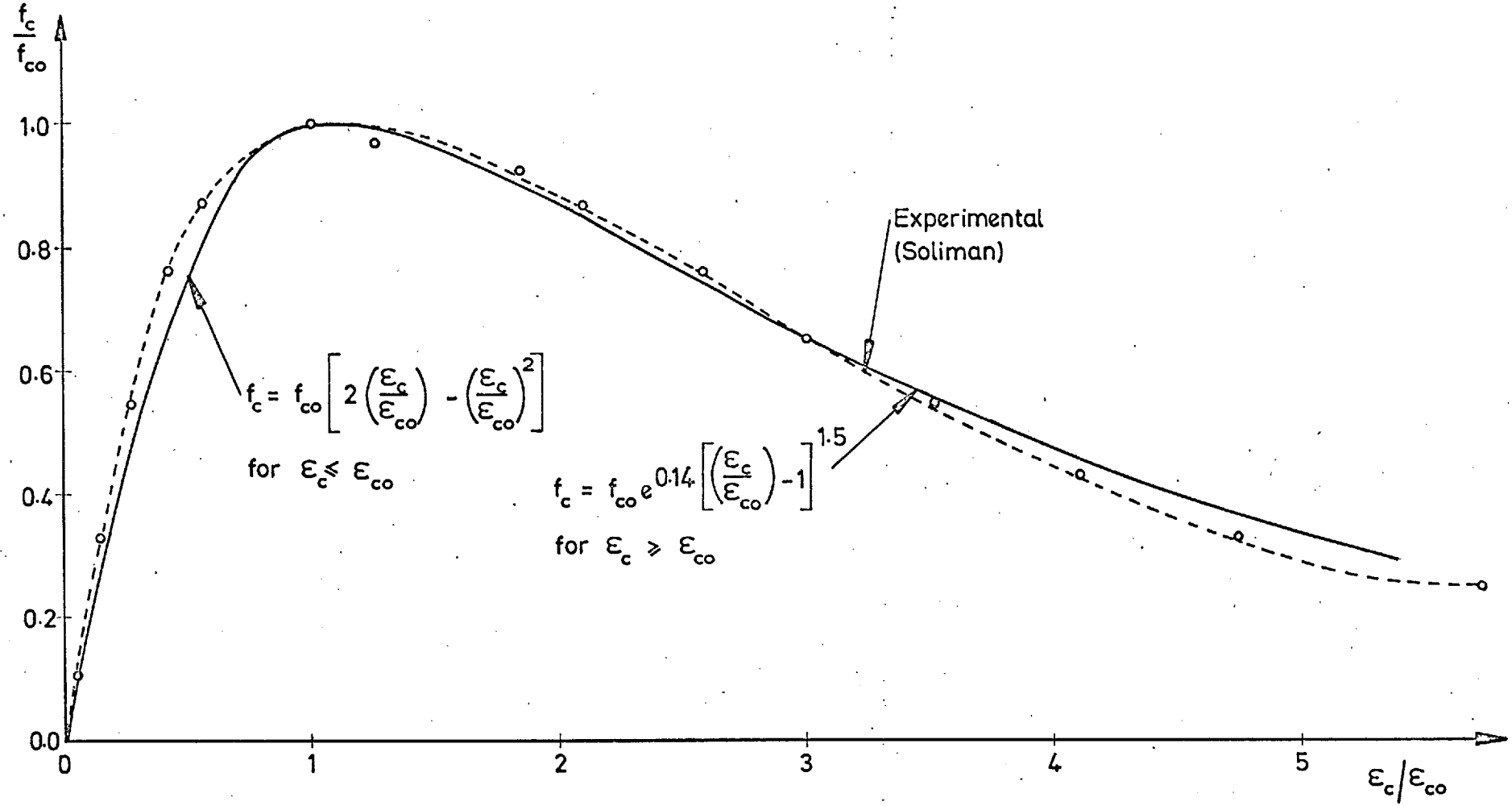

Fig 4.1: PROPOSED STRESS - STRAIN CURVE OF CONCRETE

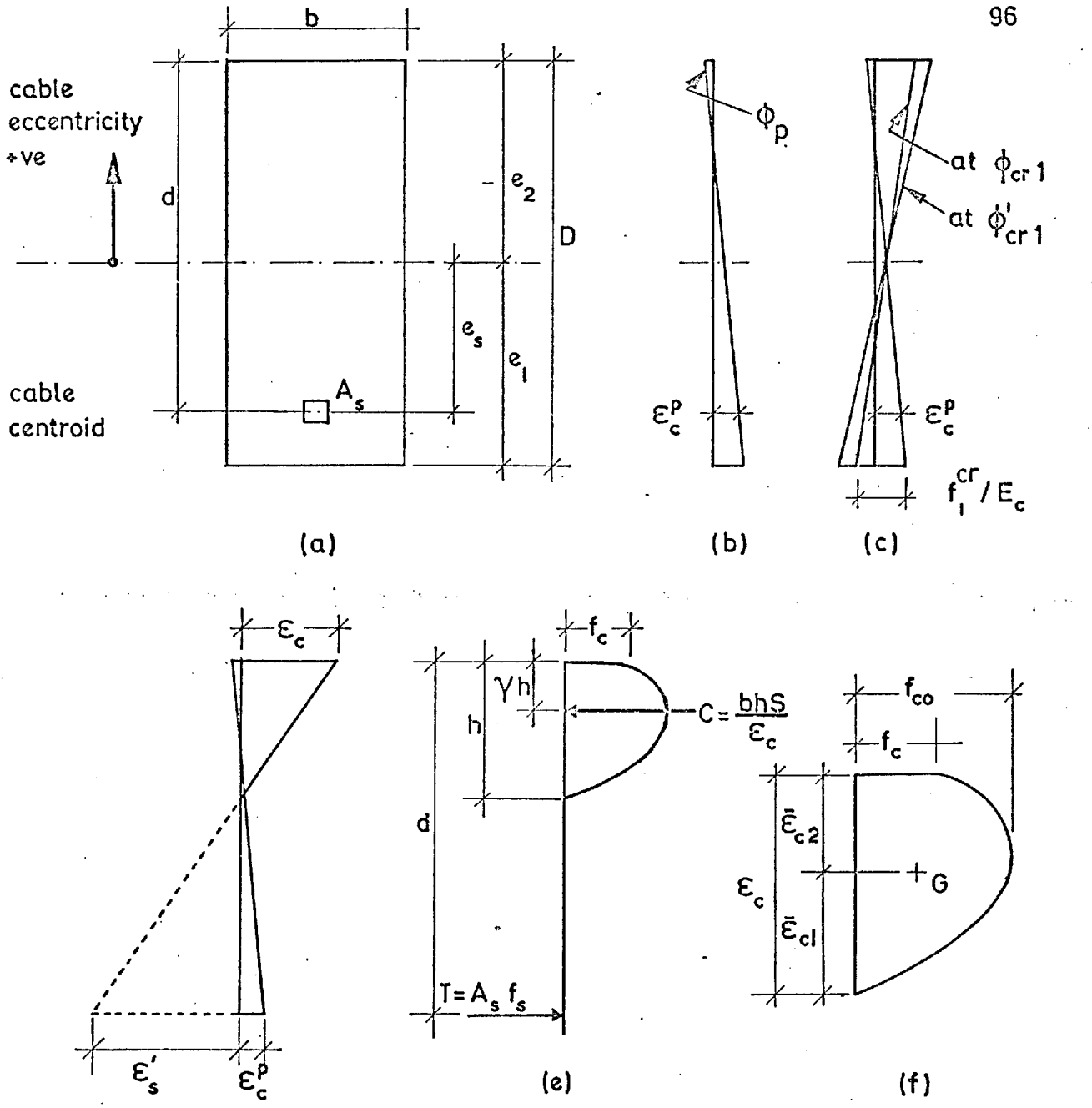

Fig. 4.2: Deformation and stresses in a section subject to flexure

(a) Section details
(b) Strain distribution at prestress
(c) Strain distribution at cracking
(d) Strain distribution after cracking
(e) Stress distribution after cracking
(f) Stress-strain diagram of concrete
(g) Strain in steel

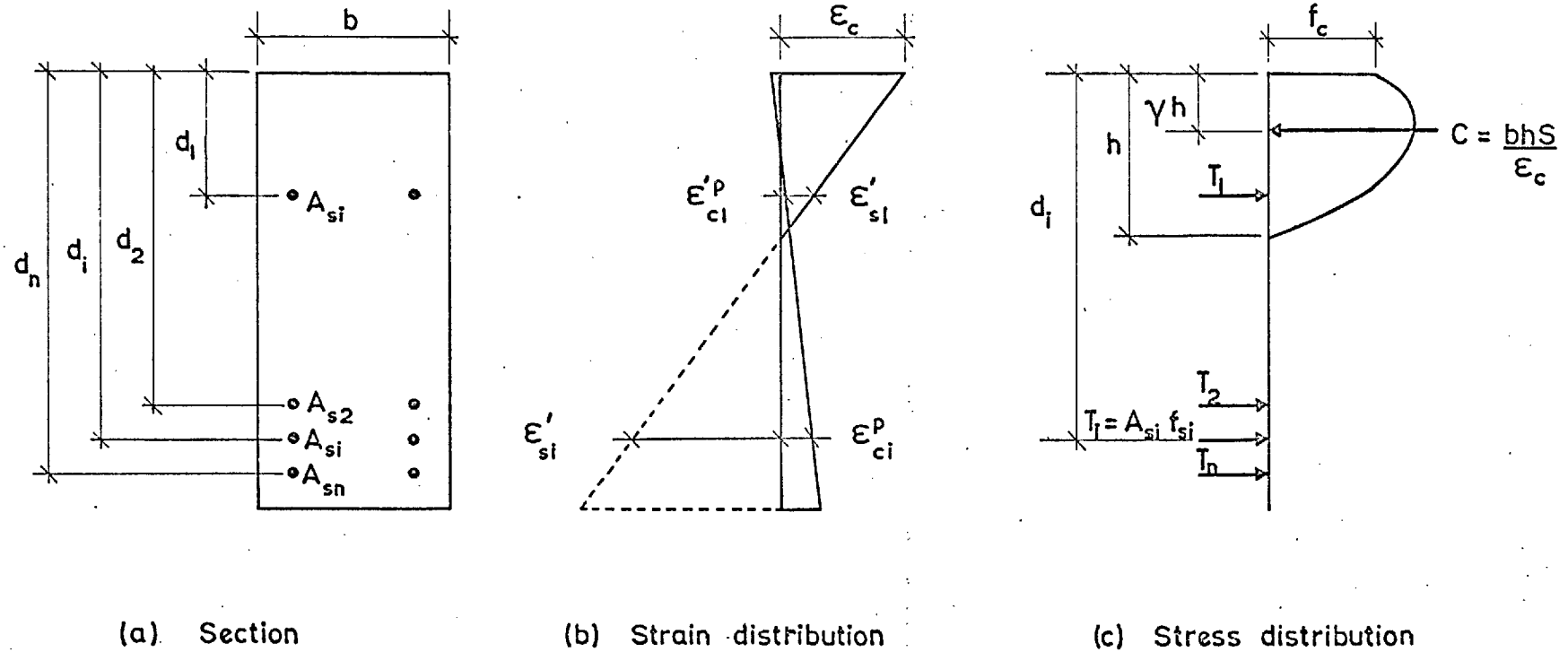

(a) Section (b) Strain distribution (c) Stress distribution

Fig. 4.3: Strain and Stress distributions in a prestressed section with several layers of steel in the post-elastic phase

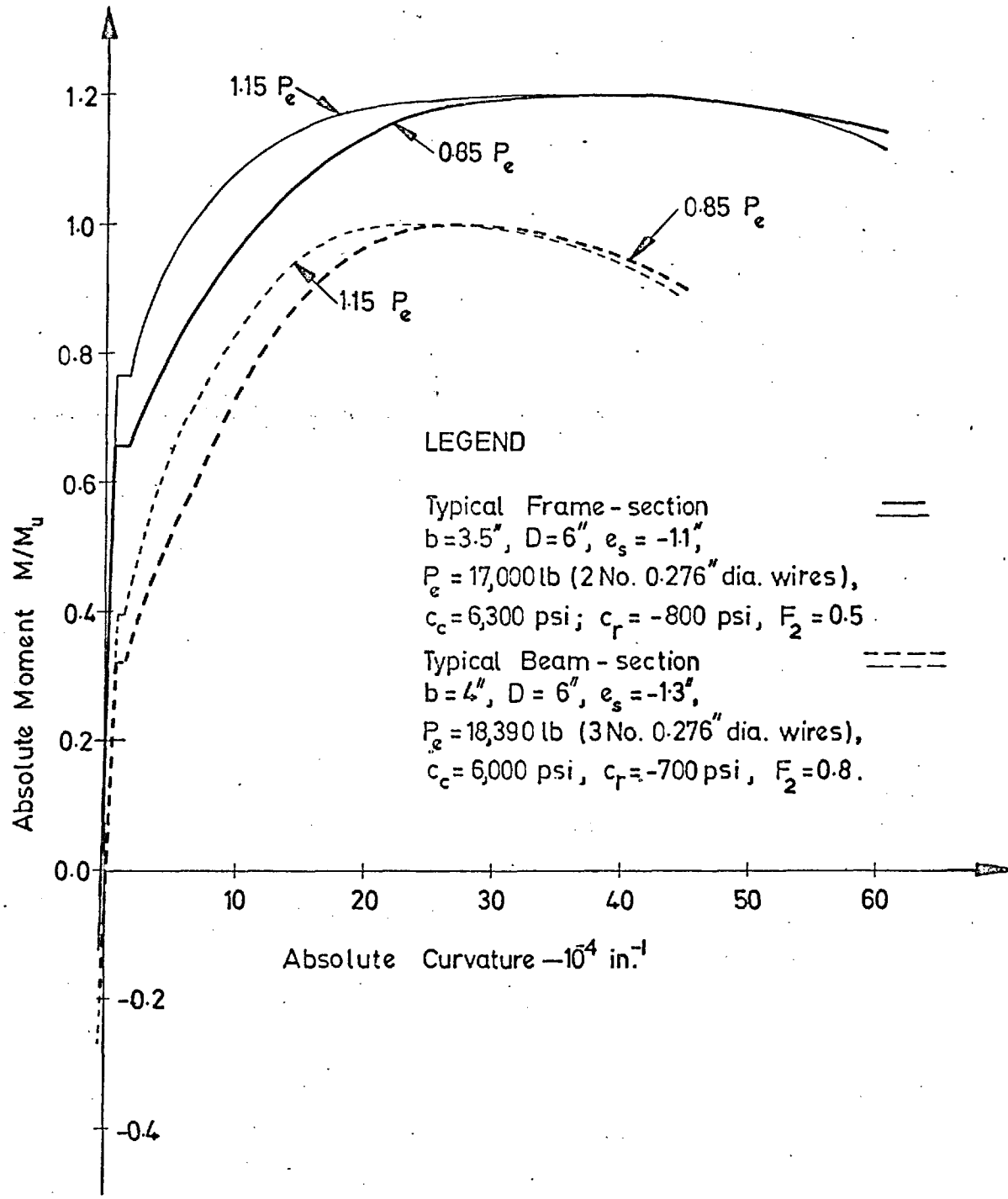

Fig. 4.4: EFFECT OF VARIATION OF PRESTRSS ON MOMENT - CURVATUR RELATIONSHIP (ε_c = 0.002, f_{co} = 1.05 c_c)

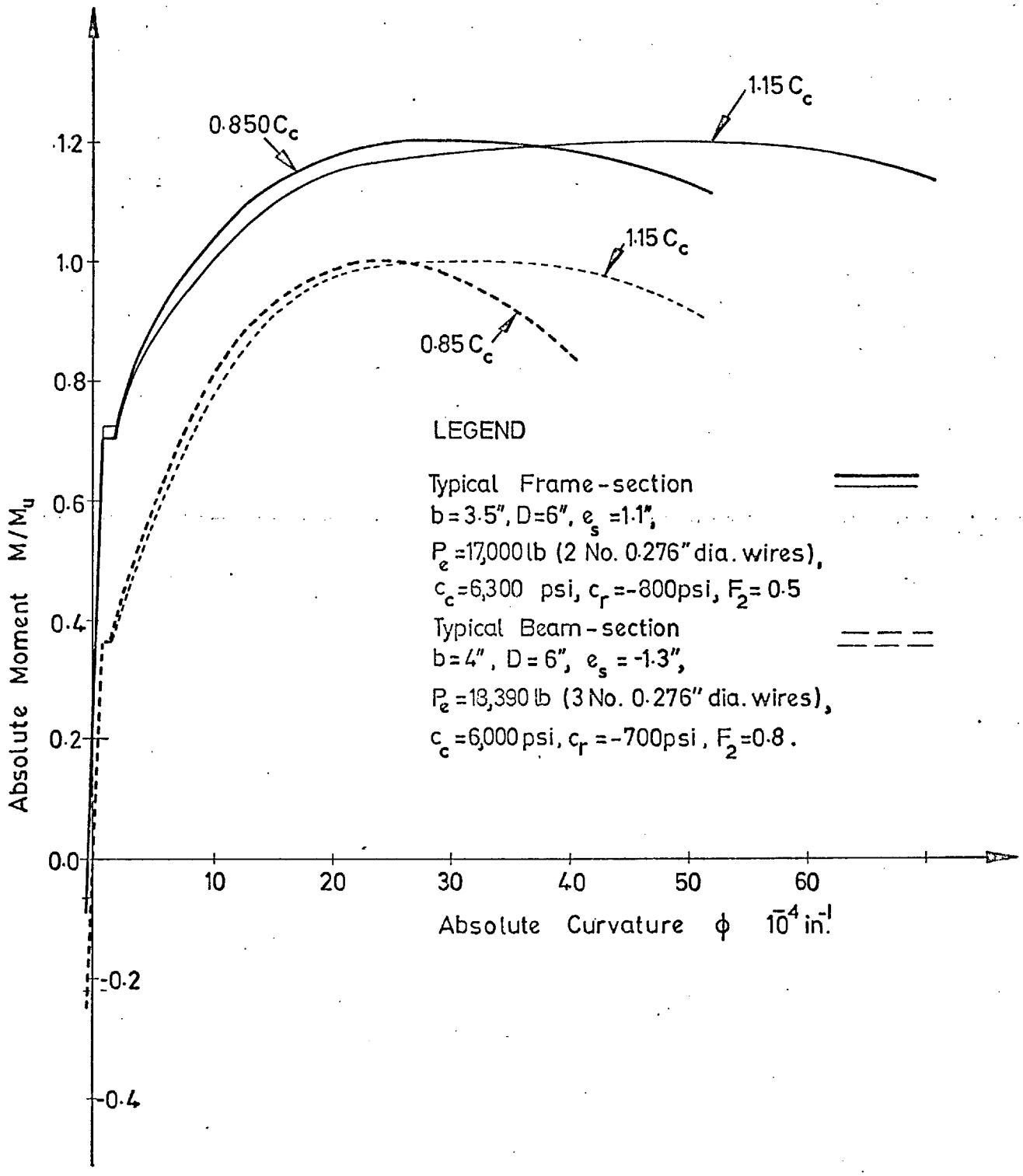

Fig. 4·5 : EFFECT OF VARIATION OF CONCRETE STRENGTH ON MOMENT - CURVATURE RELATIONSHIP

(ε_{co} = 0·002, f_{co} = 1·05 c_c)

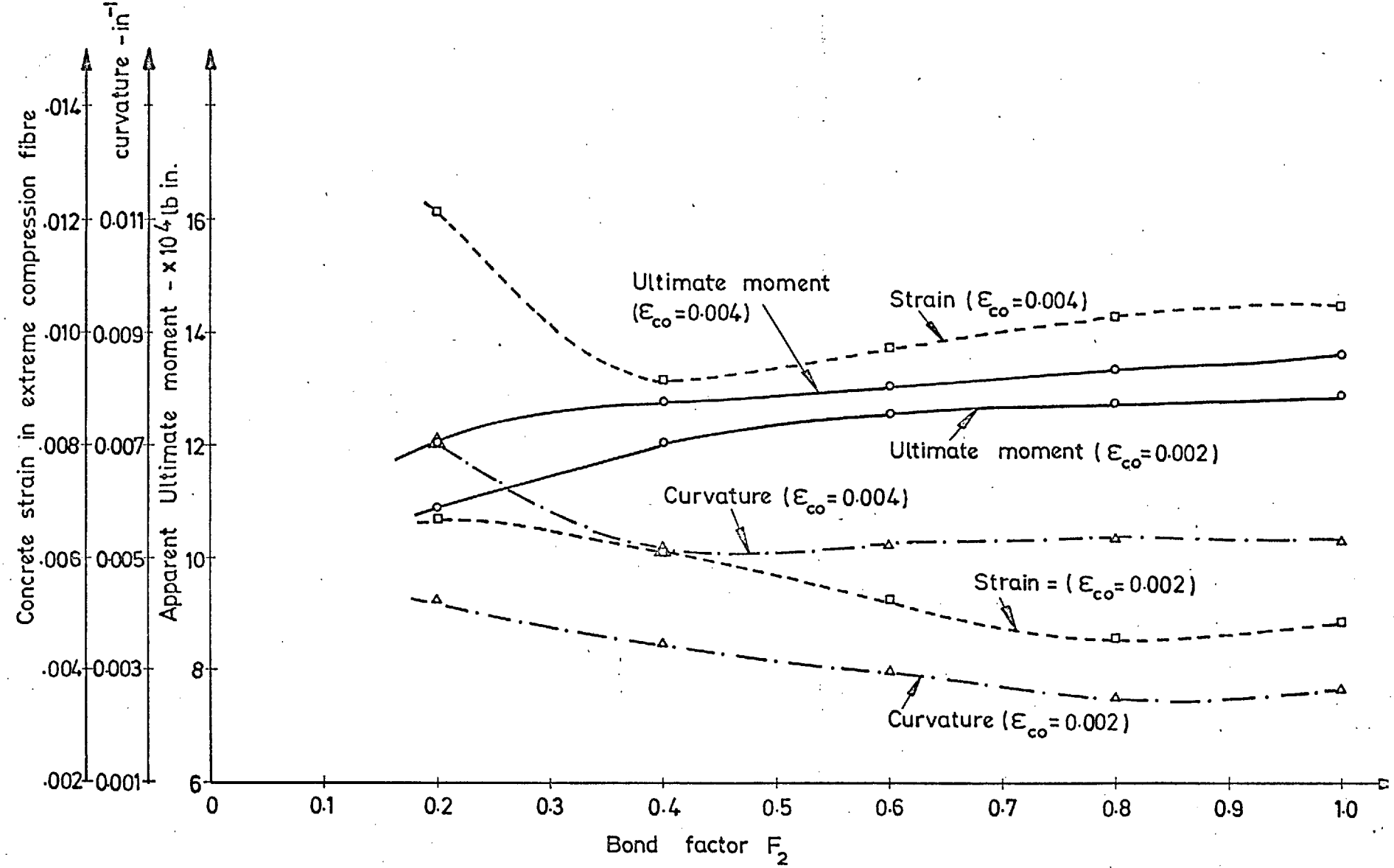

Fig. 4·6: EFFECT OF BOND FACTOR F_2 ON ULTIMATE FLEXURAL STRENGTH AND CORRESPONDING DEFORMATIONS FOR A TYPICAL BEAM - SECTION ($b = 4''$, $D = 6''$, $e_s = -1{\cdot}3''$, $P_e = 18{,}390$ lb (3 No. 0·276" dia wires) $c_c = 6{,}000$ psi, $c_t = -700$ psi)

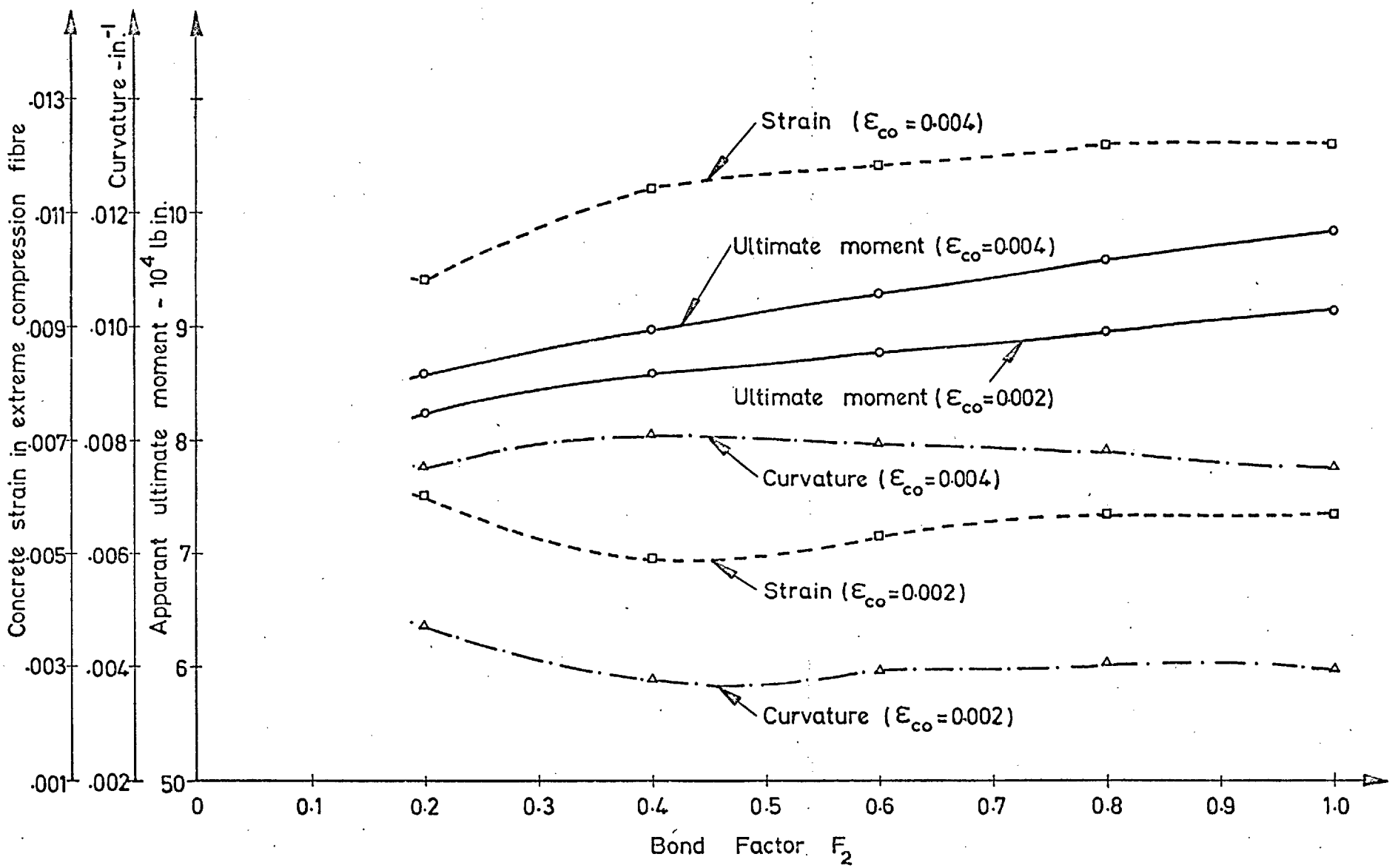

Fig. 4·7: EFFECT OF BOND FACTOR F_2 ON ULTIMATE FLEXURAL STRENGTH AND CORRESPONDING DEFORMATIONS FOR A TYPICAL FRAME-SECTION (b=3·5", D=6", e_s =-1·1", P_e =17,000 lb (2 No. 0·276" dia. wires), c_c = 6,300 psi, c_r = - 800 psi.)

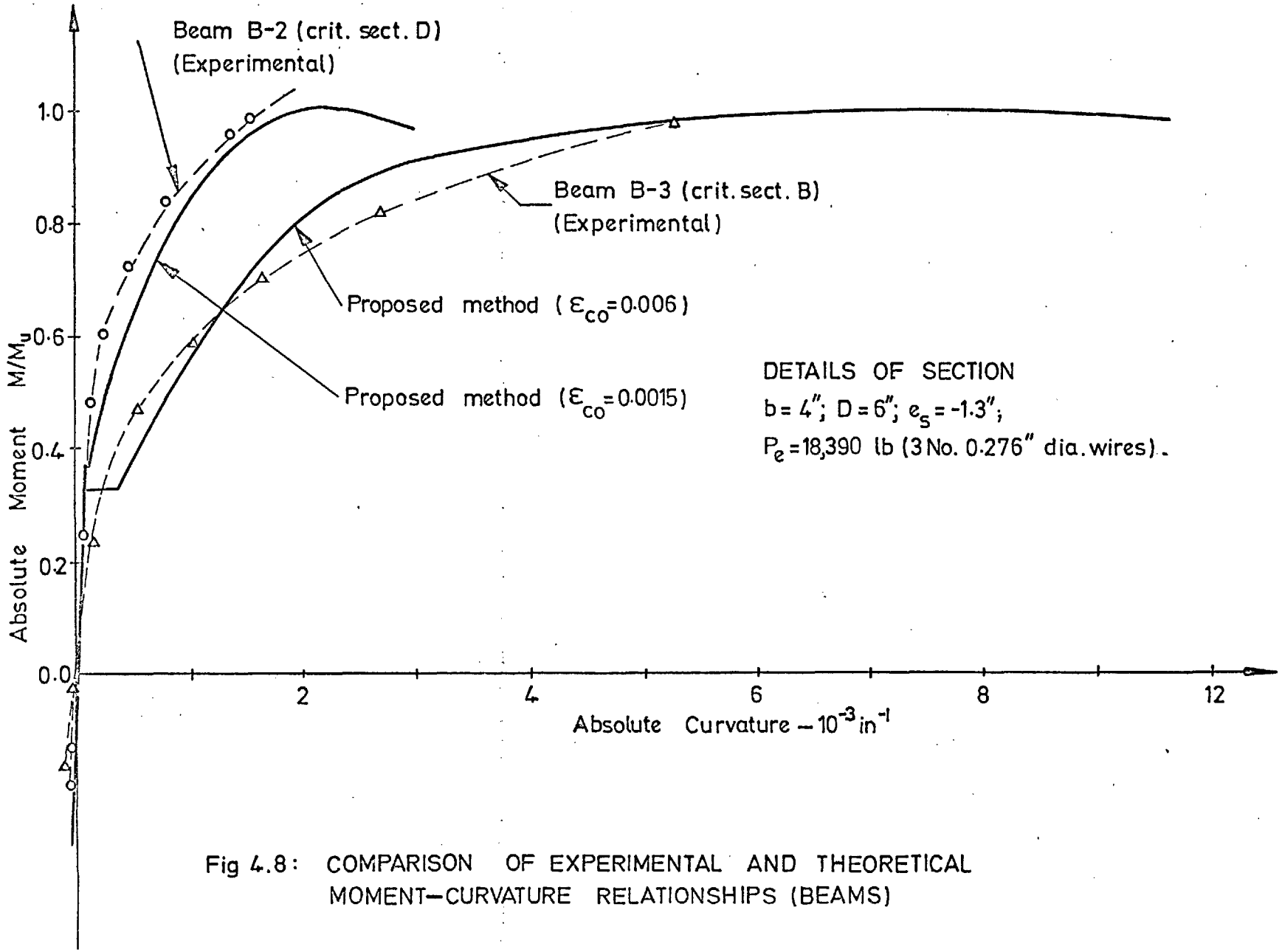

Fig 4.8: COMPARISON OF EXPERIMENTAL AND THEORETICAL MOMENT–CURVATURE RELATIONSHIPS (BEAMS)

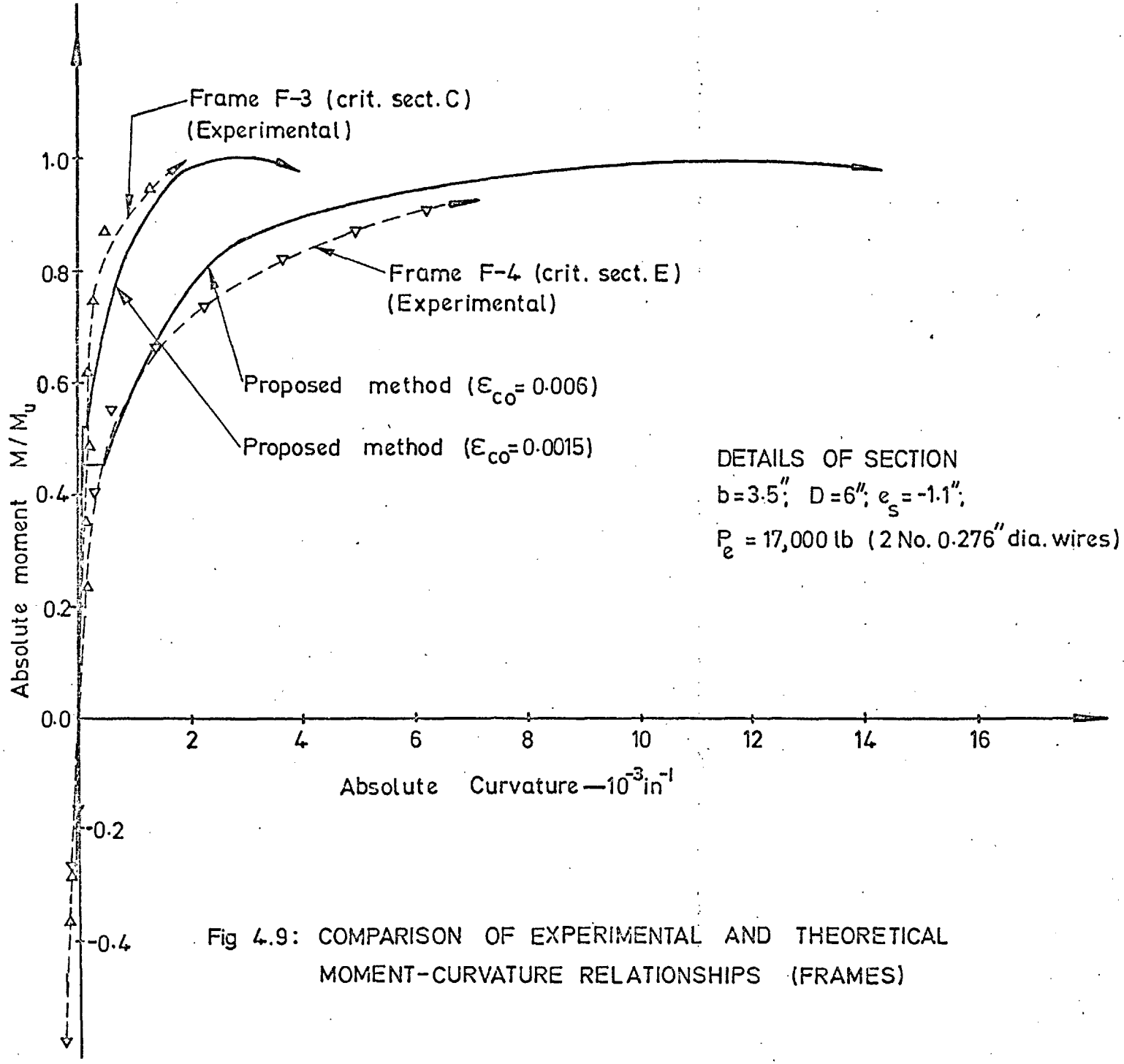

Fig 4.9: COMPARISON OF EXPERIMENTAL AND THEORETICAL MOMENT-CURVATURE RELATIONSHIPS (FRAMES)

CHAPTER 5

REDISTRIBUTION IN STATICALLY INDETERMINATE PRESTRESSED CONCRETE STRUCTURES

5.1 OBJECT AND SCOPE

The up to date research in statically indeterminate prestressed concrete structures subject to monotonically increasing load, that is all loads are increased in proportion from zero load to the ultimate load, consists of a large number of tests on different types of structures ranging from two-span beams to fixed portal frames. The results of such tests show that, in general, full redistribution does not take place in prestressed concrete structures. The object of this Chapter is to establish why, in general, full redistribution does not occur in statically indeterminate prestressed concrete structures. One explanation of this phenomenon could be the 'limited rotational capacity of concrete hinge' but, for many of the tests experimental results do not agree with those predicted by an analysis based on this concept.

The author here examines if the moment-curvature relationship with a drooping characteristic, as set out in Chapter 4, can explain all the test results satisfactorily without imposing restriction on rotational capacity of a concrete hinge. The difficulty in verifying this approach for two and three-span beams lies in the fact that in the majority of the cases moment-curvature or load-moment curves have not been obtained well past the maximum load. It has therefore been done here in an indirect manner. First it is postulated that prestressed concrete structures behave according to the moment-curvature relationship with a falling branch. It is then shown that in such a case a statically indeterminate structure would carry ultimate load with 'over-redistribution' and rarely with

'full-redistribution'; and mathematical conditions necessary for 'over-redistribution' are set up for various conditions of failure. If the conditions typical of the various tests reasonably agree with these theoretical conditions, then it would mean that the postulate is reasonable.

To this end, it is necessary that conditions typical of the various tests on two and three-span beams are first established, which is done in Sections 5.2 tnd 5.3.

5.2 TESTS ON TWO-SPAN BEAMS

Early tests on two-span prestressed concrete beams were carried out by Guyon[21], Morice and Lewis[36], Bennett[24], etc., who observed practically full redistribution in almost all cases.

LaGrange[14], in June 1961, published the results of an exhaustive series of tests on prestressed concrete beams and frames. All his beams and frames had either concordant or linearly transformed cable profiles. All his two-span beams had each span equal to 7 ft 6 in. and were loaded at mid-spans. Beams 139 and 146 were loaded in both spans and had a concrete section of $2\frac{1}{2}$ x 4 in. with 2 No. 0.2 in. diameter prestressing wires; beams 159, 164, 165, 182, 196 and 167 were loaded in one span only and had a concrete section of 3 x 7 in. and 4 wires of 0.2 in. diameter. Redistribution was complete in beams 139 and 146; beam 139 failed by the formation of all the three hinges simultaneously and beam 146 by the formation of first hinge at the support. The remaining beams failed without full redistribution and had the first hinge in the span.

Except beam 167, LaGrange's beams with concordant cable profiles had the disadvantage that the cable profiles were obtained by making the eccentricities at the critical sections proportional to elastic moments due to loads. Thus LaGrange's tests, to some

extent, can be criticized for not being carried out under severe conditions for redistribution. However, beam 167 had a straight cable profile along the centroidal axis and factor for scope for redistribution Sc was 2.37. This beam failed in a manner similar to other beams loaded in one span.

LaGrange, however, noted that whether full redistribution took place or not, the maximum loads carried by beams with linearly transformed cables were practically the same as that carried by the parent beam with the concordant cable profile.

Mallick[25], in November 1962, published the results of tests on twenty-one two-span prestressed concrete beams tested at the Indian Institute of Technology, Kharagpur. Three of the beams failed prematurely and, since no ultimate moments were reached, they were not included in the final analysis. Four of the beams were of T-section (three inverted T) and the remainder were of rectangular cross section. Except beams P11, 13 and 17 which were loaded in one span only, all beams were loaded symmetrically by single concentrated load in each span. Each span was 7 ft 6 in. and the position of the load from the central support varied from 0.27 to 0.73 of the span, giving a large variation in Sc. Redistribution is reported to be complete in all beams except P3 and P6 where, it should be noted, the first hinge was formed in the span. In beams P3 and P6 loads were applied at 0.73 of the span from the central support and Sc was 1.9 for P3 and 1.17 for P6. Beams T2 to 4, in which the effective depth was 2.5 in. at the central support and 4.5 in. under the load points, need a special mention. Sc varied from 2.40 to 3.36 and still full redistribution took place.

Beams T2 and 3 had nearly the same cube strength and were identical in all respects except that T3 has $\frac{1}{4}$ in. diameter mild-steel stirrups at 3.5 in. pitch and T2 had no shear reinforcement. The ultimate loads carried by them were 8,900 and 8,200 lb respectively. The increase in load was due to the slight increase in the ultimate

strength of the load section of beam T2. This shows the order of accuracy one should expect in practice for concrete structures.

Naughton[41], in November 1963, published the results of four prestressed concrete beams continuous over two spans each of 10 ft. Each beam had a constant rectangular cross section of 4 x 6 in. and was loaded symmetrically about the central support. Beams E1 and E3 were loaded at 6 ft 3 in. and beams E2 and E4 at 7 ft 6 in. from the end supports. Each beam was prestressed with 3 wires of 0.276 in. diameter and had a $\frac{1}{4}$ in. diameter mild steel bar in each corner. The effective depth of the prestressing wires at all the critical sections in all beams was kept equal to 4 in. The only parameter varied was the cable profile in between the critical sections, which was curved over the central support in between the load points in all beams but was straight in the remaining length for beams E3 and E4 and curved for beams E1 and E2 Each beam was tested as a concordant beam, and concordancy was obtained by adjusting the relative heights of the supports. The value of Sc for beams E1 and E3 was 1.65 and that for E2 and E4 was 2.54. Naughton's tests were thus carried out under quite severe conditions and still they showed full redistribution. All beams, except E3 which failed prematurely by rupture at load point due to the breaking of the weld in the untensioned steel, failed by the formation of the first hinge at the support.

Naughton also observed that the variation of cable profile in between the critical sections did not appreciably affect the crack pattern or the general behaviour of the beams.

Raina[37], in March 1966, published the results of six prestressed concrete beams which were continuous over two equal spans each 9 ft and loaded at the centre of each span. Each beam

had a cross section of 4 x 6 in. and was prestressed with 3 No. 0.276 in. diameter wires. Beams CB-1 and 6 had the same concordant cable profile and were similar except that CB-6 had some untensioned longitudinal steel. Beams CB-2 to 5 had linearly transformed cable profiles obtained from CB-1. Full redistribution was obtained in beams CB-1 to 4 and 6, but beam CB-5 carried an ultimate load of 6,500 lb only as against 7,440, 7,540, 7,790 and 7,620 lb carried by beams CB-1 to 4 respectively. Beam CB-5 failed by the formation of the first hinge at the support section. The moment measured at the mid-span at failure was 154,800 lb in. as against its calculated apparent ultimate moment of 181,400 lb in.

In the author's two-span beams, which are described in Chapter 7, full redistribution was obtained in all cases except beam B-1 which failed by the rupture of the span section for reasons mentioned in Chapter 7 and will be excluded here. Beams B-2 to 4 had similar geometric properties at all the critical sections; the only parameter varied was the cable profile in between the critical sections. Beams B-2 and 4 failed by the formation of both the support and span hinges simultaneously, and beam B-3 had the first hinge at the support.

From the above it is clear that, in general, full redistribution in two-span beams does not occur and whether full redistribution would occur or not is not governed by Sc or the relative rotations at the various critical sections, as also pointed out by many others[14,36]. Excluding Raina's beam CB-5, there seems to be only one difference to the author between the tests in which redistribution was complete and those where it was not, namely the difference in the place of the first hinge. In Mallick's beams P3 and 6 and LaGrange's beams 159, 164, 165, 182, 196 and 167 in which full redistribution did not take place first hinge was formed in the span.

5.3 TESTS ON THREE-SPAN BEAMS

The early tests on three span prestressed concrete beams were carried out by Macchi[22], who did not observe full redistribution. These tests, however, had the disadvantage that the evaluation of the ultimate flexural strengths of the critical sections was made by using control tests and not from the measurement of the redundant reactions. Another series of early tests on three-span beams was carried out by LaGrange[14] who observed practically full redistribution.

The exhaustive series of tests on three-span prestressed concrete beams consist of sixteen tests by Cooke[11] at the University of Leeds and twenty-seven tests by Mallick and Sastry[26] at the Indian Institute of Technology, Kharagpur. These tests were carried out under symmetrical conditions of load and span and covered several outer and inner span lengths with one or two concentrated loads in the inner span, or a concentrated load in each outer span. The overall cross section of all beams was 4 x 6 in; the other parameters varied were the cable profile and the effective depths at the critical sections. Full redistribution has not been reported in Cooke's tests, except beam 15 in which two concentrated loads at 17 in. on either side of the centre of the inner span were applied and the first hinge was formed at the supports. In the remaining beams, where only a single concentrated load at the centre of the inner span was applied and the first hinge was formed in the span, full redistribution was not observed; when ultimate load was reached, the moment measured at the support section varied from 0.86 to 0.96 of the ultimate flexural strength, which was actually measured by continuing the tests beyond the ultimate load.

On the other hand, in the majority of Mallick and Sastry's tests practically full redistribution has been reported. In these

tests, whether full redistribution was complete or not was assessed by comparing the measured ultimate load, and moments at the critical sections with the corresponding calculated quantities. The measured ultimate load, expressed as the ratio of the calculated ultimate load varied from 0.87 to 1.04 and the apparent moment measured at the second hinge at ultimate load, expressed as the ratio of the calculated apparent ultimate moment varied from 0.86 to 1.00. If due consideration is made to the order of accuracy of such calculations, the above variation is practically of the same order as observed by Cooke. Cooke's conclusion is based on the measured ultimate flexural strengths and is more refined but, as pointed out in Chapter 3, Cooke's measured moments had the inconsistency that they were not measured from the same datum. To the author, the difference in the two conclusions is merely of interpretation and both series of tests do show that, in general, full redistribution does not take place in three-span prestressed concrete beams. It would be noted that wherever full redistribution did not take place, the first hinge was formed in the span.

5.4 FULL-REDISTRIBUTION, OVER-REDISTRIBUTION AND UNDER-REDISTRIBUTION

Term 'full redistribution' has so far been used in the sense normally implied in structural steel work, that is if the ultimate load of a statically indeterminate structure is equal to the plastic load, then the structure is said to have exhibited 'full redistribution'. On the other hand, if the ultimate load of a statically indeterminate structure is less than the plastic load, the structure is said to have not exhibited 'full redistribution'. In these definitions nothing is specified about the actual moments at the various critical sections at collapse. Since the moment-curvature relationship for mild steel has a long plateau at the maximum moment of resistance (the effect of strain hardening is usually ignored), it

is implied that the moments at the critical sections at ultimate load would either correspond to the flat plateau or the rising portion. In the light of theoretical moment-curvature relationship of Chapter 4 and the experimental load-moment or load-deflection curves, it would be appropriate to assume that the moment-curvature relationship for prestressed concrete has a drooping characteristic after the maximum moment is reached. In such a case the situation would be different. In the case of 'full redistribution' being not complete, it is not necessary that the moments at some of the critical sections correspond to the peak point and those at the remaining ones to the rising portion of the moment-curvature diagram. 'Full redistribution' in a prestressed concrete structure would only occur if at collapse the moments at the critical sections which form the collapse mechanism are at the peak of their respective moment-curvature diagrams. In practice it would be quite rare, unless specially aimed at, and, in general, some of the critical sections which form the apparent collapse mechanism are beyond the peak i.e. on the drooping portion of their respective moment-curvature diagrams whilst the others are either at the peak or on the rising portion of their respective moment-curvature diagrams. In the light of the meaning assigned to 'full-redistribution', this state can be described as 'over-redistribution'. The state when some of the critical sections which form the apparent collapse mechanism are at the peak of their respective moment-curvature diagrams whilst the others are still on the rising portion would be called as 'under-redistribution'. Obviously the state of under-redistribution cannot take place in a statically indeterminate prestressed concrete structure. However, if the slope of the drooping portion of the moment-curvature diagram for most of the critical sections which form the apparent collapse mechanism is shallow and the collapse takes place when the moment at any of the critical sections of the apparent collapse mechanism is still on the steep rising portion, then 'over-redistribution' can be

mistaken for 'under-redistribution'. Similarly, if failure takes place when the moments at some of the critical sections of the apparent collapse mechanism are on the shallow drooping portion, and the moments at the remaining critical sections of the apparent collapse mechanism are on the shallow rising portion of their respective moment-curvature diagrams, then 'over-redistribution' can be mistaken for 'full-redistribution'. In order to determine whether 'full-redistribution' or 'over-redistribution' takes place in a test, the moment-curvature relationships for the critical sections which form the apparent collapse mechanism should be obtained right up to the maximum load. As pointed out in Chapter 3, it is not possible to do so through the usual methods of measuring local curvatures. The alternative is to obtain load-moment curves for all the critical sections well past the maximum load, but such relationships have been published for a few investigations only. In the absence of such data there is no confirmatory basis. If the slope of the drooping portion of the moment-curvature relationship for the earlier hinges is shallow over a long length, then it is very likely that the effect of over-redistribution remains unnoticed and it is mistaken as full-redistribution. In such a case, sometimes, even from the load-moment curves, it is not possible to detect the effect of 'over-redistribution', since it may be of the same order as the order of accuracy of experimental work.

According to the above, the cases of incomplete redistribution so far described are the cases of 'over-redistribution' in which the moments at some of the critical sections of the apparent collapse mechanism were either on the steep rising portion or on the steep drooping portion of the respective moment-curvature diagrams.

The phenomenon of 'over-redistribution' was first observed by LaGrange[14], but at present, to the author's knowledge,

there is no satisfactory method of analysis which considers this phenomenon. The author has here presented a theory which takes into consideration this phenomenon to describe the behaviour of a statically indeterminate prestressed concrete structure. This has been illustrated by applying to two and three-span beams, since the author wanted to interpret the test result of such structures only. The same can, however, be applied to other structures as a part of an extensive thesis on the subject.

5.5 ASSUMPTIONS IN THE PROPOSED ANALYSIS

(1) The 'Compatibility criterion' in a statically indeterminate structure at any stage is governed by the curvature distribution along the structure for the corresponding load stage. In the light of the theoretical moment-curvature (M-Ø) relationship set out in Chapter 4, and the experimental load-moment and load-deflection curves, it would be appropriate to assume that the moment-curvature relationship for a prestressed concrete section has a drooping characteristic. Thus, for a statically indeterminate prestressed concrete structure at an instant when some of the critical sections have reached their maximum moments of resistance, for any further increase of load some of the critical sections will be on the drooping portion and the others on the rising portion of their respective moment-curvature diagrams. There is little experimental evidence showing the distribution of curvature along the structure when a critical section is on the drooping portion of the M-Ø diagram. In the light of experimental evidence shown by Edwards[34] for simply supported reinforced concrete beams, it would be reasonable to assume that when the moment at a critical section corresponds to the drooping position of the M-Ø diagram, then the moments at all the sections between the adjoining points of contraflexure will be decreasing but with increased curvatures over the cracked length. It will be further assumed that corresponding to such small

increase in curvature (which is accompanied by decrease in moment) at a critical section, increase in curvature at any section in the adjacent cracked length is linear, and the changes in elastic curvatures over the uncracked length are neglected. Similarly, for the critical sections where the moment will be increasing, it is assumed that corresponding to a small increase in curvature at a critical section, the increase in curvature at any section in the adjacent cracked length is linear, and that changes in elastic curvatures over the uncracked length are neglected.

(2) After the instant when some of the critical sections have reached their maximum moments, changes in curvatures at the critical sections other than those forming the apparent collapse mechanism are assumed small as compared to those at the critical sections forming the apparent collapse mechanism and are neglected.

(3) The moment-curvature relationship for a critical section is assumed continuous on either side of the peak moment, which is reasonable in the light of Chapter 4.

5.6 PROPOSED THEORY FOR THE ANALYSIS OF STATICALLY INDETERMINATE STRUCTURES WITH DROOPING MOMENT-CURVATURE CHARACTERISTIC

Consider an α times statically indeterminate planar structure subjected to planar proportional loading and where only the flexural deformations are significant. Up to the instant when one or some of the critical sections have just reached their maximum moments of resistance and the others are still on the rising portion of their moment-curvature diagrams, its behaviour can be established by any well known method by satisfying both 'compatibility' and 'equilibrium' requirements. If the various

loads acting on the structure can be expressed as ratios of load W, then at any stage subsequent to the above for an increase of load δW moments at some of the critical sections will be increasing, whereas at the others they will be decreasing such that

$$\delta W = \sum_{1}^{\alpha+1} k_i \, \delta M_i \qquad \ldots\ldots (5.1)$$

where k_i's are the $(\alpha + 1)$ constants defining the equilibrium; and δM_i is the change in moment at the critical section i due to load δW.

During the application of load δW, curvatures at critical sections which are undergoing increasing moment or decreasing moment corresponding to the falling branch of the M - Ø diagram will be increasing.

If $\delta \emptyset_i$ is the change in curvature at the critical section i due to the application of load δW, then

$$\delta M_i = \left(\frac{dM}{d\emptyset}\right)^{i}_{M_i = \overline{M}_i} \delta \emptyset_i \qquad \ldots\ldots (5.2)$$

where superscript i after the round brackets denotes the critical section i; and

$\overline{M}_i$ is the absolute bending moment at the critical section i just before the application of load δW.

Substituting equation 5.2 in equation 5.1, we have

$$\delta W = \sum_{1}^{\alpha+1} k_i \left(\frac{dM}{d\emptyset}\right)^{i}_{M_i = \overline{M}_i} \delta \emptyset_i \qquad \ldots\ldots (5.3)$$

For 'compatibility' requirements to be satisfied

$$\int_S \underline{m}^T \, \delta \underline{\emptyset} \, ds = 0 \qquad \ldots\ldots (5.4)$$

where $\underline{m}$ is the functional matrix in positional co-ordinates s and corresponds to 1 x α bending moment distributions due to unit bi-action applied in turn at each release of the reduced structure; and

$\delta\underline{\emptyset}$ is the functional matrix in positional co-ordinates s and corresponds to change in curvature distribution over the structure due to load δW.

In the light of assumption (2) made under Section 5.5, $\delta\underline{\emptyset}$ can be expressed in terms of $\delta\underline{\emptyset}_i (i = 1 .. \alpha+ 1)$. Thus equation 5.4 represents α equations in $\delta\emptyset_i (i = 1,2 .. \alpha + 1)$ unknowns and can be solved in terms of say $\delta\emptyset_1$, i.e. equation 5.4 yields

$$\delta\emptyset_i = c_i \delta\emptyset_1 \quad (i = 2,3 .. \alpha + 1) \qquad .... (5.5)$$

where c_i is a constant.

Substituting equation 5.5 in equation 5.3, we have

$$\delta W = \sum_{1}^{\alpha+1} k_i c_i \left(\frac{dM}{d\emptyset}\right)_{M_i}^{i} = \bar{M}_i \quad \delta\emptyset_1$$

or

$$\frac{\delta W}{\delta\emptyset_1} = \sum_{1}^{\alpha+1} K_i \left(\frac{dM}{d\emptyset}\right)_{M_i}^{i} = \bar{M}_i \qquad .... (5.6)$$

where $K_i = k_i c_i$.

In the limit, $\frac{\delta W}{\delta\emptyset_1} \rightarrow \frac{dW}{d\emptyset_1}$ and equation 5.6 yields

$$\frac{dW}{d\emptyset_1} = \sum_{1}^{\alpha+1} K_i \left(\frac{dM}{d\emptyset}\right)_{M_i}^{i} = \bar{M}_i \qquad .... (5.7)$$

For W to assume a stationary value,

$$\frac{dW}{d\emptyset_1} = 0$$

and since minimum value is the trivial case, this is the necessary and sufficient condition for W to be maximum. Hence W will be maximum when

$$\sum_{1}^{\alpha+1} k_i \left(\frac{dM}{d\phi}\right)_{M_i}^{i} = \bar{M}_i = 0 \qquad \ldots\ldots (5.8)$$

Equation 5.8 is true for any stage after the instant when some of the critical sections have just reached their maximum moments of resistance whereas the others are still on the rising portion of their moment-curvature diagrams. Hence, starting from this instant and proceeding by step by step increment method, maximum load W will be obtained when equation 5.8 is satisfied. This can either be done on a computer, or by a semigraphical method after drawing the moment-curvature diagrams for the various critical sections forming the apparent collapse mechanism.

5.7 ANALYSES FOR TWO AND THREE-SPAN BEAMS

Case (i) Symmetrically loaded beam with two equal spans

Consider a symmetrically loaded beam ABC of two equal spans loaded at D' and D; see Figure 5.1. Consider a stage subsequent to the instant when the first hinge has just passed its maximum moment and the second hinge is still on the rising portion of its $M - \phi$ diagram. Let $\bar{M}_B$ and $\bar{M}_D$ be the absolute moments at B and D respectively at this instant. If δM_B and δM_D are the small changes in absolute moments at B and D respectively for a small increase in load δW, then from equilibrium we have

$$\beta(1-\beta)\,\delta W\, L = \delta M_D + \beta\,\delta M_B \qquad \ldots\ldots (5.9)$$

In the light of Section 5.5, for the beam in which the first hinge is formed at the support section, the bending moment and curvature distributions along the beam before and after the application of load δW can be assumed as shown in Figure 5.1.

For 'compatibility' requirements to be satisfied

$$\int_s \underline{m}_1 \, \delta\underline{\phi} \; ds = 0$$

$$\text{i.e.} \quad -\frac{1}{2}\delta\phi_B \, l_B \cdot 1 + 2 \cdot \frac{1}{2}\delta\phi_D \, l_D \, \beta = 0 \qquad \ldots\ldots (5.10)$$

Here it is assumed that the centre of gravity of curvature distribution over the cracked length near D coincides with the critical section D, which is reasonable since the difference will be of second order.

From equation 5.10 we have

$$\delta\phi_B = 2\beta \frac{l_D}{l_B} \, \delta\phi_D \text{ (Numerically)} \qquad \ldots\ldots (5.11)$$

Now

$$\delta M_D = \left(\frac{dM}{d\phi}\right)^D_{M = \bar{M}_D} \delta\phi_D \qquad \ldots\ldots (5.12)$$

and

$$\delta M_B = \left(\frac{dM}{d\phi}\right)^B_{M = \bar{M}_B} \delta\phi_B$$

$$= 2\beta \frac{l_D}{l_B} \left(\frac{dM}{d\phi}\right)^B_{M = \bar{M}_B} \delta\phi_D \text{ from eq. 5.11} \qquad \ldots\ldots (5.13)$$

Substituting equations 5.12 and 5.13 in equation 5.9, we have

$$\beta(1 - \beta)\delta W \, L = \left[\left(\frac{dM}{d\phi}\right)^D_{M = \bar{M}_D} + 2\beta^2 \frac{l_D}{l_B} \left(\frac{dM}{d\phi}\right)^B_{M = \bar{M}_B} \right] \delta\phi_D$$

For reasons given in Section 5.6, W will be maximum when

$$\left(\frac{dM}{d\phi}\right)^{D}_{M=\bar{M}_D} + 2\beta^2 \frac{l_D}{l_B}\left(\frac{dM}{d\phi}\right)^{B}_{M=\bar{M}_B} = 0 \qquad \ldots. (5.14)$$

If B is the first hinge to form, then in equation 5.14 $\left(\frac{dM}{d\phi}\right)^{B}$ will pertain to the drooping portion of the moment-curvature diagram for the critical section B and will be negative, and $\left(\frac{dM}{d\phi}\right)^{D}$ will pertain to the rising portion of the moment-curvature diagram for the critical section D and will be positive. Thus, in such a case W will be maximum when

$$\left(\frac{dM}{d\phi}\right)^{D}_{M=\bar{M}_D} = 2\beta^2 \frac{l_D}{l_B}\left(\frac{dM}{d\phi}\right)^{B}_{M=\bar{M}_B} \quad \text{(Numerically)}$$

(Rising portion) (Drooping portion) .... (5.15)

For the prestressed concrete sections usually met in practice, the slope of the falling branch of the $M - \phi$ diagram for some length adjacent to its peak is nearly constant and is smaller than that of the rising portion near the peak and since $\beta < 1$ and $l_D/l_B \simeq 1$, equation 5.15 for usual values of β will be satisfied when $\bar{M}_D$ is nearly equal to its ultimate flexural strength. In the tests referred to in Section 5.2, β was about 0.5 and in equation 5.15 $2\beta^2 \, l_D/l_B$ was approximately equal to 0.5, which explains why the moment at the critical section D at collapse was nearly equal to its ultimate flexural strength. The slope of the falling branch of the moment-curvature diagram, except for the heavily over-reinforced sections, is shallow for some length adjacent to the peak moment, and in such a case by the time maximum moment is reached at D, the moment at B is not substantially reduced, with the result the ultimate load carried by such beams is nearly equal to the plastic load. This, with the exception of Raina's beam CB-5, explains why the two-span beams in which the

first hinge was formed at the support carried practically full plastic load. Raina's beam CB-5, as against its overall depth of 6 in., had an effective depth of 1.86 in. only at the support section and constituted a heavily over-reinforced section in so much so that even the pure prestress moment equal to 1.14 x 18,390 = 21,000 lb in. was set up in the same sense as the elastic moment due to loads. At ultimate load, moments measured at the support and mid-span sections were 47,600 and 154,800 lb in. respectively. These moments, like Cooke's moments (see Chapter 3), did not include the secondary prestress moments, which was +47,700 lb in. at the support aection and +23,850 lb in. at the mid-span section. With the addition of these to the measured moments, the apparent moments at ultimate load work out to +100 lb in. at the support section and +178,650 lb in. at the mid-span section. If due consideration is made to the fact that the pure prestress moment at the support section had the sense same as that due to loads, then the apparent ultimate moments of support and mid-span sections, based on Raina's calculations, work out as 12,300 and 181,400 lb in. respectively. This shows that the apparent moment reached at mid-span at collapse was practically equal to its ultimate flexural strength. But at this time, due to over-redistribution the apparent moment at the support section was reduced well below its ultimate flexural strength, which resulted in collapse at a load lower than the plastic load. The fact that the support section was unloading is borne from Raina's graph 29 (see reference 37); but, as it is plotted for moments excluding the secondary prestress moments, the effect is not so conspicuous.

If D is the first hinge to form, then in equation 5.14 $(\frac{dM}{d\phi})^D$ will correspond to the drooping portion of the moment-curvature diagram for the critical section D and will be negative, and $(\frac{dM}{d\phi})^B$ will correspond to the rising portion of the moment-curvature diagram for the critical section B and will be positive.

That is, in such a case W will be maximum when

$$\left(\frac{dM}{d\phi}\right)^{B}_{M=\bar{M}_B} = \frac{1}{2\beta^2 \frac{l_D}{l_B}} \left(\frac{dM}{d\phi}\right)^{D}_{M=\bar{M}_D} \quad \text{(Numerically)}$$

(Rising portion) (Drooping portion) .... (5.16)

Remembering that for the prestressed concrete sections usually met in practice the slope of the falling branch of the $M - \phi$ diagram for some length adjacent to its peak is nearly constant and is smaller than that of the rising portion near the peak and since $\beta < 1$ and $l_D/l_B \simeq 1$, equation 5.16 for usual values of β can be sasisfied when the moment at D has just passed its maximum value and that at B is still far behind its peak. For Mallick's beams P3 and 6, in which full redistribution was not reached, β was 0.27 and in equation 5.16 $1/2\beta^2 \; l_D/l_B$ was approximately equal to 7, which explains why these beams failed with moment at the critical section B less than the ultimate flexural strength.

Case (ii) Two-span beam loaded in one span only - first hinge in span

Consider a two-span beam ABC loaded at point D at a stage subsequent to the instant when the critical section D has just reached its maximum moment and the critical section B is still on the rising portion of its $M - \phi$ diagram, see Figure 5.2. In this case 'compatibility' requirement yields

$$\delta\phi_B = \beta \frac{l_D}{l_B} \delta\phi_D \quad .... (5.17)$$

and equation 5.14 takes the form

$$\left(\frac{dM}{d\phi}\right)^{B}_{M=\bar{M}_B} = \frac{1}{\beta^2 \frac{l_D}{l_B}} \left(\frac{dM}{d\phi}\right)^{D}_{M=\bar{M}_D} \quad \text{(Numerically)}$$

(Rising portion) (Drooping portion) .... (5.18)

Equation 5.18 is similar to equation 5.16 and for reasons given before can be satisfied for prestressed concrete sections usually met in practice when the moment at the critical section D has just passed its peak and that at the critical section B is still far behind its peak. For LaGrange's beams 159, 164, 165, 182, 196 and 167, in which full redistribution was not reached, β was 0.5 and if l_D/l_B is approximated to 0.8, then in equation 5.18 $1/\beta^2 \; l_D/l_B$ is approximately equal to 5, which explains why the moment at the critical section B at collapse was less than the maximum moment of resistance.

Case (iii) Three-span beam loaded in central span - first hinge in span

Consider a three-span beam ABB'C with equal end spans and loaded at point D in the central span at a stage subsequent to the instant when the critical section D has just reached its maximum moment of resistance and the critical sections B and B' are still on the rising portions of their moment-curvature diagrams; see Figure 5.3. In this case 'compatibility' requirements yield

$$\delta\phi_B = (1 - \beta) \frac{l_D}{l_B} \delta\phi_D \text{ (Numerically)} \quad \ldots\ldots (5.19)$$

$$\delta\phi_{B'} = \beta \frac{l_D}{l_{B'}} \delta\phi_D \text{ (Numerically)} \quad \ldots\ldots (5.20)$$

and equation 5.8 takes the form

$$(1 - \beta)^2 \frac{l_D}{l_B} \left(\frac{dM}{d\phi}\right)^B_{M = \bar{M}_B} + \beta^2 \frac{l_D}{l_{B'}} \left(\frac{dM}{d\phi}\right)^{B'}_{M = \bar{M}_{B'}} + \left(\frac{dM}{d\phi}\right)^D_{M = \bar{M}_D} = 0 \quad \ldots\ldots (5.21)$$

For Cooke, and Mallick and Sastry's beams β was 0.5 and critical sections B and B' were identical, so that equation 5.21 reduces to

$$\frac{1}{2}\frac{l_D}{l_B}\left(\frac{dM}{d\phi}\right)^B_{M=\overline{M}_B} + \left(\frac{dM}{d\phi}\right)^D_{M=\overline{M}_D} = 0 \qquad \ldots\ (5.22)$$

Since D is the first hinge to form, $\left(\frac{dM}{d\phi}\right)^D$ will be negative and $\left(\frac{dM}{d\phi}\right)^B$ positive such that at ultimate load

$$\left(\frac{dM}{d\phi}\right)^B_{M=\overline{M}_B} = 2\frac{l_B}{l_D}\left(\frac{dM}{d\phi}\right)^D_{M=\overline{M}_D} \quad \text{(Numerically}$$

(Rising portion) (Drooping portion) .... (5.23)

In equation 5.23 l_B/l_D will be near about unity, depending upon the ratio of the outer and inner spans, and for reasons given before explains why full redistribution was not reached in Cooke, and Mallick and Sastry's beams.

Since the coefficient of $\left(\frac{dM}{d\phi}\right)^D$ was nearly 2, it was quite likely that the moment reached at the critical section B at collapse was not very much different from its maximum moment of resistance, and being a marginal case could lead to the inconsistency pointed out in Section 5.3.

5.8 TESTS ON PORTAL FRAMES

With the exception of LaGrange's tests[14] on six fixed portal frames, all reported experiments on prestressed concrete portal frames have been carried out without the measurement of redundant reactions. The tests in which reactions were not measured were carried out by Morice and Lewis[36], Guyon[21], Pietrzykowski[56], and Edwards[34], which, as ascertained from visual inspection and by comparing the measured ultimate loads with the calculated ones, showed practically full redistribution.

All portal frames tested by LaGrange had a span of 7 ft 6 in. and a height of 5 ft and were loaded vertically at

the centre of the transome and horizontally from left to right at the transome centroidal axis. The ratio of the vertical to horizontal load was 2. All members had an overall section of 3 x 6.5 in. and were prestressed with 4 No. 0.2 in. diameter wires. The strengths of the critical sections were varied by changing the effective depths by adding linear functions to the eccentricities of the concordant cable profile which was straight in between the critical sections. If the critical section identification is done as adopted for the author's frames (see Figure 7.9), then for frames P3 and 6 which had concordant cable profiles the effective depths at A, B_2, B_1, C, D and E were 3.26, 3.79, 3.44, 4.32, 4.35 and 4.26 in. respectively. It would be noted that this profile does not satisfy equation 2.15. However, the secondary prestress moments set up were small and it is reasonable to regard it as concordant cable profile.

Frames P3 and 6 had concordant cable profiles and were similar except that concrete in P6 was 30% stronger than that in P3. Behaviour of both the frames was essentially the same and there was only a difference of 6% in their maximum loads. Collapse occurred at sections C and D_2 only, but at that instant moment at section E was almost equal to its maximum value and that at A was about 0.78 of its maximum flexural strength. The ultimate loads carried by P3 and 6 were 8,050 and 8,550 lb respectively.

In an attempt to make the strongest possible frame, in P4 the effective depth at the four sections where the elastic moments due to loads were the highest, that is at A, C, D and E was increased to the possible maximum of 5 in. and that at B_2 reduced to 2.46 in. This frame also failed with the collapse of critical sections C and D and at that instant moment at A was only about 50% of its maximum value. The maximum load was 9,750 lb.

In frame P5 the effective depths at A, B_2, B_1, C, D and E were changed to 2.50, 5.00, 4.65, 4.26, 3.25 and 3.25 in. respectively. The frame failed at a load of 6,550 lb as a complete mechanism with the formation of hinges at A, C D_2 and E.

In frame P7 the effective depth at all the critical sections except C was increased to 5 in ; at C it was reduced to 3.3 in. The result was that when section C reached its ultimate moment, the rest of the structure was still strong enough to carry further load. Maximum load carried was 8,750 lb, which was reached when the section D_1 also failed but by then the moment at C was reduced to 90% its maximum.

In frame P8 the effective depth along the length AB was reduced to 2 in. and that at the other critical sections increased to 5 in. This resulted in the failure at C and D and at this instant the moments at E and B_1 were also near their maximum flexural strengths. This frame carried an ultimate load of 9,950 lb.

On the other hand, author's all portal frames (except F-3), which are described in Chapter 7, failed as mechanisms by the formation of hinges at A, C, D and E. Frames F-1 and 4 failed by the formation of all hinges almost simultaneously but in F-2, 3 and 5 the maximum loads were reached when some of the hinges had already started unloading, see Figures 7.14 to 7.18.

From the above it would appear that LaGrange's frames behaved somewhat differently from the author's frames. This was the result of design and will be discussed in Chapter 6. These tests, however, bring out clearly that, in general, full-redistribution in statically indeterminate structures would not take place, unless specially aimed at, and the ultimate load is usually reached with over-redistribution.

5.9 CONCLUSIONS

1) All test results can be explained satisfactorily on the basis of moment-curvature relationship with a drooping characteristic as set out in Chapter 4.

2) Full-redistribution, in its strict sense, cannot occur in a statically indeterminate prestressed concrete structure unless all the critical sections forming the collapse mechanism reach their maximum flexural strengths simultaneously.

3) The two and three-span beams which have been reported to undergo full redistribution can be accounted for by the assumption of a moment-curvature characteristic which has a shallow negative slope adjacent to the peak moment.

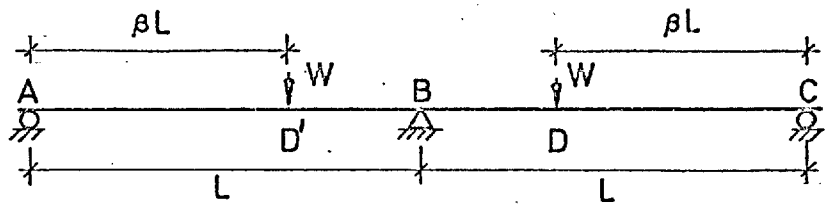

Two-Span Beam

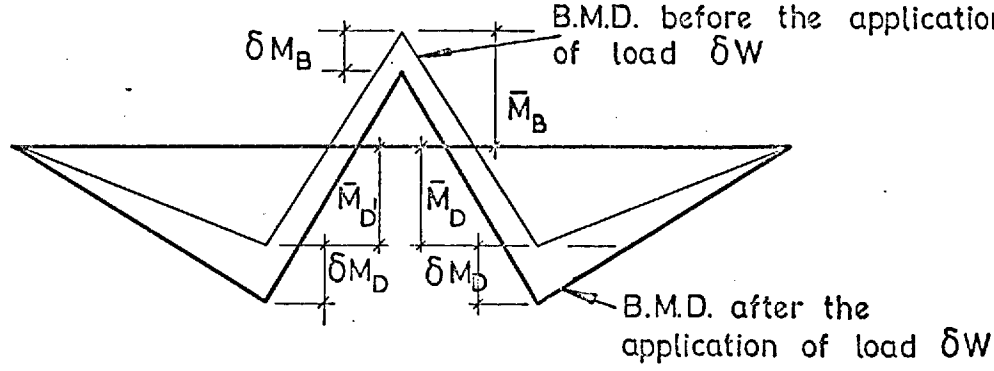

B.M. Distribution

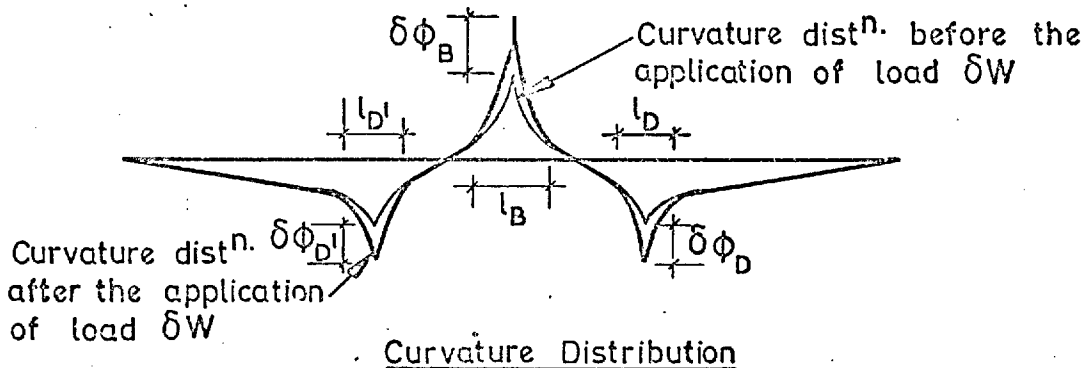

Curvature Distribution

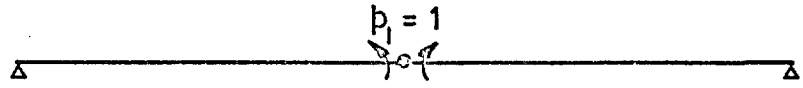

Released Structure

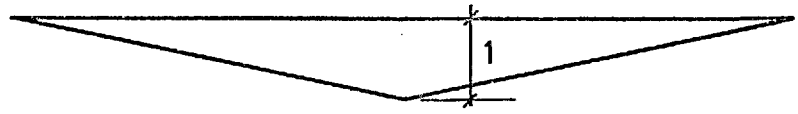

m_1 -Diagram

Fig 5.1: SYMMETRICALLY LOADED TWO-SPAN BEAM

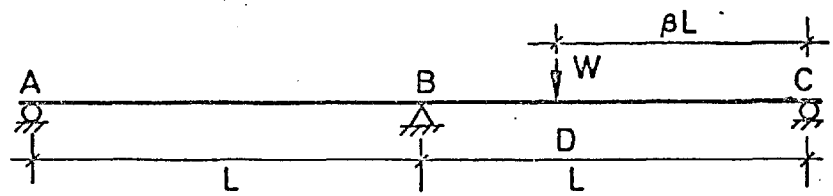

Two-Span Beam

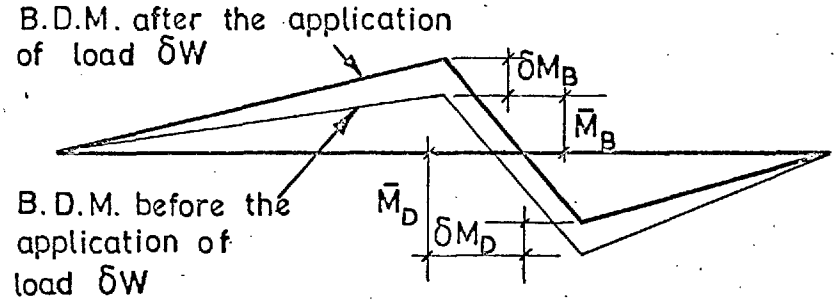

B. M. Distribution

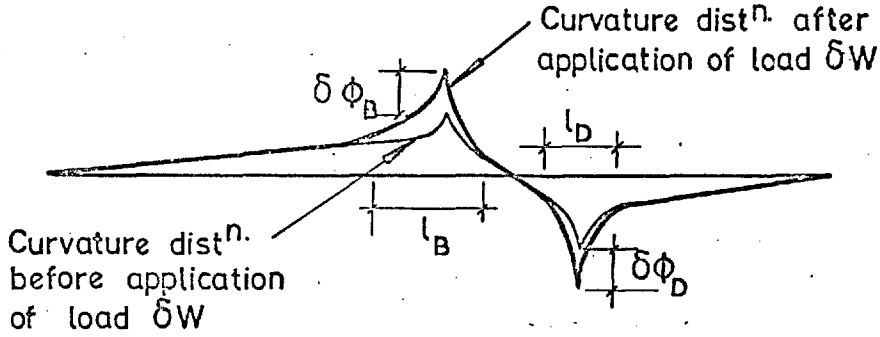

Curvature Distribution

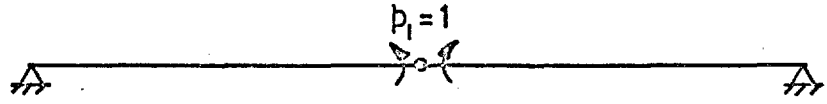

Released Structure

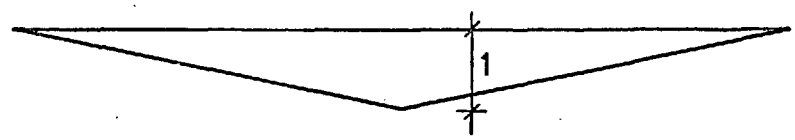

m_1 - Diagram

Fig 5.2: TWO-SPAN BEAM LOADED IN ONE SPAN ONLY

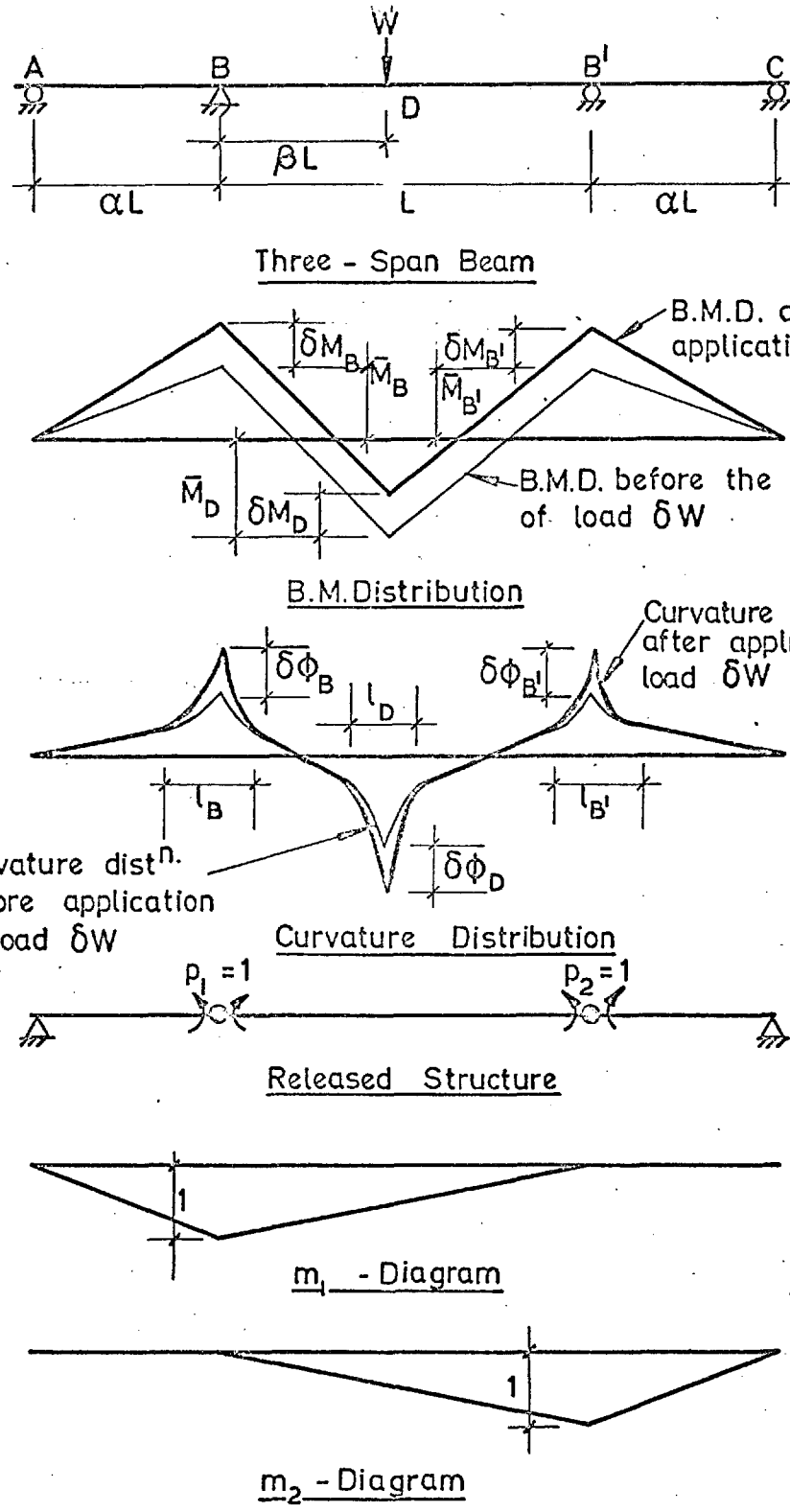

Fig 5.3: THREE-SPAN SYMMETRICAL BEAM LOADED IN CENTRAL SPAN

CHAPTER 6

PROPOSED METHOD OF ULTIMATE LOAD DESIGN OF STATICALLY INDETERMINATE PRESTRESSED CONCRETE STRUCTURES

6.1 INTRODUCTION

The basic equations that a statically indeterminate skeletal structure must satisfy at any load stage, including the ultimate load, were set up in Chapter 3. In prestressed concrete it is necessary that while applying equations 3.5 due consideration is made for the prestress moments and corresponding curvatures. The moment-curvature relationship of a prestressed concrete section is linear elastic up to cracking and thereafter it is nonlinear; it has a rising characteristic up to the maximum moment of resistance and then it starts drooping down. It is difficult to use the moment-curvature relationship with a drooping characteristic in an analysis. The author has here presented a theory for the design of statically indeterminate prestressed concrete skeletal structures so that the structure carries the ultimate load by simultaneously developing the maximum moment of resistance at each of the critical sections which form the collapse mechanism, and at the same time maximum output from each such critical section is ensured. In this connection and in respect of studies made in Sections 6.4 and 6.5 the author wishes to acknowledge the help rendered by Edwards[57].

The proposed method has the advantage that the structure would carry full plastic load, and there is no necessity to consider the drooping portion of the moment-curvature relationship.

6.2 ULTIMATE LOAD ANALYSIS OF A STATICALLY INDETERMINATE PRESTRESSED CONCRETE STRUCTURE

In the work that follows it will be assumed that only the flexural deformations are significant and the portion of the

moment-curvature relationship which need to be considered is $C'AOC^D$ only, see Figure 2.1. In this diagram $C'AC$ represents the linear elastic phase and CD the non-linear phase. In an ultimate load analysis it is often convenient to separate the variation of the bending moments due to inelastic deformations from the distribution for elastic conditions, which is often known or easily established by standard methods. If inelastic deformations at a load stage are known in a structure, then the total solution can be obtained by superimposing their effect on the elastic structure for which solution due to loads is already established. Loads for a statically indeterminate prestressed concrete structure, in general, consist of prestress and applied loads. Thus for load $\nu(d+1)$ we have from equilibrium

$$\underline{M} = \underline{M}^{o}_{\nu(d+1)} + \underline{m}\,\underline{p}_{\nu(d+1)} + \underline{M}^{o}_{p} + \underline{m}\,\underline{p}^{s}_{p} + \underline{m}\,\underline{p}_{r}$$

$$\text{or } \underline{M} = \underline{M}^{o}_{\nu(d+1)} + \underline{M}^{o}_{p} + \underline{m}\left(\underline{p}_{\nu(d+1)} + \underline{p}^{s}_{p} + \underline{p}_{r}\right) \quad \ldots\ldots (6.1)$$

where $\underline{M}$ is the functional matrix in positional co-ordinates s and corresponds to the absolute bending moment distribution at the given load $\nu(d+1)$;

$\underline{M}^{o}_{\nu(d+1)}$ is the functional matrix in positional co-ordinates s and corresponds to the bending moment distribution due to load $\nu(d+1)$ applied to the reduced structure;

$\underline{m}\ (= \underline{m}_1\ \underline{m}_2\ \ldots\ \underline{m}_\alpha)$ is the functional matrix in positional co-ordinates s and corresponds to $1 \times \alpha$ bending moment distributions due to unit bi-action applied in turn at each release of the reduced structure;

$\underline{p}_{\nu(d+1)}$ is the column matrix and corresponds to α complementary solution coefficients for load $\nu(d+1)$ applied to the elastic structure;

$\underline{M}_p^o$ is the functional matrix in positional co-ordinates s and corresponds to bending moment distribution due to prestress applied to the reduced structure;

$\underline{p}_p^s$ is the column matrix and corresponds to α complementary solution coefficients for prestress applied to the elastic structure; and

$\underline{p}_r$ is the column matrix and corresponds to α complementary solution coefficients due to the final inelastic curvatures which represent the difference between the elastic solution and the final inelastic solution applied to the elastic structure.

From compatibility

$$\int_s \underline{m}^T \underline{k} \underline{M}^o_{\nu(d+1)} \, ds + \int_s \underline{m}^T \underline{k} \underline{m} \underline{p}_{\nu(d+1)} \, ds +$$

$$\int_s \underline{m}^T \underline{k} \underline{M}^o_p \, ds + \int_s \underline{m}^T \underline{k} \underline{m} \underline{p}^s_p \, ds + \int_s \underline{m}^T \underline{k} \underline{m} \underline{p}_r \, ds +$$

$$\int_s \underline{m}^T \underline{\emptyset} \, ds = 0 \qquad \ldots\ldots (6.2)$$

where $\underline{k}$ is the functional matrix in positional co-ordinates s and corresponds to the elastic bending flexibility of the members, see Figure 2.1, and

$\underline{\emptyset}$ is the functional matrix in positional co-ordinates s ane corresponds to inelastic curvature distribution, see Figure 2.1.

But

$$\int_s \underline{m}^T \underline{k}\, \underline{M}^o_{\nu(d+1)}\, ds + \int_s \underline{m}^T \underline{k}\, \underline{m}\, \underline{p}_{\nu(d+1)}\, ds = 0 \qquad \ldots. (6.3)$$

and $$\int_s \underline{m}^T \underline{k}\, \underline{M}^o_p\, ds + \int_s \underline{m}^T \underline{k}\, \underline{m}\, \underline{p}^s_p\, ds = 0 \qquad \ldots. (6.4)$$

Therefore from equation 6.2 we have

$$\int_s \underline{m}^T \underline{k}\, \underline{m}\, \underline{p}_r\, ds + \int_s \underline{m}^T \underline{\emptyset}\, ds = 0$$

or $$\underline{p}_r = -\underline{F}^{-1} \underline{\mu}_r \qquad \ldots. (6.5)$$

where $$\underline{F} = \int_s \underline{m}^T \underline{k}\, \underline{m}\, ds \qquad \ldots. (6.6)$$

and $$\underline{\mu}_r = \int_s \underline{m}^T \underline{\emptyset}\, ds \qquad \ldots. (6.7)$$

Considering moments at the critical sections, we have from equation 6.1

$$M = M^o_{\nu(d+1)} + M^o_p + m\left(p_{\nu(d+1)} + p^s_p + p_r \right)$$

or $$M - M^o_p = M_a = M^o_{\nu(d+1)} + m\left(p_{\nu(d+1)} + p^s_p + p_r \right) \qquad \ldots. (6.8)$$

Equation 6.8 together with equations 6.3, 6.4 and 6.5 infers that specified apparent moments at the critical sections can be obtained by equilibrium of the applied loads alone, provided secondary prestress moments are set up accordingly.

Equations 6.1 and 6.2 are the basic equations for a statically indeterminate prestressed concrete structure and can be used for any problem of design or analysis, provided all critical sections are on the rising portion of their moment-curvature diagrams. In a problem of analysis it would be seldom that all critical sections are on the rising portion at collapse. In design, however, this can be overcome as suggested in Section 6.3.

6.3 DESIGN APPROACH

The object of any design approach is to determine a rational, directed evolution of a structural system which performs the specified purposes and satisfies certain criterion. There are usually two important criteria: (1) cracking (2) ultimate load. Whatever criterion is used, after fixing the design loads the problem is to ensure that the structure would withstand them as specified.

If a structure is proposed to be designed for the ultimate load criterion, then an ultimate load stress-resultant distribution in equilibrium with the applied load is established. The required section sizes, the area and position of steel are calculated at the critical sections involved in the equilibrium criterion to ensure adequate ultimate load carrying capacity. The lengths over thich inelastic deformations take place can then be approximated by marking off the cracking moments. In the work that follows, it will be assumed that all the critical sections involved in the equilibrium criterion reach their ultimate flexural strengths simultaneously, that is all such sections are at the peak of their moment-curvature relationships. It will be further assumed, for simplification, that the moment-curvature relationships for the sections in the inelastic zone adjacent to a critical section are the same as for the critical section itself. The moment-curvature

diagrams for the critical sections can be established according to the theory set out in Chapter 4.

The solution to the compatibility equation 6.5 is thus found, that is p_r is known in equation 6.8. The only unknown in equation 6.8 is p_p^s which can be evaluated.

The area dnd position of steel at the critical sections involved in the equilibrium criterion were fixed while fixing their ultimate strengths. The required area and position of steel in between the critical sections and also at the critical sections not involved in the equilibrium criterion can now be established from equation 6.4; due care may be taken that this does not result in the change of collapse mechanism.

Thus from equation 6.4 we have

$$\underline{p}_p^s = -F^{-1} \underline{\mu}_p^o \quad \ldots\ (6.9)$$

where $$\underline{\mu}_p^o = \int_s \underline{m}^T \underline{k} \underline{M}_p^o \, ds \quad \ldots\ (6.10)$$

It may be more accurate to also take into account the deformations due to axial force while calculating μ_p^o, and in that case equation 6.10 reduces to

$$\underline{\mu}_p^o = \int_s \underline{m}^T \underline{k} \underline{M}_p^o \, ds + \int_s \underline{n}^T \underline{g} \underline{N}_p^o \, ds \quad \ldots\ (6.11)$$

where $\underline{n}$ $(= \underline{n}_1 \; \underline{n}_2 \ldots \underline{n}_\alpha)$ is the functional matrix in positional co-ordinates s and corresponds to $1 \times \alpha$ thrusts due to unit bi-action applied in turn at each release of the reduced structure;

$\underline{g}$ is the functional matrix in positional co-ordinates s and corresponds to elastic thrust flexibility of members; and

$\underline{N}_p^o$ is the functional matrix in positional co-ordinates s and corresponds to thrust distribution due to prestress applied to the reduced structure.

A statically indeterminate prestressed concrete structure designed in this manner not only carries full plastic load but, as shown in Section 6.4, will also exhibit small inelastic deformations.

If cracking is the criterion of design, then a cracking load stress-resultant distribution in equilibrium with the applied load is established. The required section sizes, the area and position of steel at the critical sections involved in the equilibrium criterion are calculated to ensure adequate cracking load carrying capacity. If cracking moment of a critical section is calculated by allowing some inelasticity, then in a manner outlined above, p_r can be evaluated from equation 6.5 otherwise p_r is equal to zero. Thus, the only unknown in equation 6.8 is p_p^s which can be calculated and set up by varying the area and position of steel in between the critical sections and also at the critical sections not involved in the equilibrium criterion, by means of equation 6.9; care may be taken that it does not result in cracking at any other section.

If one wishes to design a statically indeterminate prestressed concrete structure on a criterion similar to the Russian code, then an ultimate load stress-resultant distribution in equilibrium with the applied load is assumed. The required section sizes, the area and position of steel are calculated at the critical sections involved in the equilibrium criterion to ensure adequate ultimate load carrying capacity. The assumed stress-resultant distribution is reduced in the ratio of allowable cracking load to ultimate load. The cracking moments of the critical sections involved in the equilibrium criterion are

calculated on the basis of the concordant cable. If the cracking moments at the critical sections are not satisfactory, then the above stress-resultant distribution is modified by superimposing a secondary prestress stress-resultant distribution. That is, in equation 6.8 p_p^s can be evaluated by putting $p_r = 0$ such that $M_a \leqq M_{acr}$ everywhere. It remains to ensure that p_p^s so calculated is set up. This can be done by means of equation 6.9 by varying the area and position of steel in between the critical sections and at the critical sections not involved in the equilibrium criterion; care may be taken that it does not result in cracking at any other section or change of apparent collapse mechanism.

The above method, as compared to the Russian practice, has the advantage that required secondary prestress stress-resultant distribution is set up in a statically indeterminate state and is not subjected to linear creep.

It would be appreciated that, unlike the proposed criteria, Russian criterion does neither optimize from cracking point of view nor does it ensure that the structure would withstand the specified ultimate load; it is rather an arbitrary design in between the two proposed criteria. It is reported that the Russian code recommendations are based on exhaustive test results and are found satisfactory in practice. The results of the author's test on the frame designed according to the Russian practice are set out in Section 6.6.

6.4 INELASTIC DEFORMATIONS IN THE PROPOSED DESIGN

Consider the same concrete structure prestressed in two different ways; structure 1 stressed with a concordant cable profile and structure 2 with a nonconcordant cable profile in a manner outlined in Section 6.3 for ultimate load criterion.

Let the geometric properties, that is the section and prestress at the corresponding critical sections be the same in the two structures.

Let the two structures be subjected to the same collapse load, and let the moment-curvature relationship of each of the critical sections forming the collapse mechanism be idealized with a long flat plateau at the maximum moment of resistance. In the light of discussions made in Chapter 4 it is not strictly true; but for the under-reinforced sections it is reasonably accurate, since the slope of the drooping portion adjacent to the peak moment is small for some length.

Let us postulate that there is an idealized plastic hinge rotation $\underline{\theta}$ in the concordant case, where $\underline{\theta} = (\theta_1, \theta_2 \ldots \theta_\alpha)$ is a functional matrix in positional co-ordinates s and corresponds to the idealized plastic rotations at α critical sections.

The total bending solutions for the two structures are

$$\left[\underline{M}_{au}\right]_1 = \underline{M}^{o}_{\nu(d+1)} + \underline{m}\,\underline{p}_{\nu(d+1)} + \underline{m}\left[\underline{p}^{s}_{p}\right]_1 + \underline{m}\left[\underline{p}_{r}\right]_1 \quad \ldots\ldots (6.12)$$

$$\left[\underline{M}_{au}\right]_2 = \underline{M}^{o}_{\nu(d+1)} + \underline{m}\,\underline{p}_{\nu(d+1)} + \underline{m}\left[\underline{p}^{s}_{p}\right]_2 + \underline{m}\left[\underline{p}_{r}\right]_2 \quad \ldots\ldots (6.13)$$

where suffices 1 and 2 after the square brackets refer to structures 1 and 2 respectively.

Since the corresponding critical sections of the two structures have the same geometric properties, and structure 1 has a concordant cable profile,

$$\left[\underline{M}_{au} \right]_1 = \left[\underline{M}_{au} \right]_2$$

and $$\left[\underline{p}_p^s \right]_1 = 0$$

Therefore, subtracting equation 6.12 from equation 6.13, we have on simplification

$$\left[\underline{p}_r \right]_1 - \left[\underline{p}_r \right]_2 = \left[\underline{p}_p^s \right]_2 \quad \ldots\ (6.14)$$

From compatibility we have for the two structures

$$\int_s \underline{m}^T \underline{k}\, \underline{m} \left[\underline{p}_r \right]_1 ds + \int_s \underline{m}^T \left[\underline{\phi} \right]_1 ds + \underline{m}^T \underline{\theta} = 0 \quad \ldots\ (6.15)$$

and $$\int_s \underline{m}^T \underline{k}\, \underline{m} \left[\underline{p}_r \right]_2 ds + \int_s \underline{m}^T \left[\underline{\phi} \right]_2 ds = 0 \quad \ldots\ (6.16)$$

In equations (6.15) and (6.16) $\underline{\phi}$ represents the inelastic curvature due to the same final bending moment distribution and therefore

$$\left[\underline{\phi} \right]_1 \simeq \left[\underline{\phi} \right]_2$$

Hence subtracting equation 6.16 from equation 6.15, we have on simplification

$$\left[\underline{p}_r \right]_1 - \left[\underline{p}_r \right]_2 = -\underline{F}^{-1}\, \underline{m}^T\, \underline{\theta} \quad \ldots\ (6.17)$$

Substituting for L.H.S. from equation 6.14, we have

$$\left[\underline{p}_p^s \right]_2 = -\underline{F}^{-1}\, \underline{m}^T\, \underline{\theta} \quad \ldots\ (6.18)$$

Equation 6.18 shows that the plastic hinge rotations in the concordant case can be done away by setting up an appropriate secondary prestress moment distribution; or in other words equation 6.18 infers that a statically indeterminate structure prestressed in a manner suggested in Section 6.3 for ultimate load criterion would exhibit less deformations than the corresponding structure prestressed with concordant cable profile. The idealized plastic rotation $\underline{\theta}$ in a statically indeterminate structure represents the fact that such a structure would carry the ultimate load with over-redistribution. Therefore equation 6.18, in general, infers that a statically indeterminate structure prestressed in a manner suggested in Section 6.3 for ultimate load criterion would exhibit less deformations than the corresponding structures which carry the ultimate load with over-redistribution.

6.5 EFFECT OF LINEAR TRANSFORMATION

In several cases cable profile in a statically indeterminate prestressed concrete structure is obtained by linear transformation of the parent concordant cable profile. In the past considerable experimental and theoretical research has been carried out to study the effect of linear transformation on ultimate load. The theoretical studies, to the author's knowledge, have so far been made by considering only the 'equilibrium' criterion. The author here examines this by considering both the 'equilibrium' and 'compatibility' criteria.

Consider the same concrete structure prestressed in two different ways; structure 1 has a concordant cable profile and structure 2 a linearly transformed cable profile obtained from structure 1.

Let the two structures be assumed to carry the same collapse load, that is $M_{\nu(d+1)}$ is the same in both cases.

If d is the effective depth at a section in the concordant case, then the effective in the linearly transformed case at the same section would be $(d + m \left[p_p^s\right]_2 / P_e)$, where P_e is the initial prestress. If suffices 1 and 2 after the square brackets refer to structures 1 and 2 respectively, then

$$\left[M_{au}\right]_1 = \left[k_u\right]_1 \left[P_u\right]_1 d$$

and $$\left[M_{au}\right]_2 = \left[k_u\right]_2 \left[P_u\right]_2 \left(d + \frac{m\left[p_p^s\right]_2}{P_e}\right)$$

where P_u is the force in steel at ultimate load; and

k_u is a constant.

If it is assumed that all critical sections are under reinforced before and after linear transformation, then

$$\left[P_u\right]_1 \simeq \left[P_u\right]_2 = P_u \text{ say}$$

and $$\left[k_u\right]_1 \simeq \left[k_u\right]_2 = k_u \text{ say}$$

Hence

$$\left[M_{au}\right]_1 = k_u P_u d \quad \ldots\ldots (6.19)$$

and $$\left[M_{au}\right]_2 = k_u P_u \left(d + \frac{m\left[p_p^s\right]_2}{P_e}\right) \quad \ldots\ldots (6.20)$$

From equilibrium we have for the two structures

$$\left[\underline{M}_{au}\right]_1 = \underline{M}_{\nu(d+1)} + \underline{m}\left[\underline{p}_r\right]_1 \quad \ldots\ldots (6.21)$$

and $$\left[\underline{M}_{au}\right]_2 = \underline{M}_{\nu(d+1)} + \underline{m}\left[\underline{p}_p^s\right]_2 + \underline{m}\left[\underline{p}_r\right]_2 \quad \ldots\ldots (6.22)$$

where $\underline{M}_{\nu(d+1)}$ is the functional matrix in positional co-ordinates s and corresponds to the absolute bending moment distribution due to ultimate load $\nu(d+1)$ applied to the elastic structure.

Substituting for M_{au}'s from equations 6.19 and 6.20 in equations 6.21 and 6.22, we have on subtraction and simplification

$$\left[\underline{p}_p^s\right]_2 = \frac{P_e}{(k_u P_u - P_e)}\left(\left[\underline{p}_r\right]_2 - \left[\underline{p}_r\right]_1\right) \quad \ldots\ldots (6.23)$$

If it is assumed that all sections have a moment-curvature relationship which has long flat plateau at the maximum moment before and after linear transformation then from compatibility we have for the two structures

$$\int_s \underline{m}^T \underline{k}\,\underline{m}\left[\underline{p}_r\right]_1 ds + \int_s \underline{m}^T \left[\underline{\phi}\right]_1 ds + \underline{m}^T \left[\underline{\theta}\right]_1 = 0 \quad \ldots\ldots (6.24)$$

and $$\int_s \underline{m}^T \underline{k}\,\underline{m}\left[\underline{p}_r\right]_2 ds + \int_s \underline{m}^T \left[\underline{\phi}\right]_2 ds + \underline{m}^T \left[\underline{\theta}\right]_2 = 0 \quad \ldots\ldots (6.25)$$

Subtracting equation 6.24 from equation 6.25, we have after simplification

$$\left[\underline{p}_r\right]_2 - \left[\underline{p}_r\right]_1 = \underline{F}^{-1}\left\{\int_s \underline{m}^T\left(\left[\underline{\phi}\right]_1 - \left[\underline{\phi}\right]_2\right) ds + \underline{m}^T\left(\left[\underline{\theta}\right]_1 - \left[\underline{\theta}\right]_2\right)\right\} \quad \ldots\ldots (6.25)$$

Hence from equations 6.23 and 6.26 we have

$$\left[\underline{p}_p^s\right]_2 = \frac{P_e}{(k_u P_u - P_e)} \underline{F}^{-1}\left\{\int_s \underline{m}^T\left(\left[\underline{\phi}\right]_1 - \left[\underline{\phi}\right]_2\right) ds + \underline{m}^T\left(\left[\underline{\theta}\right]_1 - \left[\underline{\theta}\right]_2\right)\right\} \quad \ldots\ldots (6.27)$$

This is a general expression relating $\underline{p}_p^s$ set up in the linearly transformed case with the inelastic curvatures and plastic hinge rotations taking place in two structures and shows that if the two structures carry the same ultimate load, then the inelastic curvatures and plastic hinge rotations in the linearly transformed case would depend upon the secondary prestress moment distribution set up on linear transformation. If $\left[\theta\right]_2$ for any critical section is large and the moment-curvature relationship for it has a falling branch with sharp slope, then it may be possible that the ultimate load carried by the linearly transformed case is appreciably different from the parent concordant case, as it happened in the case of Raina's beam CB-5 which, compared to the parent concordant beam, carried only 86% load.

It is not possible to take equation 6.27 any further. However, if we consider a two-span beam and assume that the positions of the first and the last hinges do not change, then $\left[\underline{\phi}\right]_1 \simeq \left[\underline{\phi}\right]_2$ and equation 6.27 reduces to

$$\left[\underline{p}_p^s \right]_2 = \frac{P_e}{k_u P_u - P_e} \underline{F}^{-1} \underline{m}^T \left(\left[\underline{\theta} \right]_1 - \left[\underline{\theta} \right]_2 \right) \quad \ldots\ldots (6.28)$$

For a two span beam $\underline{F}^{-1}$ is a 1 x 1 matrix which is positive definite; therefore equation 6.28 shows that if the effective depth at the first hinge is reduced, that is $\left[p_p^s \right]_2$ has a sign opposite to the sign of rotation, then plastic hinge rotation at the first hinge in the linearly transformed case would be greater than that in the concordant case. Similarly, if the effective depth at the first hinge is increased, then $\left[p_p^s \right]_2$ would have the same sign as that of rotation and in this case plastic hinge rotation at the first hinge in the linearly transformed case would be less than that in the parent concordant case. In other words, it amounts to the fact that linear transformation that increases the effective depth at the first hinge reduces redistribution, and linear transformation that reduces the effective depth at the first hinge increases redistribution. This does not appear strictly in line with the conclusion of Cooke[11] and Raina[37] that a structure with a concordant cable profile exhibits minimum redistribution, any linear transformation produces greater redistribution. However, LaGrange[14] test results for beams 159, 165 and 182 clearly bring out the above fact. If redistribution is measured as the difference between the elastic and actual apparent moments at the first hinge at ultimate load, expressed as percentage of its apparent ultimate moment, then beam 159 which had the parent concordant cable profile showed a redistribution of 10%. Compared to this, beam 165 where the linear transformation increased the effective depth at the first hinge showed a redistribution of 2.5%, and beam 182 where the linear transformation reduced the effective depth at the first hinge showed a redistribution of 21%.

Cooke and Raina's moments, as pointed out earlier, suffer from the disadvantage that they have been measured from the state of prestress, i.e. including the secondary prestress moments and it appears to the author that the above inconsistency is more of interpretation rather than reality.

6.6 TEST RESULTS AND DISCUSSIONS

Tests on five two-span beams and five fixed portal frames are described in Chapter 7. The test results are now discussed in the light of the theories presented.

Beams CB-1 and B-1

Beam CB-1 was tested by Raina and had a concordant cable profile with an effective depth of 4.46 in. at the support and 4.20 in. at the mid-span sections. The cable profile in between the critical sections was straight. This beam failed at an ultimate load of 7,440 lb, and the first hinge was formed at the support. Full redistribution was practically reached. Beam B-1, tested by the author, was designed with the same prestress and the same effective depths at the corresponding critical sections, but the cable profile in between the critical sections was varied (see Figure 7.4) by means of equation 6.9 so that the secondary prestress moments set up were +10,300 lb in. at the support and +5,150 lb in. at the mid-span sections. The first hinge in beam B-1 was formed in the span, which showed that by setting up an appropriate secondary prestress stress-resultant distribution the mode of collapse can be controlled. Because of the dislocation in the position of the duct-tubing during casting, the actual effective depths as verified after sawing, were found 4.1 in. at the support and 4.3 in. at the mid-span sections. This would mean that the secondary prestress moments set up were in excess of what is required according to the theory set out in Section 6.3.

It was also found that grouting was not efficient through the central duct of this beam; the left hand span was especially bad. Further, this was the author's first beam of the series, and the two spans were loaded by a single hydraulic cabinet, so that as soon as the first hinge was formed in the left hand span, the total load applied to the structure was determined by the response of the left hand span. The result was the left hand span ruptured at a load of 6,640 lb. Full redistribution was not complete; the ultimate load carried was 94.7% of the full plastic load. This was considered to be the result of bad grouting and loading arrangement, and will not be discussed further.

The load-moment relationships for these beams are given in Figures 7.10 and 7.10a. Figure 7.10a is same as graph 25 of reference 37 and has been reproduced with the vertical scale halved so as to facilitate comparison with the author's test results for beam B-1. The curvature and concrete compressive strain (extreme fibre) distributions along beam B-1 at a load of 0.945 W_u are shown in Figure 7.32.

This test demonstrated, at least qualitatively, that secondary prestress moments play an important role in the ultimate load behaviour of a statically indeterminate prestressed concrete structure. Taylor[58] pointed out the effect of secondary prestress moments on the disproportion factor at the Symposium on the Strength of Concrete Structures, London, May 1956. The true significance of these moments was, however, not appreciated at this Symposium[59]

These two beams were designed for practically the same ultimate load, and the best way of comparing the redistribution in the two cases is to compare their load-deflection curves (W/W_u versus δ), but the load-deflection curve for beam CB-1 is not available. The load-deflection curve for the author's beam B-1 is given in Figure 7.20. However, the measured rotations for each critical section are available for beam CB-1, and therefore redistribution

in this case has been assessed by comparing the load-rotation curves for the span section, see Figure 7.19. The points between which the rotations were measured by Raina, and the author were not identical, although they were close to the same sections. The comparison between the relationships shown in Figure 7.19 should therefore be taken as approximate. However, it does demonstrate that the deformations in a structure with secondary prestress stress-resultant distribution set up as proposed in Section 6.3 are less compared to those in the corresponding structure with a concordant cable profile.

The crack patterns of these beams are shown in Plate 7.5, which shows that cracks were spread over a longer length at each of the critical sections of beam CB-1 (concordant).

Beam B-2 and B-3

Both these beams had the same effective depth of 4.3 in. at each critical section and were prestressed with the same effective prestress, so that the geometric properties of all the critical sections were similar. The cable profile in between the critical sections was varied (see Figure 7.4) by means of equation 6.9 such that no secondary prestress moments were set up in beam B-3, and secondary prestress moments set up in beam B-2 were +17,300 lb in. at the support section and +8,650 lb in. at the mid-span sections.

Beam B-2 carried an ultimate load of 7,760 lb and failed by practically the simultaneous crushing of concrete at the critical sections B and D'. On the other hand, in beam B-3 first crushing of concrete started at B, which took place at a load of 7,600 lb, and the beam finally failed at a load of 8,220 lb by the crushing of the concrete at D. Theoretically, beam B-2 should have carried a higher ultimate load but the experimental ultimate load was higher for beam B-3. This was an experimental

scatter normally expected in concrete structures. The fact that beam B-2 carried the ultimate load with full-redistribution and beam B-3 with over-redistribution is clearly borne by their load-moment relationships (see Figures 7.11 and 7.12). When beam B-3 was carrying the ultimate load, the moment at the first hinge was reduced below its maximum value. Since there was not a conspicuous decrease in moment at the critical section B, the ultimate load carried by beam B-3 was not different from its plastic load. If the measuring instruments were not sensitive enough, then the effect of over-redistribution in this case could have remained unnoticed and mistaken for full-redistribution, as pointed out in Chapter 5.

Beams B-2 and 3 were similar to the four beams tested by Naughton, except that beam B-2 was tested with certain secondary prestress moment distributions set up, whereas the other beams were tested as concordant beams. Naughton concluded that the variation of cable profile in between the critical sections did not affect the behaviour of the beams. It means that the simultaneous formation of hinges in author's beam B-2 was due to the setting of secondary prestress moment distribution and supports the theory set up in Section 6.3.

The load-deflection curves (W/W_u versus δ) for beams B-2 and 3 are given in Figure 7.20, which confirms the theory set out in Section 6.4. The curvature and concrete compressive strain (extreme fibre) distributions along beam B-2 at a load $0.983 W_u$ are shown in Figure 7.33 and those for beam B-3 at a load of $0.953 W_u$ in Figure 7.34. They also show that beam B-2 carried the ultimate load with less deformations than beam B-3.

The crack patterns of these beams are shown in Plate 7.5, which shows that cracks were spread over a longer length at each of the critical sections of beam B-3 (concordant).

Beam B-4 and LaGrange's beams 159, 165 and 182

Beam B-4 was loaded at the centre of one span only and was similar to LaGrange's beams 159, 165 and 182. Beam B-4 had the same effective depth of 4.3 in. at the critical sections D and B and constituted a more severe case than any of LaGrange's beams which had either a concordant cable profile (beam 159) based on the working load stress-resultant distribution or a linearly transformed profile obtained from the parent concordant profile. LaGrange's beams failed by the crushing of the concrete in the span only; the moment reached at the support section at collapse varied from about 0.93 to 0.96 of the ultimate apparent moment and the ultimate load was always less than the plastic load. The author's beam B-4, on the other hand, failed at a load of 8,060 lb by practically the simultaneous crushing of the concrete at both the support and the span, and the beam carried full plastic load. Beam B-4, as mentioned in Chapter 7, had the cable profile in between the critical sections varied (see Figure 7.4) and a secondary prestress moment of -57,560 lb in. at the support section and -28,780 lb in. at the span sections were set up. This test again confirmed the theory set out in Section 6.3.

The load-moment and load-deflection curves for beam B-4 are given in Figures 7.13 and 7.20 respectively; the curvature and concrete compressive strain (extreme fibre) distributions along the beam at a load of 0.945 W_u in Figure 7.35, and the crack pattern under near maximum load in Plate 7.5.

Frames F-3, 4 and 5

All these frames had the same prestress and same effective depth of 4.1 in. at all the critical sections involved in the equilibrium criterion, i.e. at A, C, D and E, but they were prestressed and designed so that the secondary prestress moments given in Table 7.3 were set up. Frame F-3 had an arbitrary

nonconcordant cable profile and was partially stressed on the ground and partially stressed in the test rig; the cable profile in between the length BC was raised so as to result in a reduced stiffness of the transome over the length BC where there was nearly a constant positive bending moment distribution at collapse. However, to ensure that the frame did not have a mode of collapse other than that of frames F-4 and 5, the knee at B was strengthened by an angle iron at the time of testing. Frame F-4 was designed according to the theory set out in Section 6.3 and the secondary prestress moments given in Talbe 7.3 were set up by varying the cable profile in between the critical sections. However, it was not possible to set up the requisite secondary prestress moment distribution within the bounds of the structure. The moments given in Table 7.3 are therefore slightly less than what required according to Section 6.3. Frame F-5 was designed according to the Russian code of practice and the secondary prestress moments given in Talbe 7.3 were set up as a result of partially stressing the structure in a statically determinate state and partially in statically indeterminate state. The secondary prestress moments required to correspond to the ultimate load stress-resultant distribution scaled down in the ratio of cracking load to ultimate load could not be set up within the bounds of the structure, and the secondary prestress moments given in Table 7.3 are slightly less than what required according to the Russian specifications. The cable profiles employed in the three frames are shown in Figure 7.5.

Frames F-4 and 5 failed through the beam and sway mechanism by the crushing of the concrete at A, C, D and E; the ultimate loads carried were 3,960 and 3,970 lb respectively, which were nearly equal to the corresponding plastic loads. In frame F-3 at a load of 3,850 lb i.e. 97.8% of the plastic load there were no signs of crushing at C, although excessive crushing had already started at A, D(D_2) and E and the beam had swayed

horizontally by about 2.7 in., i.e. about 100% more compared to the other frames. At this instant the whole system became so unstable that the load had to be taken off. It will be seen from Figure 7.16 that at this instant the moments at the critical sections E and $D(D_2)$ had already started decreasing and that at A was at its peak with a trend to decrease. It appears to the author that the frame could not take further load since at this instant condition given by equation 5.8 was reached. Frame F-3 differed from frames F-4 and 5 in the sense that the secondary prestress moment at C was set up in a direction opposite to the direction of elastic moment at C due to applied loads and the transome was made flexible by virtue of positioning of the cable profile. Frame F-3 was therefore quite an extreme case to carry ultimate load with full-redistribution and it should not be surprising that it did not carry full plastic load. Its behaviour, however, confirms author's postulate set out in Chapter 5.

The ultimate load behaviour of frames F-4 and 5 was essentially the same; the moment at collapse at each of the critical sections forming the collapse mechanism was practically equal to its ultimate flexural strength (see Figures 7.17 and 7.18). The only difference was in the order of first cracking at the various critical sections and the order of formation of hinges (crushing of concrete). The order of formation of hinges in frame F-4 was C, E, A, $D(D_1$ and $D_2)$ whereas in frame F-5 it was E and D_2, A and C; the first hinge in frame F-4 was formed at a load of 3,775 lb and that in frame F-5 at a load of 3,750 lb. Compared to this, the first crushing of the concrete in frame F-3 took place at $D(D_2)$ and E and at a load of 3,475 lb only.

The secondary prestress moment distribution was appreciably different in the three frames, and the variation in the order of first cracking at the various critical sections and the formation of hinges can be attributed to this. The similarity

of the ultimate load behaviour of frames F-4 and 5 can be explained by the fact that the secondary prestress moment went some considerable way is satisfying equations 6.2. Neither case was the required one for theoretical full-redistribution, but both cases could correspond to over-redistribution which had an ultimate load nearer the plastic load, and which was less severe than that of the corresponding structure with a concordant profile or a profile as that of frame F-3. This view is confirmed by the load-deflection curves of the three frames (See Figures 7.23 and 7.24).

The fact that the deformations at ultimate load were least in frame F-4 and maximum in frame F-3 is clearly brought out by their load-deflection (W/W_u versus δ) relationships, according to which the horizontal and vertical deflections at the ultimate load in frames F-3 to 5 were 2.74 and 1.35, 1.18 and 0.94 and 1.40 and 0.98 in. respectively. The formation of hinges was also spaced slightly more closely in frame F-4 and 5 than in frame F-3 (see Figures 7.16 to 7.18).

At the time of collapse there were distinct signs of crushing of concrete at each of the critical sections forming the collapse mechanism. At node D crushing was observed both in the transome and the column in frame F-4, but in frames F-3 and 5 it was seen in column only, which, as verified by sawing the transome and the column at D_1 and D_2 after testing, was the result of bad grouting in the columns of frames F-3 and 5 near the critical section D.

The deformed shapes and crack patterns of these frames under near maximum load are shown in Plates 7.8 to 7.10 inclusive, and the curvature and concrete compressive strain (extreme fibre) distributions along the frame under near maximum load in Figures 7.38 to 7.40 and 7.43 inclusive. The crushing of the concrete seen at B in frame F-3 took place during unloading of the frame and should not

be taken into account. It will be seen that cracking at the dry mortar joints was confined to a single crack which was as wide as $\frac{3}{8}$ in. in certain cases. Cracking in the transome was spread over a longer length in frame F-3, which, as mentioned above, was the result of its reduced stiffness.

A comparison of the above frames with those tested by LaGrange[14] shows that the difference in the two series was that certain precalculated secondary prestress stress-resultant distributions were set up in the author's frames, which, in the author's view led to near full-redistribution in his frames F-4 and 5.

Frames F-1 and 2

Frame F-1 was designed in the conventional manner on the basis of working load stress-resultant distribution with a concordant cable profile. The cross sectional area of concrete and prestress in all the members were same as those in frames F-3 to 5. The effective depths at the critical sections A, B, C, D and E were 3.31, 3.035, 3.37, 3.75 and 4 in. respectively. Frame F-2 was same as F-1 except that its cable profile was obtained by linear transformation of the concordant cable profile of frame F-1. The effective depths so obtained in frame F-2 at the critical sections A, B, C, D and E were 4.1, 1.8, 2.575, 4.1 and 4.1 in. respectively. The cable profiles in between the critical sections were straight in both the frames and can be seen in Figure 7.5.

Both frames F-1 and F-2 failed as a beam and sway mechanism by the crushing of the concrete at A, C, D and E (see Figures 7.14 and 7.15 and Plates 7.6 and 7.7); the ultimate loads carried were 3,160 and 3,180 lb respectively, which were nearly equal to the corresponding plastic loads. The similarity of the ultimate load can be attributed to over-redistribution which had an ultimate load very near to the plastic load. This, for

frame F-2 can be clearly seen in Figure 7.15. At ultimate load the moment at the critical section C was well past the maximum moment and those at the other critical sections were slightly under or equal to their maximum moments.

The loads at which the first cracking at the various critical sections was seen differed slightly in the two frames, but the order of formation of hinges was practically the same. The first hinges in frame F-1 were formed at A, D_2 and E at a load of 3,080 lb and additional hinges at D_1 and C, whereas the first hinges in frame F-2 were formed at D_2 and E at a load of 3,060 lb and additional hinges at A and C. This similarity of behaviour was the result of linear transformation which although changes the characteristics of the critical sections also sets up secondary prestress stress-resultant distribution accordingly.

The load-deflection curves for frames F-1 and 2 are given in Figures 7.21 and 7.22, and the curvature and concrete compressive strain (extreme fibre) distributions along the frames at under near maximum loads in Figures 7.36, 7.37, 7.41 and 7.42.

The crushing of the concrete at node D was observed in both the frames in both the transome and the column.

Compared with the ultimate loads carried by frames F-4 and 5, the ultimate loads carried by frames F-1 and 2 are only 80%. This shows that by designing the frame according to the theory set up in Section 6.3, or according to the Russian code of practice an additional output of 25% can be obtained from the same concrete and prestress.

6.7 EFFECT OF TIME ON REDUNDANT REACTIONS DUE TO PRESTRESS IN FRAME F-5

The secondary prestress stress-resultant distribution in frame F-5 was set up as a result of partially stressing it in a statically determinate state with mechanical hinges placed eccentrically,

and partially in a statically indeterminate state. The reactions set up in the statically determinate state are reduced in time due to linear creep. With a view to study the variation in such reactions with time, frame F-5 was left untested for two months after final stressing and the reactions were measured regularly at each foot of the frame. The horizontal and vertical thrusts and moment measured at the right foot are plotted versus time in Figure 7.46, which shows that with time the vertical and horizontal thrusts tended to reduce, whereas the moment started increasing. Such studies, to the author's knowledge, have not been made in the past, except for two-span beams, where there was only one redundant reaction, and it cannot be said whether it was an experimental scatter or an actual phenomenon requiring investigation. In the present case above variations were quite consistent over the whole period except for the first 7 days, which may be the result of losses due to relaxation, shrinkage of grout, etc., and it was assumed that the reactions recorded on the test day were actually available.

6.8 CONCLUSIONS

(1) Linear transformation can result in an ultimate load which is much less than the ultimate load carried by the parent structure with a concordant cable profile. The actual solution can only be obtained by considering both the 'equilibrium' and the 'compatibility' criteria.

(2) The author's tests on two-span beams and fixed portal frames show that a statically indeterminate prestressed concrete structure, in general, carries ultimate load with over-redistribution and rarely with full-redistribution, unless specially aimed at.

(3) The secondary prestress moments play an important role in the behaviour of a statically indeterminate prestressed concrete structure; and if set up as suggested in Section 6.3, they can create conditions so that the structure carries the ultimate load by simultaneously developing the maximum moment of resistance at each of the critical sections which form the collapse mechanism, and at the same time maximum output from each critical section is ensured.

(4) The deformations of such a structure at collapse are less compared to those of the corresponding structures which carry the ultimate load with over-redistribution.

(5) The conventional method of design of statically indeterminate prestressed concrete structures based on the working load stress-resultant distribution with a concordant or a linearly transformed cable profile is not, in general, economical.

CHAPTER 7

AUTHOR'S TESTS ON PRESTRESSED CONCRETE TWO-SPAN BEAMS AND FIXED PORTAL FRAMES UNDER MONOTONICALLY INCREASING LOAD

7.1 OBJECT AND SCOPE

The overall objective of this investigation was to study the effect of secondary prestress, and to compare the ultimate load behaviour of statically indeterminate prestressed concrete structures designed according to the theory presented in Chapter 6 with those designed in the conventional manner, or according to the Russian practice.

An ideal test-programme for such an investigation would have consisted in testing to destruction a large number of different types of structures for various loading conditions and designed according to different methods, but this would be beyond the scope of any one thesis. The test-programme was therefore restricted according to the available time, and the facilities available in the laboratory, but at the same time it was ensured that it covered a representative range of statically indeterminate structures. From the point of view of mode of collapse, indeterminate skeletal structures can be classified as:

(1) Continuous Beams and
(2) Frames.

The collapse mechanism of a continuous beam is a special case in that collapse occurs, in general, with the formation of three hinges in any one span. The partial mechanism thus formed can only be combined with other partial mechanisms in other spans The failure mechanism for frames, on the other hand, can either be complete or partial, but, in any case, is a combination of the basic mechanisms.

The test-programme was therefore designed to consist of (1) Series A - Continuous Beams and (2) Series B - Frames. The structures included in each series were designed according to the

(i) conventional method with concordant or linearly transformed cable profile;
(ii) theory presented in Chapter 6; and
(iii) Russian practice.

Because of the limited period of availability of the test rig, the Russian method could not be applied to test-series A.

For Series A, it was thought advisable to extend the test-series recently carried out in the Department by Raina[37]. This test-programme consisted of two-span beams loaded at the centre of each span; the beams had either concordant or linearly transformed cable profiles designed in the conventional manner. This had the advantage that, without duplicating the work, a comparison was made between the behaviour of beams designed by the different methods. To cover more severe conditions, in one of the beams load was applied in one span only. The loading arrangements are shown in Figures 7.1 and 7.2.

The simplest frame structure which may fail by the combination of basic mechanisms with the total number of hinges greater than three is a portal frame with fixed ends. Therefore test-series B consisted of fixed portal frames loaded proportionally as shown in Figure 7.3. All reported experiments on the prestressed concrete continuous structures where detailed stress-resultant-deformation studies have been made, to author's knowledge, consist of two and three-span beams only, and therefore, in addition to fulfilling the above objective, the proposed tests were also intended to throw some light on the ultimate load behaviour of such structures, about which little experimental evidence is, at present, available.

The most common method of setting up a secondary prestress stress-resultant distribution is through linear transformation of a concordant

cable profile. This method has the disadvantage that the effective depths of the critical sections are also changed. Thus two effects have to be studied simultaneously, a fact which may lead to error. Such studies in the past have led to conclusions[59] which are not confirmed by the present investigation. In order to study the effect of secondary prestress, it was considered necessary to maintain the geometric properties of the critical sections constant whilst the secondary prestress stress-resultant distribution is set up. Tests on frames F-3 to 5 (labelling of the test frames has been described in Section 7.3) provided sufficient data for such a study and no additional tests on this account were included in test-series B. In test-series A, such studies were made for two cases, namely

(i) beams designed on the basis of stress-resultant distribution at working load; and

(ii) beams designed by aiming maximum output at ultimate load from all the critical sections forming the apparent collapse mechanism.

The effective depths at the critical sections in case (i) were fixed on the basis of working load design outlined in Section 2.5, whereas in case (ii) each critical section forming the apparent collapse mechanism had the maximum effective depth that could be conveniently accommodated. In either case the cable profile in between the critical sections was so varied that secondary prestress moments as given in Table 7.2 were set up.

7.2 GENERAL DESCRIPTION OF BEAMS

Reference will be made to five continuous beams tested by Raina[37] and four tested by the author. Raina labelled his beams as

CB-1 to 5 and they will be referred to here also by the same labelling. The author's beams have been labelled B-1 to 4.

All beams had a constant rectangular section, 6 x 4 in. overall and, except B-4 where the load was applied at the centre of one span only, were loaded at the centre of each span. Each beam measured 19 ft 6 in. overall and consisted of two 9 ft spans, and 9 in. overhang at either end support.

Each beam was provided with the same shear reinforcement as used by Raina, so as not to make it a variable parameter; it consisted of two rows of $\frac{1}{4}$ in. diameter mild steel bent into a sinusoidal wave form with peaks at every 10 in. centres, thereby giving 2 legs every 5 in. This arrangement had the advantage that it avoided the lateral confining effect of usual stirrups. To avoid any failure in anchorage zones, 6 in. length at either end of each beam was reinforced with nominal grills made from the steel used for shear reinforcement.

6 in. cube strengths of concrete used in beams CB-1 to 5 were 8,000, 7,760, 7,860, 7,730 and 7,910 lb/in^2 respectively and those for beams B-1 to 4 are given in Table 7.1, along with the strengths of other control specimens.

Each beam was post-tensioned with three 0.276 in. diameter wires in circular duct-tubing such that a total effective prestress of about 18,390 lb was available on the day of test. Beams CB-1 to 5 were designed in the conventional manner, that is the cable profile was based on the stress-resultant distribution at working load. CB-1 had a concordant cable profile and CB-2 to 5 had linearly transformed profiles obtained from the cable profile of CB-1; the cable profile in each beam between the critical sections was straight. Beam CB-1 had an effective depth of 4.46 in. at the support section and 4.20 in. at the mid span sections. The corresponding depths for beams CB-2 to 5 were 5.00 and 3.93, 5.50 and 3.68, 3.00 and 4.93, and 1.86 and 5.50 in. respectively.

The effective depths at the critical sections of beam B-1 were fixed as those of CB-1, that is 4.46 in. at support section and 4.20 in. at the mid span sections, but the cable profile was varied such that requisite secondary prestress stress-resultant distribution was set up. In beams B-2 to 4 the effective depth at each critical section was kept same equal to 4.3 in. and the cable profile in between the critical sections varied to obtain the requisite secondary prestress stress-resultant distribution. In beam B-4, within the bounds of the structure, it was not possible to set up the requisite secondary prestress stress-resultants by the variation of cable profile, and the difference was set up by the adjustment of the support levels at the time of placing the beam in the test-rig. The cable profiles employed in beams B-1 to 4 are shown in Figure 7.4. Details of the effective depths at the critical sections, together with the secondary prestress moments set up, are summarised in Table 7.2.

7.3 GENERAL DESCRIPTION OF PORTAL FRAMES

Five portal frames labelled F-1 to 5 were cast and tested. The frames were made up of five precast elements, the transome, two columns and two base feet. All members were of rectangular section, the transome and columns 6 x $3\frac{1}{2}$ in. overall, the base feet $15\frac{1}{4}$ x 6 in. overall with a 3 in. deep tapered slot at the centre of the bottom face in full width. This slot was provided to accommodate the prestress bearing plate and anchors, and thus keep them clear of the top plate of the reaction-transducer; it had a width of $6\frac{1}{4}$ in. at the inside face and $6\frac{3}{4}$ in. at the transducer face. Each base foot had a length of 3 ft 2 in. and was reinforced longitudinally with 4 No. $\frac{1}{2}$ in. diameter mild steel bars at both top and bottom and was reinforced transversely with common two-legged stirrups made from $\frac{1}{4}$ in. diameter cold worked steel at $2\frac{1}{2}$ in. centres. To avoid any anchorage failure, reinforcement designed according to C.and C.A. Report No. 9[60] and

13[61] was provided in the central 6 in. width. General view of the reinforcement arranged for frame F-1 is shown in Plate 7.1.

The precast elements were made continuous by post-tensioning with joints formed of $\frac{1}{2}$ in. dry mortar packing. The height from the top of the base feet to the centre line of the transome was 4 ft 6 in., the span between the column centre lines was 9 ft.

Shear reinforcement was calculated according to MacGregor[62] for frame F-4, which was expected to carry the maximum load, and provided in all frames so as not to make it a variable parameter and avoid any shear failure. It consisted of a single row of $\frac{1}{4}$ in. diameter mild steel bent into a rectangular wave form with peaks at every 8 in. centres, that is one leg every 4 in. This arrangement had an additional advantage over the sinusoidal wave form that all legs were vertical and did not contribute anything towards resisting longitudinal bending moment.

The end six inches of all transomes were reinforced with nominal grills made from 3/16 in. diameter mild steel to avoid any anchorage failure. In frames F-1, 2 and 4 no reinforcement other than the above was provided, but in frames F-3 and 5, which were intended to be stressed with mechanical hinges at the column junctions with the base feet and at the right hand end of the transome, the end six inches of the columns adjacent to these points were also provided with nominal 3/16 in. diameter mild steel grills to avoid any accidental cracking during the first phase of stressing. This could result in certain confining effect on concrete but was ignored, since we were more interested in the lengths immediately adjacent to the junctions, where it was only dry mortar packing.

All frames were loaded by a vertical load at the mid point of transome, and a horizontal load acting from left to right at the

level of the centroidal axis of the transome. The design ratio of the horizontal load to vertical load was 1.5 throughout. Frames F-1 and 2 were designed in the conventional manner with cable profiles based on the working load stress-resultant distribution. F-1 had a concordant cable profile and F-2 a linearly transformed one obtained from F-1. Effective depths at the critical sections are given in Table 7.3. The cable profile in between the critical sections was straight. Frame F-3 was originally intended to be stressed according to the Russian practice. However, it was subsequently decided to use the last frame in the test series for the Russian method so that a study could be made of the effect of creep on the secondary prestress stress-resultant distribution set up as a result of partially stressing it in a statically determinate state. Frame F-3 was then treated as a test specimen with an arbitrary non-concordant cable profile. It had the same effective depth, 4.1 in., at all the critical sections forming the apparent collapse mechanism as that in frames F-4 and 5, but, unlike F-4 and 5 which had stiff transomes, it had a flexible transome, by virtue of cable positioning. The test on such a frame was considered to provide suitable data for studying the problem of redistribution. The secondary prestress stress-resultant distribution in F-3 was kept appreciably different from those in F-4 and 5 by stressing the transome separately on the ground. In frames F-4 and 5 the effective depth at each critical section of the apparent collapse mechanism was kept the same, that is 4.1 in. so that maximum output could be obtained at ultimate load. The cable profile in between the critical sections was varied as shown in Figure 7.5 to obtain the requisite secondary prestress stress-resultant distribution.

All frames were stressed with a nett total prestress of 18,000 lb such that after losses an effective prestress of about 17,000 lb was available on the day of test. Frames F-1,2 and 4

were fully stressed in a single stage after dry mortar packing the junctions between the precast elements. The transome of F-3 was stressed and grouted on the ground and frame erected. The junctions of the precast elements were then dry mortar packed and the columns stressed in a single stage. Frame F-5 was stressed in three stages. Its transome was first stressed and grouted on the ground and the whole frame erected with mechanical hinges firmly glued at places shown in Figure 7.6. The junction between the column and the left hand end of the transome was then dry mortar packed and each column stressed in a statically determinate state with a nett prestress of 9,000 lb. The junctions of the precast elements where mechanical hinges were inserted were then packed with dry mortar, and the columns further stressed in the statically indeterminate state to a nett total prestress of 18,000 lb.

A summary of the secondary prestress moments set up at the critical sections forming the apparent collapse mechanism is given in Table 7.3, together with the effective depths.

The section 6 x $3\frac{1}{2}$ in. for members was chosen such that it was a fairly reasonable representation of the practice in industry for such structures, and had an average compressive stress of about 800 lb/in^2 due to prestress.

7.4 MATERIALS AND THEIR PROPERTIES

Rapid hardening cement (ferrocrete) was used for casting of all beams, and frames F-4 and 5, and in dry mortar packing. Frames F-1 to 3 were cast with ordinary Portland cement. Cement Fondu was used for grout.

Thames valley river aggregates were used throughout. The maximum aggregate size was $\frac{3}{8}$ in. except for beam B-1 where it was $\frac{1}{2}$ in., as used by Raina. The aggregate was obtained by mixing 55 parts by weight of $\frac{3}{8}$ in. down to 3/16 in. with 45 parts by weight

of 3/16 in. down to No. 100. The latter was obtained by mixing three parts by weight of 3/16 in. down to No. 25 with one part by weight of No. 25 down to No. 100, and it also constituted sand used for dry mortar packing.

The concrete was designed to have a 56 day 6 in. cube strength of 9,000 lb/in^2 and 6 in. diameter by 12 in. cylinder strength of 6,000 lb/in^2. The aggregate cement ratio was 4.0 and the effective water cement ratio 0.515. The dry mortar packing had a sand cement ratio of 2.0 and water cement ratio of 0.36. The grout had a water cement ratio of 0.375 for the frame members and 0.40 for the beams, and in both cases a commercial expanding agent was used.

Each beam and control specimens were cast with two batches, and each frame and control specimens with three batches of concrete. The control specimens were 3 No. 6 in. cubes, 3 No. 6 in. diameter by 12 in. cylinders and 3 No. 4 x 4 x 20 in. prisms. The results of all the control specimens tested one day after the major test are given in Table 7.1. The beams were cast in two layers; the first batch was used for the lower layer and 1 No. cube, 2 No. cylinders and 1 No. prism and the second batch for casting the upper layer and remaining control specimens. In the case of the frames the first batch was used for one of the base feet and 1 No. cube and 1 No. prism. The second batch was used for casting the transome, columns, and 2 No. cubes, 2 No. cylinders and 2 No. prisms. The third batch was used for casting the other base foot and the remaining control specimens.

The 0.276 in. diameter high tensile steel wire used was manufactured by Richard Johnson and Nephew Ltd. It was tested in the laboratory; the load-extension curve obtained was identical to that provided by the manufacturer. The material characteristics and the load-strain curve are given in Figure 7.7.

Corrugated C.C.L. duct-tubing was used in the beams, which had practically no strength; but for the frames the only commercially available $\frac{1}{2}$ in. outer-diameter duct tubing was the seamless cold-drawn

tube. This had much greater strength (ultimate 1.64 tons) than was desired. It was accepted on grounds of delivery, cost and the fact that it was discontinuous at the column junctions, and at the other critical sections located in the transome, it would be made discontinuous by sawing it through and connecting the two ends by means of rubber tubing, as seen in Plate 7.1.

The $\frac{1}{2}$ in. diameter steel used as longitudinal reinforcement in base feet, and $\frac{1}{4}$ in. diameter steel used for shear reinforcement in all members other than base feet was all mild steel with yield stresses of 48,700 and 66,200 lb/in^2 respectively. The $\frac{1}{4}$ in. diameter cold-worked steel used for shear reinforcement in base feet had a 0.2% of proof stress of 56,000 lb/in^2.

7.5 MANUFACTURE AND CURING

All members were cast in rectangular steel moulds consisting of 3/16 in. thick channel sections for bottom shutter. The beams were cast on a 4 in. face, as done by Raina. This, although somewhat unsatisfactory as explained later, was accepted since these beams were also intended for a comparative study with Raina's beams. All frame members were cast on their side, that is on the 6 in. face for the reason that, unlike simply supported beams, the same member had different compression or tension faces at adjacent critical sections. For example, the compression face at the mid span of the transome becomes the tension face at the ends. If such members were cast on the bottom $3\frac{1}{2}$ in. face, then conditions obtainable in the compression faces of two adjacent critical sections would have differed, since the compression face which had formed the bottom part during casting was well compacted, whereas the compression face which formed the top part during casting was rather less compacted. Steel moulds with 6 in. width and $3\frac{1}{2}$ in. depth were not available in stock, and one was obtained by packing the lower $3\frac{1}{2}$ in. depth of the 7 x 6 in. mould with timber treated with three coats of plastic paint. It was

important that timber formed a flat bottom with depth of the mould above the top of the timber as $3\frac{1}{2}$ in. To achieve this for subsequent castings, the timber had to be replaned, reset and repainted every time.

The cable profiles changed directions frequently and sharply in the test specimens. It was of the utmost importance that all duct-tubing was accurately positioned. To this end, special types of duct-holders as shown in Plate 7.2 were devised. Type A and B were used for the beams; type A where the duct-tubing was required to be supported from dropping down and type B where the duct-tubing had a tendency to lift. Type C and D were devised for the frames; type C for the transome and type D for the columns.

The positioning of the duct-tubing in the beams was carried out as follows. The base shutter was placed level with an approximate height of 8 in. clear of the ground. Wherever the profile changed direction, holes were drilled in the base plate to receive duct-holders. Type A duct-holders were then held at the requisite heights, and loosely locked by means of two nuts, one at the top and another at the bottom of the shutter. Three lengths of C.C.L. duct-tubing (which was $\frac{5}{8}$ in. diameter for beams B-1 and 2 and $\frac{3}{4}$ in. diameter for B-3 and 4) through which prestressing wires had previously been passed, were laid on the holders already fixed, and held by means of thin binding wire. Type B duct-holders passing over the duct-tubing were then fixed at the requisite heights, and locked like type A. The heights of all duct-holders were again checked, and adjustment, if any, made before finally locking them firmly. The shear reinforcement, which was bent previously, was laid and held by tying it with the duct-holders. The steel cages for the end blocks were then slipped from the ends, and side shutters erected and bolted. The end plates, which were previously drilled accurately, were also likewise slipped from the ends, and bolted.

For the frames, the positioning of the column duct-tubing which was in the transome end blocks and base feet posed a further practical problem. It was of the maximum importance that all such

duct-tubing was very accurately positioned so that the correct mating and alignment took place on assembly. To this end, special type of mild steel buttons which had a depth of $\frac{1}{2}$ in. and diameter equal to the internal diameter of the duct-tubing were made. Wherever the column duct-tubing passed through the transome or the base feet, these buttons were screwed down to the inner faces of the side shutters through holes previously drilled in an accurate manner. Exact lengths of such duct-tubing were sawn and slipped on to the buttons while erecting the side shutters. This arrangement worked very satisfactorily, and it was possible to assemble frames to an accuracy of $\pm\frac{1}{8}$ in., as ascertained by measuring the lengths of two diagonals.

The duct-tubing was held to the required profile by means of the duct-holders placed wherever the profile changed direction. In the transome at the mid span and the end critical sections the discontinuity, similar to that obtainable at the column junctions, was affected by laying the duct-tubing in four pieces connected by rubber tubing; two central pieces of about 54 in. and two end pieces of 6 in. were used. To hold these pieces in correct alignment additional duct-holders were necessary, which were placed sufficiently away from the critical sections. The duct-tubing was somewhat stiff to be aligned to the correct profile through tensioning of the duct-holders, especially where it had sharp curvatures. In such cases, it was roughly bent to the required profile on the ground, and the final alignment obtained by applying tension through the duct-holders. In frames F-1 to 3 the column duct was straight, and no duct-holder was used. Mild steel rods $\frac{3}{8}$ in. diameter and threaded at both ends were passed through the duct-tubing and tensioned against the shuttering. These rods had a two-fold purpose; to keep the tube positioned in the end plates and to stiffen and position the tube along the length.

The process of erecting shutters for the frame members was similar to that described for the beams. The important difference was

in the manner of holding the duct-holders. Unlike the beam duct-holders, they were held through the side shutters. Two lengths of duct-tubing, through which the prestressing wires had previously been inserted, were passed through the duct-holders positioned close to their intended locations. The duct-holders were then held to one of the side shutters clamped to the base shutter. The other side shutter was slowly brought near, care being taken that the studs of the duct-holders passed through their respective holes and the column duct-tubing, if any, slipped over its respective button. A general view of the formwork for frame F-1 ready for casting is given in Plate 7.1.

The concrete was mixed in a five cubic feet horizontal drum type mixer. 'Allam' external vibrators were used for the beams, and 'Tremix' internal poker vibrators for the frame members. The control specimens were cast at the same time. The cylinders were cast with about 3/16 in. depth unconcreted for capping, which was done next day with plycolay. The specimens were covered with wet hessian and plastic sheeting for about 48 hours after which the side shutters were removed and wet hessian and plastic sheeting replaced. After a total of seven days the members were removed from the shutters and left to air dry. Because of long lengths, the beams were removed from the base shutter after applying a nominal prestress, and lifting them at four points by a special carrier beam.

Owing to the complex nature of the project, it was not possible to test the specimens at the same age. The beams, and frames F-4 and 5, which were tested comparatively at an early age, were cast in rapid hardening cement such that all specimens had approximately the same strength on the test day.

To check the effectiveness of the duct-holders, certain sections of both beams and frames were at random chosen and sawn after tests. Maximum variation in the effective depths from the intended values was less than 2%. This was considered very satisfactory and further verification of the effective depths was not considered necessary.

7.6 PRESTRESSING

Prestressing of the frames was carried out in the test rig and the redundant reactions set up due to prestress were measured. The beams were tested in the rig belonging to the Engineering Structures Section of the Department. The rig was available for a short period, just sufficient for testing only. The prestressing and grouting of the beams was therefore carried out before hand outside the rig. In beams B-1, 2 and 4 large secondary prestress moments creating tensile stresses greater than the permissible values were set up. These beams required special care during stressing and transportation. The beam with nominal prestress was placed on three temporary supports in practically the same manner as that designed for the test, and stressing carried out. As prestressing continued, precalculated dead weights were gradually applied at about 6 in. off the centres of the spans so that at no stage excessive stresses were created. The beam was grouted next day in the same position. It was unwieldy to transport the beam along with the dead weights. While transporting, the dead weights were replaced by small screw jacks at the centres of the spans. These jacks were previously calibrated in the standard Amsler compression machine and tensioned against the carrier beam, so that they applied the required load on the specimen. The beam was transferred and aligned in the test rig with the screw jacks and carrier beam in position. The screw jacks were removed only after applying the equivalent dead weights at 6 in. off the centres of the spans. These dead weights were allowed to remain until the load applied during the test was sufficient to keep the stresses due to prestress within the permissible limits.

The prestress was measured throughout by using a previously calibrated force transducer between the stressing jack and its quick-release grip. The prestressing wires had sharp curvatures, and it was desired to verify the prestress applied at the critical sections.

To this end, PL30 electrical strain gauges manufactured by Messrs. Tokyo Sokki Kenkyujo Co., Limited were fixed to the prestressing wires of beams B-1 and 2. In each beam three wires in a single horizontal layer were used. It was preferred to fix gauges to end two wires. Two gauges at 4 in. on either side of each critical section, that is in all six gauges for each wire were used. The gauges were waterproofed and mechanically protected by using Fleming compound. No special exits were provided for the leads; they were taken out through the duct-tubing and a groove in the concrete face of the bearing plate, and connected to an amphinole plug fixed to the bearing plate. The gauges were primarily used for measurement of strain at the time of stressing, but it was also hoped to obtain a strain history during loading. Readings were taken by means of a Peekel strain box connected through a multi-switch junction box. Some of the gauges were damaged at the time of stressing; the record obtained from the remaining ones was also inconclusive. Recourse was therefore taken to verify friction losses in some other way. It was done by applying the requisite prestress at one end and measuring the available prestress at the other end by means of another jack and force transducer. After applying the requisite prestress at one end, the other end of the wire was pulled by using a special restressing stool designed to fit the wire layout. As soon as the anchor started pulling away from the bearing plate, which was verified by using a 0.0015 in. feeler gauge, the force in the force transducer at this end was measured. The difference accounted for the losses due to friction and elastic shortening, and compared favourably with the theoretically calculated figure based on the coefficients given in B.S. Code No. 115[63]. As a further check extension was also measured, which tallied within reasonable limits with the calculated one. In all subsequent work losses were calculated theoretically, and prestress applied accordingly.

A number of reasons are possible for the inconsistent behaviour of the electric strain gauges fixed to the prestressing wires; the technique of fixing gauges; the high values of strain; etc. The Fleming compound or any other similar compound used to protect the gauge makes a firm contact with the gauge and leaves an undulating surface at the outside. Such a surface, if it comes in contact with the surface of the duct-tubing during stressing, will exert considerable friction. This, on account of contact between the gauge and the protective glue, will be transmitted to the gauge and upset the strain readings. Because of the sharp curvatures, the chances of the gauge not coming in contact with the duct-tubing were little in the present case, and the above inconsistency can be explained as above. However, before any conclusive evidence is established, some research with improved technique for fixing such gauges will be necessary. One of the ways to improve the technique could be to protect the gauge without subjecting it to frictional force. It is hoped that Price's findings[64] which are aimed at developing such a technique in the Department will be useful for future.

All members except the columns were stressed from both ends. The beams were stressed by first stressing the central wire approximately to its required prestress and anchored off. The other two wires were then similarly stressed and anchored off one by one. The wires were then restressed to the exact value by using the restressing stool and shims of various sizes down to 0.002 in. For the frames the transome wires did not pose any practical difficulty since the two wires were along the minor axis and the wire nearer to the centre of the member was stressed first. The column wires were symmetrical about the minor axis but asymmetrical about the major axis. The stressing of any one wire at a time would have resulted in an asymmetrical prestress causing excessive tensile stresses across the minor axis, especially at the dry mortar joints. This could have been avoided

by stressing both the wires simultaneously by using two jacks. To stress both the columns simultaneously, four jacks were necessary; but only two jacks were available. The stressing of the frame was therefore done in stages. First, about one-quarter of the final prestress was applied simultaneously to the two diametrically opposite wires in the two columns and anchored off. The remaining two wires in the columns were then similarly stressed and anchored off. The transome was then similarly stressed with about one-quarter of its final prestress. The procedure was repeated with half and full prestress by using restressing stool and shims.

Attempts to measure the loss of prestress due to creep and relaxation were inconclusive, and in all work it was assumed that the intended prestress was available on the test day.

7.7 GROUTING

Grouting was carried out by means of a high pressure hand pump through the grout-holes especially provided in the bearing plates. Grouting was done on the day following the final stressing; the time from grouting to testing varied, but in no case was it less than 7 days.

7.8 ERECTION OF FRAMES

The precast frame members were assembled in the test rig. It was of the maximum importance that the reaction-transducers, jacks and the frame all lay in the same plane. The plane of the test rig was established by means of two plumb bobs suspended at about 5 ft 6 in. on either side of the centre line of the rig. Each plumb bob was suspended through a fine hole drilled in the centre of a small bolt which was screwed into the bottom of the rig-transome along its longitudinal axis. These bolts served as permanent marks for all subsequent alignment. The plumb lines

when transferred to the floor, established the line for the reaction-transducers. Further success of erecting the frames correctly depended upon how accurately the two reaction-transducers were aligned transversely, since all subsequent erection was carried out with reference to them. To this effect, transverse lines at 4 ft 6 in. on either side of the centre line and at right angles to the above line were marked. These established the lines along which the longitudinal and transverse axes of the reaction-transducers were aligned and levelled on three levelling screws especially provided for this purpose in their base plates. When the top plates of the two transducers were set to the same level, which was verified by means of a Dumpy level reading up to 0.001 in., the levelling screws were locked and the whole transducer raised on four bolts screwed through holes provided at the corners of the base plate. This enabled plaster of paris, which was laid on polythene sheeting in a thick layer, to be slipped under the base plate. The four bolts were then removed, and the whole transducer was allowed to rest on its levelling screws. The levels were again verified, and the plaster of paris allowed to harden for 48 hours. The transducers were then firmly bolted to the floor by means of box and I-sections. This arrangement was left untouched for all frames.

The base feet were seated on the top of the respective reaction-transducer and aligned both longitudinally and transversely. The tops of the base feet were then levelled both longitudinally and transversely by means of shimming plates used underneath. The levels were checked by means of a Dumpy level and difference, if any, made good by using shims of various sizes down to .005 in. Each foot was then tightly held down to the top plate of the transducer by means of 4 No. $\frac{7}{8}$ in. diameter bolts and 2 No. $\frac{3}{4}$ in. thick plates; see Drawing 7.1. The columns supported on the wedges were then erected vertically with their axes in line with the axes of the base feet

and held down temporarily at about three-quarters height by means of four brackets operated from two angles fixed to the rig. The levels of the column tops were checked and difference, if any, made good through wedges provided at their feet. The transome nominally prestressed previously was then raised on the Sherper hydraulic lift and placed on the top of the columns with $\frac{1}{2}$ x $\frac{1}{2}$ x $4\frac{1}{2}$ in. long metal pieces in between to allow for dry mortar packing. The column wires were then threaded from the top. The transome was then supported on two screw jacks resting on the angle irons fixed to the rig, and destressed. To cover the wires in between the spaces for the dry mortar packing the column duct-tubing was cast $\frac{1}{8}$ in. projecting and on to these 7/16 in. long metal rings were fed before erecting the columns. In frames F-4 and 5, where the cable profile had sharp curvatures, the wires in the column duct-tubing were inserted before casting and the columns erected with the wires inside. The transome in such cases was placed on the column tops by supporting it on the overhead crane as near to the rig as possible and bending the projecting wires such that the transome slid over them, when lowered slowly.

The frame was ready for dry mortar packing. The joint was dry mortar packed firmly in part length with wedges in position, using temporary wooden shutters. When this was slightly set, the wedges were taken out and whole joint dry mortar packed firmly. The curing of the dry mortar packing was carried out for 72 hours by covering it with wet hessian and plastic sheeting. The time of prestressing varied, but in no case it was carried out before 72 hours from the placing of dry mortar packing.

The height, length and diagonal dimensions of all frames were recorded. The maximum difference in the lengths of the two diagonals never exceeded $\pm\frac{1}{8}$ in.

In frame F-5 three mechanical hinges, one at each of the column feet and one at the top of the right hand column, were used, see Figure 7.6. The mechanical hinge used is shown in Plate 7.2. The bottom plates of the hinges were fixed to the base feet at the required eccentricities with certite, and left for a few hours to set. The top hinge-plates were then placed, and the columns erected, as explained above, with wedges in position. The space, if any, between the top hinge-plate and the bottom face of the column was packed with fibre glass and certite. The top hinge was also fixed in a similar manner.

7.9 RIG AND LOADING DEVICE FOR BEAM TESTS

A general view of the test rig is given in Plate 7.3. It was an internal reaction frame. The bottom girder formed the base for the beam supports. The end beam supports had roller bearings, and the central one a rocker bearing such that a symmetrical freedom in the longitudinal movement was possible. Under each bearing, a bearing type force transducer was used to measure the reaction. To avoid any eccentric transfer of load to the transducers, a spherical seating was used at the top of each end transducer; the central transducer, for stability reasons, had the rocker plate tightly fitted. The transducers were positioned at 9 ft centres along the longitudinal axis of the bottom girder and rollers adjusted such that they were immediately above the transducers. This ensured that each span of the beam was 9 ft and loads were transferred centrally to the transducers. All the three supports were then set at the same level by machining the plates resting on the spherical seatings to the exact required thicknesses.

Two jacks were used, which were fixed to the bottom flange of the rig girder. Each jack had an arrangement to move lengthwise and sideways. This enabled the jacks to be moved clear of the beam

while placing it in the rig with the carrier beam on. Each jack was a standard 20 ton Amsler jack coupled to a standard Amsler oil cabinet, which was worked on half range. For beam B-1 both the jacks had a common oil supply, but subsequently each jack was connected to a separate cabinet. For beam B-4, where load was applied in one span only, the second jack was used to hold the outer end of the other span from lifting.

7.10 PLACING OF BEAM IN TEST RIG

The jacks were moved clear of the beam, and the beam together with the carrier beam and screw jacks was placed in the rig. Owing to the long length of the beam, some casting errors were involved and it was not always possible to position it correctly. The criterion used was that the beam centre line should coincide with the centre lines of rollers and rocker to $\pm 1/16$ in. The jacks were again moved and fixed such that they were in the plane of the beam, and the loads were applied at the requisite points. No spherical seating was necessary, since Amsler jacks incorporate ball seatings at either end of the ram. To avoid concentration of stress, 2 x 4 x $\frac{1}{4}$ in. thick mild steel plates with a layer of felt paper at the concrete face were provided under each jack and at the top of each support.

The dead weights were then added, and the carrier beam and screw jacks taken off. At this stage it was important that stress-resultants caused by the self weight of the beam, the applied dead weights, and the secondary prestress were set up in the beam. This was effected by packing steel shims down to .003 in. under the supports. The secondary prestress moments set up at the critical sections are given in Table 7.2.

7.11 RIG AND LOADING DEVICE FOR FRAME TESTS

The test floor of the laboratory is designed to form the

lower member of an internal reaction frame. Steel uprights are bolted to the floor and the test rig is completed by the fixing of a steel transome. The holding down bolts in the floor are on a 3 ft square grid.

Four uprights were placed at 3, 15 and 3 ft centres. These were connected at their top by an 8 x 17 in. deep steel box girder. The twin supports, that is those at 3 ft centres, were braced at a height of approximately 3 ft 6 in. by a box girder of similar dimensions as those of above; see Drawing 7.1 and Plate 7.4.

The loading system was designed to apply constant vertical load at the mid point of the transome, and constant horizontal load acting from left to right at the level of the centroidal axis of the transome. There were separate oil circuits for each load and consisted of standard Amsler oil cabinets. Provision was made to accommodate a 3 in. side movement and $2\frac{1}{2}$ in. vertical movement of the concrete frame. In addition to the above jacks, there was a horizontal follower unit for the vertical jack. It consisted of a sealed unit of a pair of horizontal jacks with one jack (termed A) placed towards the right at the level of the centroidal axis of the transome, and another jack (termed B) at the level of the horizontal sliding plate of the vertical jack.

The design ratio of the horizontal load to vertical load was 1.5, and it was important that at all stages, including the ultimate load, the two loads were applied in the same ratio. By using Amsler jacks coupled to Amsler oil cabinets, this could have been easily achieved, including the last few load stages before collapse when the readings were proposed to be taken on the automatic scan of the data logger (Solartron), and it was not possible to check the ratio through readings on the appropriate force transducers. But, because of their sizes, they were abandoned in favour of lap jacks designed by the Engineering Structures Section of the Department.

These are compact, and have very little friction; when coupled with separate Amsler oil cabinets, they formed a satisfactory loading system. It was possible throughout to stick to the above ratio within $\pm$ 2%. The vertical jack was mounted on a sliding plate. This was the same arrangement as used by Edwards[34] and could accommodate 4 in. of movement about its mean position. The follower unit was also the same as was used by Edwards[34] and had a 20.ton Blackhawk jack at either end.

Each horizontal jack at the transome level had a dead weight and pulley arrangement for being lifted up at the time of stressing the concrete transome.

Before the frame was loaded, the jack A was brought into contact with the concrete frame by means of an extension unit, and the jack B brought into contact with the sliding base of the vertical jack by means of a similar extension piece. When the load was applied, the frame was deflected sideways and oil was displaced from jack A to jack B. The vertical jack thus moved through the same horizontal distance as the concrete frame. The frames were primarily intended to be tested under the monotonically increasing load and only the follower unit moving the vertical jack towards the right was incorporated. However, to ascertain that all critical sections had reached their ultimate strengths, the test was continued well past the maximum load, and, owing to friction, the vertical jack could slide back easily towards the left without a follower unit.

An attempt was made to minimise the large bending stresses that might be induced into the rams of the horizontal jacks at transome level by providing a vertical roller bearing between the concrete frame and the spherical seating of the force transducer. A general view of the jacking arrangement is given in Plate 7.4 and Drawing 7.1.

7.12 INSTRUMENTATION

Complete load-stress-resultant-deformation history was necessary to assess a fairly accurate picture of the behaviour of tested structures, as ultimate load was reached. Since only short term loading was to be investigated, the length of any one test programme was restricted to that which could be carried out in one day. The stress-resultants at any load stage were obtained by measuring all applied loads and reactions by means of load transducers, or directly reading on the Amsler cabinets. Measurement of reactions in excess of the redundancy number provided checks on the accuracy of data and enabled its adjustment logically, as set out in Appendix 1. The curvatures and longitudinal strains in the extreme compression fibre were deduced by measurement of longitudinal strains in concrete at three levels in the compression zone on both sides of the member. A fairly long length exceeding the inelastic region was covered with gauges at each critical section so that curvature distribution along the structure could be plotted with reasonable accuracy. On grounds of cost and other conveniences, Demec gauge points were used for the beams and Japanese PL30 electric gauges for the frames. In addition to these, deflexions by means of dial gauges or linear potentiometers, and slopes by means of clinometers were measured.

In an investigation of this type it is essential that all measuring devices are extremely accurate. The development of load transducers of requisite standard presented many practical difficulties, which are described in some detail in Chapter 8.

All readings were taken either by means of Peekel strain box or data logger manufactured by Messrs. Solartron Electrical Group Ltd. which read up to $\pm$ 1 division.

In the beam tests the applied load was read directly on the Amsler cabinets working on the 10 ton range. An Amsler jack

coupled to an Amsler oil cabinet forms Grade 1 loading equipment, and in the present case read up to 0.005 ton i.e. about 10 lb. All the three reactions were measured by means of bearing type force transducers connected to a Peekel strain box. Each end force transducer was of 10 ton capacity, and the central one of 25 ton capacity; they had repeatability within $\pm$ 1 division, and sensitivities of about 0.3 and 0.1 division per pound respectively; linearity as assessed on the basis of first differences was within $\pm$2.5%. It was necessary that the Amsler cabinets and the force transducers were calibrated with the same standard. The transducers which were calibrated in the standard Amsler compression machine were checked by loading them by means of the jacks and hydraulic cabinets used in the tests, and the two calibrations were found to tally within $\pm\frac{1}{2}$%, which was considered satisfactory.

In the frame tests the applied load was measured at three positions; at the vertical jack, and at each of the horizontal jacks at the transome level. All three force transducers were of 5 ton capacity with repeatability within $\pm$ 2 divisions. The vertical force transducer had a sensitivity of about 1.57 divisions per pound and the horizontal ones of about 1.18 divisions per pound. The linearity as assessed on the basis of first differences was within $\pm$ 2%. The three reactions at each foot were measured by means of a specially devised force-moment transducer, which is fully described in Chapter 8. This had nine force transducers, which formed three tripods. Their outputs when suitably combined linearly gave both the vertical and horizontal reactions, and moment. Each of the force transducer used for the purpose was of 2.5 ton capacity and had a sensitivity of about 1.6 divisions per pound; the repeatability was within $\pm$ 2 divisions and linearity, as assessed as the basis of first differences, within $\pm$ 2%.

The mid span deflexions of the beams were measured by means of the dial gauges having a 2 in. travel and the smallest division of

0.001 in. The support deflexions which were measured with the dial gauges reading up to 0.0001 in. were found insignificant.

The horizontal and vertical deflexions of the frames were measured by means of linear potentiometers having 4 and 3 in. travels respectively. The vertical potentiometer was fixed to the vertical jack so that it could move horizontally as the frame swayed, and the point of application remained the same. The vertical movement was measured at 2 in. left of the mid point of the transome, and the horizontal movement at the face of the anchor plates of the transome. The linear potentiometers were calibrated three times in a 0.0001 in. micrometer calibration unit; the linearity as assessed on the basis of first differences was within $\pm 3\%$, and sensitivity varied from 8,400 to 15,900 divisions per inch. The support deflexions and rotations were measured by means of dial gauges and clinometers reading up to 0.0001 in. and 0.000025 radians respectively. The deflexion of the mid point of the rig transome was measured with a 0.0001 in. dial gauge and was found insignificant.

Slopes near some of the critical sections were measured by means of clinometers, originally used by Bremner[65].

The longitudinal strains in the beams were measured at $\frac{1}{2}$, 1 and $1\frac{1}{2}$ in. depths from the extreme compression fibre, and 4 in. Demec demountable extensometer, which read up to 10 microstrains, was used. In the frames the corresponding distances were $\frac{3}{8}$, $\frac{3}{4}$ and $1\frac{1}{8}$ in. and electric strain gauges connected to the Solartron, which read up to 1 microstrain were used. The measurement at three levels had the advantage that it enabled the calculation of the strain distribution across the section through the Method of Least Squares, which smoothens out the experimental errors to a certain extent.

7.13 DESCRIPTION OF TESTS

The critical section identification used for the beams is to name the three supports as A, B and C, and the mid spans as D' and D (figure 7.8) when viewed from other side of the loading cabinets, see

Plate 7.3. The identification system used for the frames is to name the nodes as A to E inclusive (Figure 7.8) when viewed from other side of the loading cabinets, see Plate 7.3. The identification system used for the frames is to name the nodes as A to E inclusive (Figure 7.9) as viewed from the data logger, see Plate 7.4.

The first load increment for the beams was the self weight, prestress and dead weights. The reactions measured at the time of placing the beam in the test rig were inclusive of the effect of the dead weights. To obtain the stress-resultant distribution due to the self weight and prestress only, it was necessary to deduct the effect of the dead weights, which was obtained by subtracting the reactions recorded after the removal of the weights from those recorded before their removal. This was justified since the beam was still uncracked and the principle of superposition was applicable.

The first load increment for the frames was the self weight. The reactions due to this were small, and, if measured, would be unreliable since the accuracy of a load transducer for the first small load is little and also they would have been subjected to drift, for the erection of the frame continued for 3-4 days. For this and other practical reasons it was decided to ignore them being small. The first load increment considered was, therefore, the prestress. Reactions due to the prestress were measured by means of a Peekel strain box and recording of the measurement continued till the test day. This enabled the study of the effect of creep on prestress. For reasons similar to those given for the beams, frame F-4 was stressed with certain horizontal load applied by means of screw jacks, previously calibrated. The procedure adopted to obtain the effect of the dead weights in the beams could not be applied in this case, since the value of the horizontal load was continuously varying on account of deformations due to prestress and creep. The horizontal load could therefore be estimated approximately and the secondary prestress moments given in Table 7.3, which were obtained by

deducting the effect of such horizontal load from the measured values, should be considered as approximate only. However, they compare fairly well with the theoretical values.

All beams and frames were tested under proportional loading. The load was applied in steps of 15% of the expected ultimate load in the early load stages nearly up to cracking. Thereafter, it was reduced to about 10%. As deformations became excessive towards collapse, the load increment was further reduced.

Except B-4, all the beams were loaded by applying equal loads at the centres of the two spans simultaneously. It was seldom that both the spans failed simultaneously. After one span had failed, the other span was loaded until it also failed so that the ultimate flexural strengths of all the critical sections were measured. Unlike the other beams, B-1 failed by the rupture of section D'. The test was continued like the other beams until all the critical sections failed, and their ultimate strengths measured. The critical sections of beams B-1 were sawn through after the test; it was found that grout had not gone through the central duct. The difference in failure in this case is attributed to bad grout and loading arrangement. The two spans in this case were loaded through a single cabinet. As soon as the first hinge was formed at D', the total load applied to the structure was determined by the response of the left hand span. The result was the left hand span ruptured at a load of 6,640 lb.

The design ratio of horizontal to vertical load was 1.5 for all frames. During the tests, this ratio was adhered to within $\pm 2\%$, but after the correction of the data it varied within $\pm 4\%$. All frames except F-3 failed through a combined beam and sway mechanism by the formation of hinges at A,C,D and E. At the maximum load distinct signs of crushing of concrete were visible at all the critical sections. In frame F-3 at a load of 3,850 lb there were no signs of crushing at C, although excessive

crushing had already started at A,D and E, and the frame had swayed by 2.7 in., that is about 100% more as compared to the other frames. At this instant the whole system became so unstable that load had to be taken off. The ultimate strength of the critical section C was then obtained by slightly increasing the ratio of the vertical load. The ratio of the horizontal to the vertical load at the time of crushing at C was 1.33.

At node D crushing was observed both in the transome and the column in all cases, except frames F-3 and 5; the maximum moments reached at the critical section D in F-3 and 5 were also somewhat less than those reached at the other critical sections which had practically the same effective depth. The column and transome of frames F-3 and 5 were therefore sawn at the node D after the test. It was found that the grout had not properly gone through the column ducts, which explained the above difference of behaviour.

In all beams and at the critical section C of all the frames (except F-5), crushing of concrete took place in the region of bending moment diagram with shallower gradient. In frame F-5, however, crushing of concrete took place in the region CD where the bending moment diagram has a steeper gradient.

The deformed shapes of the structures along with the crack pattern under near maximum load are shown in Plates 7.5 to 7.10 inclusive.

Both the test rigs behaved well under load conditions. 0.001 in. dial gauges were placed at nodes B and D in the plane at right angles to the plane of the frame; the maximum recorded values of deflexions were 0.07 and 0.20 in. respectively. The maximum deflexion of the rig transome was observed as 0.0215 in.

7.14 TEST RESULTS

It was seldom that the measured reactions and applied loads satisfied the equations of equilibrium. It was necessary to apply smallest possible corrections to the measured values such that they satisfied all the equations of equilibrium. In the past, either the data was left uncorrected[37] or the above corrections made by trial and error[14] or the error was distributed in an arbitrary manner[11]. In the present case the number of quantities involved were large and any of the above procedures was neither convenient nor rational. Lagrange's method of undetermined multipliers which logically makes such corrections easily possible was used. This gave very consistent results and is described in Appendix 1.

It was mentioned in Section 7.6 that the beams were stressed outside the test rig. The conditions at the time of stressing were somewhat different from what they would have been if the beams were stressed in the test rig. Therefore to record concrete strains after stressing would have been of little value. Attempts to relate the 'Demec' readings taken before stressing with those taken after the beams were correctly placed in the test rig were also inconclusive due to changes of temperature and humidity to which the specimens were subjected. Unfortunately, at that time the temperature and humidity system of the laboratory had broken down. The gauges over the dry mortar packing of the frames were not fixed until after the stressing had taken place. Thus actual curvatures corresponding to the prestress were not measured, although the prestress moments were known. The curvatures corresponding to the prestress were extrapolated by continuing downward the initial linear portion of the moment curvature diagram obtained for the applied loads. This had the advantage that the curvature corresponding to the prestress so obtained excluded the effect of creep.

The important results obtained from the tests are presented in Figures 7.10 to 7.46 inclusive and consist of the following. The loads at which visual cracking and crushing of concrete occurred are also marked on the appropriate Figures.

(1) Load-Moment Relationships for the critical sections (Figures 7.10 to 7.18)

(2) Load-Rotation Relationships for beams CB-1 and B-1 (Figure 7.19).

(3) Load-Deflection Relationships (Figures 7.20 to 7.24)

(4) Moment-Curvature Relationships for the critical sections (Figures 7.25 to 7.31).

(5) Curvature and Strain Distributions along the structure near collapse (Figures 7.32 to 7.45).

(6) Prestress Redundant Reactions versus Time Relationships for frame F-5 (Figure 7.46).

The graphical representation of horizontal movement of nodes B and D of the frames is almost identical and an average value has been given. The actual values obtained, however, enabled the relative movement of the two nodes to be examined. Before cracking node B moved towards node D, and after cracking node D moved away from node B. The measuring devices were sufficiently sensitive to record this effect even at low cracking loads.

CONCRETE CONTROL TESTS

(all results in lb/in^2)

Struct	6 x 12 in. cylinder strength			Avg.cyl. strength	6 in. cube strength			Avg.cube strength	Modulus of rupture			Avg. M. of R.	cyl.str. / cube str.
B-1	5790	5880	5450	5706	8470	9150	8400	8673	747	716	-	732	0.66
B-2	5800	5690	6450	5980	8770	9150	8580	8833	866	726	692	761	0.68
B-3	5800	6350	6160	6103	8700	8760	8510	8657	735	695	713	714	0.70
B-4	5920	6010	6140	6023	8520	8840	8950	8770	725	713	670	703	0.69
F-1	6050	6180	6180	6137	9200	9580	9400	9393	888	666	1032	862	0.65
F-2	5920	6150	6470	6180	8700	9100	8910	8903	-	-	-	-	0.70
F-3	6650	6510	6150	6437	8950	8780	9510	9080	974	917	974	955	0.71
F-4	6250	6730	6740	6573	9950	9510	10100	9853	610	743	893	749	0.67
F-5	6240	6510	6300	6350	9600	8950	9340	9296	980	1040	1015	1012	0.69

Avg.0.68

TABLE 7.1

EFFECTIVE DEPTHS AND SECONDARY PRESTRESS MOMENTS IN TEST BEAMS

Struct	Design description	Critical section	Effective depth, in.	Secondary prestress moment, lb in.
CB-1	concordant cable profile	D'	4.20	0
	based on working load	B	4.46	0
	design	D	4.20	0
B-1	Geom. properties of the			
	critical sections as	D'	4.3	5,150
	those of CB-1 but cable	B	4.1	10,300
	profile designed as per	D	4.3	5,150
	the proposed theory			
B-2	As per the proposed	D'	4.3	8,650
	theory	B	4.3	17,300
		D	4.3	8,650
B-3	Geom. properties of the	D'	4.3	0
	critical sections as	B	4.3	0
	those of B-2 but	D	4.3	0
	concordant cable profile			
B-4	As per the proposed theory	D'	5.1	-28,780
	(loaded at D only)	B	4.3	-57,560
		D	4.3	-28,780

TABLE 7.2

EFFECTIVE DEPTHS AND SECONDARY PRESTRESS MOMENTS IN TEST FRAMES

Struct	Design description	critical section	Effective depth, in.	Secondary prestress moment, lb in.
F-1	Concordant cable profile based on working load design	A	3.31	660
		C	3.37	-30
		D_1	3.69	-110
		D_2	3.65	-90
		E	4.00	330
F-2	Linearly transformed cable profile obtained from F-1	A	4.10	-12,200
		C	2.57	-14,000
		D_1	4.06	-7,300
		D_2	3.98	-6,500
		E	4.10	1,200
F-3	Arbitrary nonconcordant with geom. prop. of the crit. sections as those of F-4 and F-5	A	4.10	-12,500
		C	4.10	-5,500
		D_1	3.98	2,000
		D_2	3.98	2,500
		E	4.10	3,500
F-4	As per the proposed theory	A	4.10	-5,400
		C	4.10	21,300
		D_1	4.10	12,500
		D_2	4.10	10,400
		E	4.10	-23,200
F-5	As per the Russian Code of Practice but with geom. prop of the crit. sections same as those of F-4 and F-3	A	4.10	-5,100
		C	4.10	2,600
		D_1	4.10	1,600
		D_2	4.10	900
		E	4.10	-10,900

TABLE 7.3

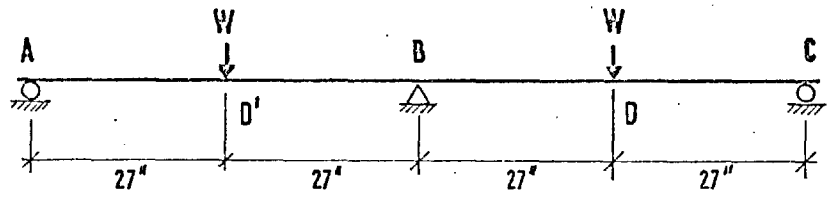

Fig. 7·1: LOADING FOR BEAMS B-1 to 3 AND CB-1 to 5

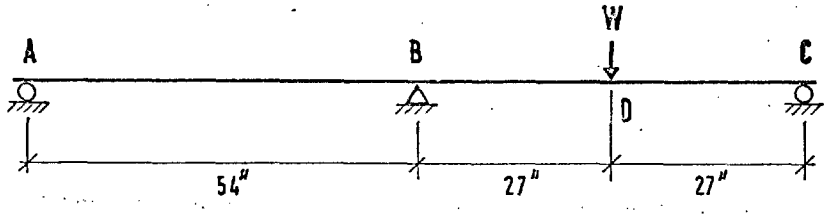

Fig. 7·2: LOADING FOR BEAM B-4

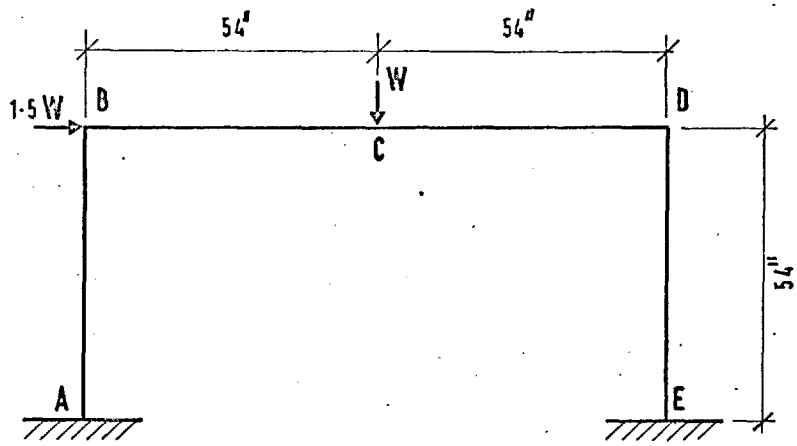

Fig. 7·3: LOADING FOR TEST FRAMES

Beam Ref.	Cable Profile: Designed as	shown thus
B-1	Nonconcordant with ecc. at crit. sect. same as in Raina's Beam CB-1 [NC]	——
B-2	Nonconcordant according to Proposed Theory [NC-E (Proposed)]	- - -
B-3	Concordant with equal max. ecc. at all crit. sect. [C-E]	—·—
B-4	Nonconcordant according to Proposed Theory [NC-E (Proposed)]	—··

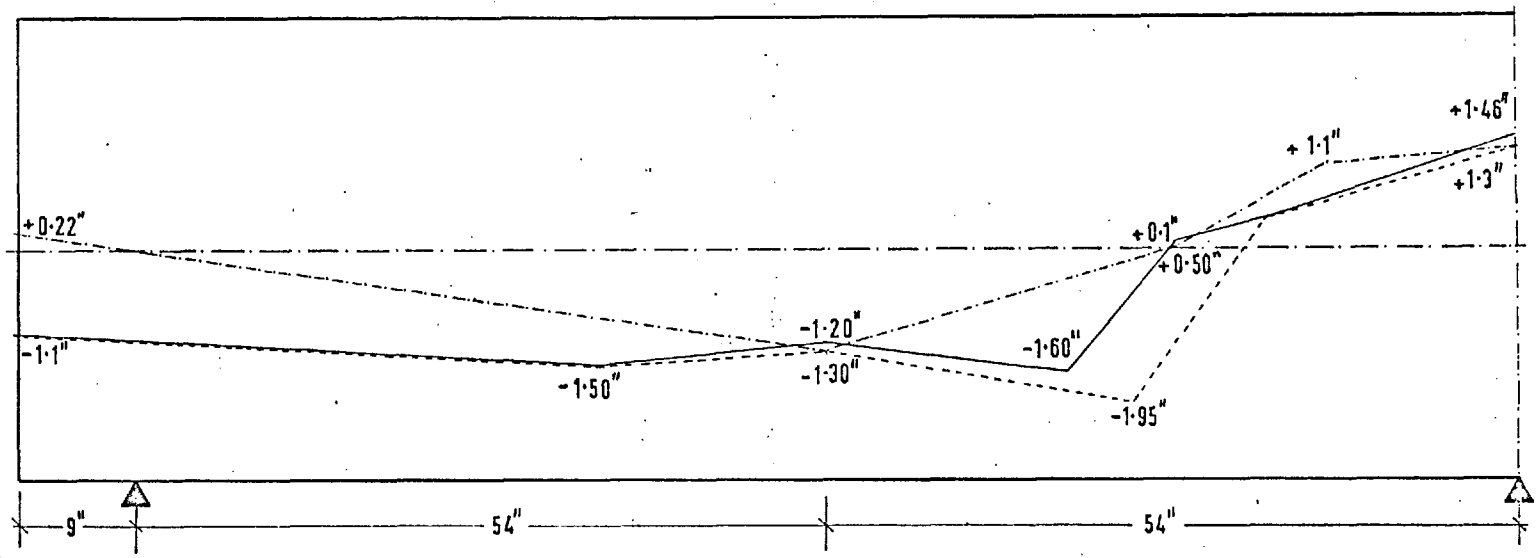

BEAMS B-1, 2 & 3 — CABLE PROFILES

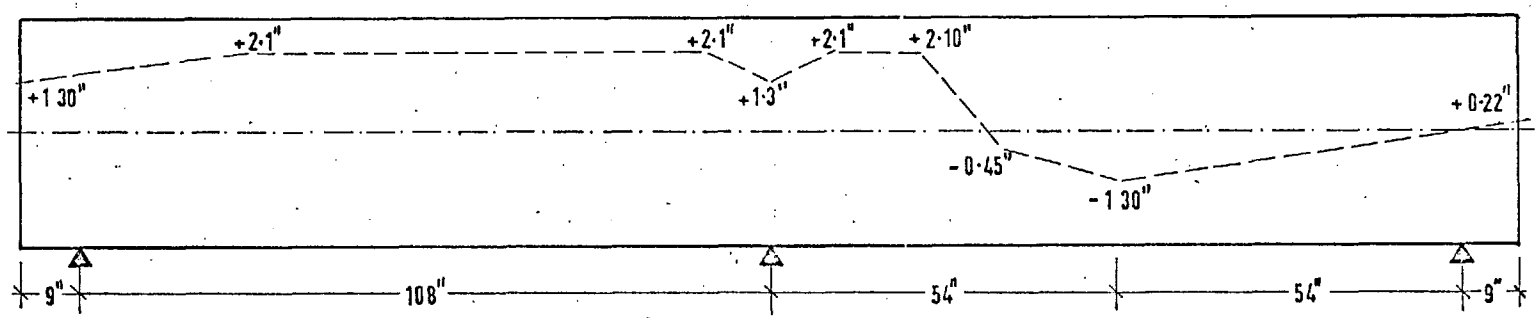

BEAM B-4 — CABLE PROFILE

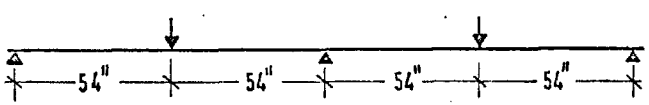

BEAMS B-1, 2 & 3

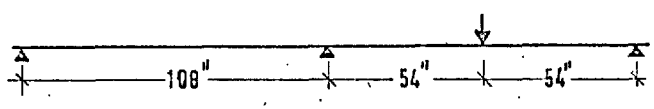

BEAM B-4

Fig. 7·4: TEST BEAMS — CABLE PROFILES

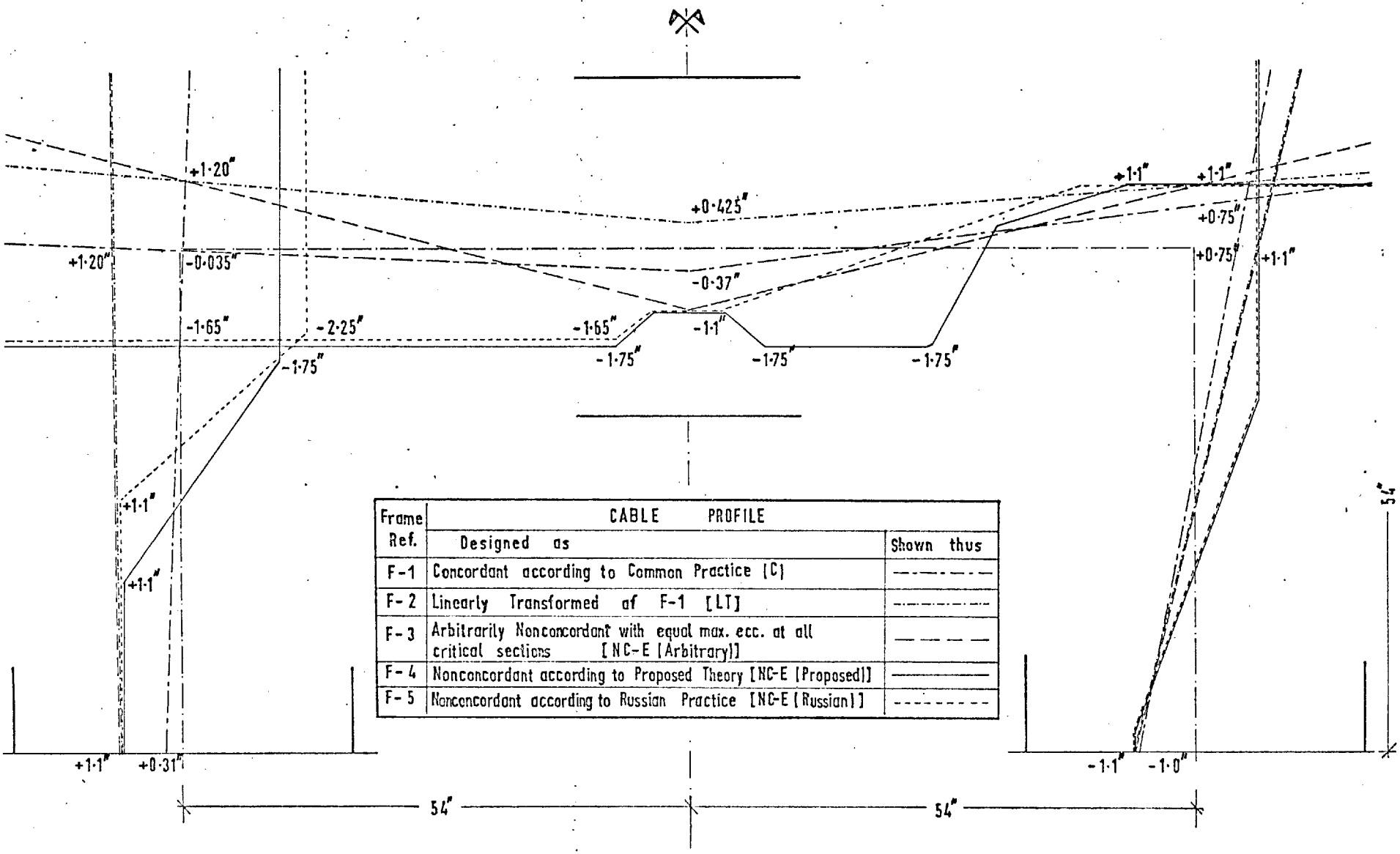

Frame Ref.	CABLE PROFILE	
	Designed as	Shown thus
F-1	Concordant according to Common Practice [C]	
F-2	Linearly Transformed of F-1 [LT]	
F-3	Arbitrarily Nonconcordant with equal max. ecc. at all critical sections [NC-E [Arbitrary]]	
F-4	Nonconcordant according to Proposed Theory [NC-E [Proposed]]	
F-5	Nonconcordant according to Russian Practice [NC-E [Russian]]	

Fig. 7.5: TEST FRAMES — CABLES PROFILES

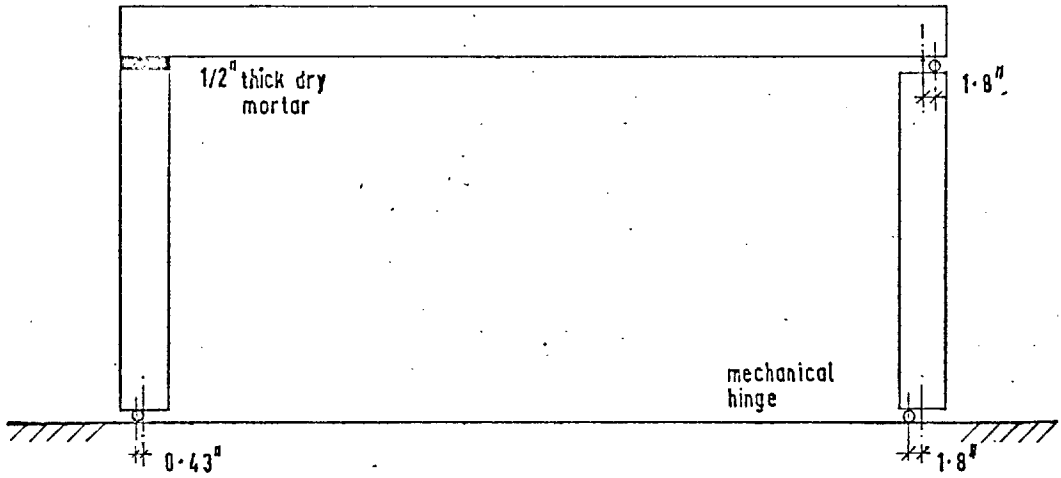

Fig. 7·6 : MECHANICAL HINGES IN FRAME F-5

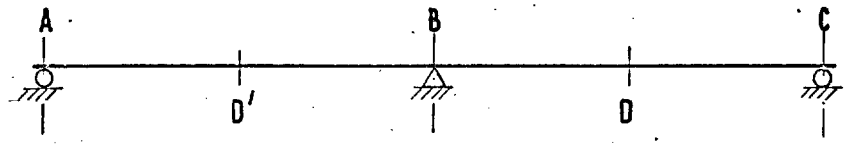

Fig. 7·8 : CRITICAL SECTION IDENTIFICATION OF TEST BEAMS

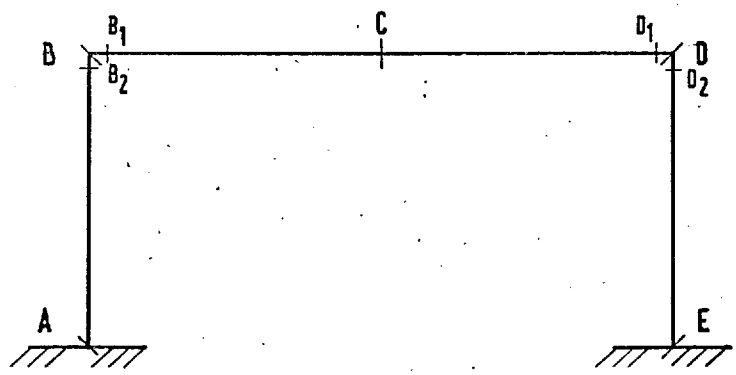

Fig. 7·9 : CRITICAL SECTION IDENTIFICATION OF TEST FRAMES

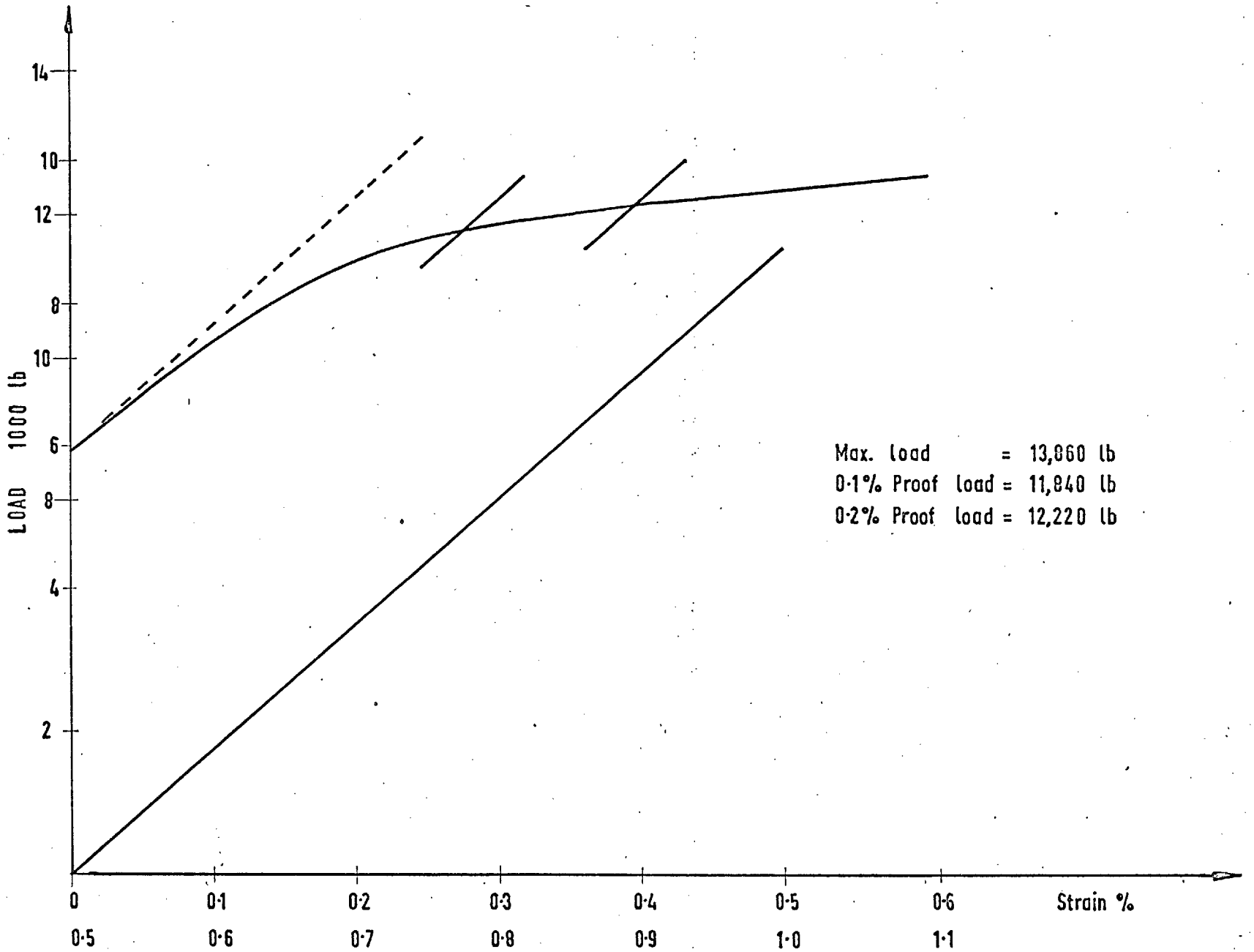

Fig. 7·7 : LOAD-STRAIN CURVE OF 0·276" DIA. WIRE

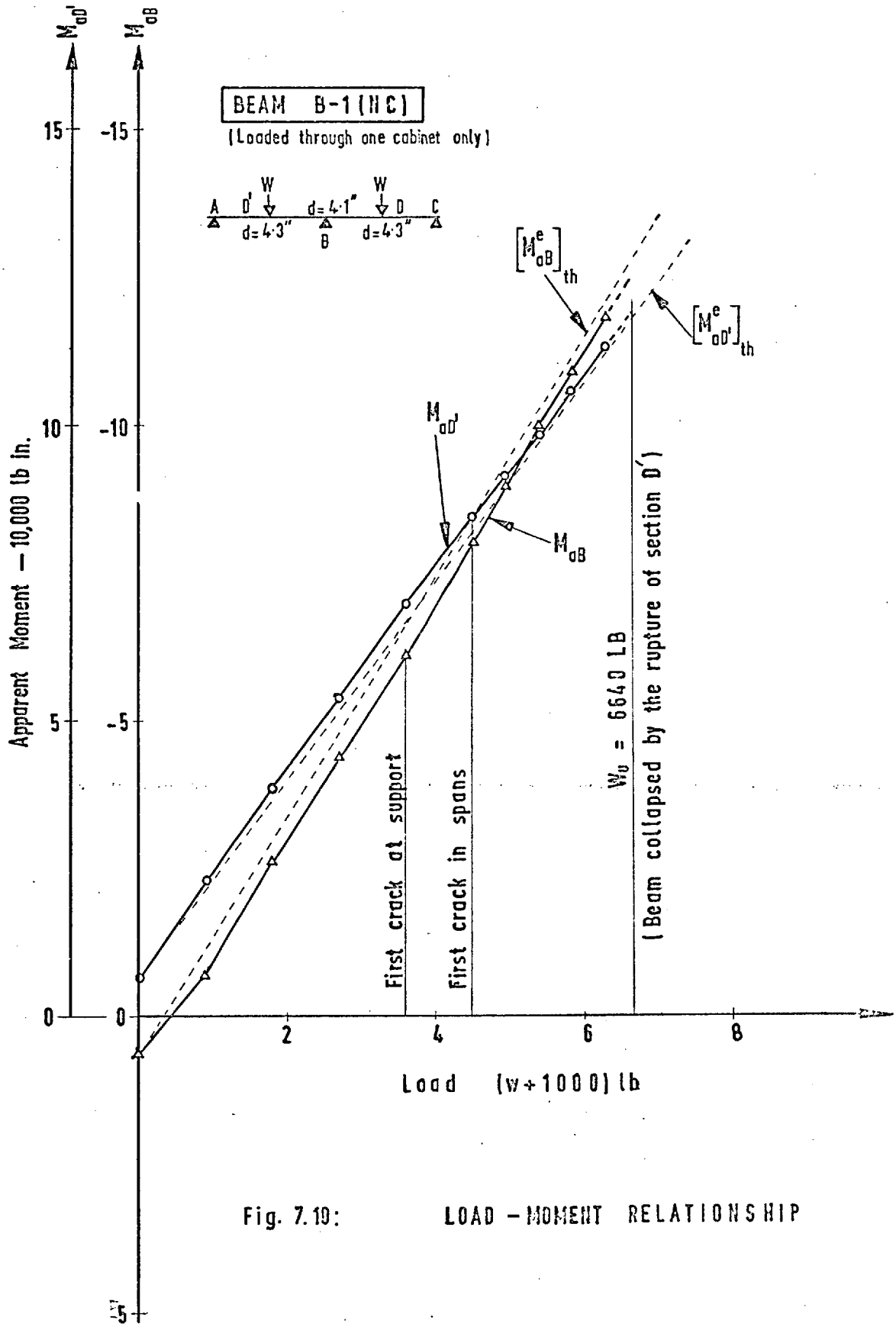

Fig. 7.19: LOAD – MOMENT RELATIONSHIP

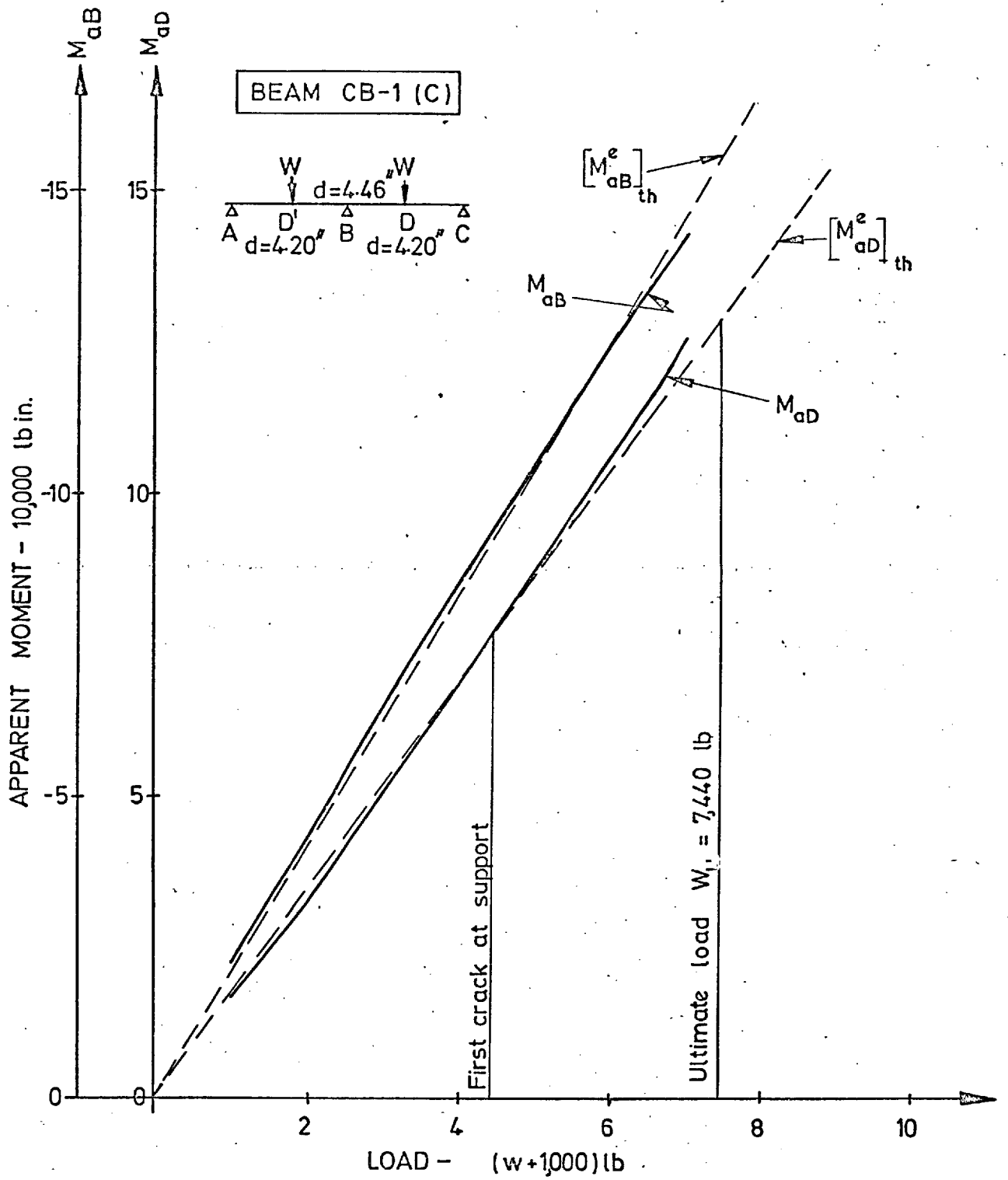

Fig 7.10a LOAD – MOMENT RELATIONSHIP

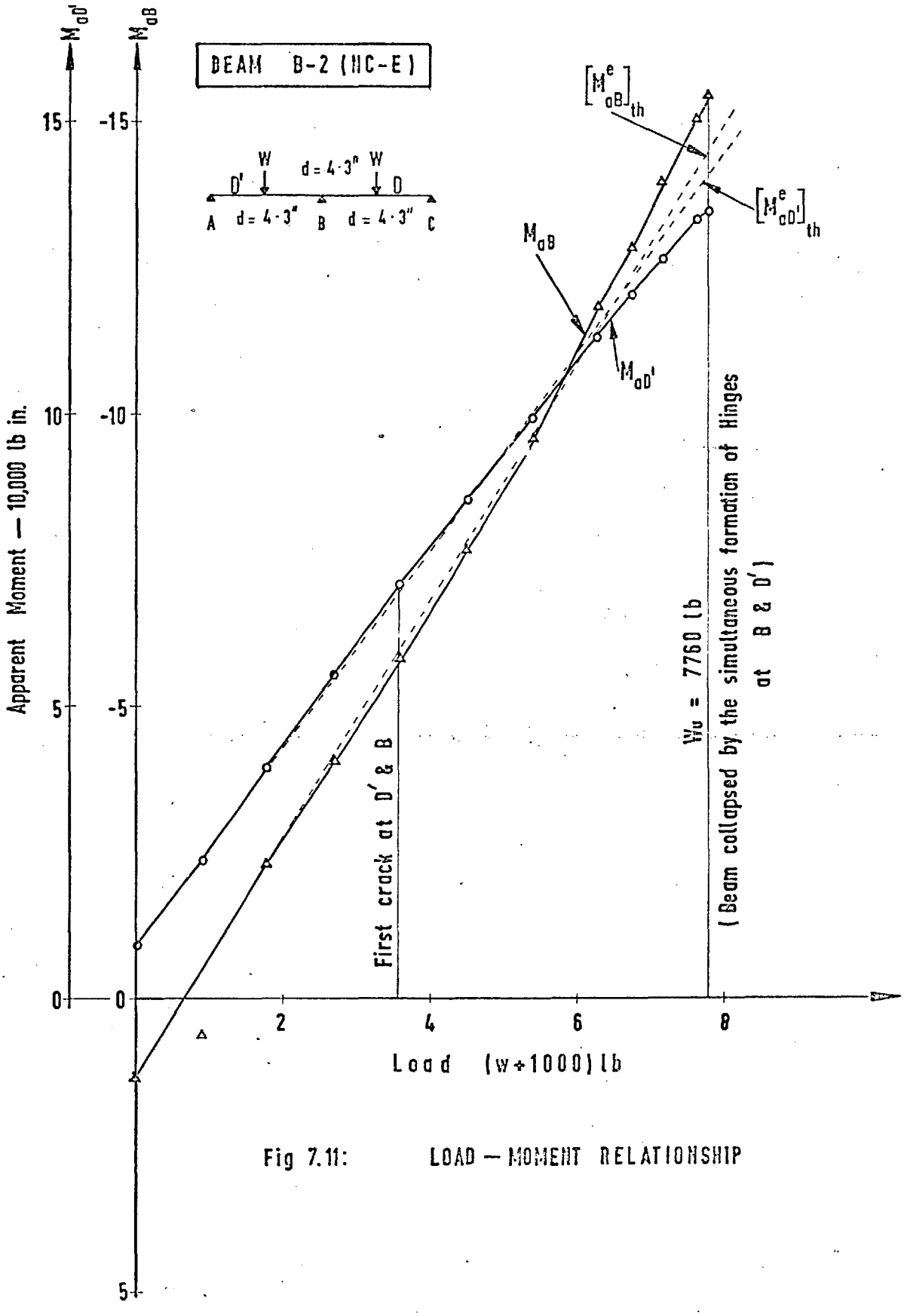

Fig 7.11: LOAD — MOMENT RELATIONSHIP

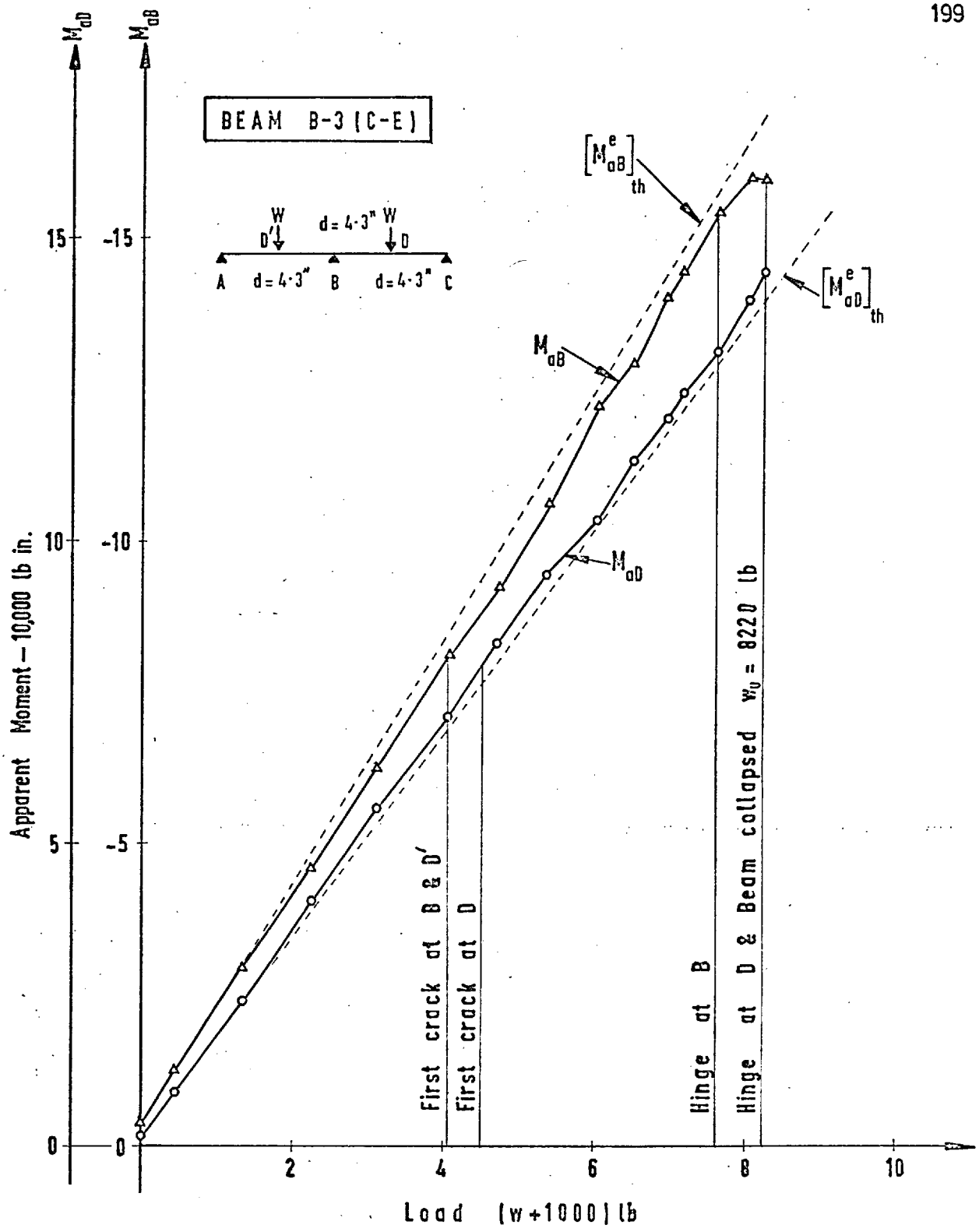

Fig. 7.12: LOAD — MOMENT RELATIONSHIP

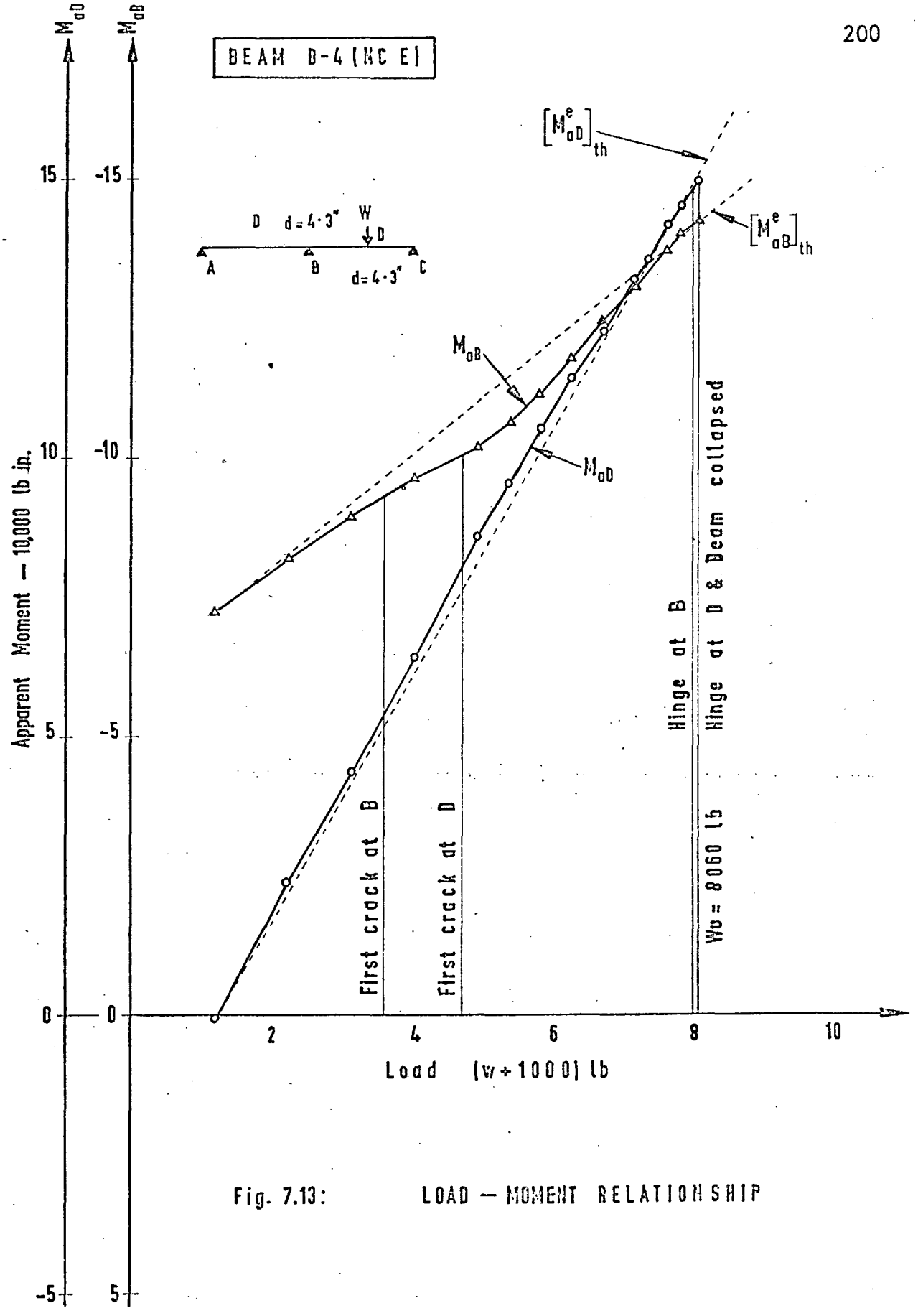

Fig. 7.13: LOAD — MOMENT RELATIONSHIP

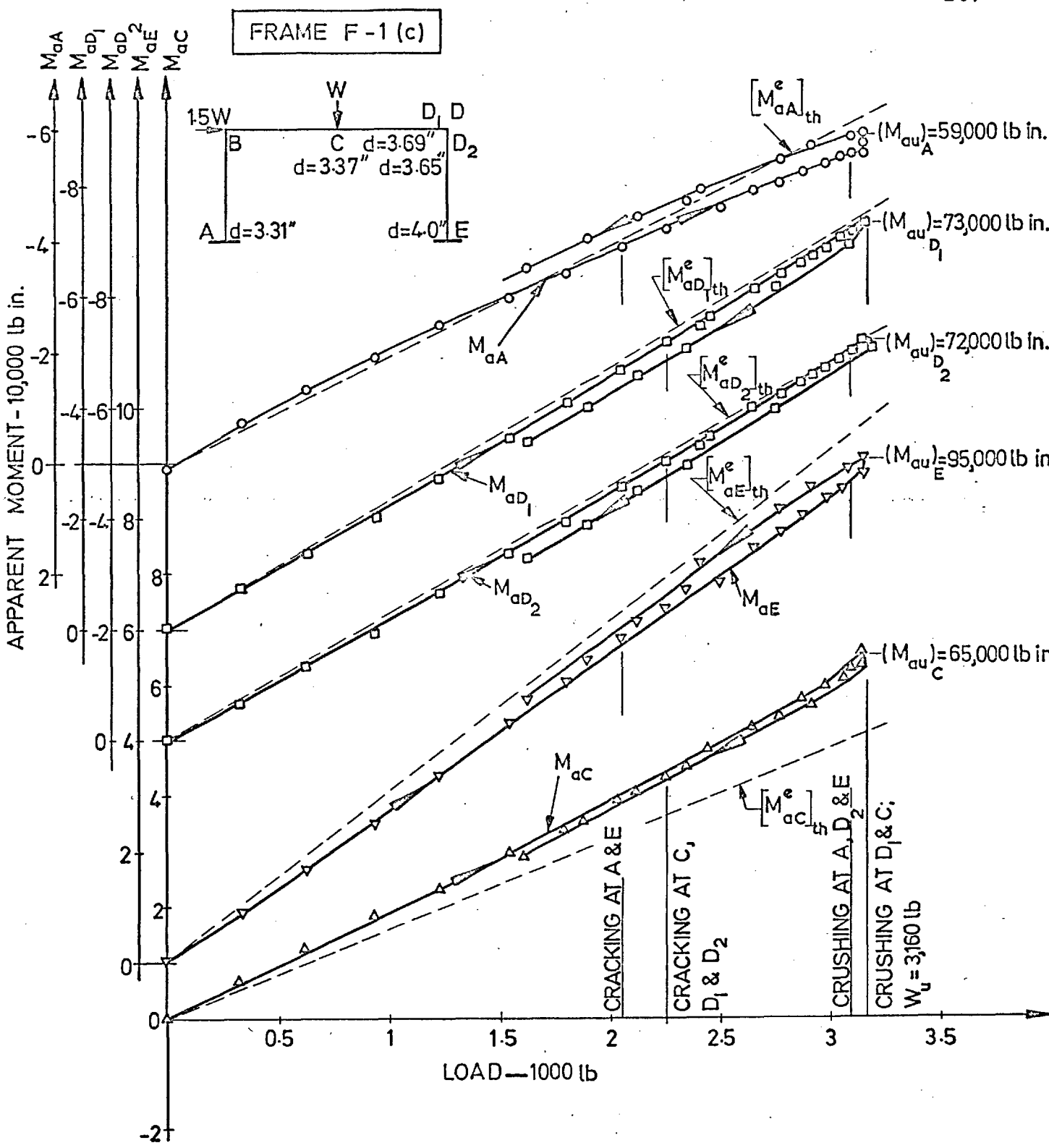

Fig.7.14: LOAD — MOMENT RELATIONSHIP

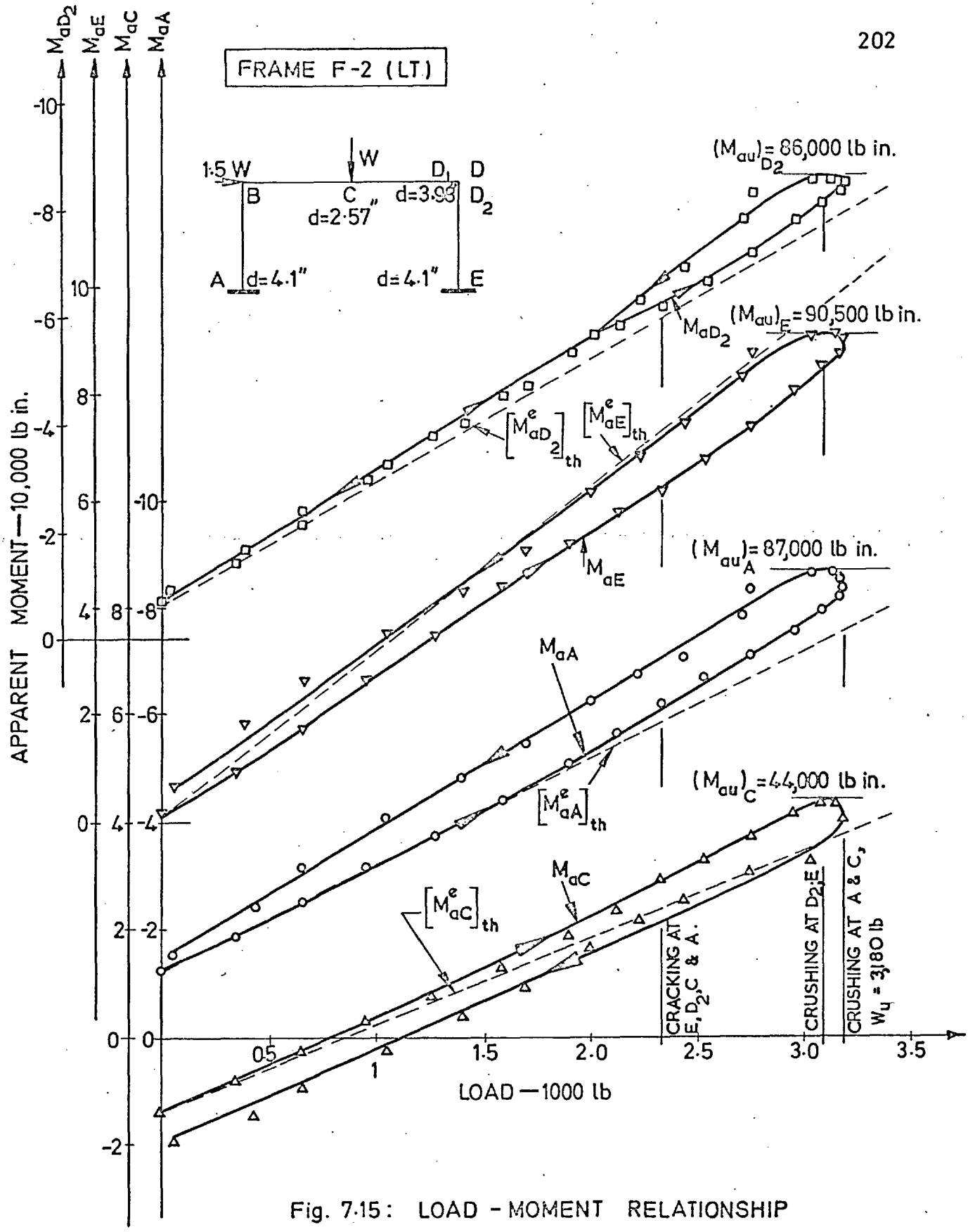

Fig. 7.15: LOAD - MOMENT RELATIONSHIP

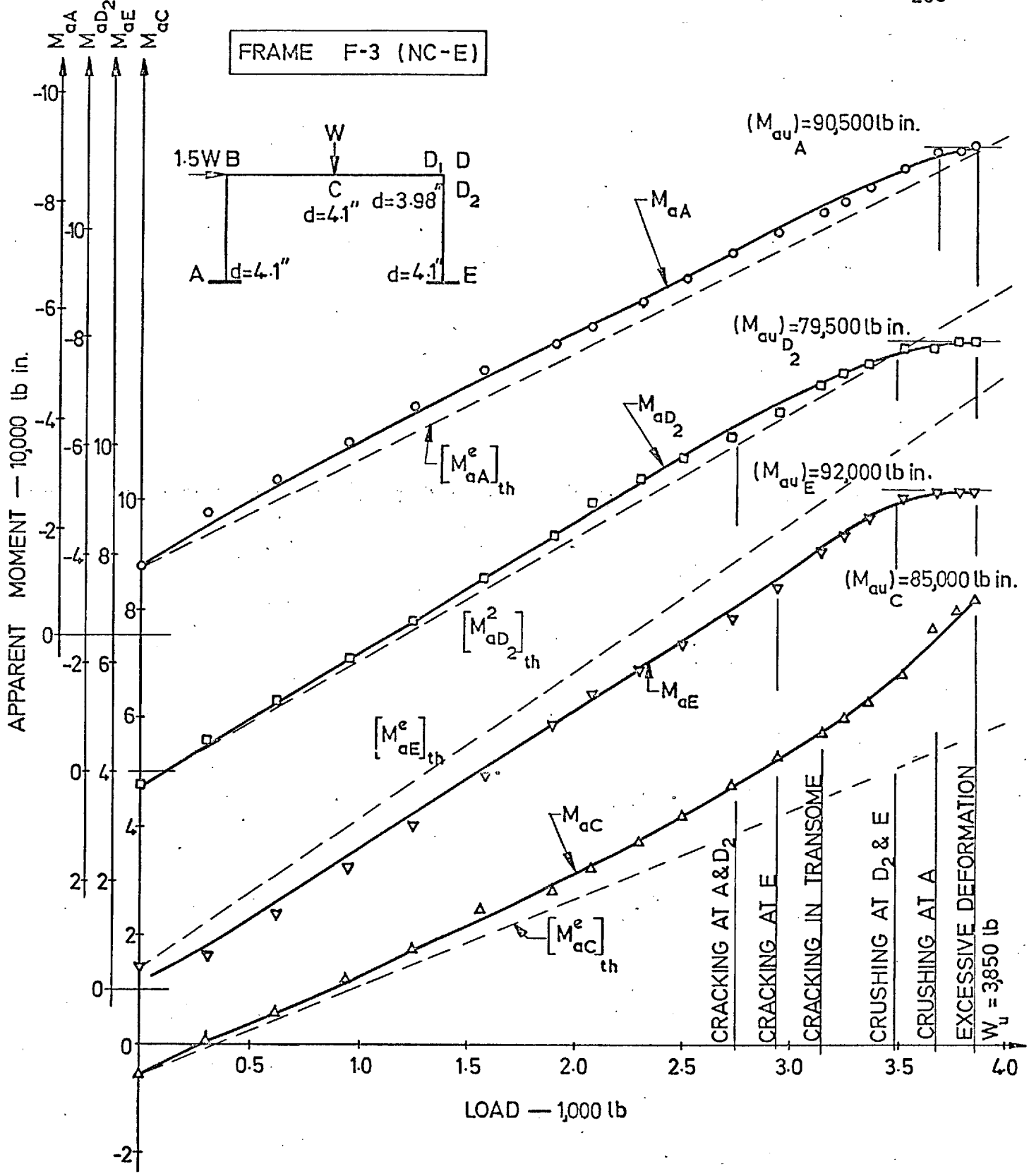

Fig. 7.16: LOAD – MOMENT RELATIONSHIPS

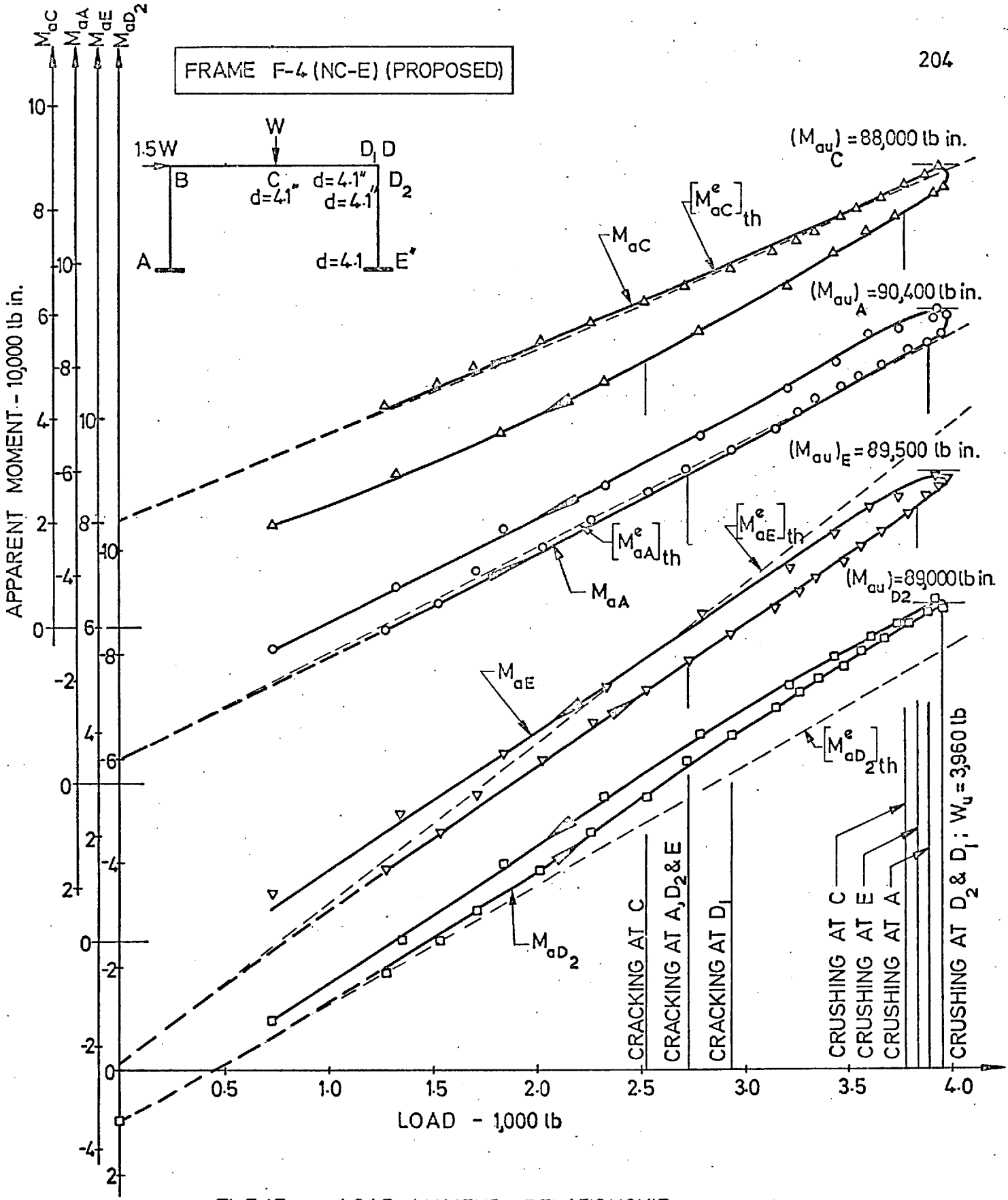

Fig 7.17: LOAD - MOMENT RELATIONSHIP

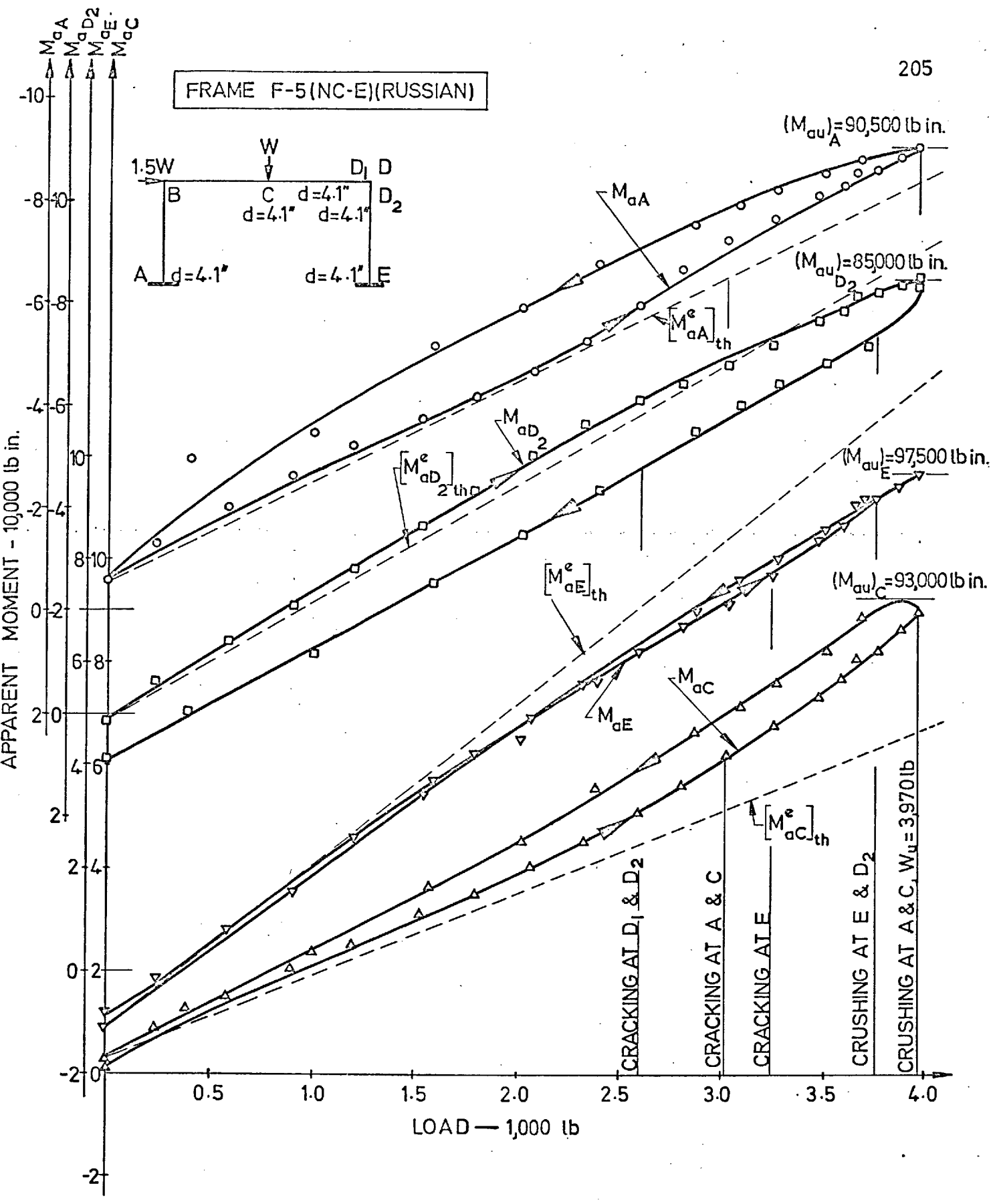

Fig. 7.18: LOAD—MOMENT RELATIONSHIP

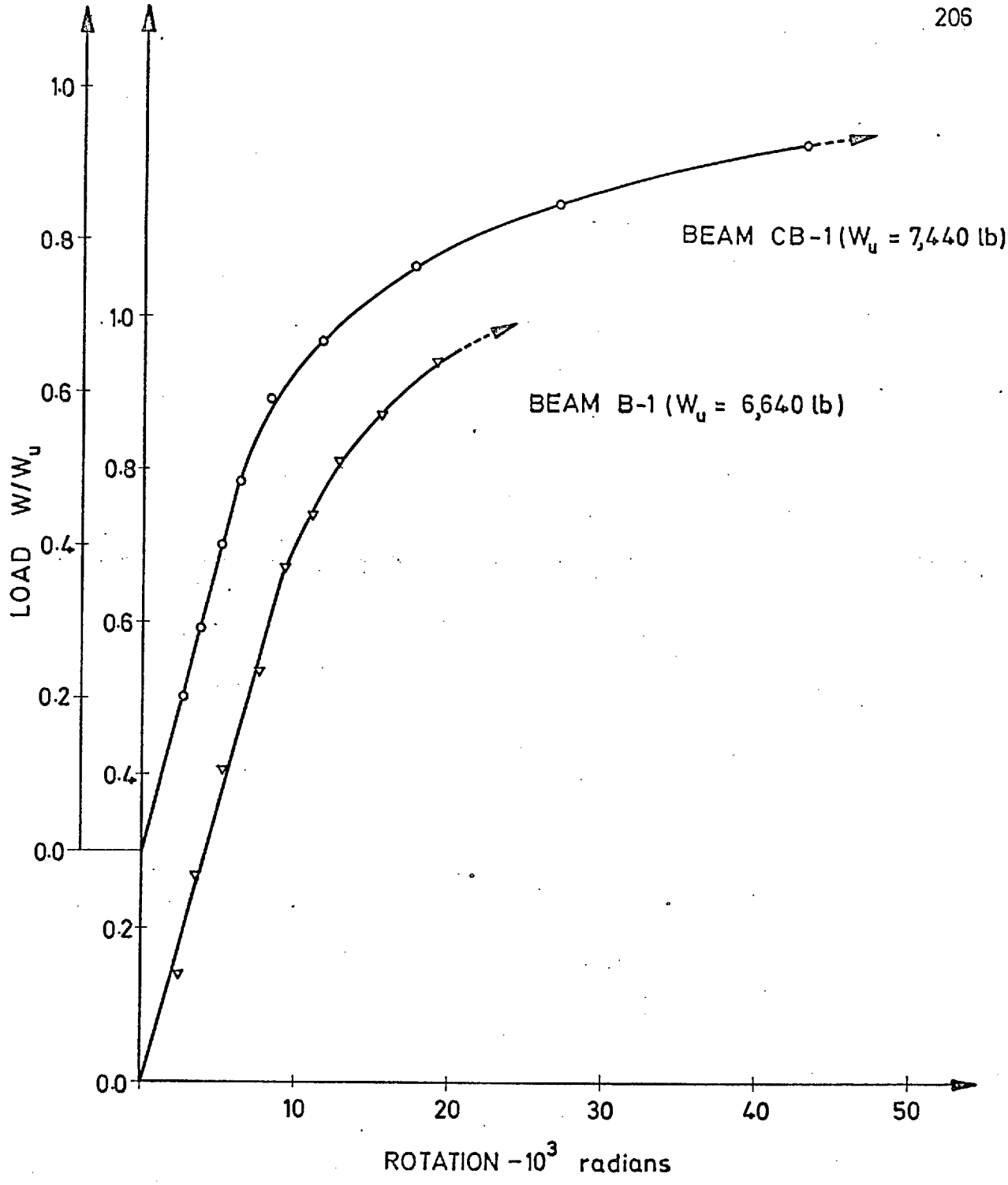

Fig 7.19: LOAD-ROTATION (as measured from clinometers) RELATIONSHIPS FOR BEAM CB-1 & B-1

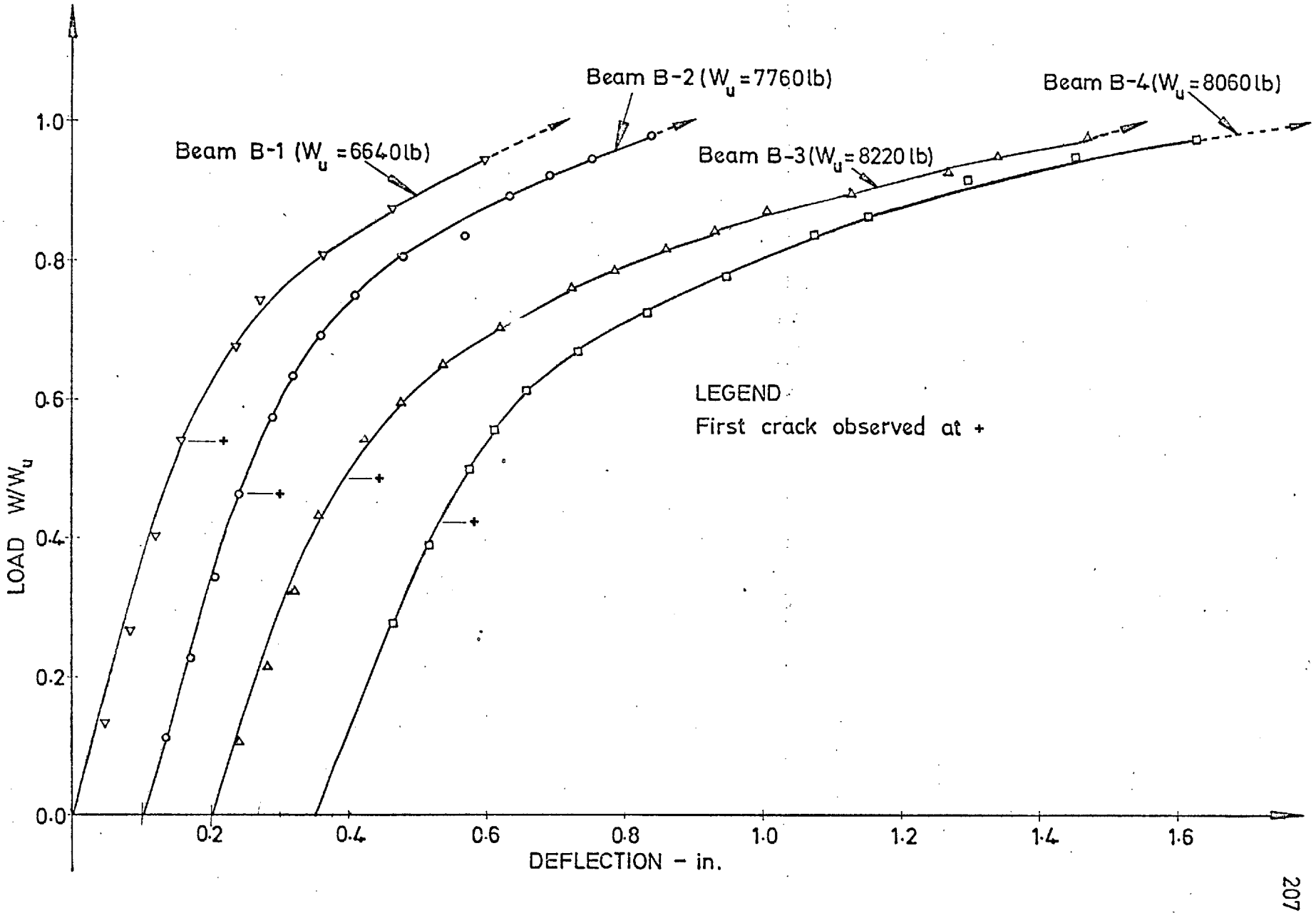

Fig 7.20: LOAD DEFLECTION CURVES FOR BEAMS

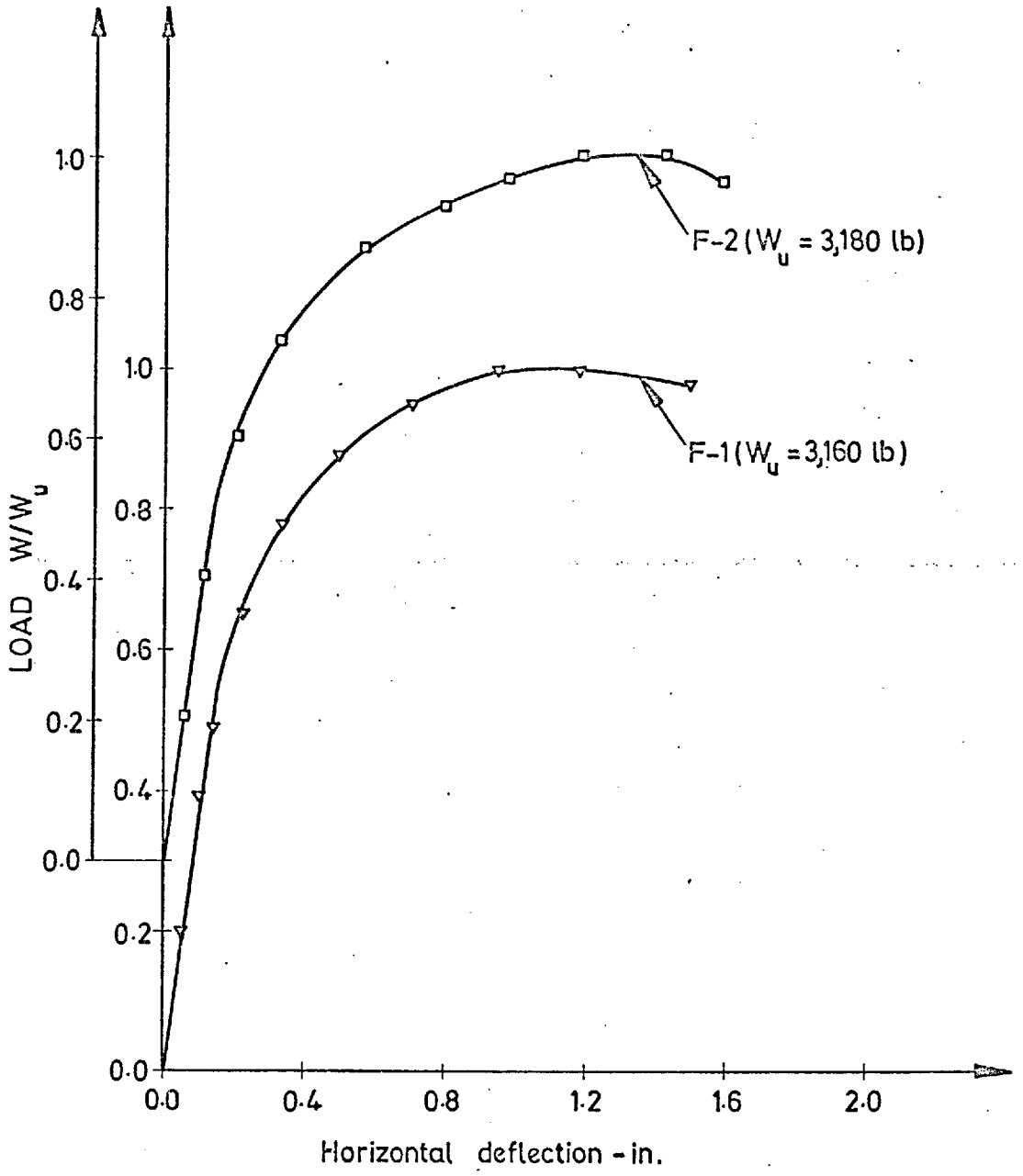

Fig. 7.21: LOAD - HORIZONTAL DEFLECTION CURVES FOR FRAMES F-1 & 2

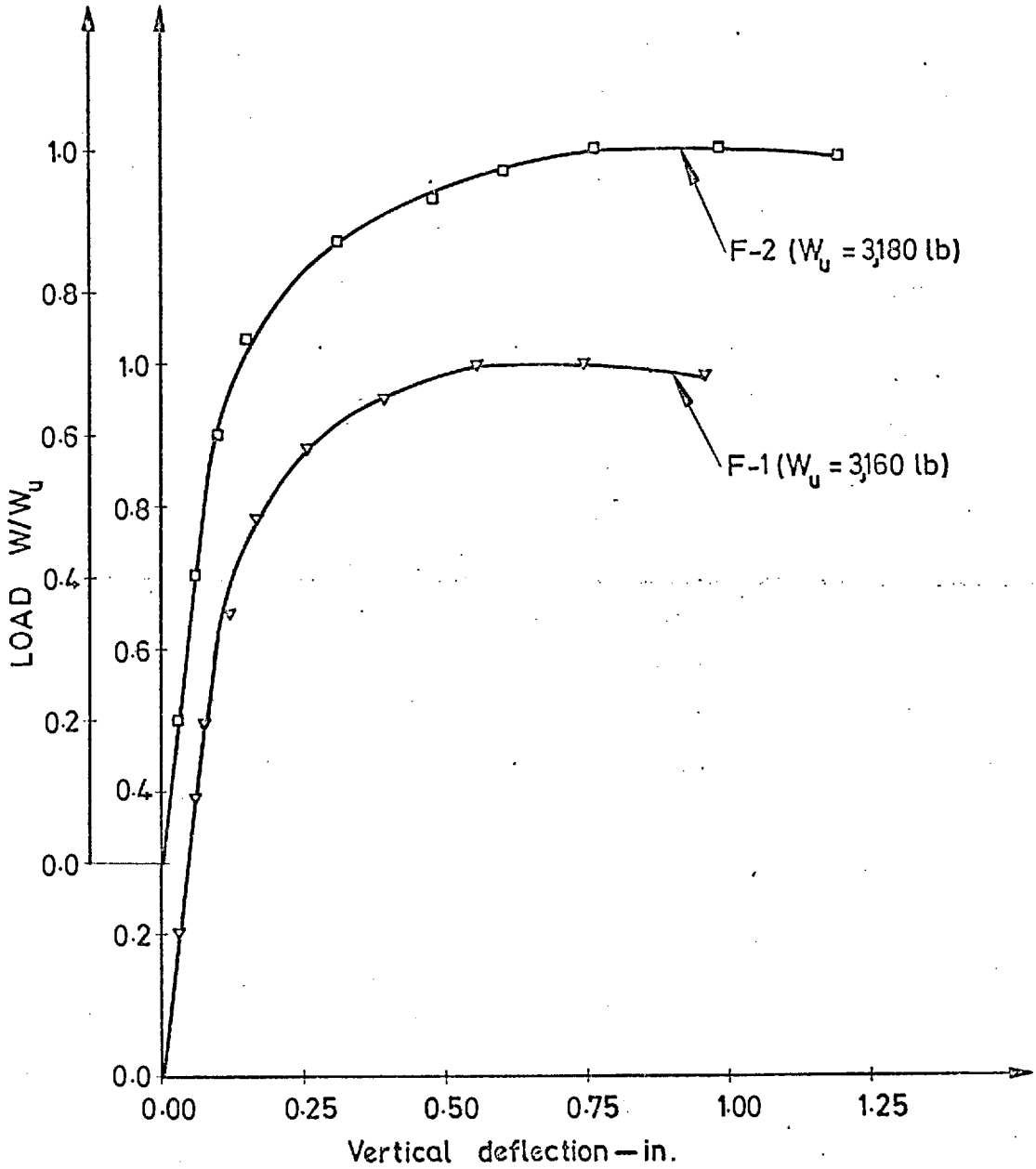

Fig. 7.22: LOAD-VERTICAL DEFLECTION CURVES FOR FRAMES F-1 & 2

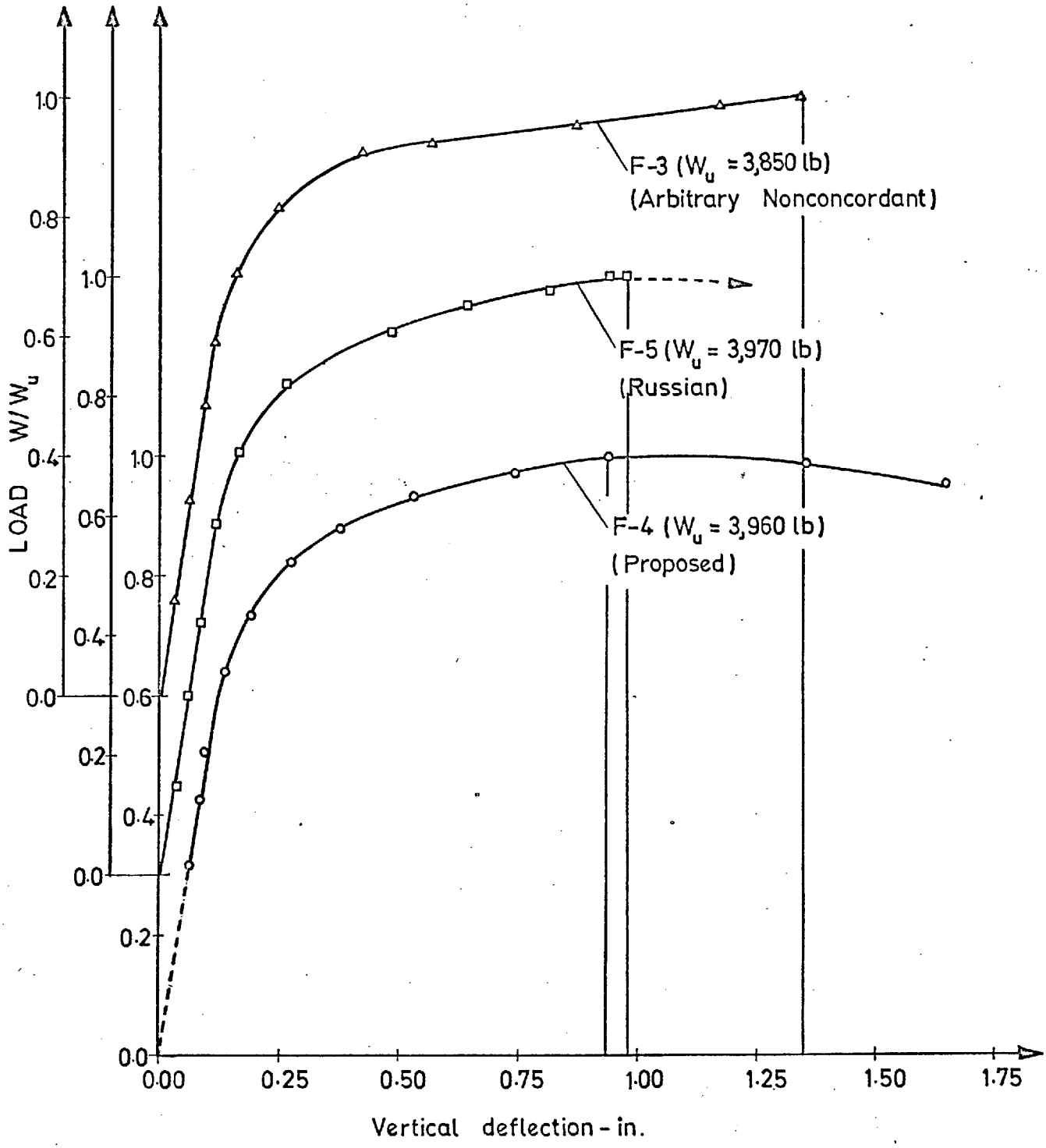

Fig. 7.24: LOAD - VERTICAL DEFLECTION CURVES FOR FRAMES F - 3, 4 & 5

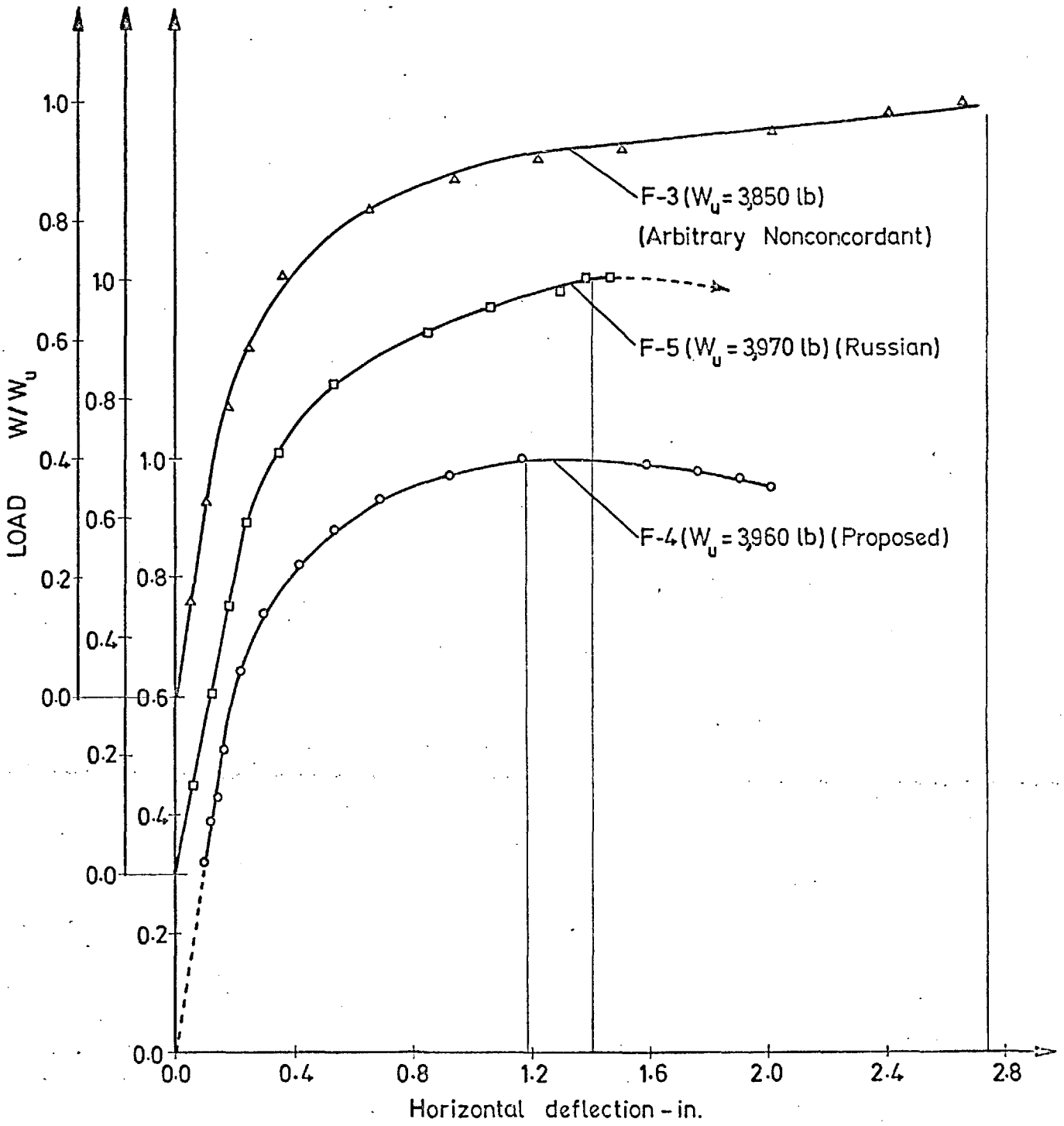

Fig. 7.23: LOAD - HORIZONTAL DEFLECTION CURVES FOR FRAMES F-3 , 4 & 5

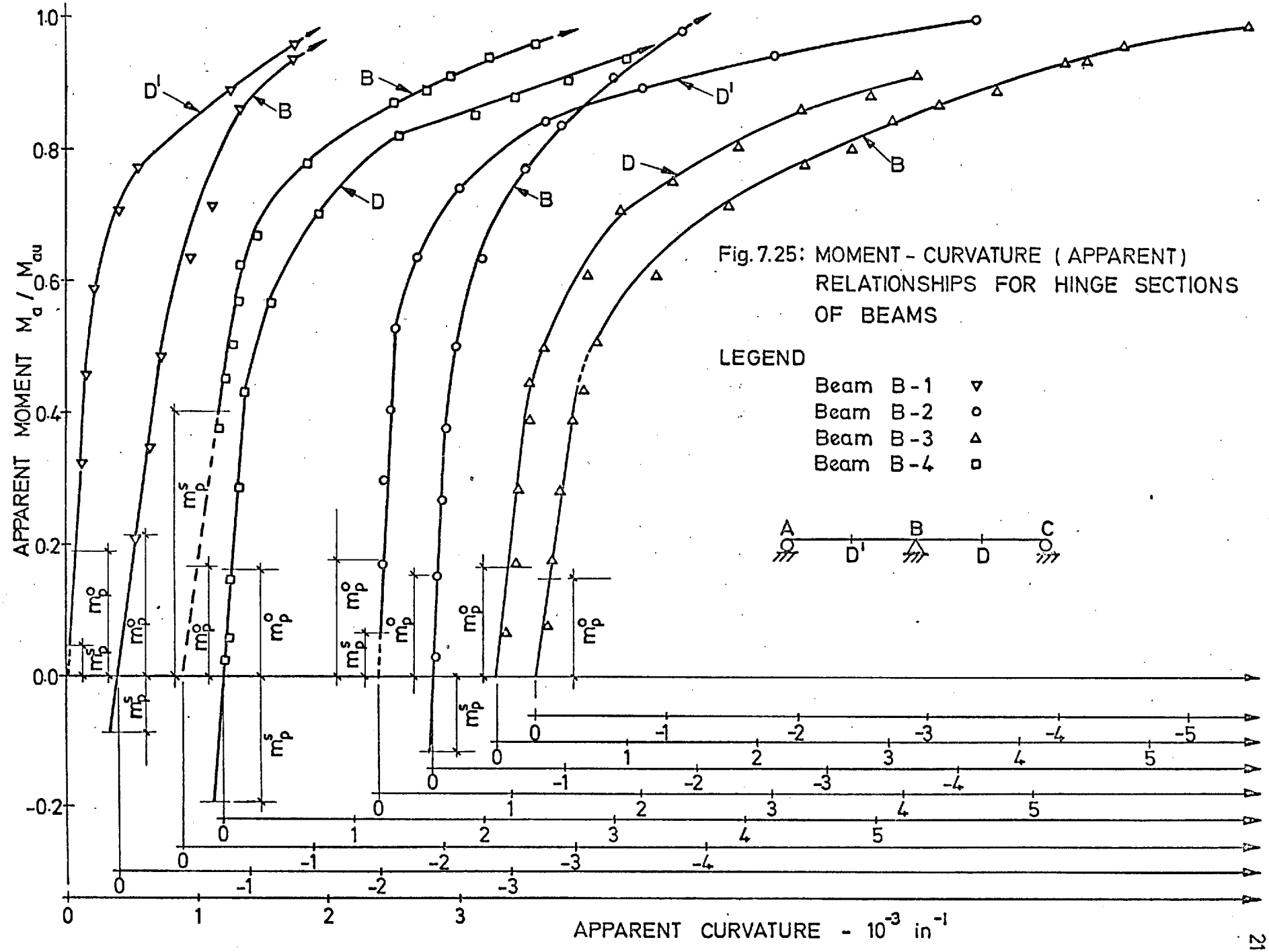

Fig. 7.25: MOMENT - CURVATURE (APPARENT) RELATIONSHIPS FOR HINGE SECTIONS OF BEAMS

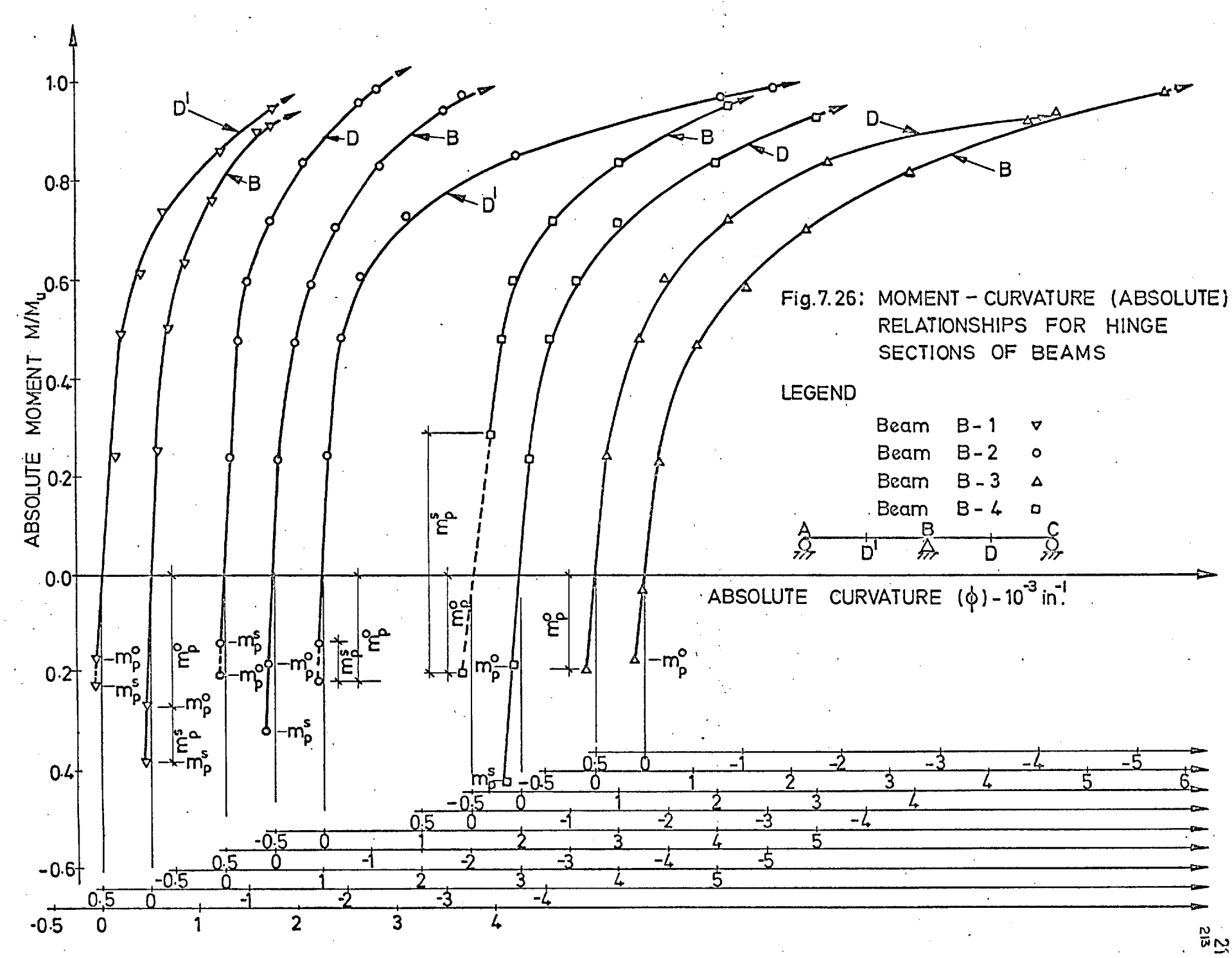

Fig.7.26: MOMENT – CURVATURE (ABSOLUTE) RELATIONSHIPS FOR HINGE SECTIONS OF BEAMS

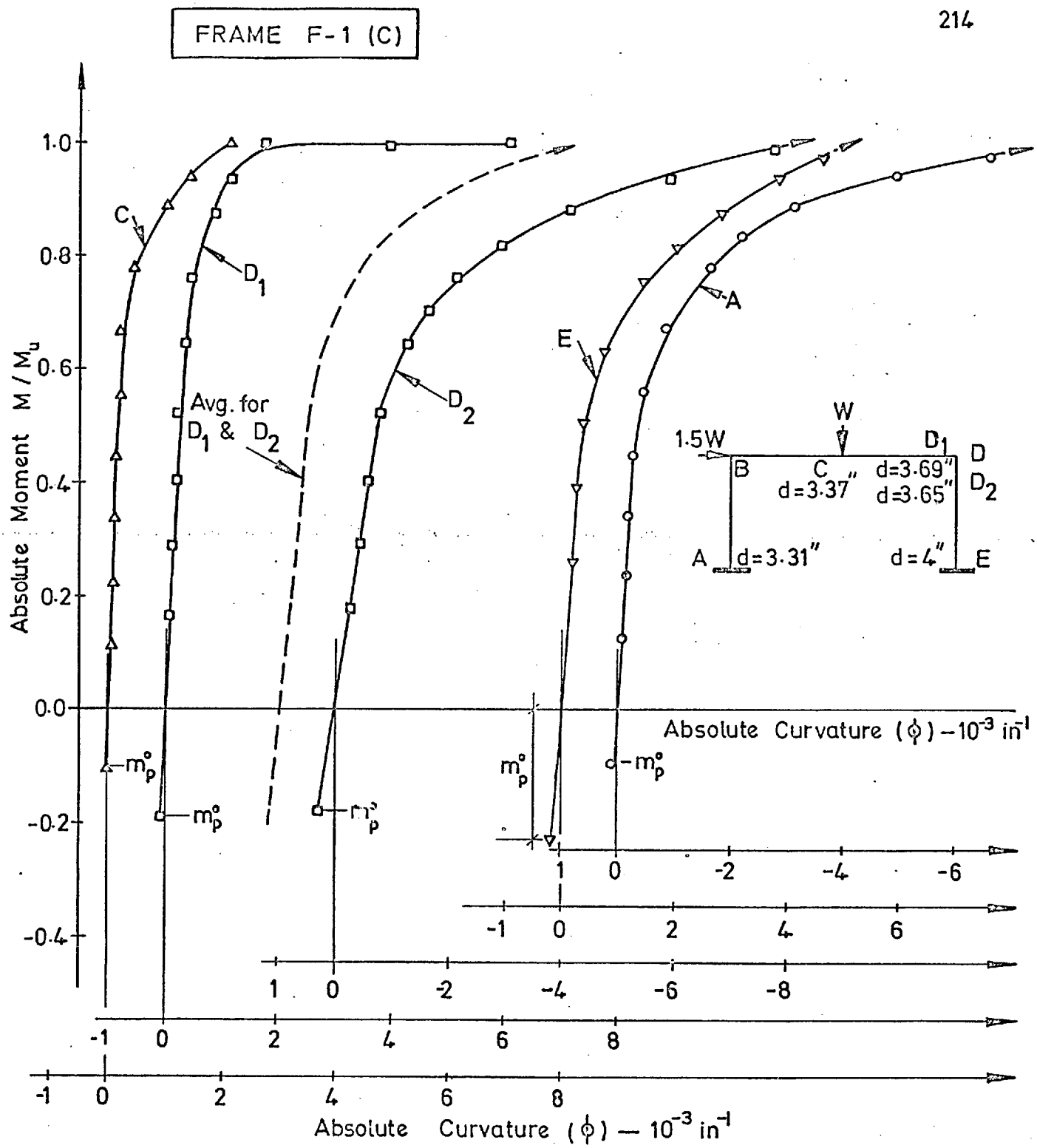

Fig 7.27 : MOMENT — CURVATURE ABSOLUTE RELATIONSHIPS FOR CRITICAL SECTIONS

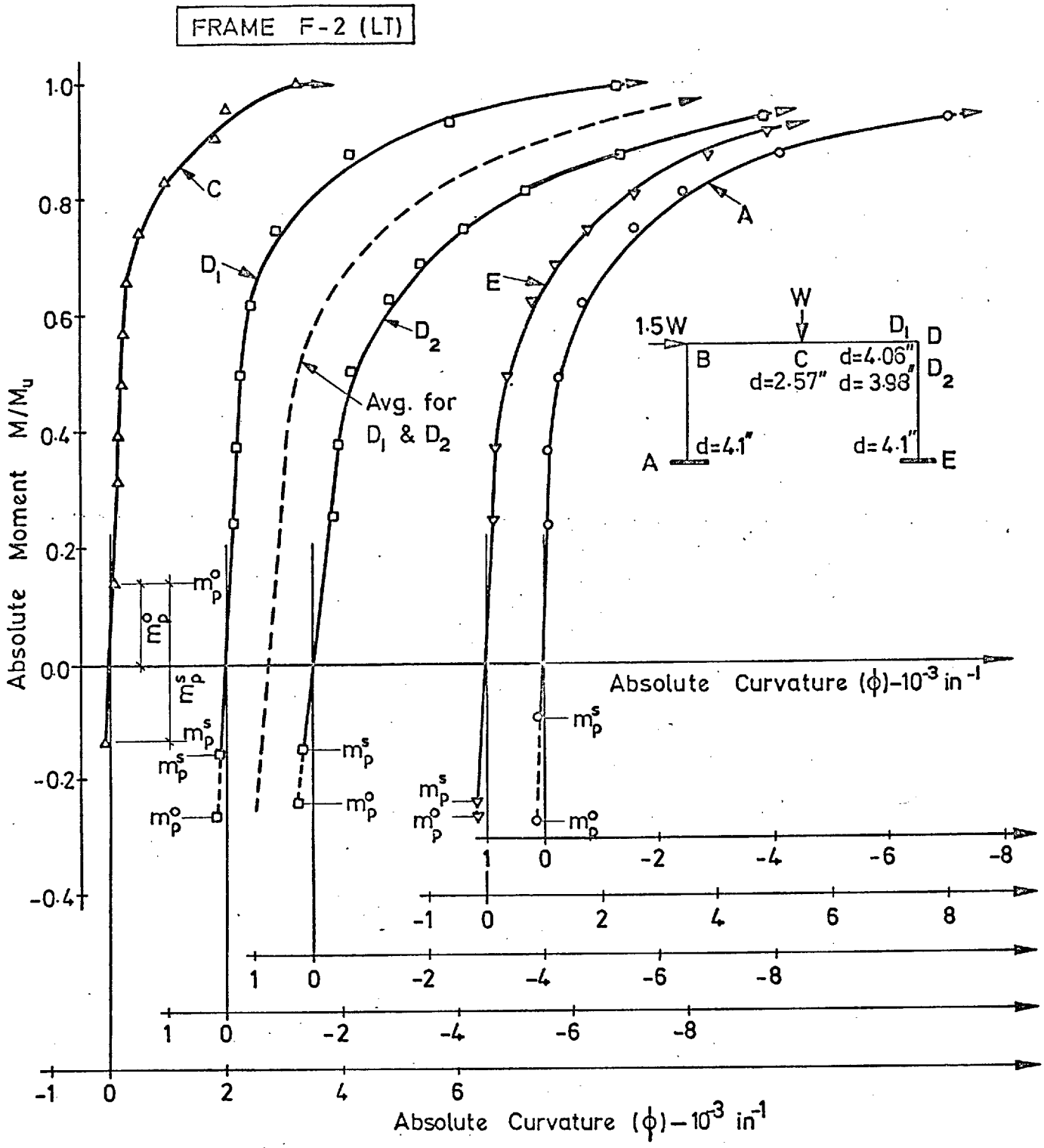

Fig. 7.28: MOMENT - CURVATURE (ABSOLUTE) RELATIONSHIPS FOR CRITICAL SECTIONS

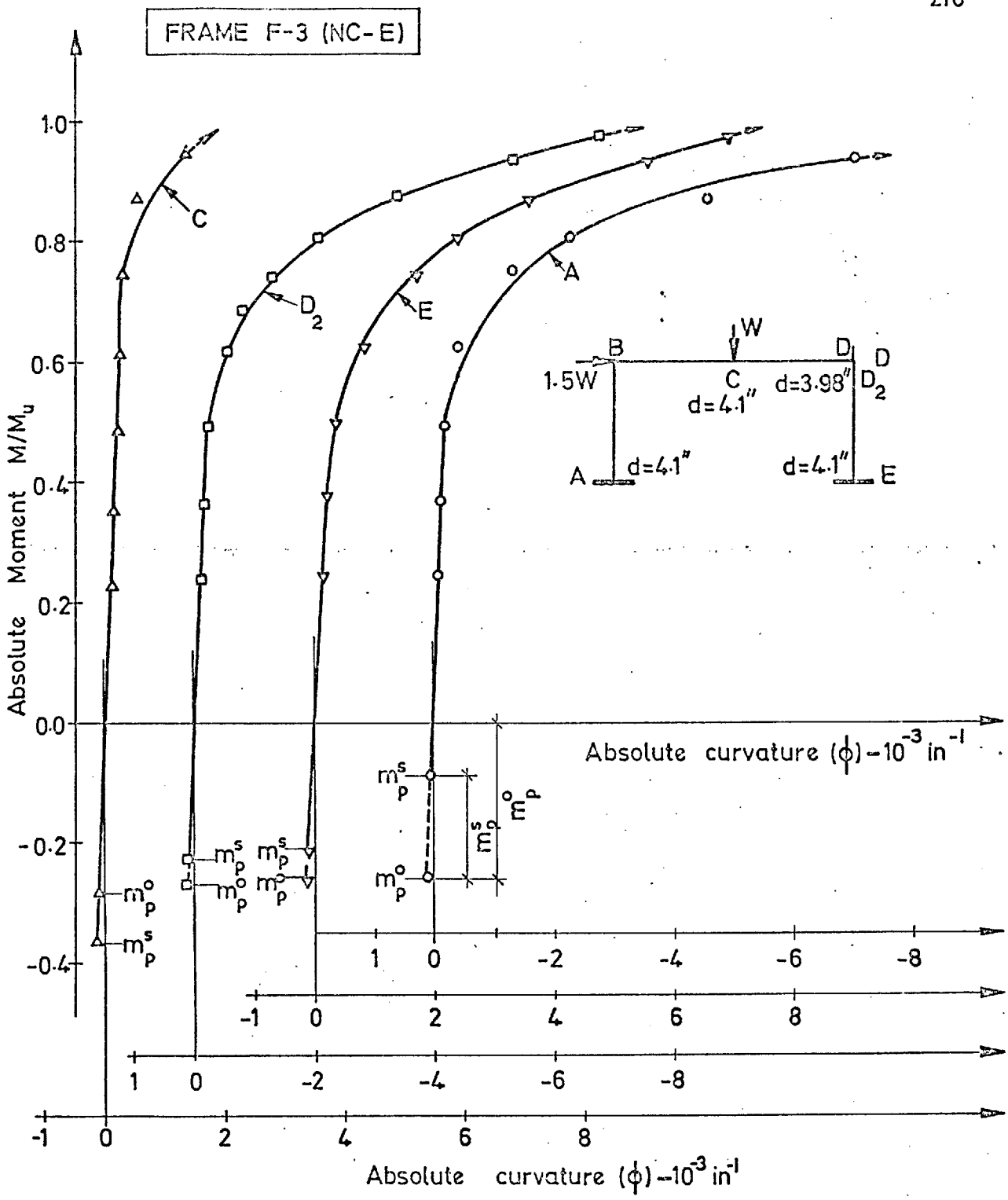

Fig. 7.29: MOMENT-CURVATURE (ABSOLUTE) RELATIONSHIPS FOR CRITICAL SECTIONS

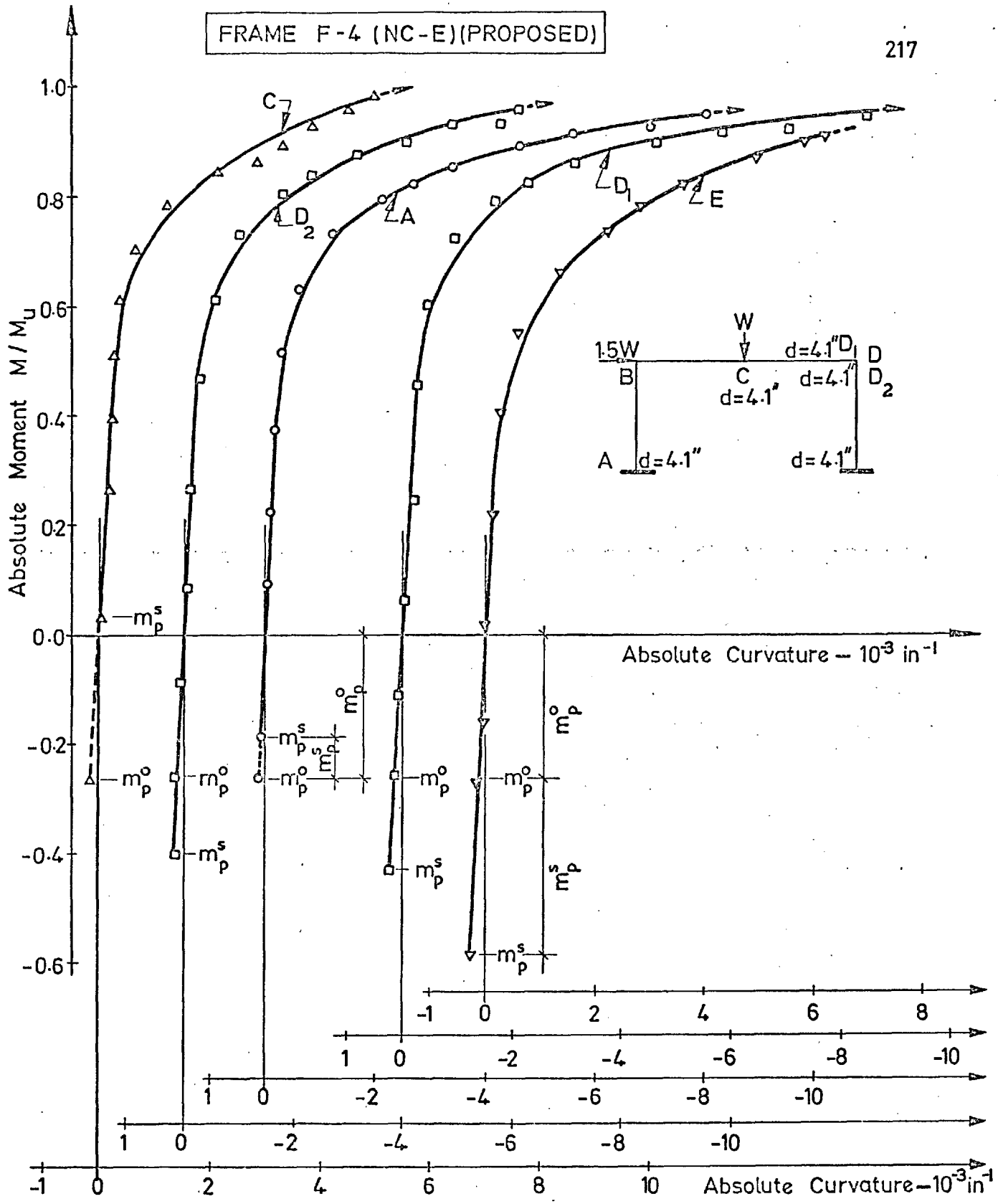

Fig. 7.30: MOMENT-CURVATURE (ABSOLUTE) RELATIONSHIPS FOR CRITICAL SECTIONS

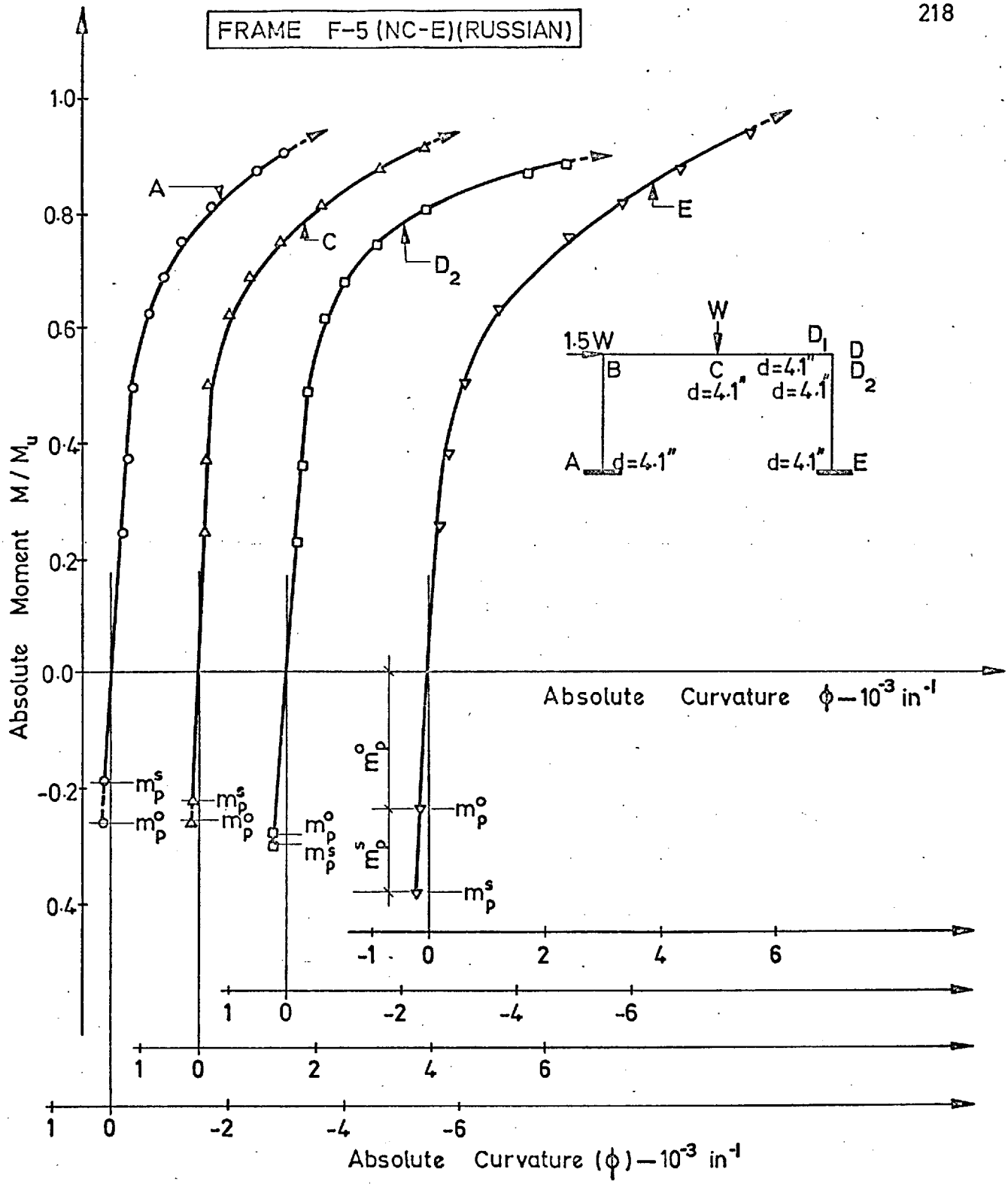

Fig. 7.31: MOMENT - CURVATURE (ABSOLUTE) RELATIONSHIPS FOR CRITICAL SECTIONS

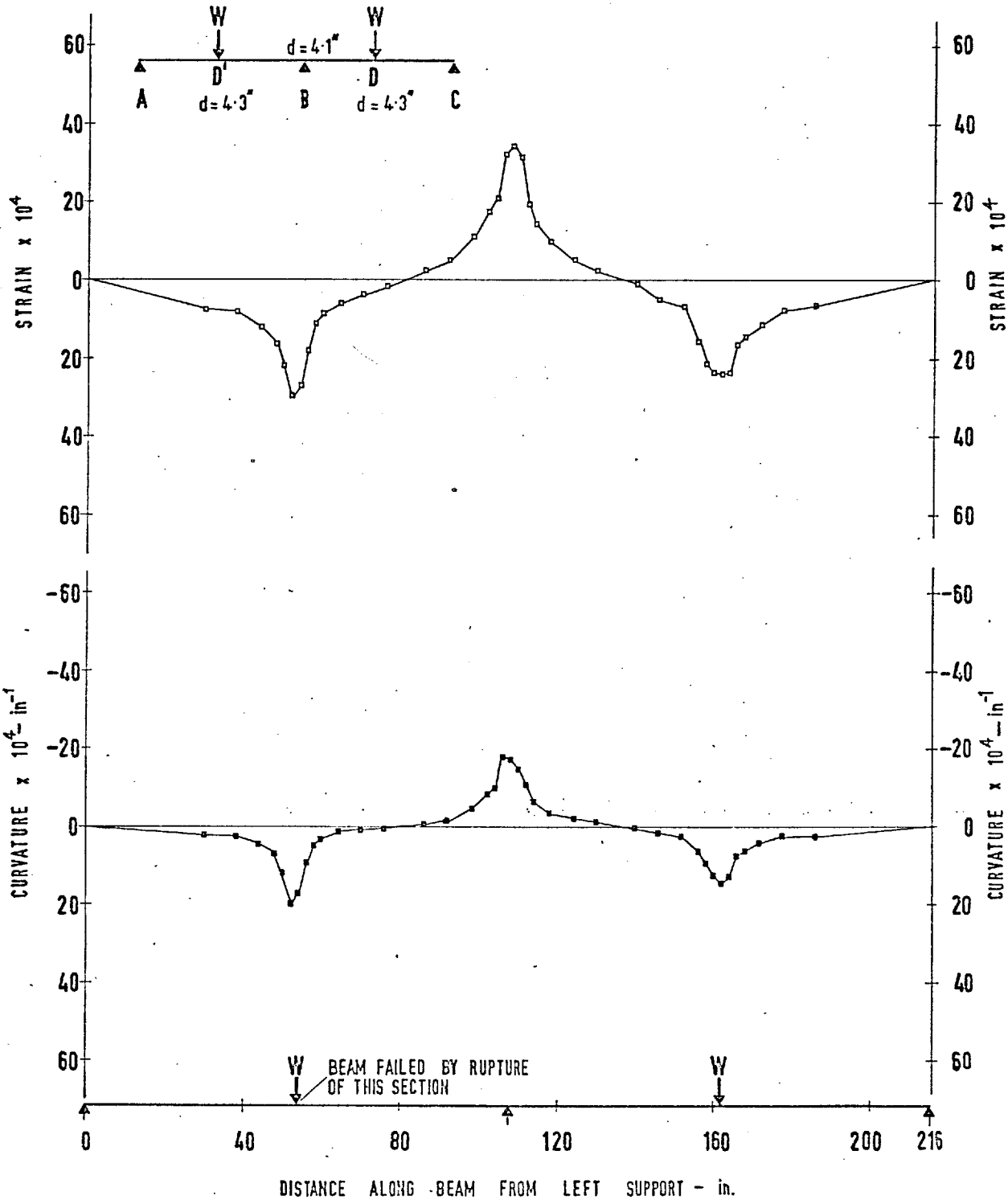

Fig. 7·32 : DISTRIBUTION OF EXTREME COMPRESSION FIBRE STRAIN AND CURVATURE ALONG BEAM AT 0·945 W_u

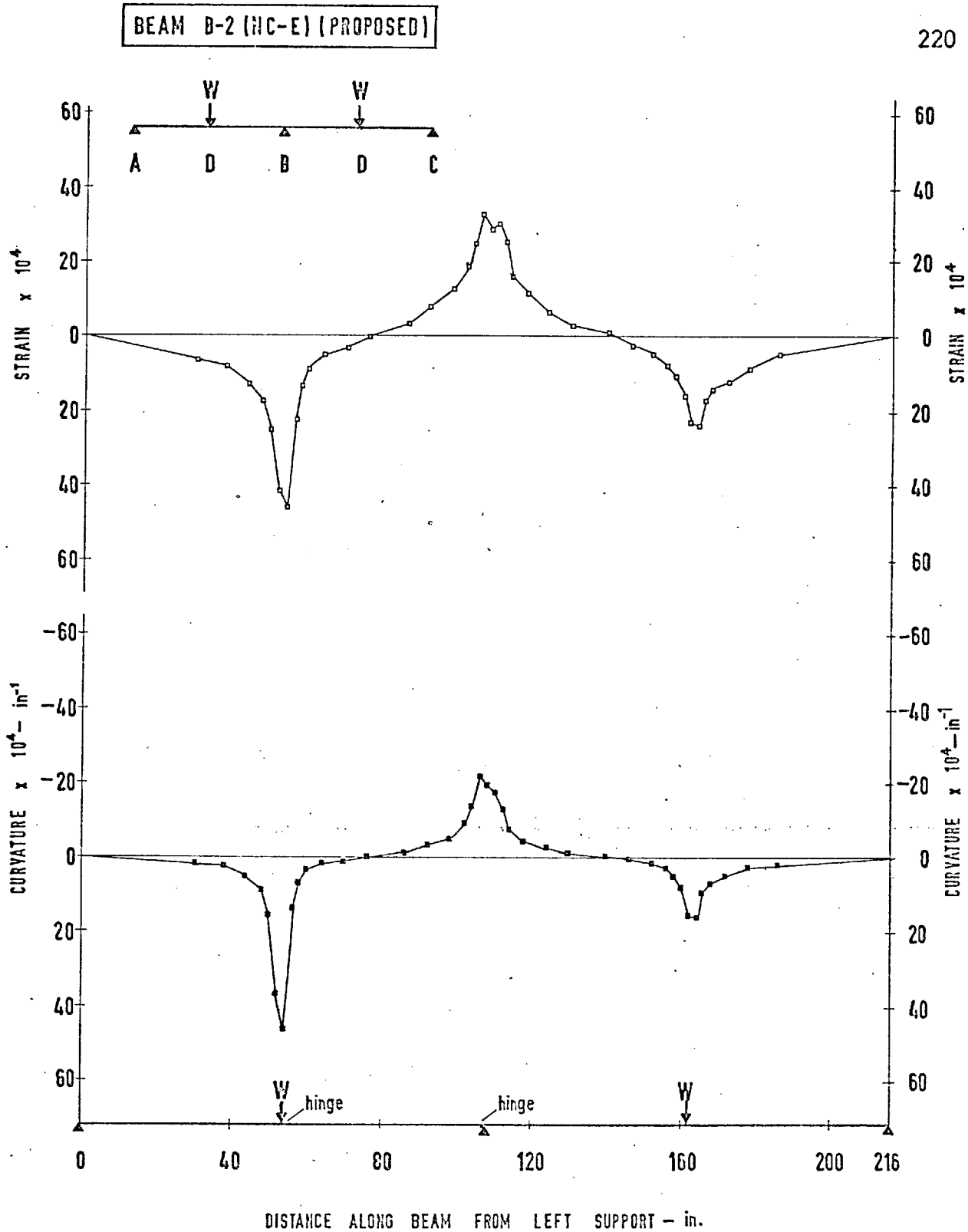

Fig. 7·33 : DISTRIBUTION OF EXTREME COMPRESSION FIBRE STRAIN AND CURVATURE ALONG BEAM AT 0·983W_u

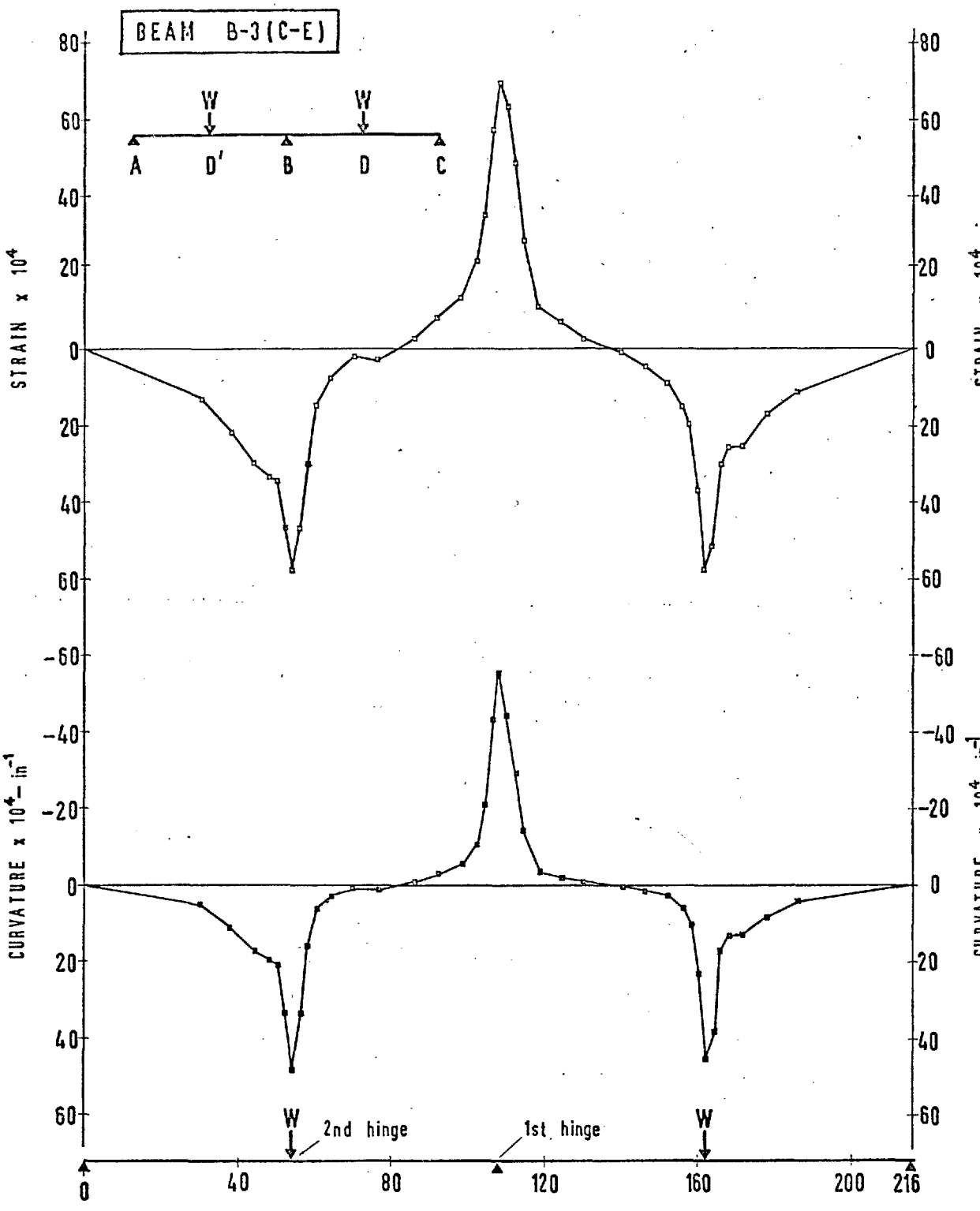

Fig. 7-34: DISTRIBUTION OF EXTREME COMPRESSION FIBRE STRAIN AND CURVATURE ALONG BEAM AT 0·953 W_u

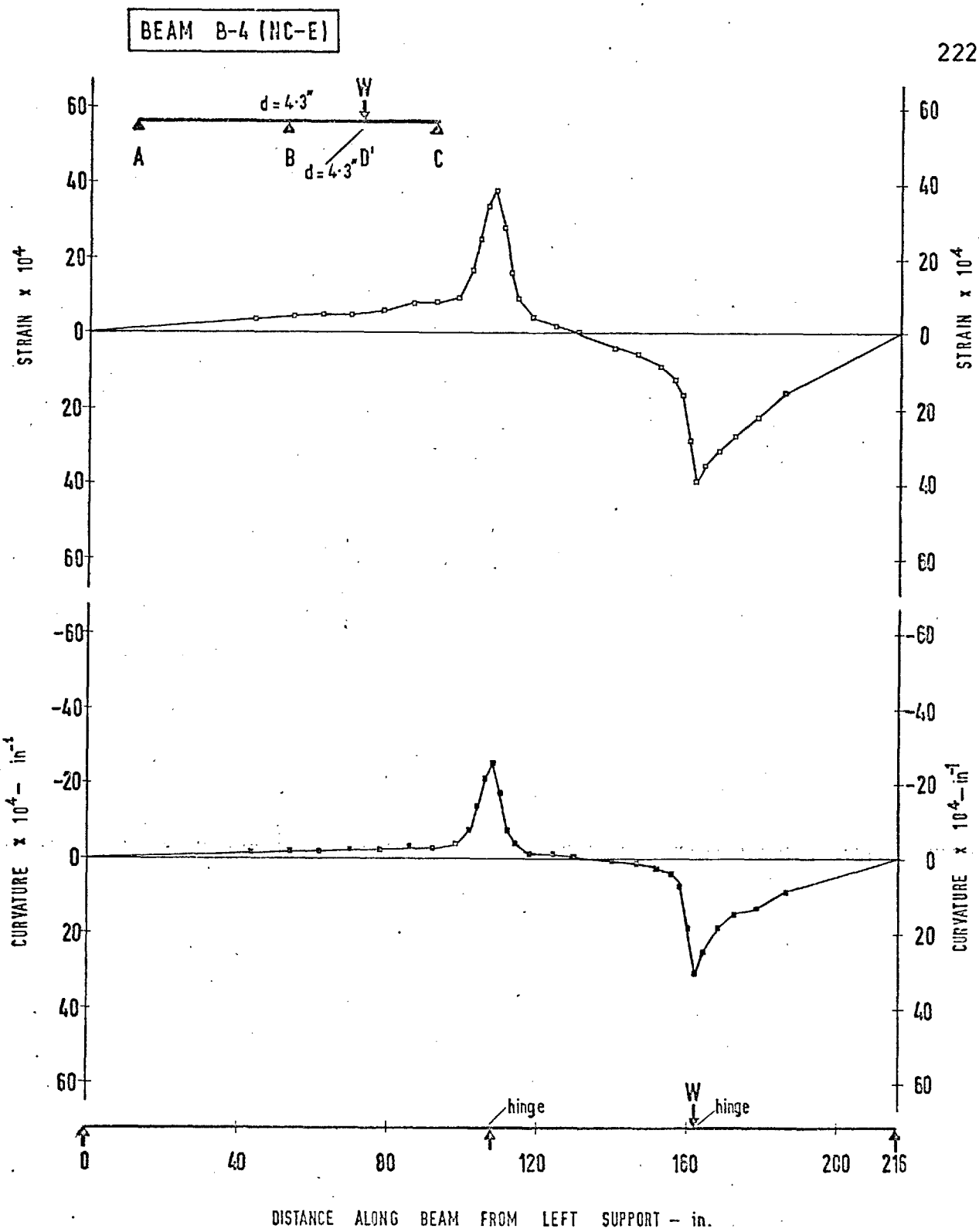

Fig. 7·35 : DISTRIBUTION OF EXTREME COMPRESSION FIBRE STRAIN AND CURVATURE ALONG BEAM AT 0·945 Wu

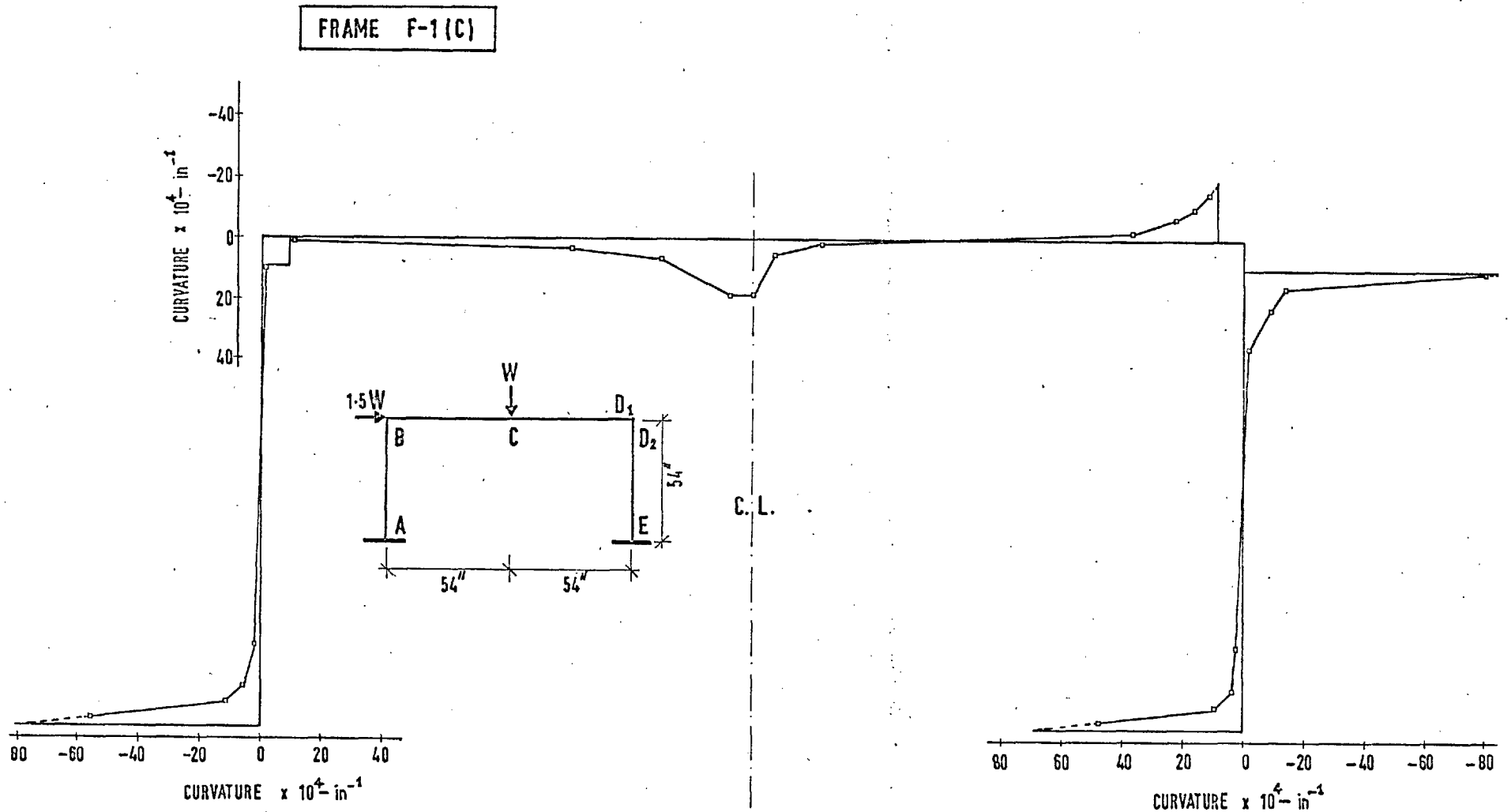

Fig. 7·36 : DISTRIBUTION OF CURVATURE ALONG THE FRAME AT W_u

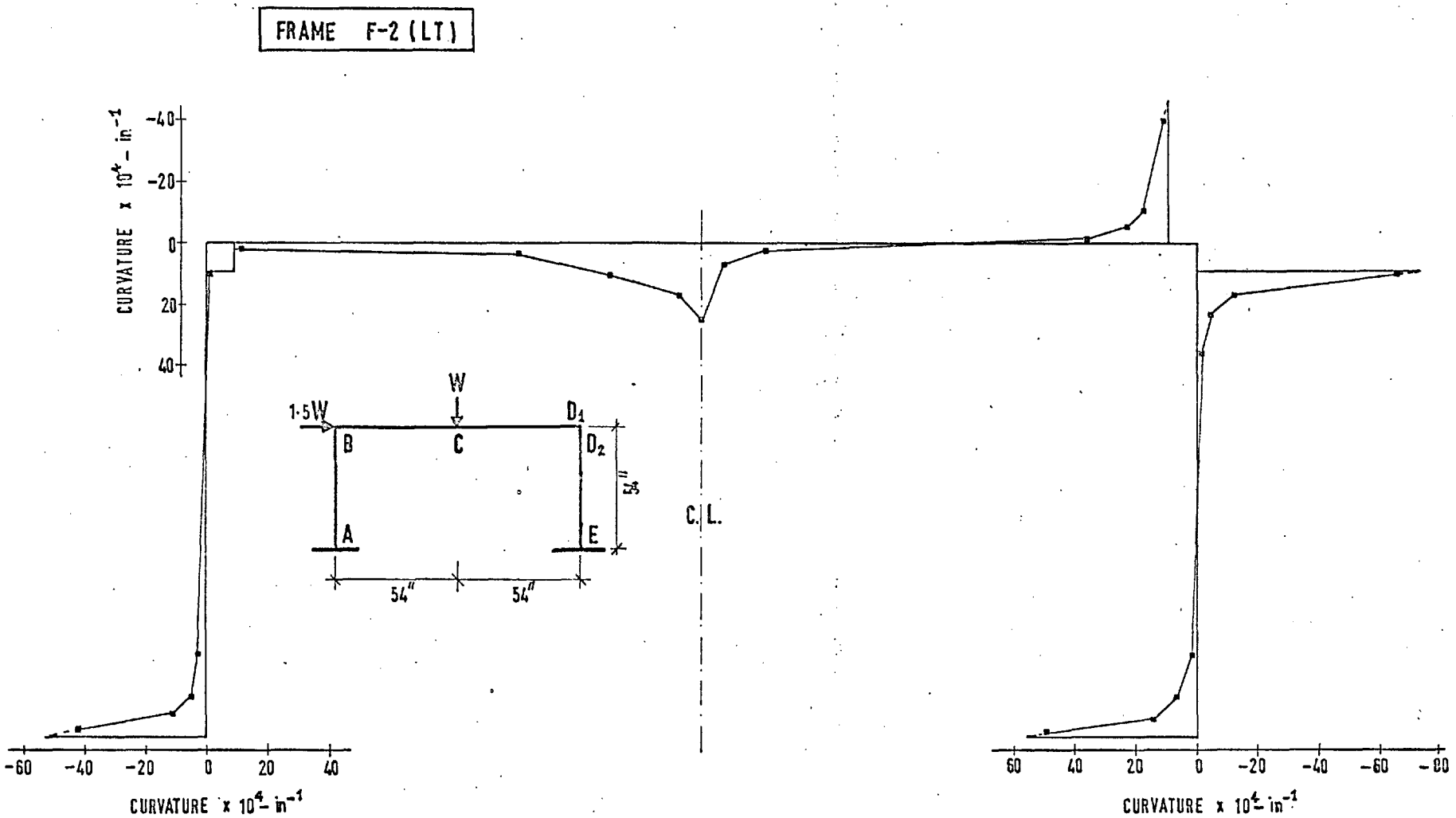

Fig. 7·37 : DISTRIBUTION OF CURVATURE ALONG THE FRAME AT 0·965W_u

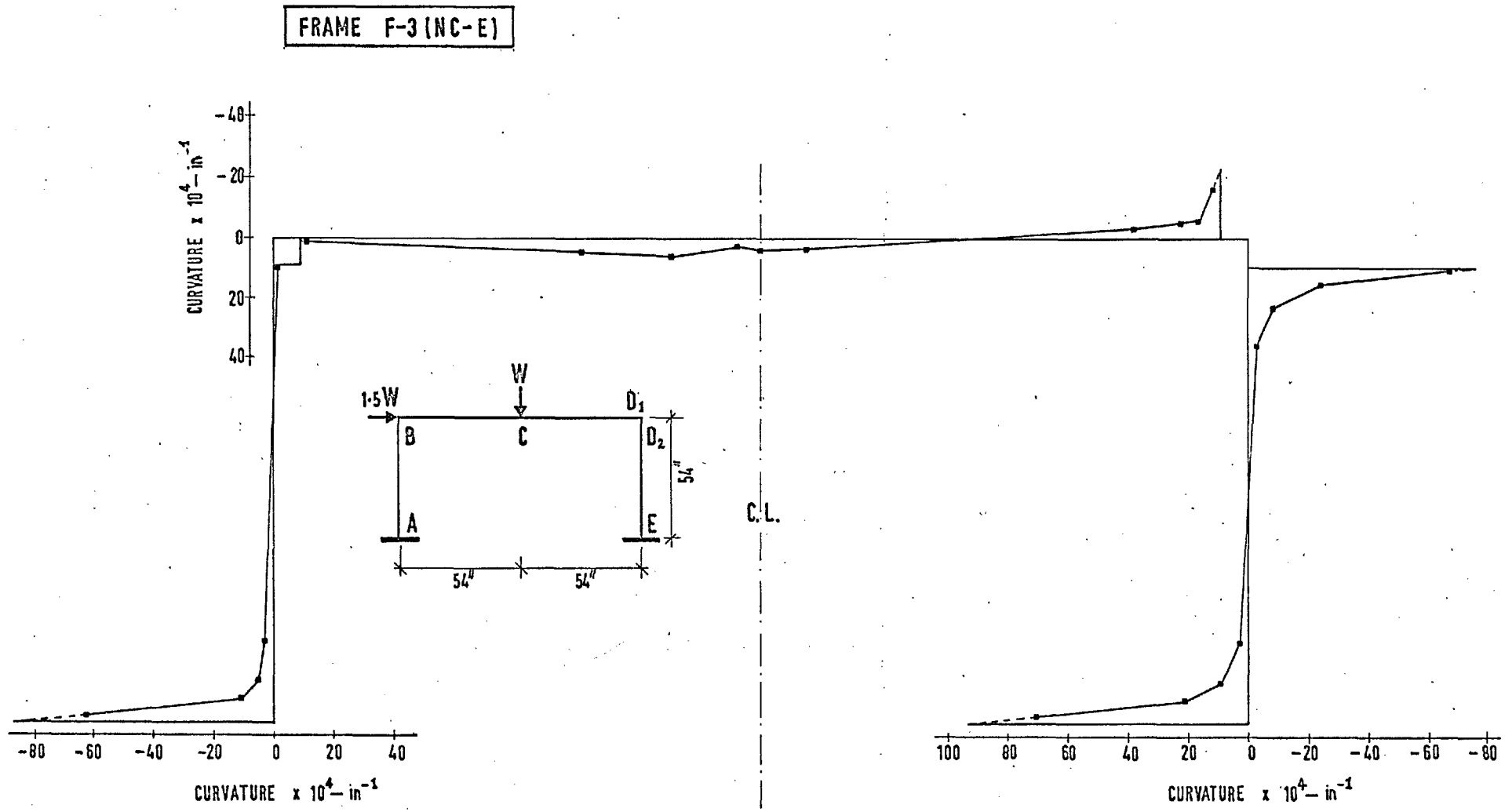

Fig. 7-38: DISTRIBUTION OF CURVATURE ALONG THE FRAME AT $0{\cdot}88W_u$

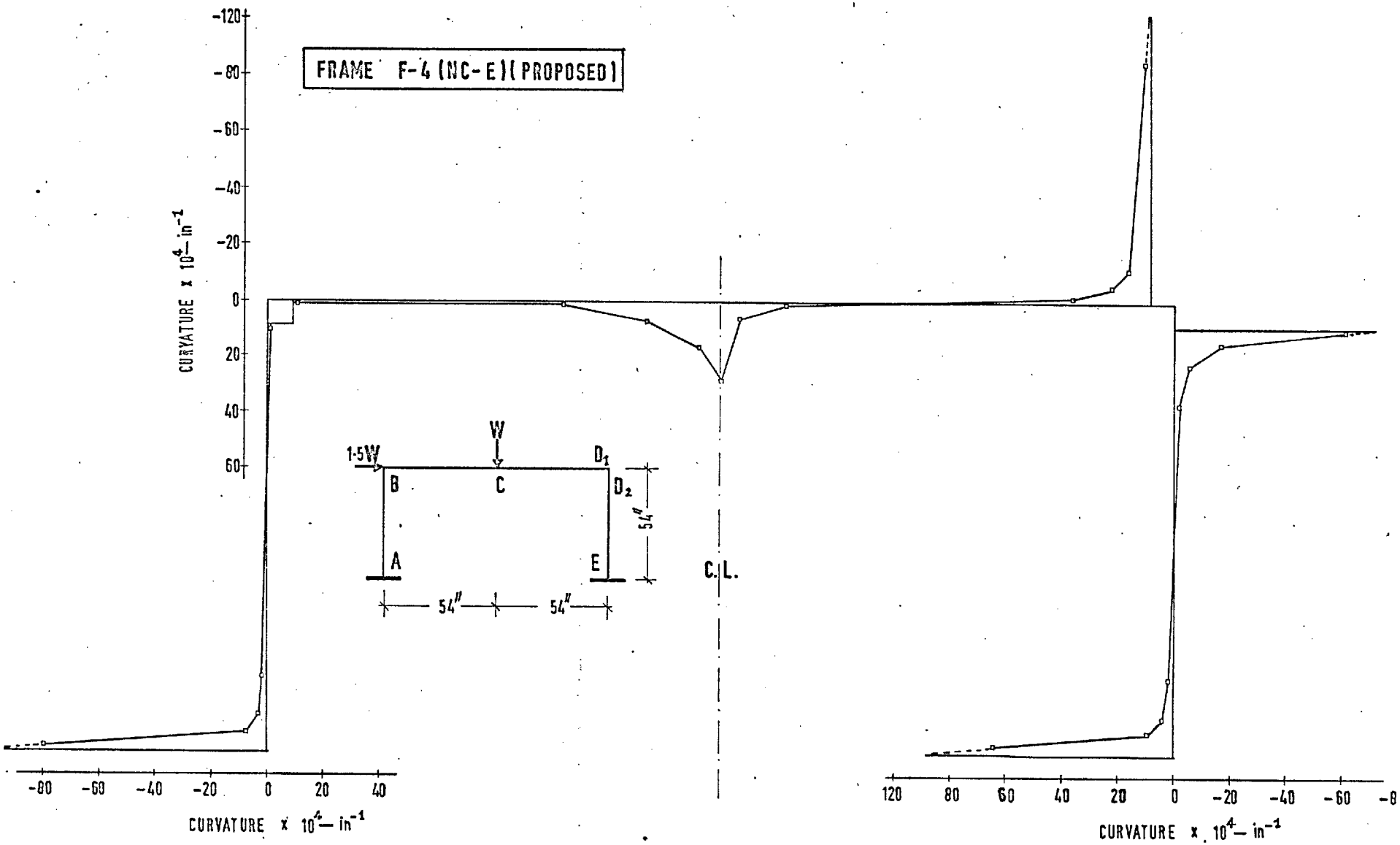

Fig. 7·39 : DISTRIBUTION OF CURVATURE ALONG THE FRAME AT 0·990W_u

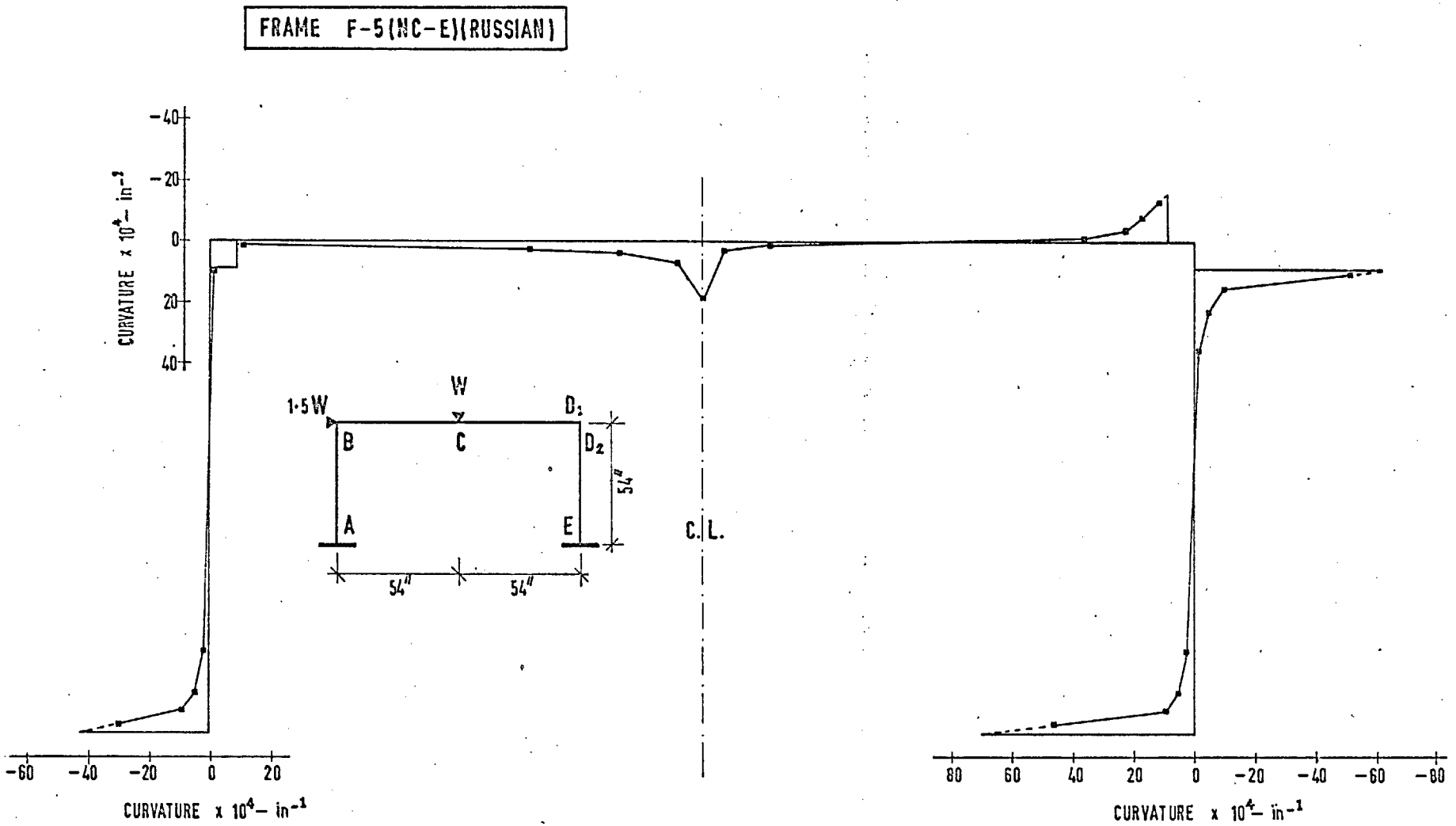

Fig. 7·40: DISTRIBUTION OF CURVATURE ALONG THE FRAME AT 0·905 W_u

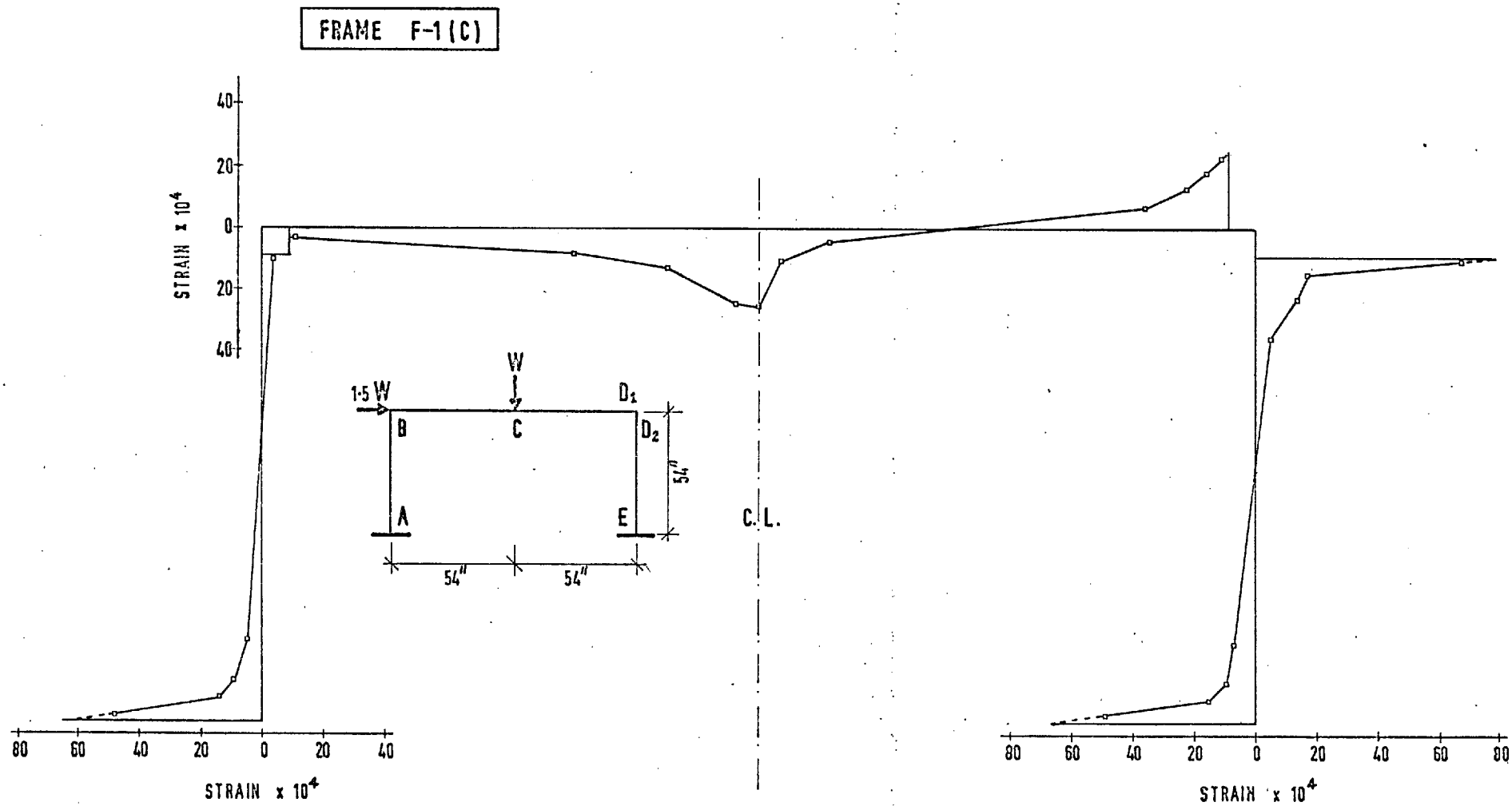

Fig. 7·41: DISTRIBUTION OF EXTREME COMPRESSION FIBRE STRAIN ALONG FRAME AT W_u

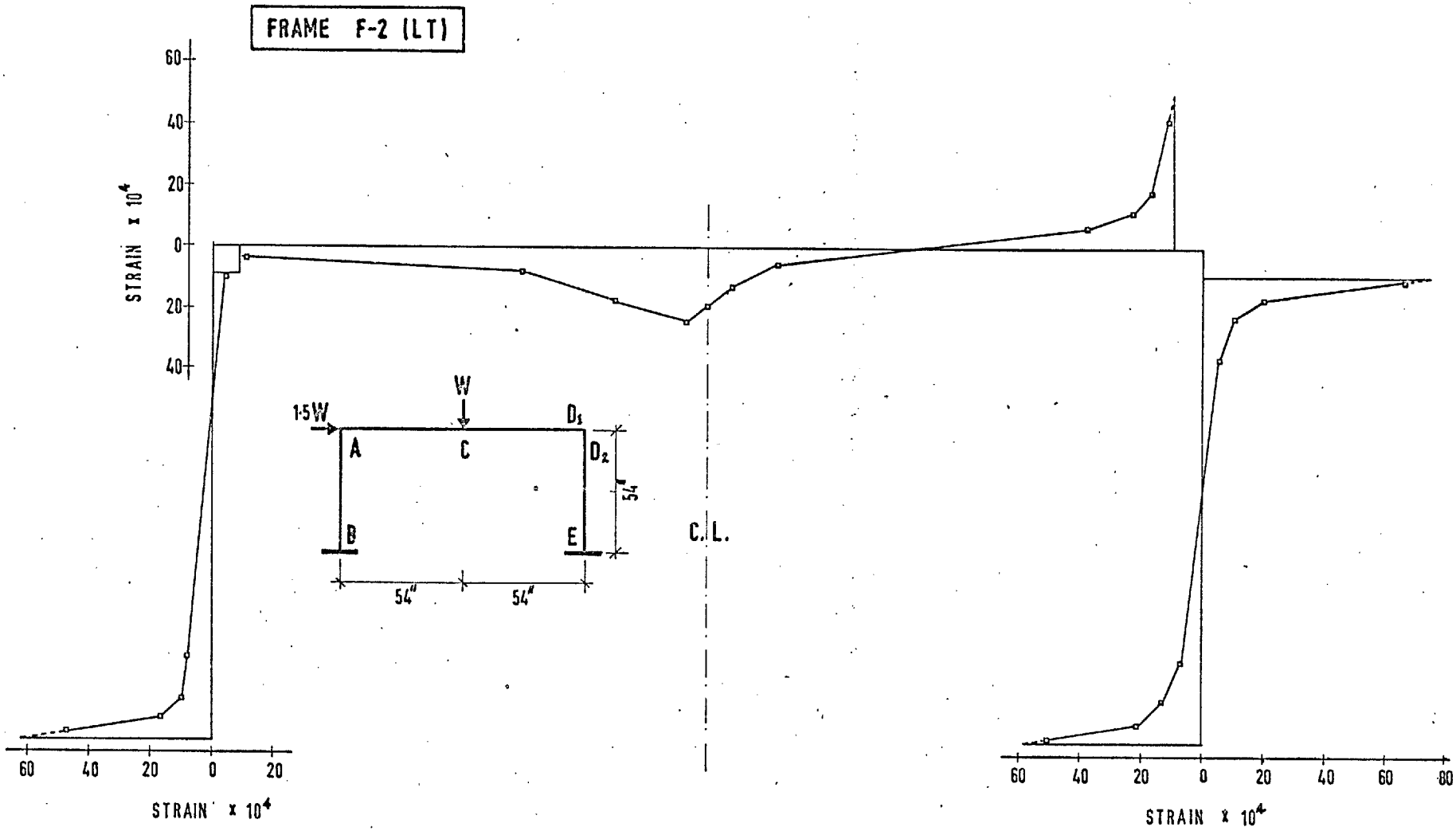

Fig. 7·42: DISTRIBUTION OF EXTREME COMPRESSION FIBRE STRAIN ALONG FRAME AT 0·965 W_u

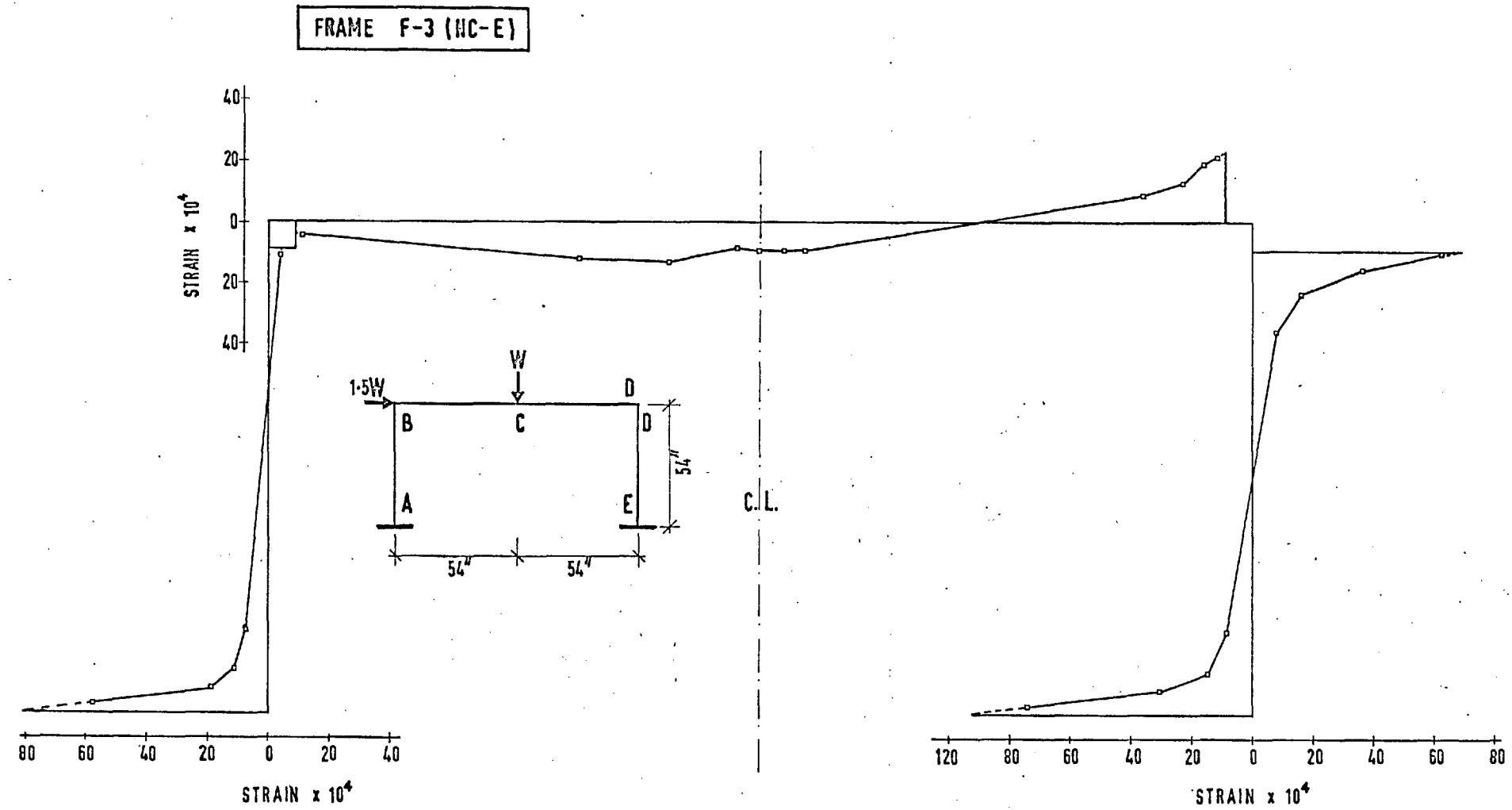

Fig. 7·43: DISTRIBUTION OF EXTREME COMPRESSION FIBRE STRAIN ALONG FRAME AT 0·80 W_u

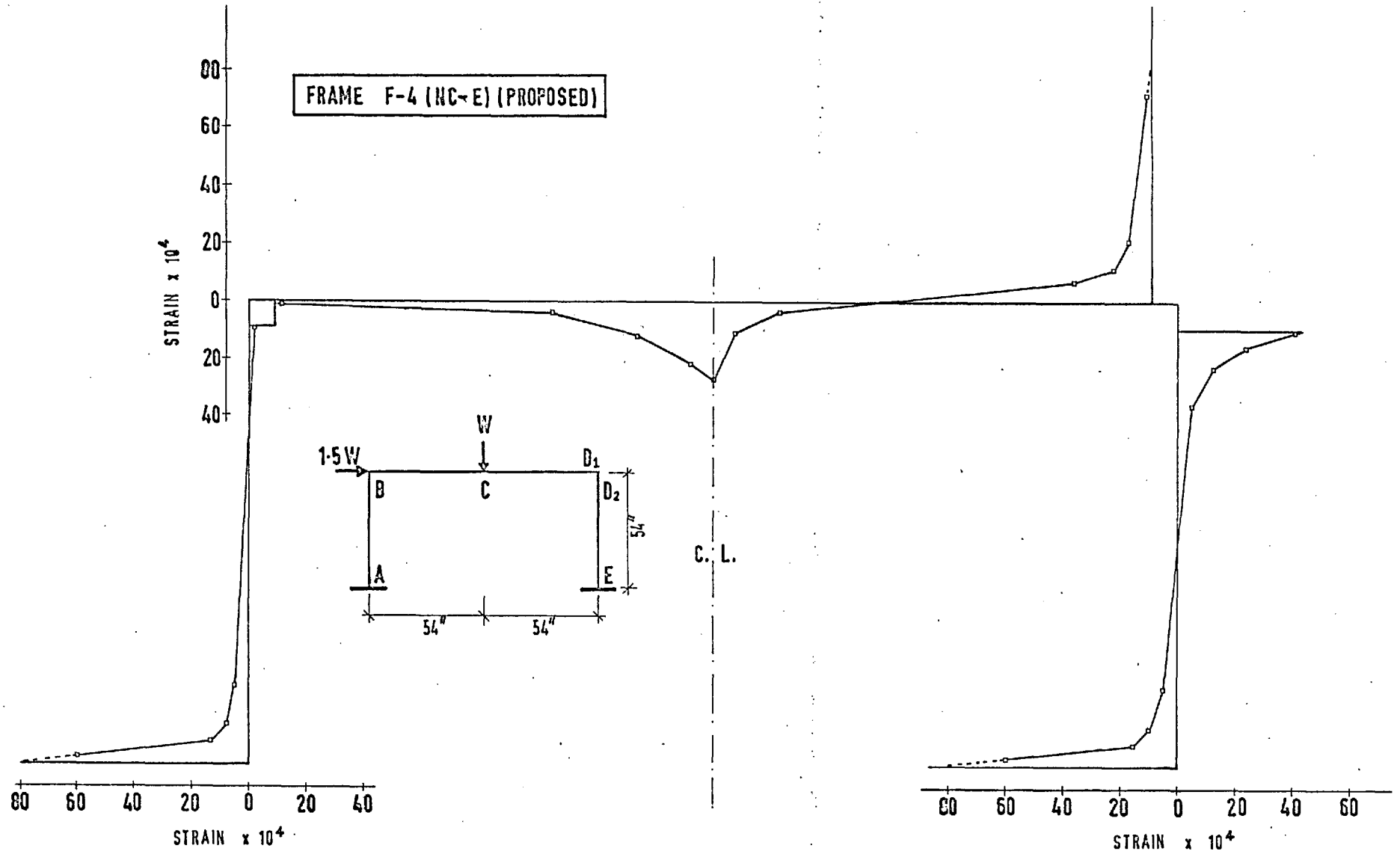

Fig. 7·44 : DISTRIBUTION OF EXTREME COMPRESSION FIBRE STRAIN ALONG FRAME AT 0·998 W_u

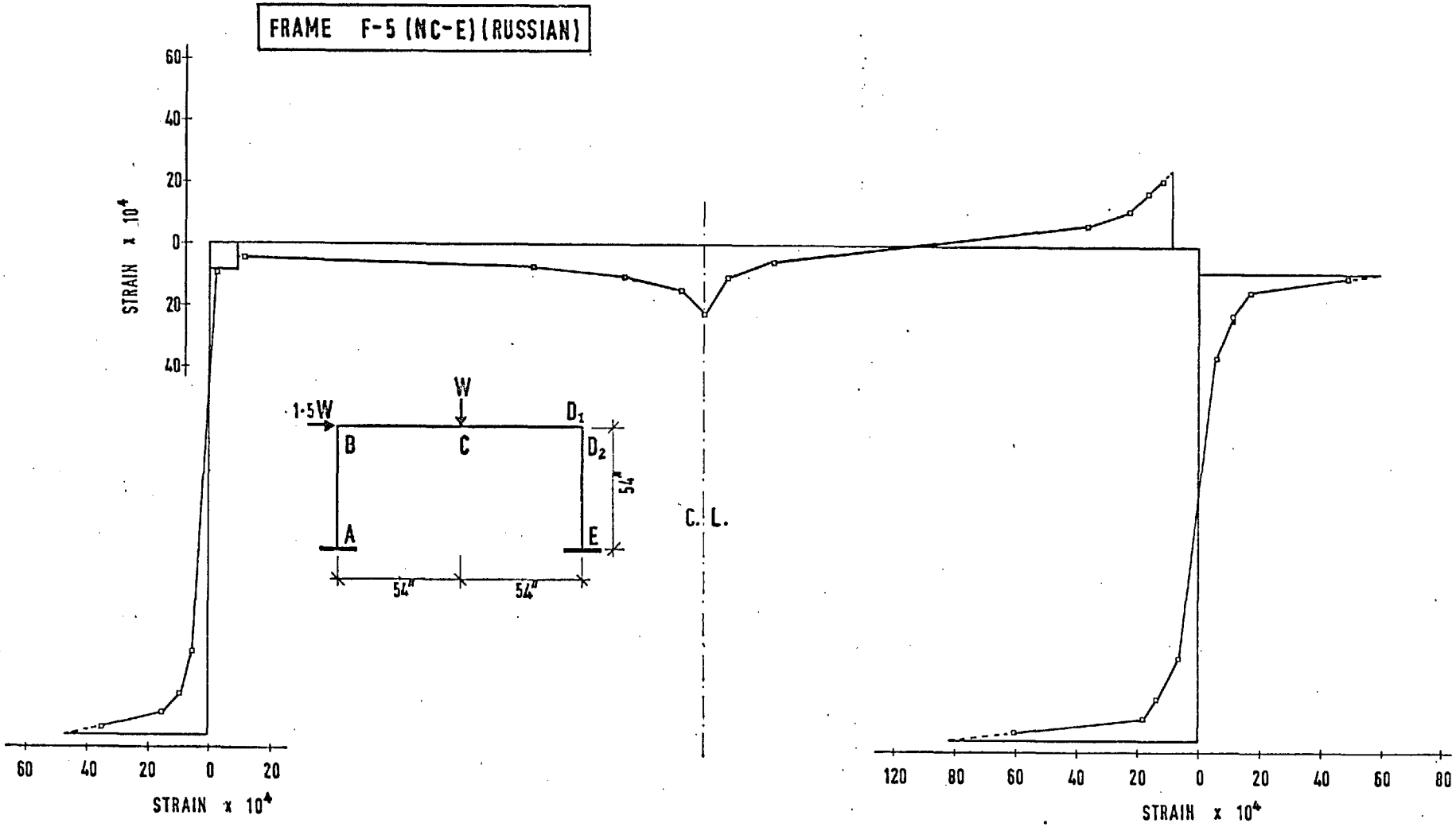

Fig. 7·45 : DISTRIBUTION OF EXTREME COMPRESSION FIBRE STRAIN ALONG BEAM AT $0{\cdot}905W_u$

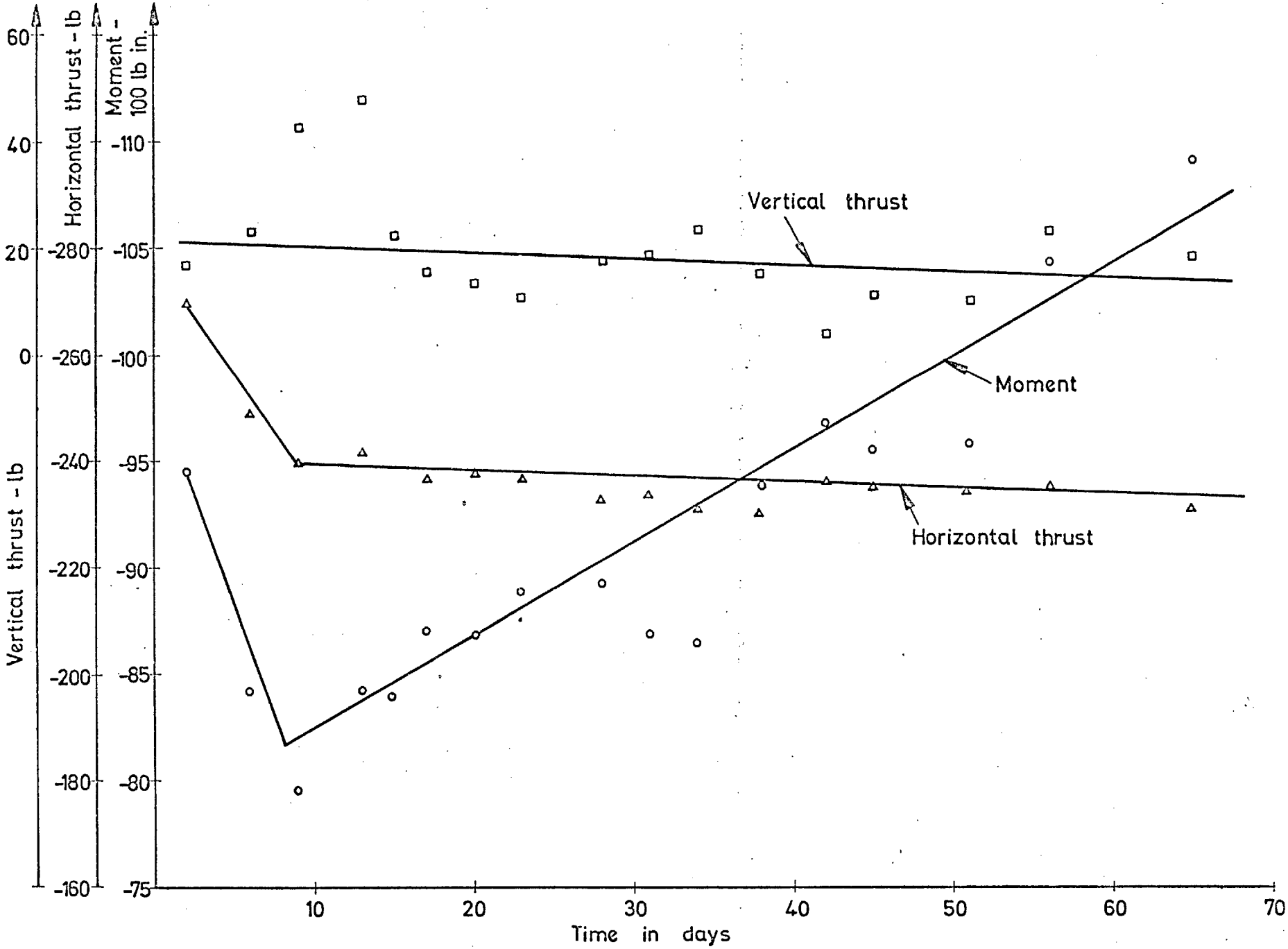

Fig. 7.46: EFFECT OF TIME ON REDUNDANT REACTIONS DUE TO PRESTRESS (FRAME F5)

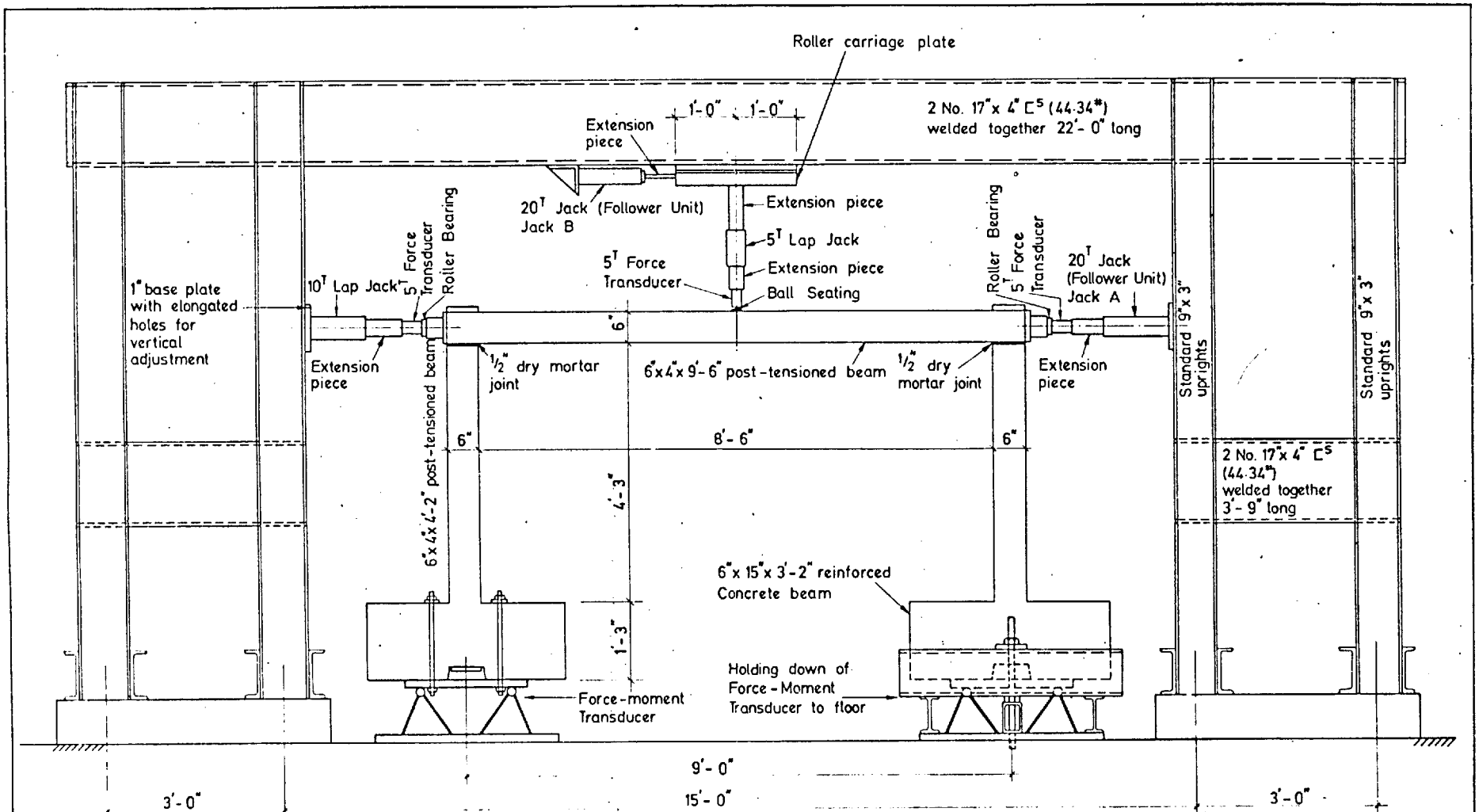

SCALE :- 1" to 1'-0"	RIG DETAILS FOR FRAME TESTS	DRG. No. 7.1

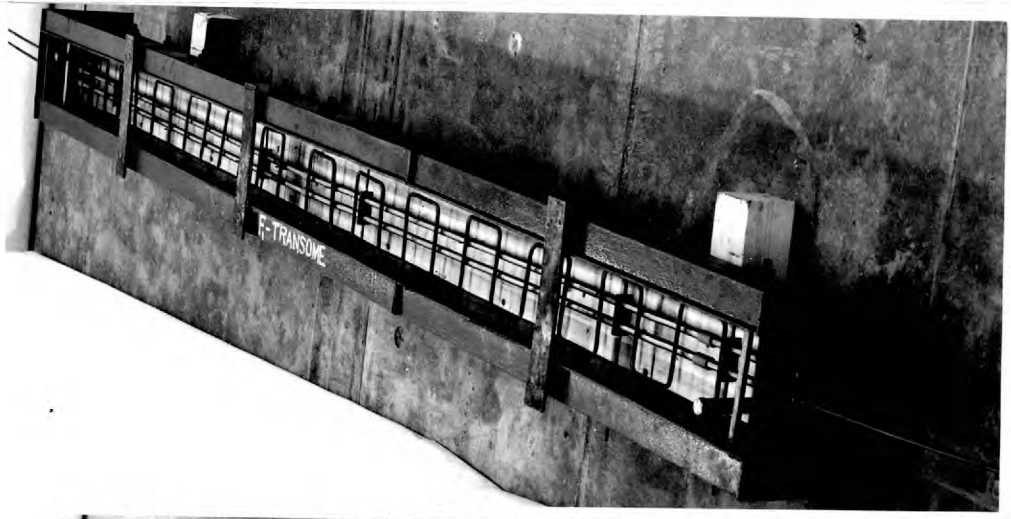

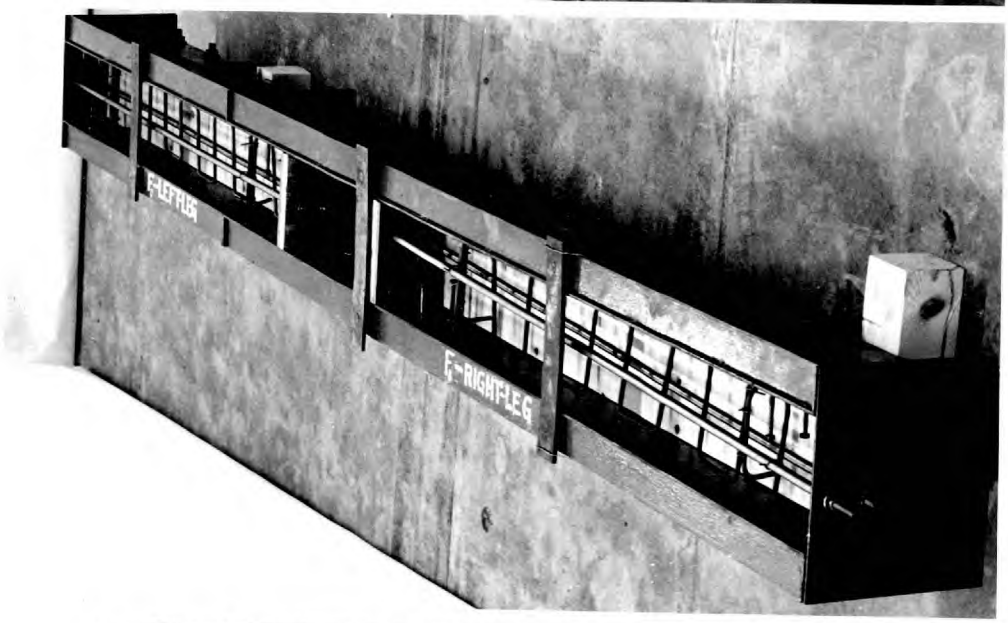

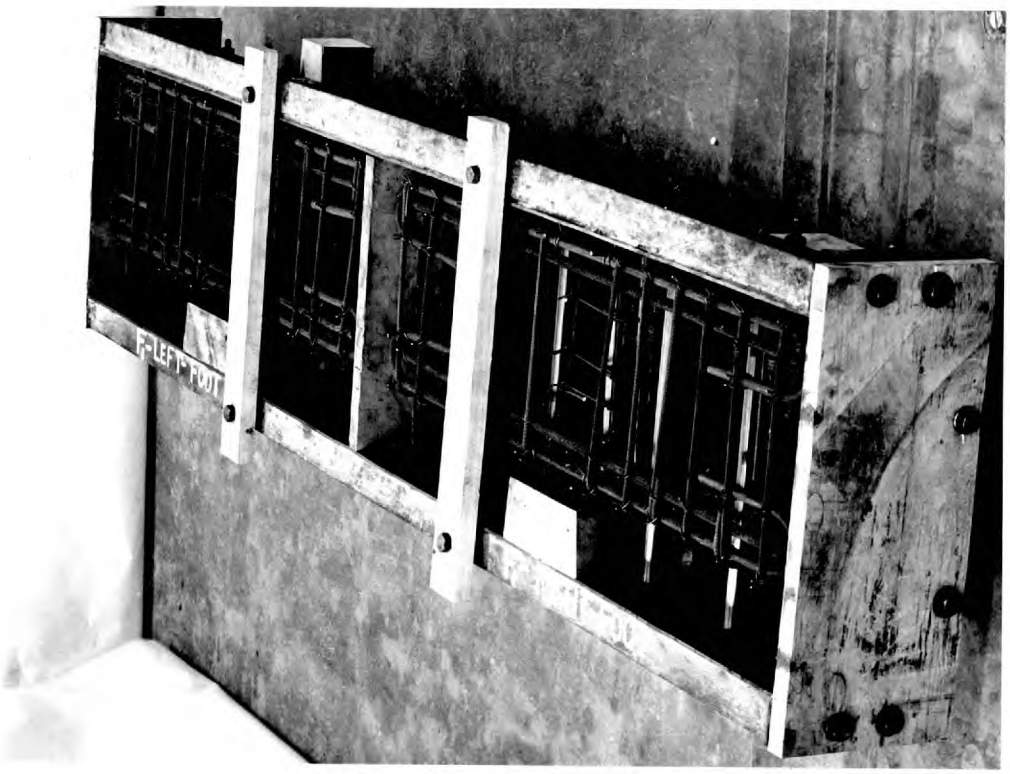

Arrangement of Reinforcement and Duct-Tubing in Frame F-1

PLATE 7.1

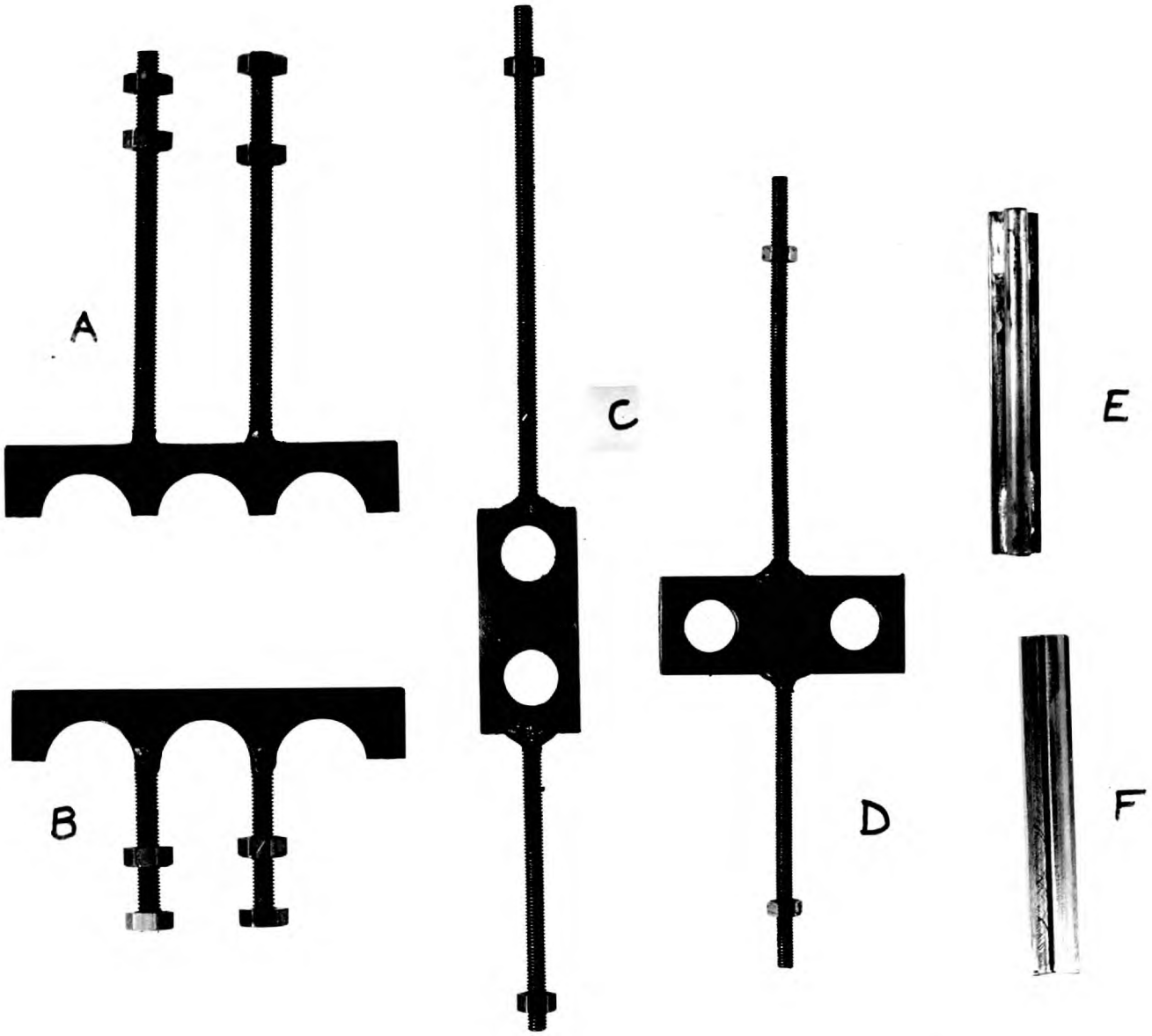

Details of Duct-Holders and Mechanical Hinges

PLATE 7.2

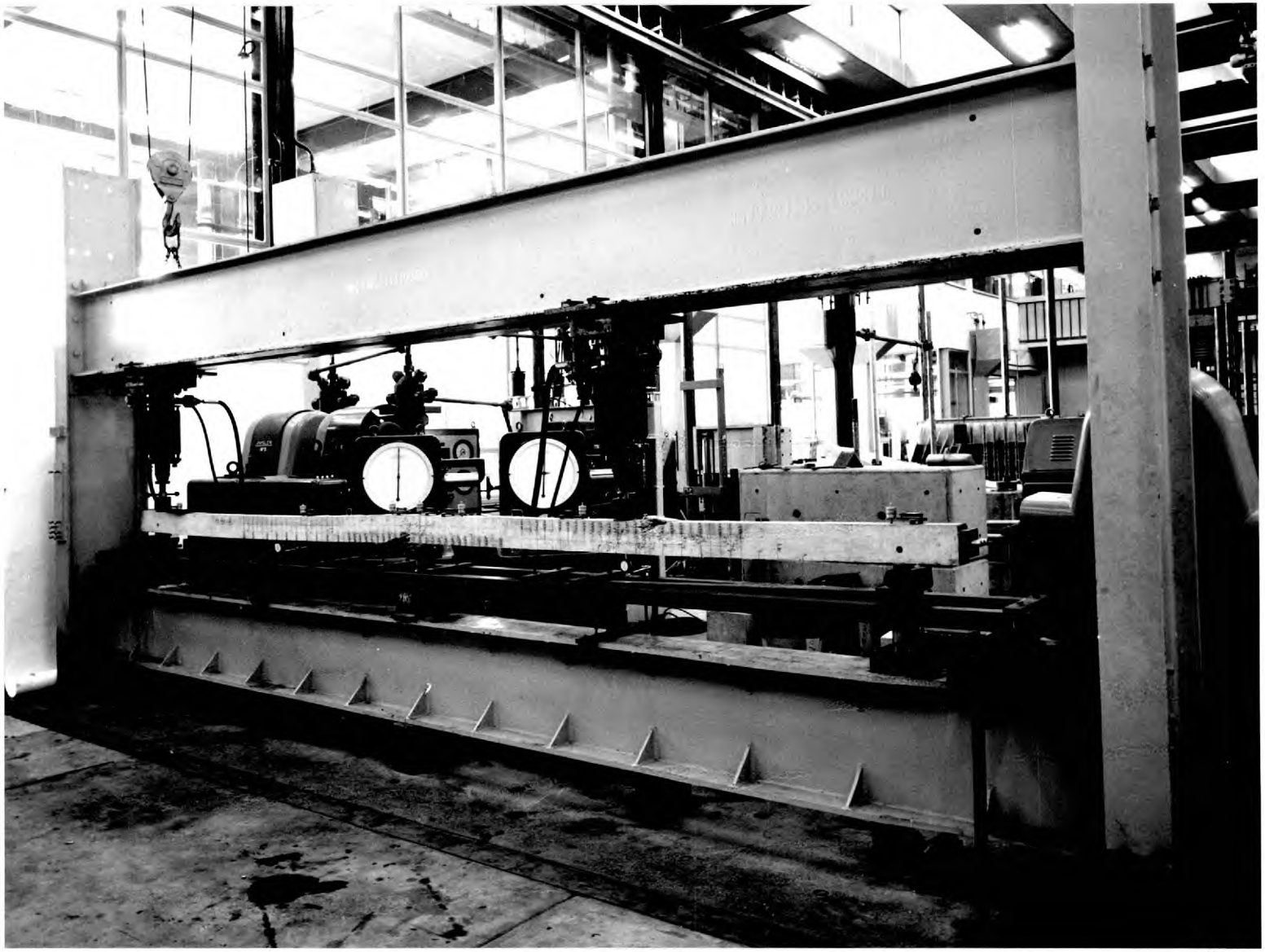

General View of Rig for Beam Tests

PLATE 7.3

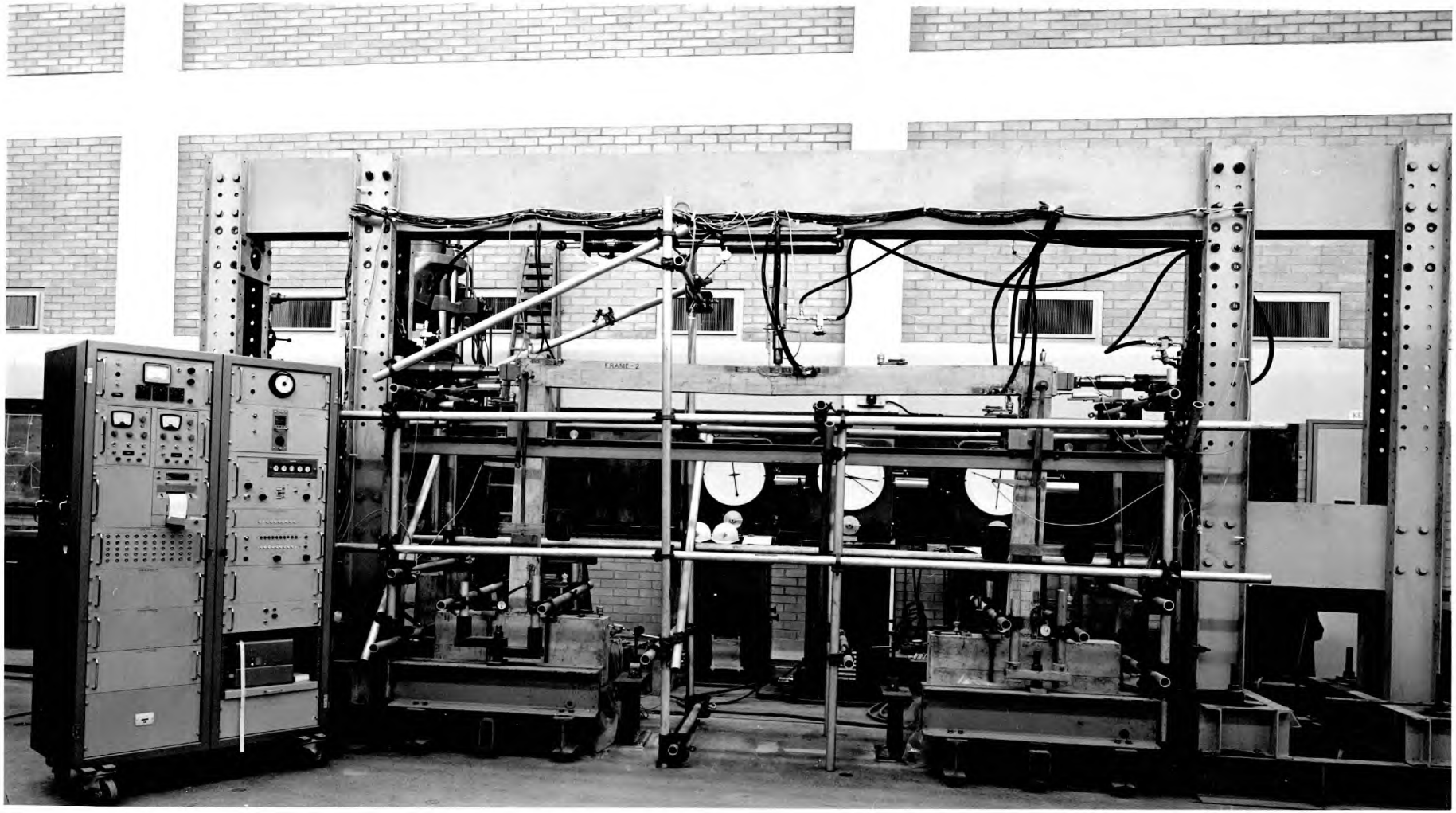

General View of Rig for Frame Tests

PLATE 7.4

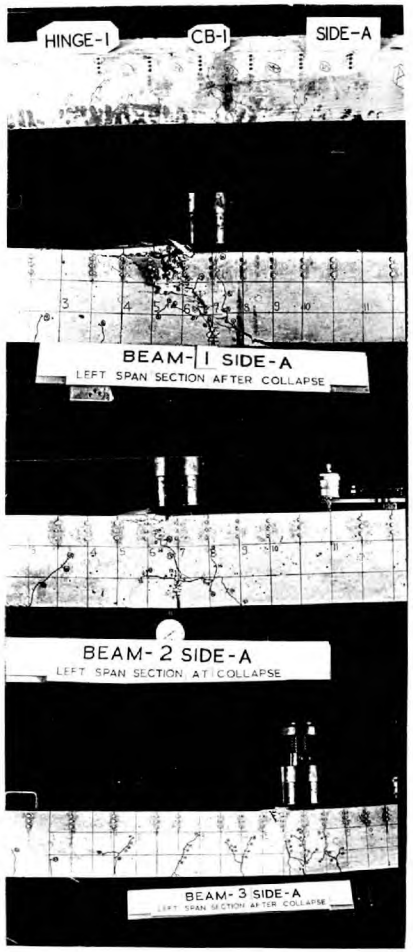

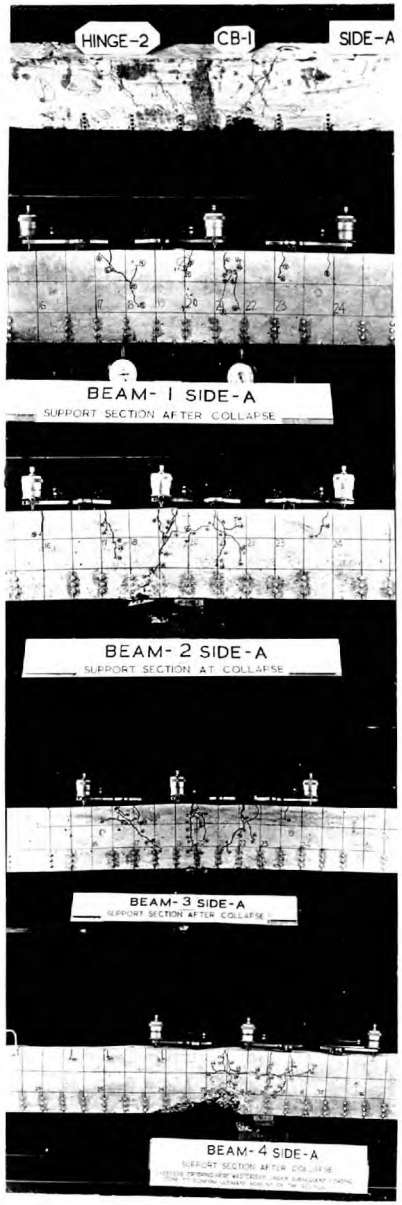

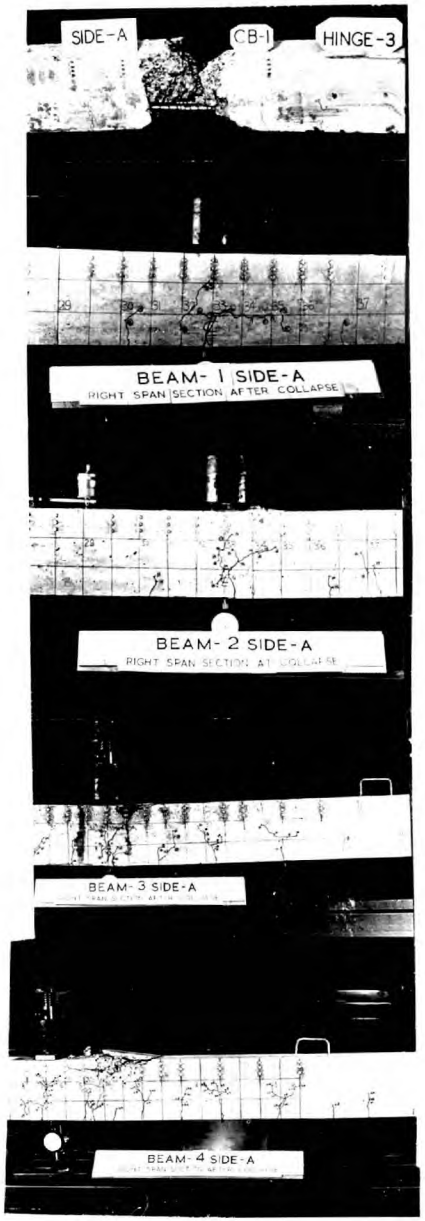

Test Beams: Crack Patterns and Crushing of Concrete at Critical Sections

PLATE 7.5

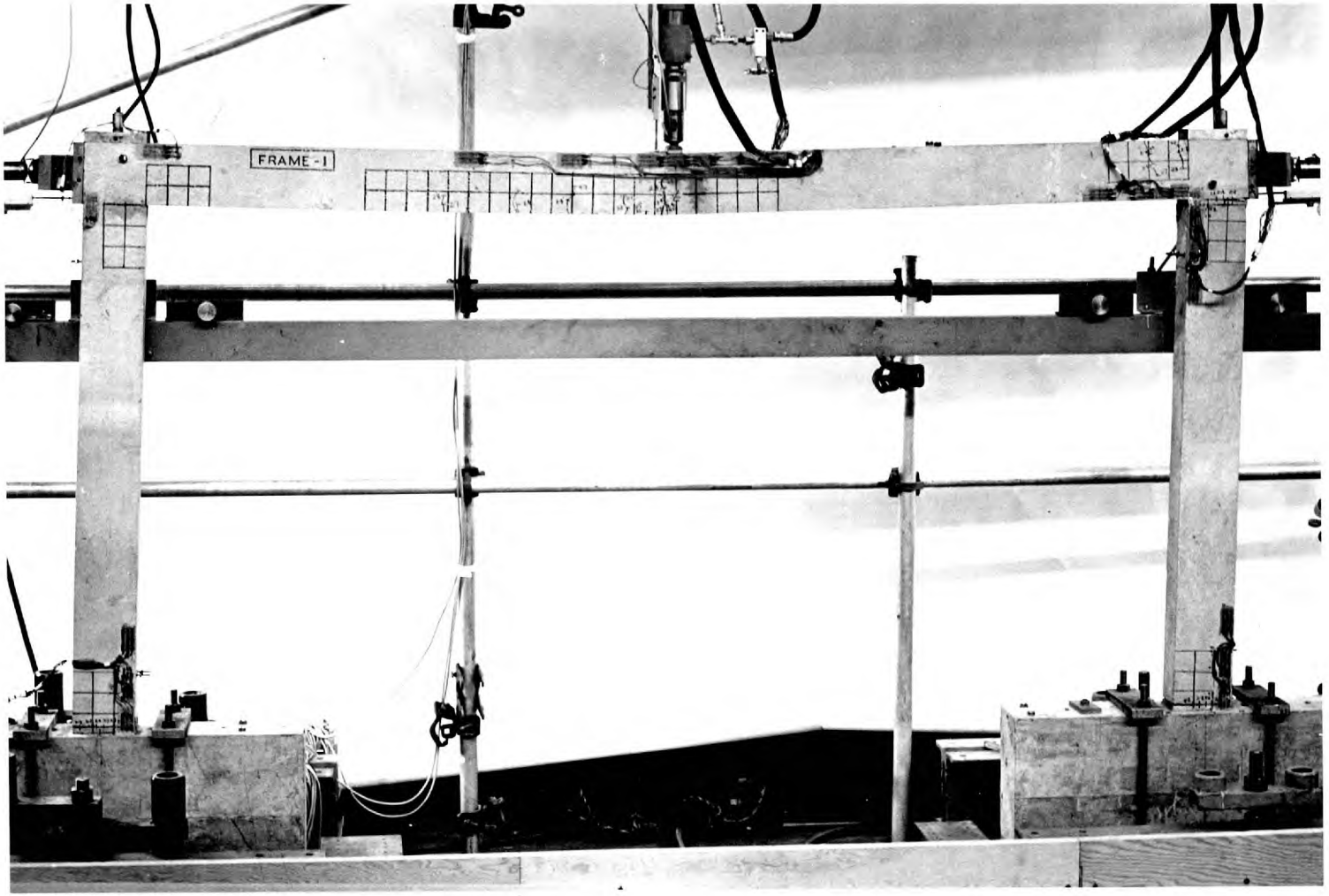

Frame F-1: Deformed Shape and Crack Pattern

PLATE 7.6

Frame F-2: Deformed Shape and Crack Pattern

PLATE 7.7

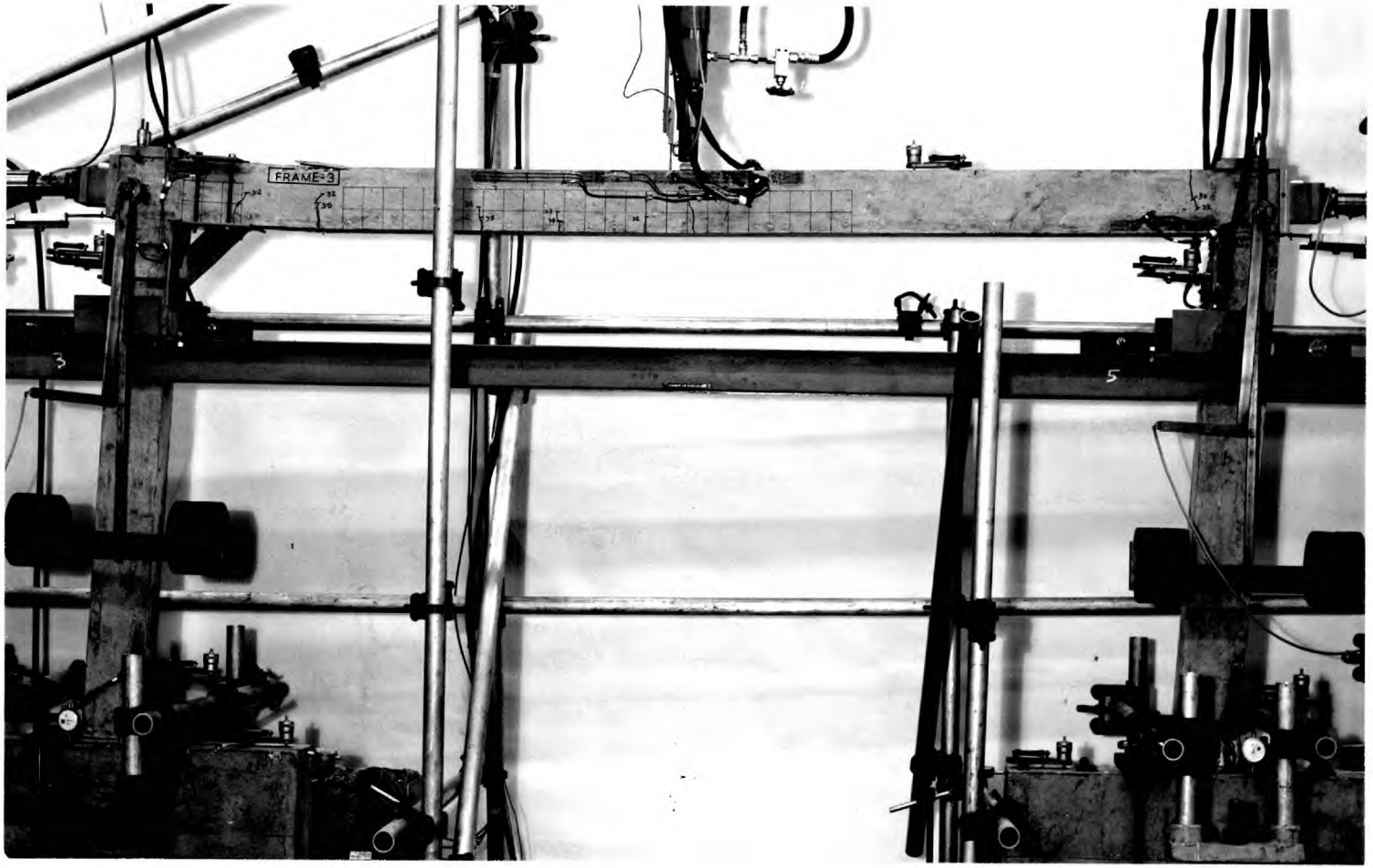

Frame F-3: Deformed Shape and Crack Pattern

PLATE 7.8

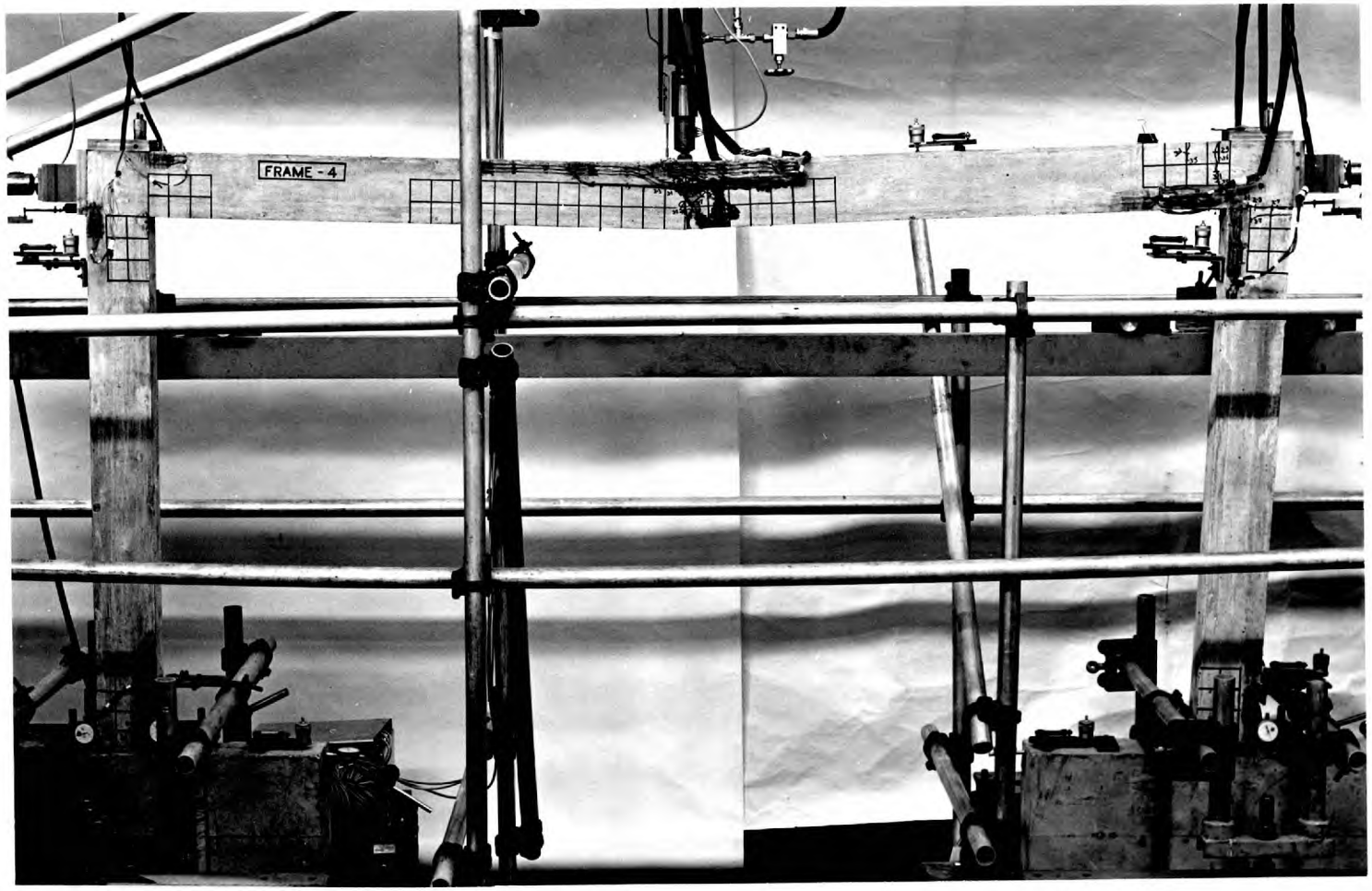

Frame F-4: Deformed Shape and Crack Pattern

PLATE 7.9

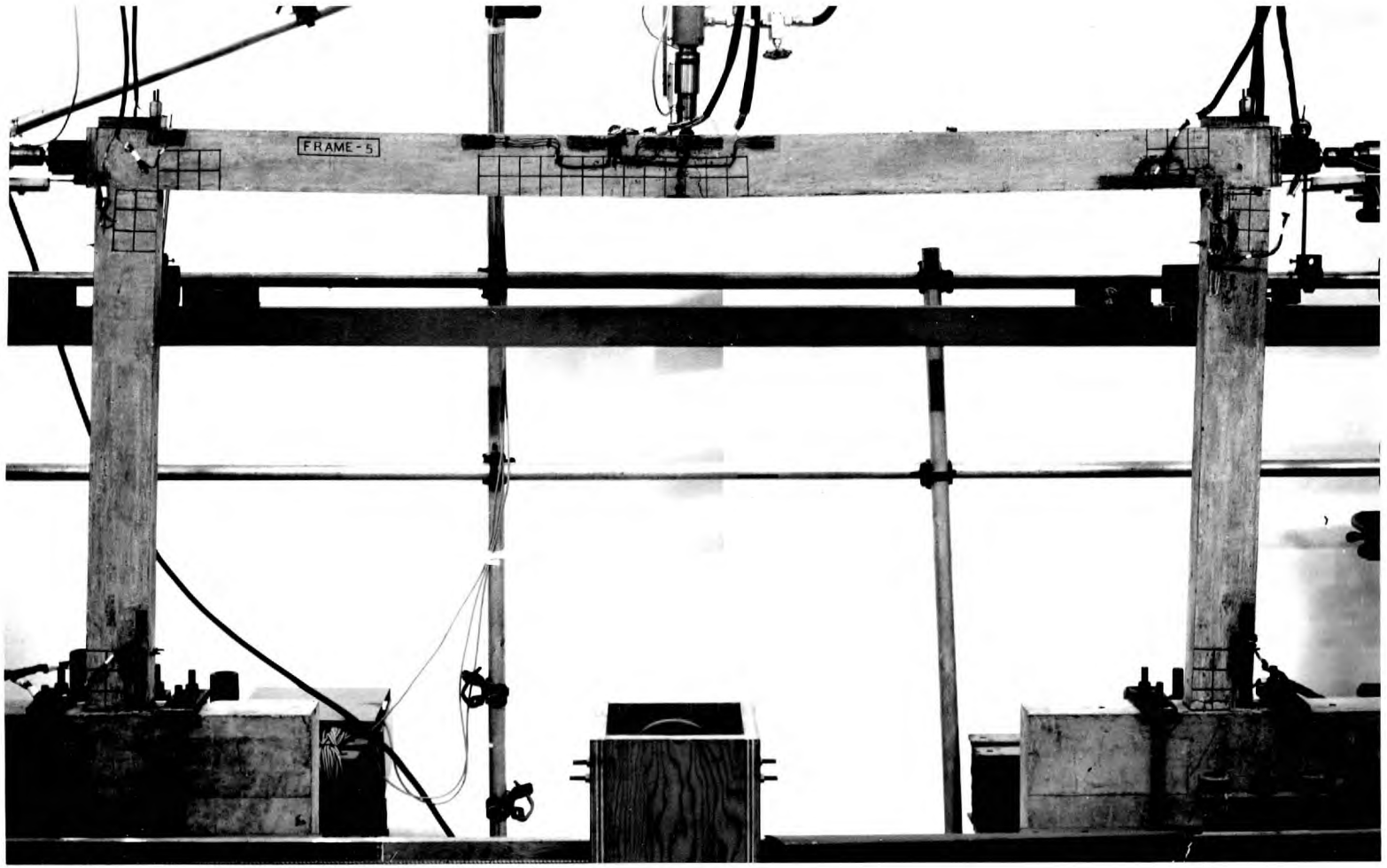

Frame F-5: Deformed Shape and Crack Pattern

PLATE 7.10

CHAPTER 8

DEVELOPMENT OF A FORCE-MOMENT TRANSDUCER

8.1 INTRODUCTION

In the present investigation all applied loads (except those in the beam tests) and reactions were measured by means of load transducers. The use of such a device for measuring an axial tensile or compressive force is very common and needs no comment. However, the development of an accurate force transducer suitable for this investigation posed many practical problems, which will be described here in some detail.

The reactions at each base foot of the portal frame comprised of a vertical force, a horizontal force and a moment. LaGrange[14] made an attempt to measure these reactions; his method consisted of measuring only the restraining moment and the horizontal force at each foot by means of two ordinary load capsules. His arrangement was somewhat cumbersome and unreliable. As LaGrance pointed out, the arrangement of capsules allowed restraining moments to be measured in one direction only. It had the further disadvantage that the horizontal reaction, which plays a most important role in the evaluation of stress-resultant distribution, was measured as the difference of two large quantities, and the whole system had only one equation to check the accuracy of the data. In the present investigation it was decided to measure all the six reactions so that the accuracy of the data could be checked against the three equations of equilibrium, and the errors adjusted logically. In order to measure the three reactions simultaneously, a special load transducer capable of measuring both the vertical and horizontal forces, and moment was devised.

8.2 MEASURE OF ACCURACY OF A LOAD TRANSDUCER

For the present investigation it was important that all load transducers were extremely accurate. Accuracy of a load transducer can be judged by the degree of repeatability it exhibits. It was desirable to have repeatability to ± 2 divisions (data-logger scale). Linearity, although not so essential, would considerably facilitate the calibration of the instrument, and the analysis of the experimental data.

True repeatability in as much that the same readings were obtained under the same load was not obtained. However, repeatability of the change in readings corresponding to the given loads was obtained within the desired accuracy.

8.3 DEVELOPMENT OF AN ACCURATE FORCE TRANSDUCER

Calibration tests on certain force transducers revealed the following unexpected facts. The force transducers which had reasonable repeatability for three calibrations carried out on the same day did not repeat to the same extent when calibrated on different dates; for example, a transducer which was calibrated on March 21st, and March 25th, 1966 in the 1.75 ton range of the standard Amsler compression machine had Solartron data logger outputs of 4302, 4305 and 4316 (average 4308) divisions on March 21st, and 4262, 4255 and 4266 (average 4261) divisions on March 25th. These transducers had duralium cores and 'Tinsley' gauges fixed with 'Araldite' cement. A newly manufactured transducer with a core made from duralium and gauged with Japanese gauges using Japanese cement, C.N. adhesive, had different calibrations in tension and compression; the output in compression being about 5% less than that in tension. A similar phenomenon was also observed while calibrating the transducer described in Section 8.4,

when it was gauged with Japanese gauges using C.N. adhesive. For an applied horizontal load, the tripod in tension had about 7% higher vertical output than the two tripods which were in compression. Because of the other complexities involved in this transducer, it was not possible to draw any conclusion from this, but it did suggest a thorough study of the load transducers before they were used in the present investigation.

A force transducer with a core manufactured from duralium and gauged with 'Budd' metal film strain gauges, using 'Araldite' strain gauge cement, was found to have repeatability within ± 2 divisions and linearity as assessed on the basis of 'first differences' within $\pm 2\%$. This transducer had practically the same calibration in both compression and tension, and also satisfied the test of repeatability in terms of reading on the data logger, that is for any loading process it had practically the same reading on the data logger for the same load. All load transducers used in the frame tests were produced in the above manner in the Department.

Early attempts using 'Budd' gauges were not very successful; at a tensile strain of about 3500 microstrains the transducer exhibited drift. This was eliminated by first etching the surface with phospheric acid and restricting the tensile output to about 3000 microstrains, which is a low output according to the manufacturer's recommendations but one which resulted in a very satisfactory performance. It is therefore suggested that the cores for load transducers should be designed such that the stress does not exceed one-third the proportional limit and the tensile output is restricted to about 3000 microstrains and the compressive output to about 4000 microstrains, unless special precautions are taken for fixing the gauges.

The above studies could not be pursued further because of the time involved. They do, however, draw attention to the importance of choice of gauges, core material, cement and workmanship

in the development of an accurate load transducer. Since a load transducer is a basic measuring device in any structural test, and without its reliability all studies through its use would be of little value, further research would be useful.

The standard Amsler loading machine, which is a Grade 1 machine, was chosen as the standard for calibration, but it was soon discovered that even this machine had calibrations differing by $\frac{1}{2}\%$ when used on different ranges. This error was accepted provided all the measuring devices used in any particular test series were calibrated in this machine using the same loading range.

8.4 DEVELOPMENT OF A FORCE-MOMENT TRANSDUCER

The tripod which is the simplest type of space structure has been used by many[66,67] as a transducer for measuring the three components of a force acting at a point. It was conceived that if three such tripods were fixed between two plates such that their apexes formed a triangle, then they could be used to measure the six components, that is three forces and three moments acting at a point. A force-moment transducer to measure the six components has been developed at the Wayne State University by Lebow[68] by force and moment separation with strain gauges. The principal difference between the two methods is that the present investigation uses a force transducer measuring axial compression or tension as the basic unit, and obtains the six components by suitable linear combination of their electrical outputs, whereas Lebow's basic unit is a strain gauge recording either direct or flexural or torsional strain, and the six components are obtained by combining their outputs. It is difficult to say which would form a better transducer without trying each type in similar conditions. The latter which is solely based on the position

and alignment of the strain gauges may pose more practical difficulties for the same accuracy.

The present investigation was concerned with planar frames and only three components, namely the horizontal and vertical components of force, and moment acting in the plane of the frame were required. Theoretically, they could have been obtained by using only two tripods, but in the event of any force acting outside the plane of the tripods the whole system would have become unstable. Three tripods arranged as shown in fig. 8.1 with $a_o = 9$ in. were therefore used. Details of the transducer are given in Drawing 8.1 and its complete assembly is shown in Plate 8.3.

8.5 CALIBRATION OF FORCE-MOMENT TRANSDUCER

Referring to Figure 8.1, we have

$$V \propto \sum_{1}^{9} x_i \qquad \ldots\ldots (8.1)$$

$$H \propto \left[\frac{1}{2}(x_5 + x_6 + x_8 + x_9 - x_2 - x_3) + x_1 - x_4 - x_7 \right] \qquad \ldots\ldots (8.2)$$

$$(M + Hh_o) \propto \left[\sum_{1}^{3} x_i + \sum_{4}^{9} x_i \right] \qquad \ldots\ldots (8.3)$$

If the applied load consists of a vertical load only, then according to equation 8.2 the electrical output represented by $\left[\frac{1}{2}(x_5 + x_6 + x_8 + x_9 - x_2 - x_3) + x_1 - x_4 - x_7 \right]$ must be zero.

Similarly, if the applied load consists of a horizontal load only, then by virtue of equation 8.1 electrical output denoted by

$\sum_{1}^{9} x_i$ must be equal to zero. In the early stages of development of the transducer, Japanese gauges manufactured by Tokyo Sokki Kenkyujo Co. Ltd. were used. It was found that while the transducer was calibrated for vertical force V, equation 8.2 was satisfied within 2%; but while calibrating it for horizontal force H, equation 8.1 was not satisfied even within 10%. This was serious and meant that the principle of superposition would not apply, and it would be necessary to calibrate the transducer for V, H and M all acting simultaneously. This would have posed considerable practical difficulty.

The only difference in the behaviour of the tripods in the two calibrations was that all tripods were in compression while the vertical load was applied, whereas at the time of the horizontal load tripod 1-2-3 was in tension and tripods 4-5-6 and 7-8-9 were in compression. There could be many reasons for the above discrepancy such as different behaviour of tripods in tension and compression, different gauge factors of strain gauges or their alignment, different calibrations of strain gauges in compression and tension, etc. For want of time, it could not be pursued to a final conclusion. It was, however, decided to use all 'Budd' metalfilm strain gauges from the same lot and commence the calibrations from the basic unit, that is each leg before being assembled into the tripods was calibrated and so was each tripod and then finally the complete force-moment transducer.

Each leg was therefore calibrated in the standard Amsler loading machine in tension or compression depending upon what it would resist in the actual tests. Where it was not easily possible to foresee, each leg was calibrated in both compression and tension. The two calibrations were practically the same, which led to much simplification. Then the legs were assembled; a complete tripod is shown in Plate 8.1. The tripods were then calibrated by

positioning them in the manner they would be placed in the actual tests. All tripods resisted horizontal force acting from left to right but the vertical force was either tensile (tripod 1-2-3) or compressive (tripods 4-5-6 and 7-8-9) and accordingly calibration of each tripod was carried out. The calibration of a tripod in compression is shown in Plate 8.2. If H and V denote the expected maximum horizontal and vertical forces acting at the tripod ball in the tests, then the tripod was calibrated twice for the vertical load with $H = 0, \frac{1}{2}H$ and H, and similarly for the horizontal load with $V = 0, \frac{1}{2}V$ and V. The same linear calibration was obtained for the corresponding cases. The individual leg calibrations had to be slightly adjusted in order to be compatible with the tripod calibrations. This was probably due to the machining or assembly errors, bending effects, etc. The tripods were then fixed between two plates to form the force-moment transducer, see Plate 8.3. To prevent any damage occuring during transportation or testing, four 1 in. diameter columns were fixed to the top plate with specified clearances at their bottoms. When the transducer is not in use the gaps are wedged to prevent damage to the transducer. During the test the wedges are removed, and the loads transmitted through the tripods; load exceeding the permissible value would close certain gaps, which would be reflected on the electrical output, and help to prevent the transducer from being damaged.

The transducer was then fixed in position as intended in the tests, and checked three times by applying a horizontal load; see Plate 8.4. The transducer had linear and consistent behaviour throughout and equation 8.1 was reasonably satisfied, but to match with the individual tripod calibrations small factors had to be applied. This was probably necessary to cater for the assembly and other practical errors and restraint caused by the top plate which modifies the bending effects otherwise exhibited by the individual tripod.

In the tests two such transducers were used and each of them behaved consistently throughout. The sensitivities of the leg transducers varied between 1.56-1.59 divisions per pound, and it was possible to record horizontal and vertical loads to the extent of about 0.41 and 0.57 lb respectively by individual tripod.

8.6 SOME ASPECTS OF DESIGN OF TRIPODS

The sensitivities of a tripod to measure the three components of a force can be adjusted by varying the angle of the legs. Ideally, the angle should be such that the tripod measures all the three components with equal sensitivity. In the present case the ratio between the vertical and horizontal components varied greatly and without changing the angle in each tripod, it was not possible to obtain the same sensitivity for the two components. On the grounds of manufacturing convenience all tripods had the same angle.

The accuracy of a tripod depends upon having very small deformations so that geometry does not change under the application of load. Other things being equal, the deformations of a tripod depend upon the degree to which the ends of the legs are restricted from movement. Welding which accomplishes this without much complication could not be used since the legs were manufactured from duralium. Tests on the tripod with legs fixed by means of screws but with or without dowels showed that the use of three dowels in a total of six screws reduced the vertical deflection by about 50%. It was therefore decided to locate the ends of the legs in slots with 0.002 in. clearance as shown in Drawing 8.1. Tripods produced in this manner behaved satisfactorily.

8.7 CONCLUSIONS

1) The accuracy of a load transducer should be thoroughly checked at an interval of a few days before use in tests.

2) A reasonably accurate transducer measuring axial compression or tension may be obtained by working to about one-third the proportional limit of the core material, and restricting the tensile output to about 3000 microstrains and the compressive output to about 4000 microstrains, unless special precautions are taken in fixing the gauges.

3) Amongst different gauges 'Budd' metalfilm strain gauges gave the most satisfactory performance.

4) The accuracy of the proposed force-moment transducer depends upon having very small deformations of tripods so that geometry of the system does not change with the application of load. The deformations of a tripod, other things being equal, depend upon the degree to which the ends of the legs are restricted from movement.

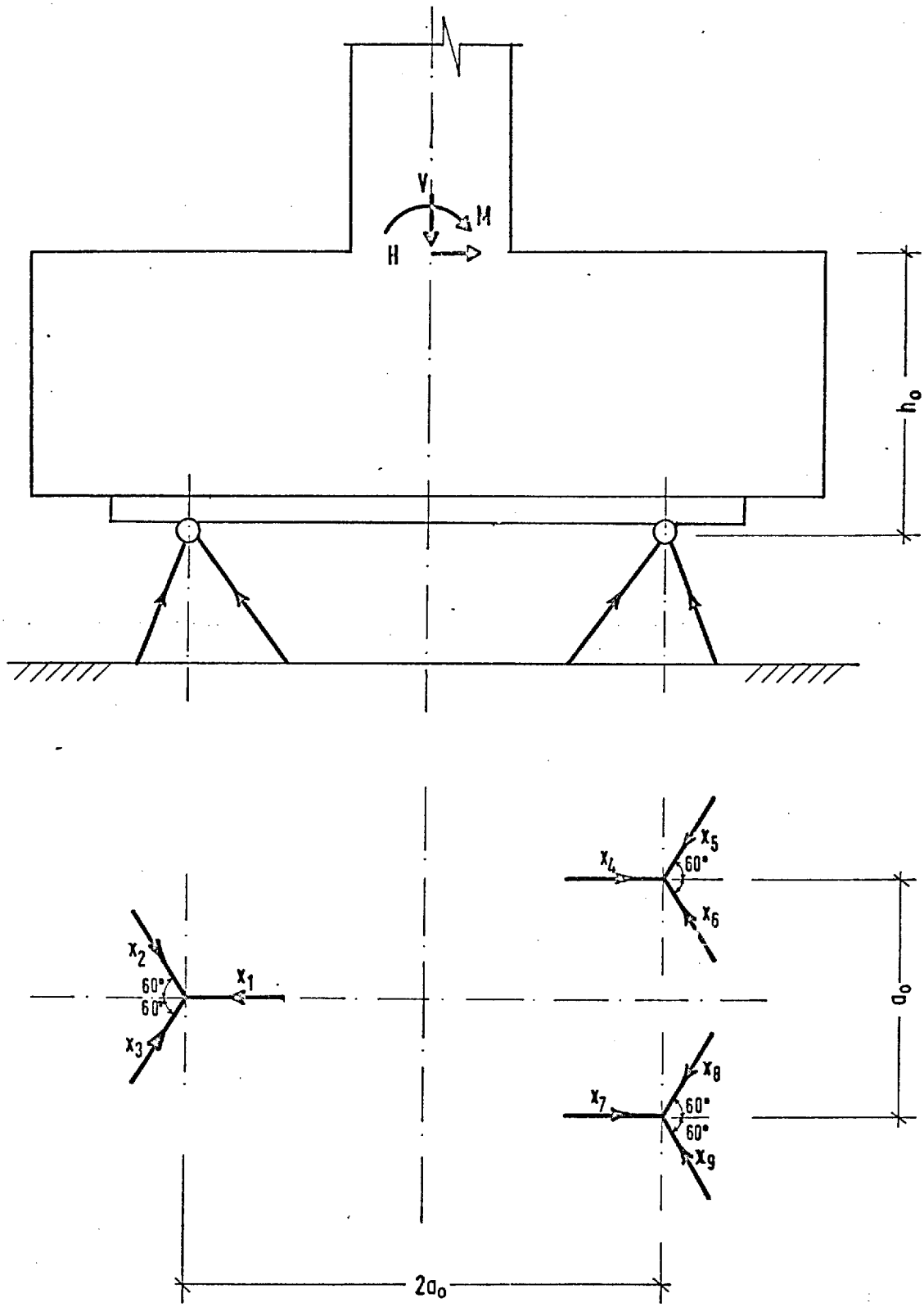

Fig. 8·1: SCHEMATIC ARRANGEMENT OF THE PROPOSED FORCE – MOMENT TRANSDUCER

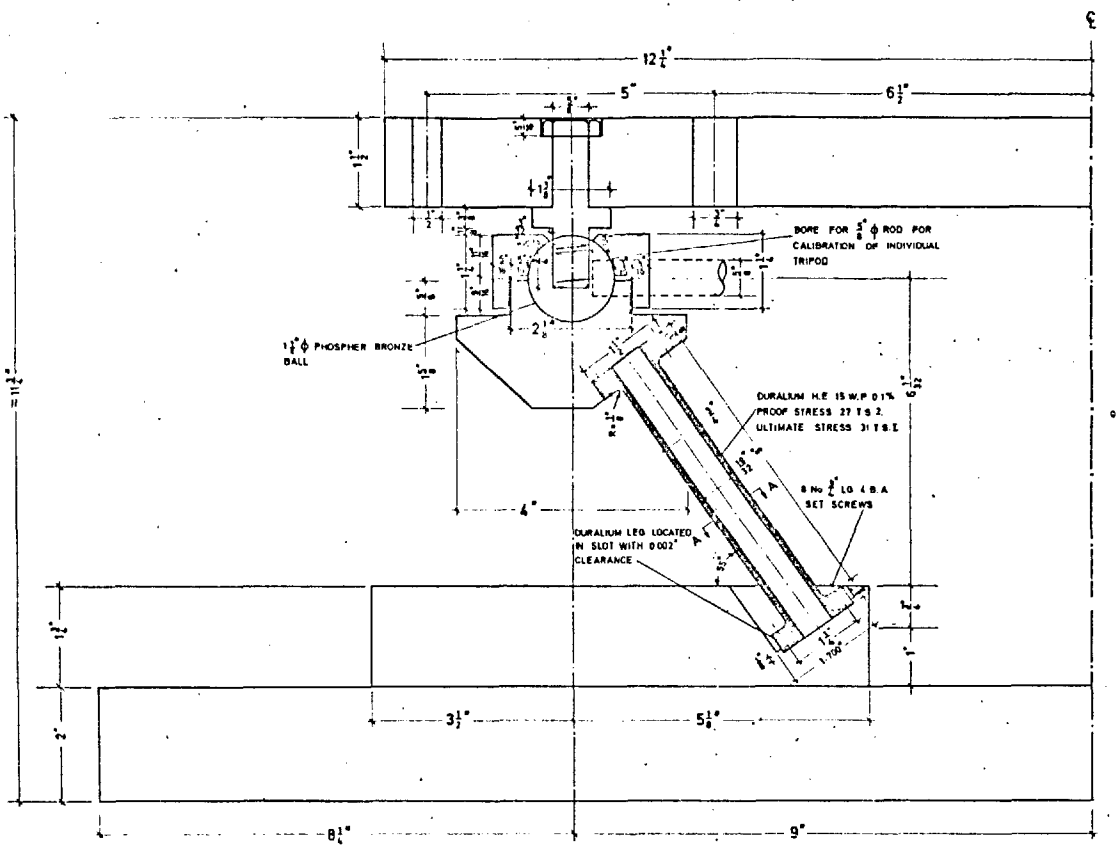

SECTIONAL ELEVATION
SCALE 1" to 1"

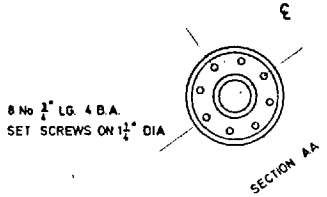

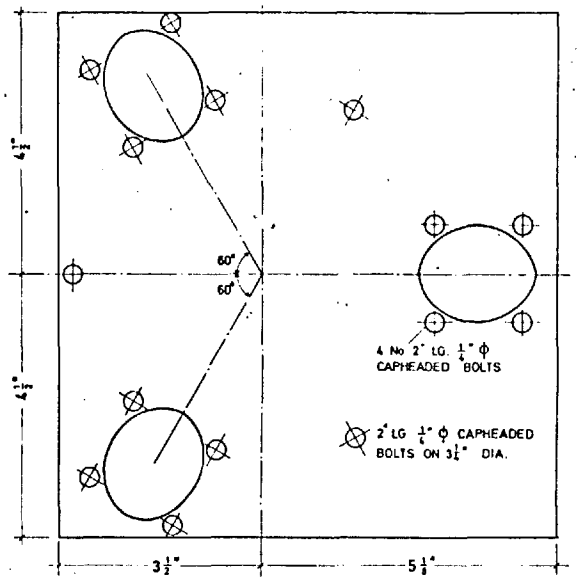

SCHEMATIC PLAN OF BOTTOM PLATE OF INDIVIDUAL TRIPOD
SCALE 1" to 1"

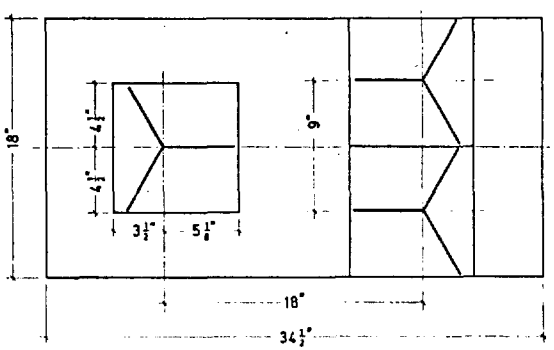

ASSEMBLY OF TRIPODS
SCALE 1" to ½"

SCALE 1" to 1" 1" to ½"	FORCE – MOMENT TRANSDUCER DETAILS	DRG No 8.1

Tripod Transducer

PLATE 8.1

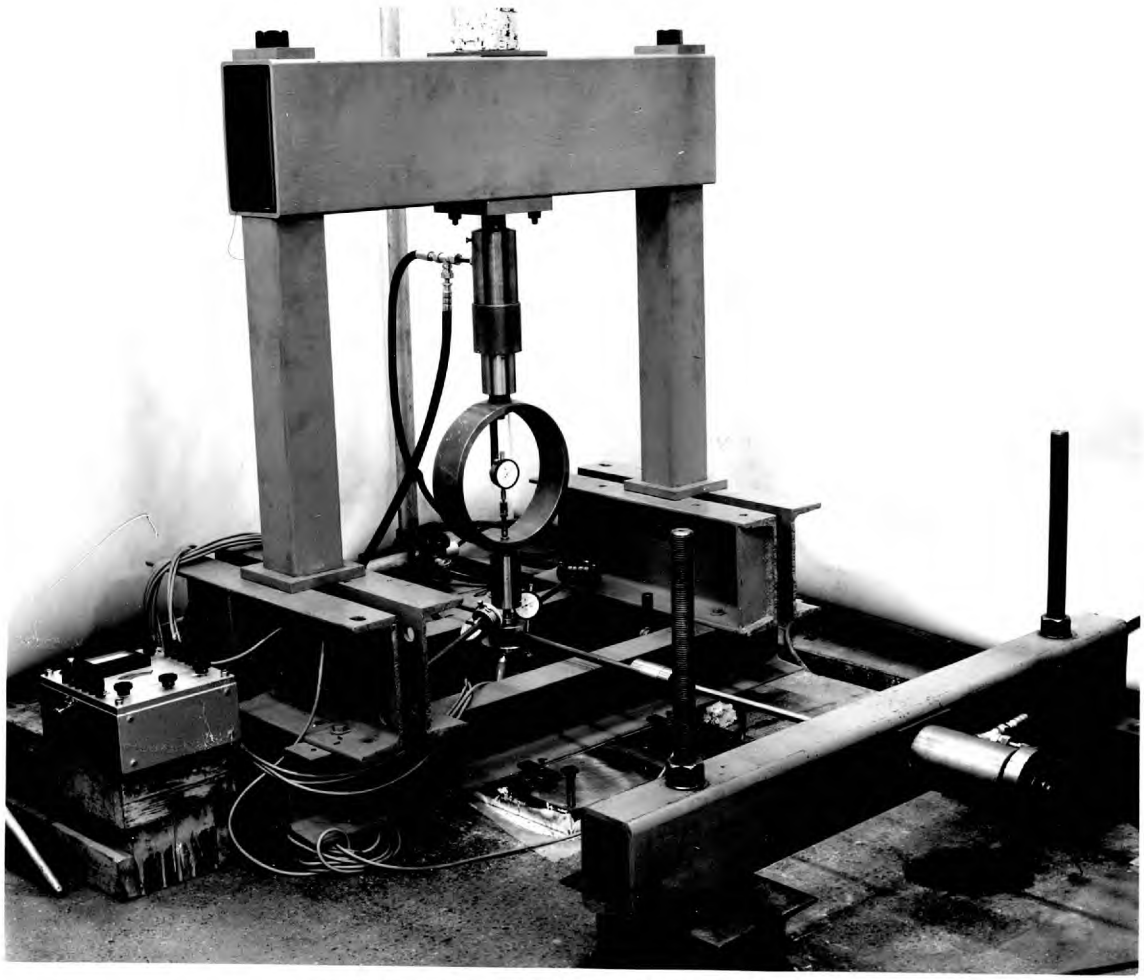

Calibration of Tripod Transducer

PLATE 8.2

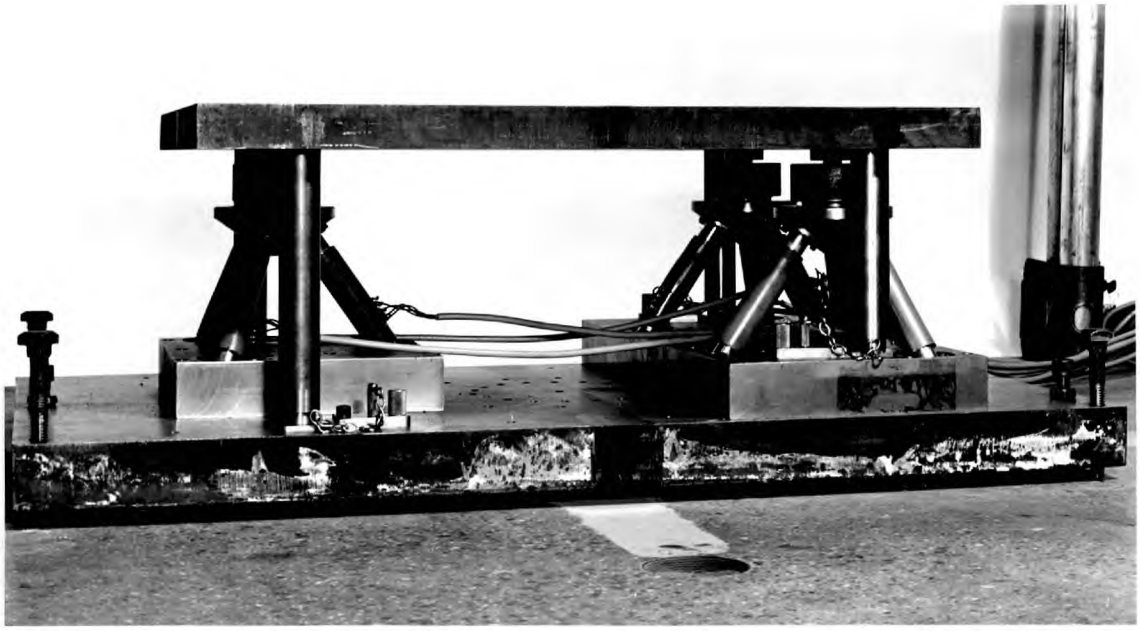

Force-Moment Transducer

PLATE 8.3

Calibration of Force-Moment Transducer

PLATE 8.4

CHAPTER 9

SUMMARY OF CONCLUSIONS

The conclusions derived from each stage of the work have been listed at the end of the appropriate Chapter. However, the following is a summary of the more important points.

(1) The flexural ultimate strengths measured at the actual points of crushing of the concrete were in reasonable agreement with those estimated according to the C.E.B. recommendations, but the corresponding curvatures, concrete compressive strains (extreme fibre), and the flexural stress-resultant-deformation characteristics for sections with similar geometric properties showed a considerable divergence.

(2) It is suggested that the enhanced flexural strength of the theoretical critical sections of a prestressed concrete structure at collapse is the result of the displacement of the actual point of crushing of the concrete from the theoretical critical section, and the gradient of the apparent bending moment distribution.

(3) The theory presented for the analysis of flexural stress-resultant-deformation characteristic of a prestressed concrete section shows that the maximum moment of resistance of a section would not occur at any fixed value of concrete strain in the extreme compression fibre, and requires the stress-strain curve of concrete in flexural compression to be completely defined, including the falling position. The following equations are tentatively suggested

$$f_c = f_{co}\left[2\left(\frac{\varepsilon_c}{\varepsilon_{co}}\right) - \left(\frac{\varepsilon_c}{\varepsilon_{co}}\right)^2\right] \quad , \text{for } \varepsilon_c \leqslant \varepsilon_{co}$$

and $$f_c = f_{co}\, e^{-0.14\left[\left(\frac{\varepsilon_c}{\varepsilon_{co}}\right) - 1\right]^{1.5}}, \text{ for } \varepsilon_c \geqslant \varepsilon_{co}$$

(4) The above theory for the calculation of the complete moment-curvature relationship, and the experimental load-moment and load deflection relationships for the critical sections of the tested structures establish that the moment-curvature relationship for a prestressed concrete section has a drooping branch after the maximum moment is reached.

(5) The divergence in the experimental moment-curvature relationships for sections with similar geometric properties could result from the variation in the concrete strain corresponding to the maximum stress of the stress-strain curve of concrete, which depends upon the degree of restraint available at a particular critical section.

(6) It is concluded that, in general, full redistribution will not take place in a statically indeterminate prestressed concrete structure. Test results can be explained satisfactorily by the theory presented, which assumes that the moment-curvature characteristic of a prestressed concrete section has a drooping branch after the maximum moment is reached.

(7) It has been shown by tests on two-span beams and fixed portal frames that by setting up a suitable secondary prestress stress-resultant distribution, conditions can be created in a statically indeterminate prestressed concrete structure so that it will carry the ultimate load by simultaneously developing the maximum moment of resistance at each of the critical sections forming the collapse mechanism, and at the same time maximum output from each such section is ensured.

For practical engineering purposes the theory presented provides a simple and economical solution for the design of such structures at ultimate load.

(8) The deformations of such a structure at collapse are less compared to those of the corresponding structures which carry the ultimate load with over-redistribution.

(9) The conventional method of design of statically indeterminate prestressed concrete structures based on the working load stress-resultant distribution with a concordant or a linearly transformed cable profile is not, in general, economical.

(10) Linear transformation can result in an ultimate load which is much less than the ultimate load carried by the parent structure with a concordant cable profile. The actual solution can only be obtained by considering both the 'equilibrium' and the 'compatibility' criteria.

REFERENCES

1. EVANS, R.H. The plastic theories for the ultimate strength of reinforced concrete beams. Proceedings of the Institution of Civil Engineers. Vol.21. December 1943. p.98.

2. HOGNESTAD, E. A study of combined bending and axial load in reinforced concrete members. Urbana, University of Illinois Engineering Experiment Station, November 1951. pp.128. Bulletin No. 399.

3. HABERSTOCK, K.B. Die n-freien Berechnungsweisen des einfach bewehrten rechteckigen Stahlbetonbalkens. Berlin, Deustscher Ausschurs fur Stahlbeton, 1951. pp.160. Bulletin No. 103.

4. HOGNESTAD, E., HANSON, N.W. and McHENRY, D. Concrete stress distribution in ultimate strength design. Journal of the American Concrete Institute, Proceedings. Vol. 52, No. 28. December 1955. pp. 455-480.

5. MOENART, R. Experimental study of failure in reinforced concrete members subjected to combined axial load and flexure. Imprimerie G.1C., Brussels, 1953. pp. 162.

6. RÜSCH, H. Tests on the strength of the flexural compression zone. Berlin, Deutsche Ausschuss für Stahlbeton, 1955. pp. vi, 94. Bulletin No. 120.

7. WHITNEY, C.S. Design of reinforced concrete members under flexure or combined flexure and direct compression. Journal of the American Concrete Institute, Proceedings. Vol. 33, No. 25. March-April 1937. pp. 483-498.

8. JENSON, V.P. Ultimate strength of reinforced concrete beams as related to the plasticity ratio of concrete. Urbana, University of Illinois Engineering Experiment Station, June 1943. pp. 62. Bulletin No. 345.

9. GASTON, G.R. An investigation of load-deformation characteristics of reinforced concrete beams up to the point of failure. M.Sc. Thesis. Urbana, Civil Engineering Department, University of Illinois, December 1952. pp.271.

10. BILLET, D.F. and APPLETON, J.H. Flexural strength of prestressed concrete beams. Journal of the American Concrete Institute, Proceedings. Vol.50, No. 49. June 1954. pp.837-856.

11. COOKE, N. The redistribution of bending moments in continuous prestressed concrete beams. Ph.D. thesis. University of Leeds, September 1965. pp.145.

12. SOMES, N.F. Moment-rotation characteristics of prestressed concrete members, Stage 1: Rectangular sections. London, Cement and Concrete Association, September 1966.

13. MATTOCK, A.H. Rotational capacity of hinging regions in reinforced concrete beams. Miami, FLA., Proceedings of the International Symposium on Flexural Mechanics of Reinforced Concrete, November 1964. pp. 143-181.

14. LAGRANGE, L.E. Moment redistribution in prestressed concrete beams and frames. Ph.D. Thesis. University of Cambridge, June 1961. pp. 153.

15. BARNARD, P.R. The collapse of reinforced concrete beams. Miami, Florida, Proceedings of the International Symposium on Flexural Mechanics of Reinforced Concrete, November 1964. pp. 501-520.

16. STURMAN, G.M., SHAH, S.P. and WINTER, G. Microcracking and inelastic behaviour of concrete. Miami, Florida, Proceedings of the International Symposium on Flexural Mechanics of Reinforced Concrete, November 1964. pp. 473-499.

17. KAZINCZY, G.V. Die Plastizitat des Eisenbetons (The plasticity of reinforced concrete). Beton o Eisen. Vol. 32. 1933.

18. GLANVILLE, W.H. and THOMAS, F.G. The redistribution of moments in reinforced concrete beams and frames. Proceedings of the Institution of Civil Engineers. Vol. 3. June 1936. p. 291.

19. BAKER, A.L.L. A plastic theory of design for ordinary reinforced and prestressed concrete, including moment redistribution in continuous members. Magazine of Concrete Research. Vol. 1, No. 2. June 1949. pp.57-66.

20. BAKER, A.L.L. The ultimate load theory applied to the design of reinforced and prestressed concrete frames. 1st edition. London, Concrete Publications Limited, 1956. pp. 90.

21. GUYON, Y. Prestressed concrete, volume II. 1st edition. London, Contractors Record Limited, 1960.

22. MACCHI, G. Etude experimentale de poutres continues précontraintes dans le domaine plastique et a la rupture. Proceedings of the Second Congress of Fédération Internationale de la Précontrainte, 1955. Session IIIa. Paper No. 2. pp. 501-543. London, Cement and Concrete Association, 1958.

23. BENNETT, E.W. Discussions on Paper Item 22. Ditto pp. 645-46.

24. BENNETT, E.W. The redistribution of bending moments in continuous prestressed concrete beams. Ph.D. thesis. University of Leeds, 1960. pp. 87.

25. MALLICK, S.K. Redistribution of moments in two-span prestressed concrete beams. Magazine of Concrete Research. Vol. 14, No. 42. November 1962. pp. 171-183.

26. MALLICK, S.K. and SASTRY, M.K.L.N. Redistribution of moments in prestressed concrete continuous beams. Magazine of Concrete Research. Vol. 18, No. 57. December 1966. pp. 207-220.

27. INSTITUTION OF CIVIL ENGINEERS. Ultimate load design of concrete structures. Report of the Research Committee, with discussion. London, 1964. pp. 104.

28. CRANSTON, W.B. A computer method for inelastic analysis of plane frames. London, Cement and Concrete Association, March 1965. pp. 38. Technical Report No. TRA/386.

29. EUROPEAN CONCRETE COMMITTEE (C.E.B.). Recommendations for an international code of practice for reinforced concrete. London, American Concrete Institute and Cement and Concrete Association, 1964.

30. KANAKVELU, S. and MALLICK, S.K. Redistribution of moments in reinforced concrete portals. Indian Concrete Journal. July 1964. pp. 266-269.

31. MAGNEL, G. Prestressed concrete. 3rd edition. London, Concrete Publications, 1954.

32. GUYON, Y. Prestressed concrete, Vol. I. 4th edition. London, Contractors Record Limited. 1960.

33. EVANS, R.H. and BENNETT, E.W. Prestressed concrete. London, Chapman and Hall, 1958.

34. EDWARDS, A.D. The elastic behaviour and ultimate strength of reinforced and prestressed concrete frames. Ph.D. thesis. University of London, August 1965.

35. MORICE, P.B. A direct method for statically indeterminate prestressed concrete structures. San Francisco, California, Proceedings of the World Conference on Prestressed Concrete, July 1957. pp. 22-1-22-10.

36. MORICE, P.B. and LEWIS, H.E. The strength of prestressed concrete continuous beams and simple plane frames. London, Proceedings of the Symposium on the strength of concrete structures, May 1956. Session C. Paper No. 3. pp. 377-400. London, Cement and Concrete Association, 1958.

37. RAINA, V.K. Ultimate moment distribution in continuous prestressed concrete beams. Ph.D. thesis. University of London, March 1966.

38. SAEED-UN-DIN, K. and HALL, A.S. The effect of creep upon redundant reactions in continuous prestressed concrete beams. Magazine of Concrete Research. Vol. 10, No. 30. November 1958. pp. 109-114.

39. JENKINS, R.S. Linear analysis of statically indeterminate structures. Euler Society, May 1954.

40. ARGYRIS, J.H. and KELSEY, S. Energy theorems and structural analysis. London, Butterworths, 1960.

41. NAUGHTON, L.P. Study of some statically indeterminate structures in prestressed concrete. M.Sc. Thesis. University of Leeds, 1963.

42. FROCHT, M.M. Photoelasticity, Vol. II. New York, John Wiley and Sons, Inc. 1948. pp. 104-117.

43. AMERICAN CONCRETE INSTITUTE. A.C.I. 318-63. Standard building code requirements for reinforced concrete. Detroit, Michigan.

44. WARWARUK, J. Strength and behaviour in flexure of prestressed concrete beams. Urbana, University of Illinois, September 1960. Structural Research Series No. 205.

45. YAMASHIRO, R. and SIESS, C.P. Moment rotation characteristics of reinforced concrete members subjected to bending, shear and axial load. Urbana, University of Illinois, December 1962. pp. 221. Structural Research Series No. 201.

46. BAKER, A.L.L. and AMARKONE, A.M.N. Inelastic hyperstatical frames analysis. Miami, Florida, Proceedings of the International Symposium on Flexural Mechanics of Reinforced Concrete, November 1964. pp. 85-142.

47. ROSENBLUETH, E. and de COSSIO, R.D. Instability considerations in limit design of concrete frames. Miami, Florida, Proceedings of the International Symposium on Flexural Mechanics of Reinforced Concrete, November 1964. pp. 439-463.

48. SHALIN, S. Effects of far advanced compressive strains of concrete in reinforced concrete beams subjected to bending moments. Stockholm, Division Building Station Structural Engineering, Royal Institute Technology, 1955. Bulletin No. 17.

49. NYLANDER, H. and SAHLIN, S. Investigations of continuous concrete beams as far advanced compressive strains in concrete. Stockholm, Division Building Statics Structural Engineering, Royal Institute of Technology, 1955. Bulletin No. 18.

50. RAMALEY, D. and McHENRY, D. Stress-strain curves for concrete strained beyond the ultimate load. Engineering and Geological Control Division, U.S. Bureau of Reclamation. March 7, 1947. Laboratory Report No. SP-12.

51. HOGNESTAD, E., HANSON, N.W. and McHENRY, D. Concrete stress distribution in ultimate strength design. Journal of the American Concrete Institute, Proceedings. Vol. 52, No. 28. 1955-56. pp. 455-79.

52. RÜSCH, H. Researches towards a general flexural theory for structural concrete. Journal off the American Concrete Institute, Proceedings. Vol. 57. July 1960. pp. 1-28.

53. SOLIMAN, M.T.M. Ultimate strength and plastic rotation capacity of reinforced concrete members. Ph.D. thesis. University of London. July 1960.

54. DESAYI, P. and KRISHNAN, S. Equation for the stress-strain curve of concrete. Journal of the American Concrete Institute, Proceedings. Vol. 61, No. 3. March, 1964.

55. DAVIES, R.D. Unpublished work (see item 4.7 of reference 14).

56. PIETRZYKOWSKI, J. The elastic-plastic behaviour of prestressed concrete frames. Magazine of Concrete Research. Vol. 16, No. 48. September 1964. pp. 123-128.

57. EDWARDS, A.D. Private communication to author.

58. TAYLOR, A.J. Discussion on paper at item No. 36. London, Proceedings of the Symposium on the Strength of Concrete Structures, May 1956. Session C. pp. 426-429.

59. LEWIS, H.E. Reply to Taylor's discussions. Ditto. pp. 440-441.

60. ZIELIŃSKI, J. and ROWE, R.E. An analysis of stress distribution in the anchorage zones of post-tensioned concrete members. London, Cement and Concrete Association, September 1960. pp. 32. Research Report No. 9.

61. ZIELIŃSKI, J. and ROWE, R.E. Ths stress distribution associated with groups of anchorages in post-tensioned concrete members. London, Cement and Concrete Association, October 1962. pp. 39. Research Report No. 13.

62. MacGREGOR, J.G. The relationship between design specifications and the behaviour of prestressed concrete beams subjected to combined bending and shear. Transactions of the Engineering Institute of Canada. Paper No. EIC-63-BR & STR 15, Vol. 6, No. A-12. November 1963. pp. 32 + figs.

63. BRITISH STANDARDS INSTITUTIONS. B.S. CP 115: 1959. The structural use of prestressed concrete in buildings. London. pp. 43.

64. PRICE, K.M. Ph.D. Thesis. University of London (to be submitted).

65. BREMNER, T.W. The influence of the reinforcement on the elastic and inelastic properties of reinforced concrete members. M.Sc. thesis. University of London 1962.

66. HATCHER, D.S., SOZEN, M.A. and SIESS, C.P. A study of tests on a flat plate and a flat slab. Urbana, University of Illinois. Civil Engineering Studies, July 1961. Structural Research Series No. 217.

67. CHUEN, C.H. The interaction between slab and columns in flat slab construction. Ph.D. thesis. University of London. June 1965.

68. LEBOW, M.J. pp. 238-243 of reference at item 69.

69 PERRY, C.C. and LISSNER, H.R. The strain gauge primer. 2nd edition. London, McGraw-Hill Book Company.

APPENDIX 1

METHOD FOR CORRECTING THE OBSERVED STRESS-RESULTANT DATA

Let the total number of reactions and applied loads measured in a test be m. If $x_i (i = 1,2 \ldots m)$ are the required corrections to the measured quantities, then they must have values such that $\sum_1^m x_i^2$ is minimum and at the same time they must satisfy the equations of equilibrium.

Let the equations of equilibrium be denoted by

$$\phi_r (x_1, x_2 \ldots x_m) = 0 \quad (r = 1, 2 \ldots k) \qquad \ldots\ (1)$$

and let

$$\sum_1^m x_i^2 \equiv f(x_1, x_2 \ldots x_m) \qquad \ldots\ (2)$$

According to Lagrange's theorem of undetermined multipliers we can find k numbers $\beta_i (i = 1,2 \ldots k)$ as well as m values of the variables $x_i (i = 1,2 \ldots m)$ which satisfy

(i) the k equations at 1 and also

(ii) m equations

$$\frac{\partial f}{\partial x_s} + \beta_1 \frac{\partial \phi_1}{\partial x_s} + \beta_2 \frac{\partial \phi_2}{\partial x_s} + \ldots = 0 (s = 1, 2 \ldots m) \qquad \ldots\ (3)$$

and for m such values of the variables $x_i (i = 1,2 \ldots m)$ the value of $f(x_1, x_2 \ldots x_m)$ is a stationary value.

The effect of equation 3 is that if $\beta_i (i = 1,2 \ldots k)$ exists, then

$$\frac{\partial f}{\partial x_s} = 0 (s = 1, 2 \ldots m) \qquad \ldots\ (4)$$

But equations 4 represent the m normal equations obtained from function $f(x_1, x_2 .. x_m)$. These are true only if $f(x_1, x_2 .. x_m)$ is minimum. That is, the values of $x_i (i = 1, 2 .. m)$ so obtained are the values of corrections which make $\sum_1^m x_i^2$ the minimum and also satisfy the k equations of equilibrium at 1.

This will now be illustrated by applying to the data of the frame tests.

By using the individual tripod calibrations the outputs from the three legs of a tripod can be expressed as horizontal and vertical components acting at the centre of the tripod ball. Since the balls of all the tripods of a force-moment transducer are at the same level, the horizontal components can be combined into one. Thus the various measured forces $W_i (i = 1, 2 .. 9)$ would act as shown in Figure 1.

If $x_i (i = 1, 2 .. 9)$ are the required corrections, then the normal equations are

$$x_i = 0 \quad \text{weight} = \frac{1}{w_i} (i = 1, 2 \ldots 9) \qquad \ldots\ (5)$$

where $\frac{1}{w_i}$ is the weight of the corresponding observation.

For equilibrium to be satisfied

$$\left.\begin{aligned}
&x_1 - x_4 - x_5 - x_7 - x_8 = -W_1 + W_4 + W_5 + W_7 + W_8 \\
&x_2 - x_3 - x_6 - x_9 = -W_2 + W_3 + W_6 + W_9 \\
&-x_2 b_o + x_3 b_o + x_4 (\tfrac{1}{2} - a_o - c_o) + x_5 (\tfrac{1}{2} + a_o - c_o) \\
&-x_6 (h + h_o - b_o) - x_7 (\tfrac{1}{2} + a_o + c_o) - x_8 (\tfrac{1}{2} - a_o + c_o) \\
&-x_9 (h + h_o - b_o) = \\
&\qquad W_2 b_o - W_3 b_o - W_4 (\tfrac{1}{2} - a_o - c_o) \\
&-W_5 (\tfrac{1}{2} + a_o - c_o) + W_6 (h + h_o - b_o) + W_7 (\tfrac{1}{2} + a_o + c_o) \\
&+W_8 (\tfrac{1}{2} - a_o + c_o) + W_9 (h + h_o - b_o)
\end{aligned}\right\} \qquad \ldots\ (6)$$

Equations 6 are equivalent to k equations at 1.

Differentiating equations 5 and 6 and forming equations similar to those at 3, after taking due account of weight of equations 5, we have

$$\left.\begin{aligned}
&\frac{x_1}{w_1} - \beta_1 = 0 \\
&\frac{x_2}{w_2} - \beta_2 + \beta_3 b_o = 0 \\
&\frac{x_3}{w_3} + \beta_2 - \beta_3 b_o = 0 \\
&\frac{x_4}{w_4} + \beta_1 - \beta_3 (\tfrac{1}{2} - a_o - c_o) = 0 \\
&\frac{x_5}{w_5} + \beta_1 - \beta_3 (\tfrac{1}{2} + a_o - c_o) = 0 \\
&\frac{x_6}{w_6} + \beta_2 + \beta_3 (h + h_o - b_o) = 0 \\
&\frac{x_7}{w_7} + \beta_1 + \beta_3 (\tfrac{1}{2} + a_o + c_o) = 0 \\
&\frac{x_8}{w_8} + \beta_1 + \beta_3 (\tfrac{1}{2} - a_o + c_o) = 0 \\
&\frac{x_9}{w_9} + \beta_2 + \beta_3 (h + h_o - b_o) = 0
\end{aligned}\right\} \quad \ldots\ (7)$$

Substituting $x_i (i = 1,2 \ldots 9)$ from equation 7 into equation 6, we have

$$\begin{bmatrix} \Lambda_{11} & \Lambda_{12} & \Lambda_{13} \\ \Lambda_{21} & \Lambda_{22} & \Lambda_{23} \\ \Lambda_{31} & \Lambda_{32} & \Lambda_{33} \end{bmatrix} \begin{bmatrix} \beta_1 \\ \beta_2 \\ \beta_3 \end{bmatrix} = \begin{bmatrix} B_1 \\ B_2 \\ B_3 \end{bmatrix}$$

or $$\underline{\Lambda}\,\underline{\beta} = \underline{B} \qquad \ldots\ (8)$$

where

$$A_{11} = w_1 + w_4 + w_5 + w_7 + w_8$$

$$A_{12} = 0$$

$$A_{13} = -w_4(\tfrac{1}{2} - a_o - c_o) - w_5(\tfrac{1}{2} + a_o - c_o) + w_7(\tfrac{1}{2} + a_o + c_o) + w_8(\tfrac{1}{2} - a_o + c_o)$$

$$A_{21} = 0$$

$$A_{22} = w_2 + w_3 + w_6 + w_9$$

$$A_{23} = -w_2 b_o - w_3 b_o + (w_6 + w_9)(h + h_o - b_o)$$

$$A_{31} = -w_4(\tfrac{1}{2} - a_o - c_o) - w_5(\tfrac{1}{2} + a_o - c_o) + w_7(\tfrac{1}{2} + a_o + c_o) + w_8(\tfrac{1}{2} - a_o + c_o)$$

$$A_{32} = -w_2 b_o - w_3 b_o + (w_6 + w_9)(h + h_o - b_o)$$

$$A_{33} = w_2 b_o^2 + w_3 b_o^2 + w_4(\tfrac{1}{2} - a_o - c_o)^2 + w_5(\tfrac{1}{2} + a_o - c_o)^2 + w_6(h + h_o - b_o)^2 + w_7(\tfrac{1}{2} + a_o + c_o)^2 + w_8(\tfrac{1}{2} - a_o + c_o)^2 + w_9(h + h_o - b_o)^2$$

$$B_1 = -W_1 + W_4 + W_5 + W_7 + W_8$$

$$B_2 = -W_2 + W_3 + W_6 + W_9$$

$$B_3 = W_2 b_o - W_3 b_o - W_4(\tfrac{1}{2} - a_o - c_o) - W_5(\tfrac{1}{2} + a_o - c_o) + W_6(h + h_o - b_o) + W_7(\tfrac{1}{2} + a_o + c_o) + W_8(\tfrac{1}{2} - a_o + c_o) + W_9(h + h_o - b_o)$$

Thus evaluating β's from equation 8, $x_i (i = 1, 2 \ldots m)$ can be obtained from equation 7.

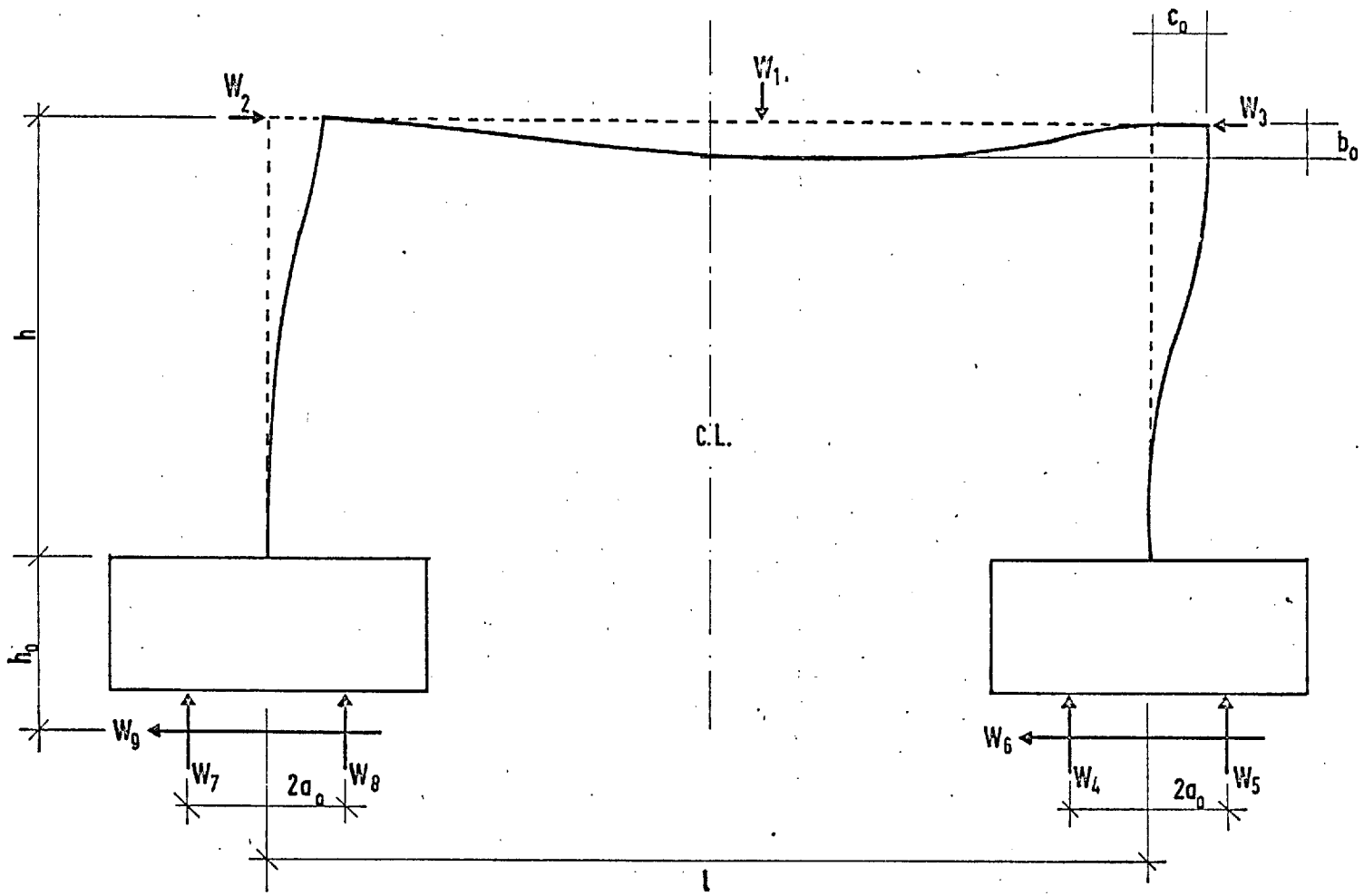

Fig. 1